UNIVERSIDADE DE LISBOA
FACULDADE DE CIÊNCIAS

Renewable and resilient power systems under future climate variability

"Documento Definitivo"

Doutoramento em Sistemas Sustentáveis de Energia

Raquel Vaz Pato Figueiredo

Tese orientada por:
Professor Doutor Miguel Centeno Brito
Doutor Pedro Nunes

Documento especialmente elaborado para a obtenção do grau de doutor

2020

UNIVERSIDADE DE LISBOA

FACULDADE DE CIÊNCIAS

Renewable and resilient power systems under future climate variability

Doutoramento em Sistemas Sustentáveis de Energia

Raquel Vaz Pato Figueiredo

Tese orientada por:

Professor Doutor Miguel Centeno Brito

Doutor Pedro Nunes

Júri:

Presidente:

- Doutor João Manuel de Almeida Serra, Professor Catedrático e Presidente do Departamento de Engenharia Geográfica, Geofísica e Energia, da Faculdade de Ciências da Universidade de Lisboa

Vogais:

- Doutora Maria Júlia Fonseca de Seixas, Professora Associada com Agregação da Faculdade de Ciências e Tecnologia da Universidade Nova de Lisboa
- Doutora Paula Fernanda Varandas Ferreira, Professora Associada da Escola de Engenharia da Universidade do Minho
- Doutor Carlos Augusto Santos Silva, Professor Auxiliar do Instituto Superior Técnico da Universidade de Lisboa
- Doutor Miguel Centeno da Costa Ferreira Brito, Professor Auxiliar com Agregação da Faculdade de Ciências da Universidade de Lisboa (orientador)

Documento especialmente elaborado para a obtenção do grau de doutor

Doutoramento financiado pela Fundação para a Ciência e a Tecnologia

(PD/BD/114174/2016)

2020

Acknowledgments

This thesis would not have been possible without the help and support of several parties, and I am grateful to all of those that in one way or another have contributed to this work.

I would like to start by expressing my deepest gratitude to both my supervisors, Professor Miguel Brito and Dr. Pedro Nunes, for always being very supportive, without them this thesis would not be possible. I wish to give my especial thanks to Professor Miguel Brito for always being available to discuss my work giving me a boost of motivation and new ideas to overcome the problems, and also for his patience and understanding. I would also like to extend this special thanks to Dr. Pedro Nunes for his rigor and constructive criticism that have continuously improved my work, and also for always pushing me to do better and all the knowledge shared.

I am grateful to Fundação para a Ciência e a Tecnologia (FCT) for funding my PhD through the doctoral grant PD/BD/114174/2016, under the framework of MIT Portugal Program in Sustainable Energy Systems. I also wish to show my appreciation for all the help and financial support provided by Instituto Dom Luiz (IDL).

I would like to thank Professor João Serra for his supervision during the first year of my PhD, and for guiding my advanced training course as the MIT Portugal Program coordinator at FCUL. I am also grateful to Professor Carla Silva who followed the coordination of MIT Portugal Program at FCUL in the last years.

I would like to express my gratitude to Professor Henrik Lund, Dr. Jakob Thellufsen and the rest of their team at Aalborg University, for allowing me to stay there and learn EnergyPLAN with them. They were always patient and available to answer all my questions and to discuss how some limitations of the software could be overcome.

During the course of this PhD, the acquisition of data from different sources was critical and, thankfully, I was able to count with the help of several people and institutions. I would like to thank the Portuguese Energy Agency (ADENE) for providing access to the EPC database, especially to Eng. Rui Fragoso e Eng. Susana Soares. I would also like to acknowledge the data on heat pumps' sales provided by APIRAC and show my gratitude for all the support and insights provided by Eng. Fonseca e Silva, Eng. Ruben Martins and Dr. Nuno Roque. I am also grateful to Dr. Patrícia Fortes and Professor Júlia Seixas for their availability to share the results from RNC2050 and being always very supportive

and helpful. I would like to acknowledge the help provided by some elements of the *Climate change, atmosphere-land-ocean processes and extremes* research group of IDL in the acquisition of climate data and the assistance provided: João Careto, Manuel Nascimento, Dr. Pedro Soares and Dr. Rita Cardoso.

I wish to extend my special thanks to the following people who have also contributed to my work with fruitful discussions and insights on several topics: Professor Ana Estanqueiro (LNEG), Eng. António Couto (LNEG), Professor António Vallêra (FCUL), Dr. João Pedro Gouveia (FCT-UNL), Professor Marília Antunes (FCUL), Dr. Pedro Soares (IDL), Dr. Rita Cardoso (IDL), Dr. Sofia Simões (FCT-UNL), Dr. Tânia Sousa (IST) and Dr. Zeus Guevara. I would also like to thank Professor Marta Panão for participating in a significant part of this work, and for always showing the availability to help and provide assistance when I asked.

And because work is not everything, I want to thank all my incredible friends.

Thanks to Ana, Guilhermes, Hugo, Ivo, Joana, João, Joel, Lena, Mendi, Rita, Rodrigo and Sara for the lunch/coffee/tea breaks, non-sense discussions and stupid jokes; you were always very important to share complaints, frustrations, to procrastinate and mostly to laugh. To Ângelo, 'colega', a special thanks for being an amazing friend from the beginning of this experience.

Thanks to Ana, Bruno, Daniel and André for all the adventures, dinners, and for putting up with my bad temper. To Andreia, thanks for your unconditional friendship and for keeping me insane with your singing. To Catarina, my 'kitkat', thanks for being my partner in crime in the last ten years, and for offering me chocolate in my worst moments. To Inês, you have been there in all my ups and downs for the last 20+ years, I owe you more than I could ever express. I could not have asked for better friends.

Lastly, I would like to thank all my family. To my brothers, my sisters-in-law and my nephews, that were always amazing role models and are always a good excuse to go away and restore batteries. To my parents, that have never stop believing that I could finish this stage and for their willingness to help in every step of the way. And above all, thanks to Miguel for everything, you have been my rock.

Abstract

The concern about the consequences of carbon-intensive activities across all socio-economic sectors is accelerating the path towards renewables-based power systems. However, larger renewable energy penetration allied with unknown future demand adds vulnerability and uncertainty to the design of power systems.

This work assesses the impact of climate variability and energy demand in renewables-based power systems. An hourly-based modelling tool is used to simulate the power system for Portugal in 2050. A multiyear model calibration is proposed, enabling a more reliable simulation. Regarding climate, two representative concentration pathways (RCP4.5 and RCP8.5), totaling 473 climate realizations, are tested. Five electricity demand-flexibility scenarios are tested for each activity sector, assuming diverging levels for electricity demand, storage and demand-side management. The impacts of climate variability on supply and demand are simultaneously analyzed and quantified.

Energy demand plays a crucial role in the power system. Results show that residential demand may increase between 4 and 60%, which are used to define scenarios. The cross-border interconnection needs quadruplicate from low to high demand, while the renewable generation share decreases 16 p.p.

Climate variability, depending on the scenario, leads to changes in residential demand between -8 to +5% around its median, while renewables generation share might oscillate between -15 and +15 p.p. Cross-border interconnection energy trading needs may vary by a factor of two due to climate variability, from -62 to +226% around its median.

Fully renewables-based power systems are especially vulnerable to climate. The system power capacity required under a climatic median year varies 3-fold according to demand-flexibility scenarios. For that same system to be resilient under unfavorable years, it is required an increase of up to 200-fold in storage or doubling of cross-border interconnection. A power system designed for unfavorable years requires 54% more installed capacity. Hence, future climate variability will be critical in the power systems' operation, thus pivotal to evaluate and consider in its planning.

Keywords: climate variability, power system, renewables, resilience, future electricity demand

Resumo

Para combater as alterações climáticas, muitos países têm feito esforços para promover uma transição energética. Um dos principais objetos dessa transição são os sistemas elétricos e as suas emissões, os quais têm registado rápidas e elevadas penetrações de energia renovável. Estes futuros sistemas elétricos enfrentarão novos desafios: o aumento da sua exposição ao clima (já que a maioria das energias renováveis depende deste) e a incerteza na evolução do consumo. Devido à crescente vulnerabilidade dos sistemas elétricos a estes fatores, o seu estudo carece de uma análise mais detalhada que inclua simultaneamente diferentes cenários para a produção e consumo elétricos.

O trabalho proposto pretende avaliar o impacto da variabilidade climática e de diferentes cenários de evolução do consumo elétrico em sistemas elétricos renováveis. O caso de estudo é o sistema elétrico Português em 2050. O sistema elétrico é simulado com o auxílio de uma ferramenta de modelação com resolução horária, tendo sido aplicada uma calibração multianual do modelo que é proposta e validada neste trabalho. Para analisar a variabilidade climática, consideram-se dois patamares de concentração representativos (RCP4.5 e RCP8.5, definidos pelo IPCC) para o período 2045-2055, perfazendo 473 realizações de clima possíveis. Para testar o consumo elétrico no futuro, cinco cenários de procura e flexibilidade são traçados para cada setor económico (mobilidade, residencial, serviços, indústria e agricultura) assumindo trajetórias divergentes para o consumo elétrico, armazenamento de energia e gestão da procura. O impacto da variabilidade climática na produção de energia e no consumo elétrico é analisado e quantificado, simultaneamente. Três configurações do sistema elétrico são sugeridas: duas considerando uma elevada penetração de renováveis (diferindo na disponibilidade de biomassa: atual e ilimitada) e outra 100% renovável.

A variabilidade climática afeta severamente o sistema elétrico. Neste trabalho, entre os diversos setores económicos apenas o consumo residencial foi determinado considerando a variabilidade climática. No consumo elétrico residencial anual, o impacto da variabilidade climática é mais acentuado com o aumento da eletrificação dos equipamentos de climatização, devido à resposta dos mesmos à temperatura ambiente. Este resulta numa oscilação entre -8 e +5% em torno do consumo médio.

Para além da procura de energia, a variabilidade climática afeta também outros indicadores do desempenho do sistema elétrico. O potencial desperdício (*curtailment*) de

energia varia muito acentuadamente para cenários de baixa procura, sendo que o seu valor mediano e a sua variabilidade decrescem com o aumento da eletrificação. A mediana de desperdício é de 44% para os cenários de baixo consumo e nula para os cenários de elevado consumo. A sua variabilidade (ou seja, a diferença entre o valor mínimo e máximo) oscila entre 8 e 36 p.p. para cenários de elevado e de baixo consumo, respetivamente. A interligação transfronteiriça necessária varia entre -62 e +226% em torno do valor mediano. Para cenários com elevado consumo, a fração de produção renovável oscila entre -15 a +15 p.p. em torno da mediana, enquanto as emissões de dióxido de carbono apresentam uma flutuação entre -50 e +50% em torno da mediana.

Alterando a capacidade de potência eólica e fotovoltaica do sistema, é possível observar que capacidades mais elevadas destas fontes renováveis levam a uma maior variabilidade nos indicadores de desempenho do sistema. Tomando o balanço líquido de importações num cenário de elevado consumo como exemplo, a capacidade requerida para obter um sistema com balanço nulo (ou seja, com importações e exportações anuais semelhantes) pode aumentar 25% ao mudar de um ano mediano para um ano desfavorável.

Para além da variabilidade climática, os cenários de consumo e flexibilidade são também críticos. Entre estes cenários, o consumo elétrico residencial aumenta entre 4 e 60%, sendo maioritariamente potenciado pelo aumento das necessidades de arrefecimento até 21 vezes superiores aos valores atuais. As necessidades residenciais de aquecimento apresentam uma redução de 1 a 35%. O consumo elétrico nacional total (incluindo os setores da mobilidade, residencial, serviços, indústria e agricultura) é esperado que diminua até 15% para os cenários futuros de baixo consumo e que duplique nos cenários de elevado consumo, comparando com o consumo atual.

Evoluções divergentes do consumo e flexibilidade podem implicar sérias alterações no desempenho do sistema elétrico. O desperdício de energia varia entre 10 e 61%, enquanto a interligação transfronteiriça quadruplica dos cenários de baixo consumo para os cenários de alto consumo. Entre os cenários de baixo e de elevado consumo, decréscimos até 16 p.p. e 36% são esperados para a fração de produção renovável e para as emissões de dióxido de carbono, respetivamente. Ao alterar as potências eólica e fotovoltaica, os diferentes cenários de consumo e flexibilidade divergem na sua capacidade de conseguir atingir as metas propostas. Dentro do espetro de potência testado, os cenários de baixo consumo conseguem atingir ou ficar perto das metas estabelecidas para a fração de produção renovável (perto dos 100% renovável) e da interligação necessária para

importações (abaixo dos 5 GW). Os cenários com elevado consumo tendem a apresentar um melhor desempenho em relação às emissões totais de dióxido de carbono.

Em relação à flexibilidade presente nos cenários de evolução do consumo e flexibilidade, o seu impacto no sistema elétrico varia significativamente, dependendo do indicador de desempenho do mesmo. O nível de flexibilidade não altera substancialmente a importação ou a interligação necessárias, mas pode representar uma melhoria até 2 p.p. na fração renovável.

Conclui-se que a evolução do consumo elétrico e flexibilidade resulta em grandes alterações no desempenho do sistema elétrico. Estes impactos são geralmente mais fortes do que os resultantes da variabilidade climática, o que revela o importante papel que a implementação de políticas pode ter para influenciar esta evolução do consumo. Tais medidas podem passar pela promoção da eficiência energética, novas tecnologias, melhorias no parque habitacional, etc.

Nesta tese, o desempenho de um sistema 100% renovável foi também explorado sobre diferentes condições climáticas e de consumo e flexibilidade. Para tal, considerou-se uma remoção considerável de produção despachável do sistema elétrico (centrais térmicas a gás natural), agravando a vulnerabilidade do sistema ao clima.

Os resultados mostram que num sistema projetado para um ano mediano, a capacidade de potência eólica e fotovoltaica necessária pode triplicar, considerando um cenário de baixo consumo para um de elevado consumo. Para que esse mesmo sistema elétrico seja resiliente em condições climáticas desfavoráveis, poderá ser necessário o dobro da interligação transfronteiriça. Para evitar o reforço da interligação, poderá ser necessário duplicar o armazenamento de energia presente no sistema elétrico (incluindo o armazenamento hídrico). Caso a meta de 15% de capacidade de interligação definida para a Europa para 2030 se cumpra em Portugal, não será necessário um acréscimo significativo da capacidade de armazenamento de energia. No entanto, é importante frisar que esta meta é ambiciosa e o seu cumprimento implica um grande investimento nas interligações transfronteiriças de Portugal-Espanha e Espanha-França.

Ao projetar um sistema para anos desfavoráveis (em vez do ano mediano), a capacidade de eólico e fotovoltaico necessária aumenta entre 36 e 77%, dependendo da evolução do consumo. Apresentando uma maior resiliência ao clima, este sistema assegura um balanço nulo das suas importações líquidas para climas desfavoráveis e requer uma

capacidade de interligação inferior em 2 GW à requerida num sistema planeado para o ano mediano. Um sistema mais resiliente necessita de um sobredimensionamento da capacidade instalada para que possa assegurar a viabilidade do sistema sob condições climáticas desfavoráveis. Isto leva a que o desperdício de energia seja mais expressivo, aumentando de 35% num sistema planeado para o ano mediano para 48% num sistema planeado para anos desfavoráveis.

Assim, esta tese evidencia a importância da variabilidade climática e da evolução do consumo elétrico no planeamento e desempenho de sistemas elétricos com elevada penetração de energias renováveis. Apesar de se ter focado no sistema elétrico português, os resultados qualitativos poderão ser transpostos para outras regiões com características semelhantes. Existem ainda várias oportunidades para continuar a explorar com mais detalhe esta análise, destacando-se a determinação do consumo elétrico dos serviços, indústria e agricultura considerando a variabilidade climática e a simulação do sistema elétrico com maior resolução espacial e temporal.

Palavras-chave: variabilidade climática, sistema elétrico, renováveis, resiliência, consumo elétrico futuro

Contents

Acknowledgments i
Abstract iii
Resumo v
Contents ix
List of Figures xii
List of Tables xv
Acronyms xviii
Nomenclature xx
List of Greek nomenclature xx
List of Latin nomenclature xxi
1. Introduction 1
1.1. Impacts of climate change and variability on the power system 2
1.2. Societal change 7
1.3. Research questions and general framework 10
1.4. Outline of the manuscript 12
2. Literature review 17
2.1. Electricity demand 17
2.2. Electricity supply 20
2.3. Performance of the power system 25
2.4. Energy modelling tools 30
2.5. Research opportunities 31
3. Portuguese power system 33
3.1. Case study – The Portuguese power system 33
3.2. Future projections 35
4. Power system modelling 39
4.1. General approach 39

4.2. Climate models 43
4.2.1. Representative Concentration Pathways (RCPs) scenarios 43
4.2.2. CORDEX climate models 45
4.2.3. Data processing 48
4.2.3.1. Air temperature 50
4.2.3.2. Global horizontal irradiance 53
4.2.3.3. Wind speed 58
4.2.3.4. Precipitation 61
4.2.4. Overview of future climate parameters 62
4.3. Supply and power system modelling 65
4.3.1. Energy Modelling tool - EnergyPLAN 65
4.3.2. Multiyear model calibration 69
4.3.2.1. Case study specifics 70
4.3.2.2. Methods 71
4.3.2.3. Calibration results 75
4.3.2.4. Validation 78
4.3.3. Modelling the supply sources 83
4.3.3.1. Thermal power plants 83
4.3.3.2. Photovoltaic generation 85
4.3.3.3. Wind generation 87
4.3.3.4. Hydropower and run-of-the-river generation 90
4.3.4. Future power system 94
4.4. Power system model – Demand-flexibility 99
4.4.1. Scenarios for the evolution of society 99
4.4.1.1. Mobility 100
4.4.1.2. Residential sector 109
4.4.1.3. Services, Industry and Agriculture sector 119

4.4.1.4. Energy storage – Second-life batteries 122
4.4.2. Modelling the demand sectors 124
4.4.2.1. Mobility 124
4.4.2.2. Residential sector 128
4.4.2.3. Services, Industry and Agriculture sector 134
4.4.2.4. System flexibility strategies: Demand-side management and energy storage 135
4.4.3. Summary of electricity demand-flexibility scenarios 138
4.5. CO_2 emissions 139
4.5.1. Power system 139
4.5.2. Non-electric uses of energy 140
4.6. Approach limitations 145
5. Results 149
5.1. Residential electricity demand 149
5.1.1. Sensitivity analysis 154
5.2. Highly renewables-based power system 157
5.2.1. Reference Power Systems 157
5.2.2. Solar-wind power capacity 163
5.3. Fully renewable power system 169
5.3.1. Approach 169
5.3.2. Reference Power System 171
5.3.3. Required solar-wind power capacity 173
6. Conclusions and final remarks 181
6.1. Opportunities for further research 185
References 187
Supplementary Material 203

List of Figures

Figure 3.1. Historical annual precipitation 35

Figure 4.1. Scheme of modelling the power system 41

Figure 4.2. Scheme of climate ensemble 48

Figure 4.3 Validation of the temporal downscaling – Air temperature 51

Figure 4.4. Absolute and relative errors for the temporal downscaling – Air temperature 53

Figure 4.5. Scheme of temporal downscaling of global horizontal irradiance 55

Figure 4.6. Validation of temporal downscaling – Global horizontal irradiance 56

Figure 4.7. Absolute and relative errors for the temporal downscaling – Global horizontal irradiance 57

Figure 4.8. Validation of temporal downscaling – Wind speed 60

Figure 4.9. Distributions resulting from the temporal downscaling – Wind speed 60

Figure 4.10. Absolute and relative errors for the temporal downscaling – Wind speed 61

Figure 4.11. Probability density functions of climate parameters under historical and RCPs data 63

Figure 4.12. Histograms of annual climate parameters – RCP4.5 64

Figure 4.13. Histograms of annual climate parameters – RCP8.5 64

Figure 4.14. Outline of EnergyPLAN inputs and outputs 67

Figure 4.15. Scheme for the multiyear model calibration 72

Figure 4.16. Correlation of calibration parameters and independent variables 76

Figure 4.17. Linear regression models chosen for the multiyear calibration 77

Figure 4.18. Comparison of standard and multiyear calibrations for the validation period 79

Figure 4.19. Power curve of wind turbine 88

Figure 4.20. Monthly water supply and precipitation in Portugal 91

Figure 4.21. Yearly distribution of water supply 92

Figure 4.22. Yearly distribution of run-of-the-river generation 93

Figure 4.23. Demand-flexibility scenarios 100

Figure 4.24. Driving patterns..... 106

Figure 4.25. Area and age distribution of occupied housing stock 117

Figure 4.26. Space heating and cooling..... 118

Figure 4.27. Literature on energy consumption of services, industry, and agriculture 119

Figure 4.28. Schematic of the Monte Carlo approach..... 129

Figure 4.29. Age of housing stock..... 133

Figure 4.30. Sizing of the dedicated stationary energy storage..... 137

Figure 4.31. Final energy needs for domestic hot water and cooking..... 141

Figure 4.32. CO_2 emissions and electricity demand for industry and agriculture..... 142

Figure 5.1. Residential load profiles..... 150

Figure 5.2. Residential electricity consumption per type of demand – RCP4.5..... 151

Figure 5.3. Sensitivity analysis on different housing stock development characteristics RCP4.5 – Histograms 155

Figure 5.4. Sensitivity analysis on different housing stock development characteristics RCP4.5 – Average 156

Figure 5.5. Highly renewable power systems – RCP4.5 158

Figure 5.6. Biomass consumption in highly renewable power systems – RCP4.5 160

Figure 5.7. Renewable share and CO_2 emissions from the power systems HiRES and HiRES+UB – RCP4.5 160

Figure 5.8. Total CO_2 emissions – RCP4.5 162

Figure 5.9. Annual net imports and cross-border interconnection in varying PV+Wind capacities – RCP4.5..... 164

Figure 5.10. Annual net imports and cross-border interconnection in varying PV+Wind capacities – RCP4.5..... 166

Figure 5.11. Level of resilience of the power system..... 170

Figure 5.12. General approach for the fully renewable power system..... 170

Figure 5.13. Fully renewable power system – RCP4.5 171

Figure 5.14. Biomass consumption in the fully renewable power system – RCP4.5... 173

Figure 5.15. Analysis of the required photovoltaics and onshore wind capacity in Central scenario – RCP4.5 174

Figure 5.16. Required photovoltaic and wind capacity – RCP4.5 174

Figure 5.17. Cross-border interconnection requirements – RCP4.5 175

Figure 5.18. Dedicated stationary energy storage – RCP4.5..... 177

Figure 5.19. Sensitivity analysis on the cross-border interconnection for High demand + Low flexibility – RCP4.5 178

Figure 5.20. Potential energy curtailment – RCP4.5..... 179

List of Tables

Table 2.1. Literature on the impacts of climate change and variability on demand..... 19

Table 2.2. Literature on the impacts of climate change and variability on the supply... 23

Table 2.3. Literature on the performance of power system under the impact of climate change and variability..... 29

Table 2.4. Examples of energy planning models 30

Table 3.1. Portuguese power system in 2011-2015..... 34

Table 3.2. Historical weather characteristics..... 35

Table 3.3. Literature on the future electricity demand in Portugal..... 38

Table 3.4. Literature on the future residential demand in Portugal..... 38

Table 4.1. Representative Concentration Pathways 44

Table 4.2. Three-hourly climate models..... 46

Table 4.3. Daily climate models..... 47

Table 4.4. Comparison of the temporal downscaling methods – Air temperature..... 51

Table 4.5. Temporal downscaling for daily and three-hourly data – Air temperature... 52

Table 4.6. Temporal downscaling for daily and three-hourly data – Global horizontal irradiance 57

Table 4.7. Comparison of the temporal downscaling methods – Wind speed 59

Table 4.8. Independent weather and energy variables..... 74

Table 4.9. Standard calibrations for the period 2011-2015 76

Table 4.10. Historical weather characteristics – Validation..... 78

Table 4.11. Deviations of standard and multiyear calibration for the validation period 81

Table 4.12. Photovoltaic system..... 87

Table 4.13. Photovoltaic and wind onshore power in literature..... 94

Table 4.14. Proposed high renewable penetration power system 95

Table 4.15. Future cross-border interconnection in Portugal 96

Table 4.16. Central scenario – Mobility 102

Table 4.17. Relative differences between Low and High electricity demand paths – Mobility 104

Table 4.18 Electricity demand paths – Mobility 105

Table 4.19. Relative differences between Low and High flexibility paths – Mobility 108

Table 4.20. Flexibility paths – Mobility 109

Table 4.21. Housing stock characteristics remaining constant 111

Table 4.22. Average characteristics of new dwelling as of 2017 111

Table 4.23. Central scenario – Residential sector 113

Table 4.24. Relative differences between Low and High electricity demand paths – Residential sector 115

Table 4.25. Electricity demand paths – Residential sector 116

Table 4.26. Relative differences between Low and High flexibility paths – Residential 118

Table 4.27. Flexibility paths – Residential sector 119

Table 4.28. Central scenario – Services, Industry and Agriculture 120

Table 4.29. Electricity demand paths – Services, Industry and Agriculture 121

Table 4.30. Relative differences between Low and High flexibility paths – Services, Industry and Agriculture 121

Table 4.31. Flexibility paths – Services, Industry and Agriculture 122

Table 4.32. Relative differences between Low and High flexibility paths – Second-life batteries 123

Table 4.33. Flexibility paths – Second-life batteries 123

Table 4.34. Electricity consumption and flexibility – Mobility 127

Table 4.35. Electricity demand-flexibility scenarios 138

Table 4.36. CO_2 emission factor for each type of fuel 139

Table 4.37. Efficiency of electric and natural gas systems 141

Table 4.38. Fuel consumption from freight and heavy-duty passenger vehicles 144

Table 4.39. Non-electric CO_2 emissions 144

Table 5.1. Metrics for residential electricity consumption per type of demand..... 152

Acronyms

AeV	–	Shared autonomous electric vehicle
100%RES	–	100% renewable power system
ADENE	–	Portuguese Energy Agency
APIRAC	–	Portuguese Association of the Refrigeration and Air Conditioning Industry
APREN	–	Portuguese Renewable Energy Association
BPIE	–	Buildings Performance Institute Europe
CDD	–	Cooling Degree Days
CHP	–	Combined Heat and Power
COP	–	Coefficient of Performance
CORDEX	–	Coordinated Regional Climate Downscaling Experiment
CSP	–	Concentrated Solar Power
DGEG	–	Portuguese Department of Energy and Geology
DHW	–	Domestic Hot Water
ENTSO-E	–	European Network of Transmission System Operators
EV	–	Electric Vehicles
GA	–	Genetic-algorithm
GCM	–	Global Climate Model
GDP	–	Gross Domestic Product
GHG	–	Greenhouse Gases
HDD	–	Heating Degree Days
HiDe	–	High demand
HiFlex	–	High flexibility
HiRES	–	Highly Renewable power system
HVAC	–	Heating, Ventilation, and Air Conditioning
ICE	–	Internal Combustion Engine
IDL	–	Instituto Dom Luiz
IPCC	–	Intergovernmental Panel on Climate Change
LoDe	–	Low demand
LoFlex	–	Low flexibility
MIBEL	–	Electricity Iberian Market
MY	–	Multiyear
NUTS	–	Nomenclature of Territorial Units for Statistical Purposes
PDF	–	Probability Distribution Function
PEV	–	Pure electric vehicles
PHEV	–	Plug-in hybrid electric vehicles
PP	–	Thermal Power Plant
PV	–	Photovoltaics

RCM	–	Regional Climate Model
RCP	–	Representative Concentration Pathway
REN	–	Portuguese Energy Networks
RES	–	Renewable energy sources
RNC2050	–	Portuguese Roadmap for Carbon Neutrality 2050
UB	–	Unlimited Biomass
V2G	–	Vehicle-to-Grid

Nomenclature

List of Greek nomenclature

α	–	solar altitude [rad]
$\hat{\beta}$	–	estimated coefficients of the independent variables [dimensionless]
β_{module}	–	tilt of the photovoltaic modules [º]
δ	–	declination angle [rad]
ε	–	error [depends]
η_{cables}	–	efficiency of cables [fraction]
$\eta_{inverters}$	–	efficiency of inverters [fraction]
$\eta_{PP,supply}$	–	efficiency of thermal power plants for each supply source [fraction]
η_{module}	–	efficiency of photovoltaic modules [fraction]
$\eta_{nominal}$	–	nominal efficiency of the photovoltaic modules [fraction]
η_{syst}	–	efficiency of the photovoltaic system [fraction]
$\eta_{system,supply}$	–	efficiency of residential equipment depending on the supply [fraction]
$\eta_{thermal}$	–	thermal efficiency of the photovoltaic modules [fraction]
θ_z	–	zenith angle [rad]
κ	–	(first) shape factor of Weibull and Burr distributions
λ	–	geographic longitude [rad] or scale factor of Weibull and Burr distributions [dimensionless]
λ_{zone}	–	time zone of the location [rad]
ν	–	second shape factor of Burr distribution [dimensionless]
ρ_{H_2O}	–	density of water [kg/m^3]
φ	–	geographic latitude [rad]
ψ	–	Linear thermal transmittance [Wm^{-1}K^{-1}]
ψ_{module}	–	orientation of the photovoltaic modules [º]
ω	–	hour angle [rad]
ψ	–	azimuth [rad]
ψ_a	–	real azimuth [rad]

List of Latin nomenclature

ac	–	autoregressive coefficient [dimensionless]
ACH	–	air changes per hour [ACH]
A_{floor}	–	Floor area [m^2]
$AGen_{ren}$	–	annual electricity generation of each renewable source [TWh]
$AGen_{total}$	–	annual total electricity generation [TWh]
A_i	–	Area of internal envelope [m^2]
AOI	–	angle-of-incidence of beam irradiance on a tilted surface [rad]
A_{op}	–	Area of opaque envelope [m^2]
$A_{windows}$	–	Area of windows [m^2]
B_{fleet}	–	energy capacity of the battery of one vehicle [kWh]
B_h	–	beam irradiance on the horizontal surface [W/m^2]
B_i	–	beam irradiance on a tilted surface [W/m^2]
c_{AeV}	–	specific electricity consumption for shared autonomous electric vehicle [kWh/km]
C_{DSM}	–	annual electricity demand available for demand-side management [TWh]
$C_{dumb/smart,\ fleet}$	–	total annual energy consumption for the dumb-charged or the smart charged of each fleet [TWh]
$c_{fleet,\ electric}$	–	specific electricity consumption for each fleet [kWh/km]
$c_{fleet,\ fossil\ fuel}$	–	specific fossil fuel consumption for each fleet [kWh/km]
$C_{freight,electric,\ RNC2050}$	–	electricity consumption of the freight based on the 'Roadmap for Carbon Neutrality 2050' [TWh]
c_{H2O}	–	specific heat capacity of water [$J.kg^{-1}K^{-1}$]
CO_2 emissions	–	Total CO_2 emissions [Mton]
$CO_{2electric}$	–	CO_2 emissions for the power system [Mton]
$CO_{2nonelectric,\ sector}$	–	CO_2 emissions of non-electric uses of energy for each sector [Mton]
$Cons_{fossil\ fuel,\ activity}$	–	annual consumption of fossil fuel resource for each activity [TWh]
c_{rate}	–	C-rate [h^{-1}]
C_{RoR}	–	run-of-the-river coefficient [dimensionless]
C_{sector}	–	annual electricity consumption from each sector [TWh]
d	–	julian day [day]
D_{AeV}	–	daily travelled distance per shared autonomous electric vehicle [km/day]
d_{dwell}	–	average number of occupants in one dwelling [#/dwelling]
demand	–	electricity demand in each hour [MW]

D_h	–	diffuse irradiance on the horizontal surface [W/m^2]
D_i	–	diffuse irradiance on a tilted surface [W/m^2]
D_{PEV}	–	daily travelled distance per pure electric private vehicle [km/day]
$D_{PHEV,\ electric}$	–	daily travelled distance per plug-in hybrid private electric vehicle in electric mode [km/day]
$D_{PHEV,\ fossil\ fuel}$	–	daily travelled distance per plug-in hybrid private electric vehicle in internal combustion mode [km/day]
$D_{pr.veh.,\ fossil\ fuel}$	–	daily travelled distance by light passenger private internal combustion vehicle [km/day]
E_0	–	eccentricity correction factor of earth's orbit [dimensionless]
EoT	–	equation of time [hour]
f_{corr}	–	correction factor for wind offshore generation [dimensionless]
$f_{curtailment}$	–	Fraction of potential energy curtailment [fraction]
$f_{DSM,\ sector}$	–	fraction of demand available for DSM in each sector [fraction]
fe_{fuel}	–	emission factor from fossil-fuels [kgCO_2/GJ]
f_h	–	factor to convert G_h to D_h - CLIMED2 model [dimensionless]
$f_{occupation}$	–	occupation factor of residential dwellings [fraction]
Gen_{supply}	–	generation of each supply source in each hour [MW]
$g_{gl\perp}$	–	glazed surface g-value for normal incidence [dimensionless]
G_h	–	global horizontal irradiance [W/m^2]
G_i	–	global incident irradiance on a tilted surface [W/m^2]
G_{obs}	–	observations of hourly global horizontal irradiance [ºC]
g_{shaded}	–	shading g-value for windows [dimensionless]
h	–	ceiling-to-floor height [fraction]
H_0	–	null-hypothesis
H_a	–	alternative hypothesis
h_{hub}	–	hub height [m]
$h_{near\text{-}surface}$	–	Near-surface height (10 m) [m]
h_p	–	hour where the peak of wind speed normally occurs [hour]
I	–	extraterrestrial global irradiance [W/m^2]
i	–	each calibration parameter
i_d	–	diurnal pattern strength [dimensionless]
$imports/exports_{residual}$	–	hourly imports or exports that surpass a given cross-border interconnection limit [GW]
I_{SC}	–	solar constant [W/m^2]
j	–	each year for the calibration
k	–	shape factor of the Weibull distribution [dimensionless]

K	–	number of independent variables
K_t	–	clearness index with a three-hourly or daily resolution [dimensionless]
k_t	–	clearness index with an hourly resolution [dimensionless]
l_ψ	–	length of linear thermal bridges [m]
m	–	number of calibration parameters
MAE	–	mean absolute error [depends]
MAXAD	–	maximum absolute difference [depends]
MAXRD	–	maximum relative difference [%]
min_{PPs}	–	minimum power capacity of thermal power plants [MW]
min_{stab}	–	minimum stabilization share of dispatchable generation [%]
n	–	number of years of historical data used to calibrate the model
N	–	number of observations
n_{days}	–	number of days in the year
N_{dwell}	–	number of existing dwellings
net $imp_{residual}$	–	hourly balance for net imports considering the imports/exports that surpass a given cross-border interconnection limit [GW]
N_{fleet}	–	total number of vehicles for each fleet
NMAE	–	normalized mean absolute error [%]
$N_{occupied\ dwell}$	–	number of occupied dwellings
NOCT	–	normal operating cell temperature [ºC]
NRMSE	–	normalized root mean square error [%]
OF_{max}	–	objective function for daily maximum wind speed [m/s]
OF_{mean}	–	objective function for daily mean wind speed [m/s]
$P_{2nd\ life\ bat}$	–	power capacity available for the charging/discharging of the second-life batteries [MW]
P_{DSM}	–	maximum power capacity available for demand-side management [MW]
P_{G2V}	–	total power capacity for grid-connection [MW]
pr_{mm}	–	daily or three-hourly precipitation [mm]
P_{RoR}	–	power capacity installed of each supply source [MW]
$pr_{original}$	–	daily or three-hourly precipitation in original units [$kg.m^{-2}.s^{-1}$]
PTE	–	percentage of timesteps' error [%]
P_{V2G}	–	total power capacity for grid-connection for V2G services [MW]
PV_{gen}	–	photovoltaics' generation in each hour [W/m^2]
R^2	–	determination coefficient
RMSE	–	root mean square error [depends]

$S_{dumb/smart}$	–	share of dumb or smart charged vehicles [fraction]
S_{EV}	–	share of electric vehicle's penetration on the private light passenger vehicles' fleet [fraction]
SIA_{norm}	–	normalized hourly electricity demand profile of services, industry and agriculture [dimensionless]
$S_{max\ EV\ rush}$	–	maximum share of electric vehicles driving during rush hours [fraction]
$S_{max\ fleet\ rush}$	–	maximum share of vehicles driving during rush hours for each fleet [fraction]
$S_{SOCavail.}$	–	maximum available fraction of capacity energy available for smart charging purposes [fraction]
$Storage_{2nd\ life\ bat}$	–	energy capacity of the second-life batteries [GWh]
$Storage_{smart,fleet}$	–	total capacity of electric vehicle battery storage available to smart charge for each fleet [GWh]
S_{V2G}	–	share of V2G penetration on the fleet [fraction]
t	–	hour of the year [hour]
T_{air}	–	hourly air temperature [ºC]
T_{avg}	–	average daily air temperature [ºC]
TC_{MPP}	–	temperature coefficient at the maximum point [%/ºC]
t_{day}	–	hour of the day [hour]
$T_{initial/final}$	–	initial or final temperature of water [ºC]
T_{max}	–	maximum daily air temperature [ºC]
T_{min}	–	minimum daily air temperature [ºC]
T_{module}	–	temperature of the photovoltaic modules [ºC]
T_{obs}	–	observations of hourly air temperature [ºC]
$t_{resolution}$	–	number of hours equivalent to the temporal resolution [hours]
t_{solar}	–	solar hour [hour]
$t_{step\ resolution}$	–	timestep considering temporal resolution, i.e., is the day or the three-hour timestep [hours]
U_e	–	Overall thermal transmittance of the external envelope [$Wm^{-2}K^{-1}$]
U_i	–	Overall thermal transmittance of the internal envelope [$Wm^{-2}K^{-1}$]
V_{H2O}	–	volume of hot water used per person per day [m^3]
v_{hub}	–	wind speed at the hub height [m/s]
v_{max}	–	maximum wind speed [m/s]
v_{mean}	–	mean wind speed [m/s]
$v_{near-surface}$	–	wind speed at near surface [m/s]
v_w	–	hourly wind speed generated [m/s]
v_{wobs}	–	observations of hourly wind speed [m/s]
WS	–	distribution of water supply [dimensionless]

w_{sector}	–	relative weight of each sector in the annual consumption [sector]
WS_{norm}	–	annual water supply [MWh/MW]
X	–	independent variable
Y	–	synthetized values of each downscaling method or calibration parameters [depends]
$\hat{Y}$	–	obtained values for each calibration parameter [depends]
$\hat{y}$	–	observations [depends]
z_0	–	mean roughness parameter [m]

1. Introduction

In the last decades, an aggravation of climate change has been observed, promoted by the increasing anthropogenic greenhouse gases (GHG) emissions. The first effects of climate change are noticed on the basic parameters of climate (precipitation, temperatures, etc.), leading to changes in ecosystems and also resulting in negative impacts on human life [1], [2]. Even though the impacts of climate change in the future can be significantly more serious than they are now, some of them have already been experienced, such as in water resources (e.g. sea-level rise, ocean acidification, and reduction of ice sheets) and temperature increases (both of air and ocean temperatures) [2].

To decelerate climate change, nations worldwide have been showing a strong determination to create joint policies and actions to foment a more sustainable society. A core focus of several of those strategies is related to the decarbonization of power systems, such as the shut-down of coal-fired power plants. Critical challenges arise for those future power systems on both their supply and demand dimensions. On the supply side, renewable power systems with high penetration levels of variable renewables are more vulnerable to climate due to the inconstant generation of those sources. On the demand side, the main challenge is the uncertainty in the development of electricity demand [3]. In both dimensions, technology innovation allied with socio-economic development contributes to the higher complexity of the power system, making it harder to predict. Some of the causes are the introduction of new concepts such as distributed generation, electrification of heat loads and transportation, energy management mechanisms, energy efficiency, and the smart grid [4]. As the level of complexity of the system increases, the planning and management of the power system become even more crucial.

Since climate change may impact the whole power system chain, from the supply to the demand, and also the infrastructures [5], the performance of future power systems should include the impact of climate on both supply and demand dimensions. Besides the impacts of long-term climate change, the power system has to also be prepared for extreme

weather events (such as floods, heatwaves, storms, etc.), which are becoming "*more intense, frequent and longer-lasting*" and trigger even stronger effects on the system [6].

For those reasons, climate change impacts on the electricity demand and supply must be understood in detail. This is the main motivation for this work.

Bellow, the impacts of climate change on the demand, supply, and on the performance of the power system are addressed. Then, the future evolution of society is discussed, highlighting the uncertainty on the many possible paths society may take. Next, the research questions proposed in this manuscript are introduced (section 1.3). Finally, the outline of the manuscript is presented (section 1.4).

1.1. Impacts of climate change and variability on the power system

Power system operation relies on the instantaneous balance between demand and supply, which makes the system vulnerable to their modifications and variability. Planning is a crucial phase in the system operation to guarantee its reliability, thus it should carefully consider the variability of supply sources and demand. Uncertainty also plays an important role in power systems' planning, and it should be addressed by including a vast range of possibilities for: 1) supply generation, e.g. changing the renewables' capacity factor; and 2) demand, e.g. choosing distinct levels of future demand development [3]. It should be dynamic to allow the adjustment of power systems to changes in the projection of demand and supply, enabling it to keep up with those changes.

Changes in electricity demand may lead to adjustments in the power systems to ensure they are properly prepared to fulfill it. For example, the projection of higher electricity demand in the future should promote a reinforcement of the whole power system's infrastructure from the transmission lines to the supply installed capacity.

As for supply, the large-scale renewables' integration into the power system can be a major challenge due to variability and uncertainty in the resource [3], [7]. However, improved self-sufficiency and reliability of power systems are attainable with a proper adaptation of power system's infrastructures (e.g. cross-border interconnection and transmission lines) to the increasing penetration of variable renewables [8]. Still, the projection of future power systems with a high share of renewables and the assessment

of its resilience should account for variations in the energy resource, which may be intensified by climate change [9].

Below, the main impacts of climate change and climate variability on electricity demand and supply are explored.

The **electricity demand** is not static and its typical pattern depends on different features such as geography, seasonality, building stock, culture and socio-economic parameters (activity sector, population, Gross Domestic Product (GDP), income, behavior habits, etc.) [6], [10]–[14]. Concerning climate change, the energy used for control of indoor temperature is presumably the most affected, with heating and cooling requirements either for thermal comfort purposes or for industrial processes [12], [15].

In very general terms, warming weather causes a general shift towards electricity usage increase: the heating, ventilation, and air-conditioning (HVAC) demand shifts from heating to cooling which is mostly supplied by electricity [16]. The overall impact on the actual demand depends on the extent of the changes that are strongly dependent on region and season. In warmer regions, the overall demand tends to increase because the increase of cooling needs offsets the decrease in heating needs. In contrast, in colder regions, the heating decrease has a stronger expression than the increase of cooling, which results in lowering the overall demand [15]. The same happens within seasons. As for demand peaks, those are expected to increase due to the increasing use of electricity, mostly during extreme weather events [17].

The energy mix of each region is responsible for changes in GHG emissions. For instance, a shift from fossil-based energy use towards electricity could mean more emissions within a fossil-based electricity mix, mainly due to losses on electricity transmission and generation, resulting in increased fossil fuel consumption. On the other hand, in a renewables-based electricity mix, a decrease in emissions could be possible, considering the replacement of fossil-based space heating by efficient electric devices based on clean electricity (depending on the change on heating/cooling needs of the location).

Across all sectors, the buildings' infrastructure has a significant weight on the energy demand of a region. Buildings have a long lifespan (usually, 50 to 100 years [18]), thus their largest fraction of energy consumption occurs during its operational time. The energy consumption of a building depends on location, weather, its own characteristics (construction materials), its purpose, occupation, type, etc. For instance, higher buildings

tend to have higher energy demand per inhabitant since high consumption systems like lifts and water pumps must be in place. Another example concerns office buildings, which have a large fraction of their consumption related to air-conditioning. On the other hand, an insulated building (e.g. double-glazed windows [19]) alters its cooling and heating demand compared to a less insulated building, generally, increasing the former and decreasing the latter. Besides changes in consumption, some of the impacts of climate change in buildings can be the weakening/degradation of the structure, and the degrading air quality and thermal comfort. These are due to wind speed, precipitation, humidity and temperature variability and also due to prolonged exposure to ultraviolet radiation [1]. As buildings are long-lasting infrastructures, they should be built considering climate change to avoid or mitigate some of these impacts [20].

Broadly speaking, a reduction of the overall power demand, still largely fossil-based in most parts of the world, contributes to the decreasing of GHG emissions, which decelerates climate change. To achieve that, both mitigation and adaptation measures should be applied to reduce energy needs without compromising basic comfort needs. The reduction of energy consumption in buildings can be achieved by improving buildings' characteristics (e.g. materials, insulation, shading mechanisms, etc.) and technology efficiency [16], [17]. Increasing the indoor temperature set-point during the cooling season allied with the reduction of lighting (which can often be achieved while maintaining sufficient thermal and visual comfort) and electric equipment use are two adaptation measures that reduce the cooling needs of a building without requiring investment or large alterations [21], [22]. The introduction of renewable energy generation can also reduce the ecological footprint of a building [23].

The **power system supply** is also affected by climate change in a variety of aspects. The vulnerability of the power system depends on its planning, whose quality improves when it considers the variability of the different supply sources. To ensure energy security and reliability and to avoid shortages or large curtailment of electricity, it is crucial to understand the variability of each source, both due to their own characteristics and climate change impacts.

Climate change can affect supply at two levels: the energy resources and the operation of the power plants [24]. The former regards changes on availability/variability and accessibility of resources while the latter is mainly associated with efficiency losses,

especially for thermal power plants and photovoltaics (for which ambient temperature increase is detrimental).

Renewable electricity generation depends on weather-related factors, including temperature, wind speed, and precipitation. In the context of increasing renewable energy share, forecasting of renewable generation is crucial to schedule supply [25]. Dispatchable power plants can also contribute to enabling higher renewable penetration on the energy mix by acting as a backup of its production [26], [27].

Below, the impacts of climate change and variability on most affected generation sources are addressed.

Solar generation potential depends on several factors such as irradiation, temperature and cloudiness [24]. Typically, positive changes in irradiation lead to better performance of solar electricity technologies, as opposed to increases in temperature and cloudiness. Different solar electricity technologies are differently affected by climate change. While for solar photovoltaics (PV) a decrease in efficiency is expected due to higher temperatures, the concentrated solar power (CSP) technologies are expected to decrease their generation potential with increasing cloudiness (i.e., reduction in direct irradiation) [28].

Projections for solar electricity potential are strongly dependent on the location. Generally, in regions where cloudiness increases photovoltaic generation decreases, and vice-versa. Depending on the magnitude of the changes, regions with higher irradiation might see their photovoltaics' potential unchanged because of potential increases in air temperature that affect its efficiency (aggravated with higher occurrence of heat waves) [29]. Air pollution might negatively impact solar electricity due to the higher fraction of diffuse irradiation as well as soiling of PV modules [28], [30].

Wind generation potential is highly dependent on the region, season, terrain, wind speed variability and inter-decadal variability [31]–[33]. One of the major drivers for wind speed changes and variability are the large-scale atmospheric circulation patterns [34]. It alters the typical patterns of wind power generation in several time scales from hourly to monthly [35]. Extremely low and high wind speeds lead to decreasing generation since wind turbines' operation is constrained to bottom and upper wind speed limits (cut-off limits) [36]. Wind power infrastructure may be damaged by future climate [35]. Extremely low temperatures contribute to the degradation of turbines' blades if they are

covered with ice [28]. Sea level rise and drifting sea ice (related to ice melting) might jeopardize the base foundations of both offshore and onshore coastal wind turbines [35]. Moreover, drastic changes in wind behavior (e.g. wind speed, wind direction or turbulence) might require an adjustment in the design of turbines to avoid their faster degradation and to make them better prepared for the changing weather conditions [35].

Hydropower potential is closely related to the hydrological cycle, i.e., with water availability and variability [37], [38]. The two main hydropower electricity generation infrastructures (i.e., run-of-the-rivers and dams) are differently affected by climate change. Dams (i.e., hydropower plants with storage capacity) occasionally are able to compensate dry periods with stored water in the reservoir during wet periods, whereas run-of-the-rivers show a more rigid and less dispatchable generation [38].

Hydropower plants with storage capacity are dispatchable, providing a quick response. Furthermore, hydropower plant operation is fossil-fuel free, hence its major role in power systems wherever the resource is available. Its variability and output changes are extremely important, especially if the system relies on them to ensure the supply-demand balance [26]. A decrease in hydropower reliability may jeopardize the operation of the whole system, leading it towards a stronger reliance on fossil fuel power plants, not only increasing GHG emissions but also its operational cost [37], [38].

Currently, hydropower plants are seen as one of the most important supply sources due to their reliability (higher predictability) and their dispatchable characteristics. However, its increasing variability, and other priority uses of water reservoirs such as water for local consumption or other uses (such as irrigation [24]), may lead to a change in the role it plays on the power grid balance. The improvement of water management and higher storage capacity can attenuate the effect of the hydropower variability and help to ensure energy security [26].

As for fossil fuel power plants, two main effects ought to be highlighted. First, access to some fossil fuels (such as oil and natural gas) can be promoted by climate change through ice cover melting on the Artic [5], [31]. On the other hand, coal can suffer negatively with climate change, due to the increase of floods that may difficult its quality and transportation, leading to higher prices of the raw material [5], [31]. Secondly, thermal power plants suffer efficiency losses and increase its cooling water needs as a result of temperature increase. Low water availability and higher water temperature can also

represent a serious impact on the power system since it can lead not only to efficiency losses but also to production shut-downs for safety reasons.

Still in the supply chain, extreme weather events can damage infrastructures, reduce the current-carrying capacity of transmission lines (due to hot weather) or even lead to forced generation shut-downs [5], [31], [39]. Moreover, water scarcity may also be boosted by extreme weather events like droughts.

Even though renewables are seen as pivotal to fight climate change and reduce GHGs emissions, climate change can contribute to a decrease in their reliability. However, renewable penetration is promoted through the reduced competitiveness of fossil-fueled thermal power plants, mainly caused by: 1) their lower efficiency; 2) their increasing needs for cooling water, which may contribute to their increasing cost [15]; 3) their need for fuel purchasing (as opposed to the majority of renewables, which operate at zero marginal cost); and 4) the introduction of carbon taxes. Therefore, efficient distribution of the roles and uses of each available resource of a power system should be in place to maintain an environmentally and economically sustainable power system [40].

1.2. Societal change

The assessment of the impacts of climate change on the power system should consider not only the innovation on supply technology but should also account for the evolution of energy demand. The latter will, of course, depend immensely on human habits and behavior, which might change dramatically with the development of society. Thus, the uncertainty on future trends makes the long-term future of power systems unpredictable.

Recent electrification tendencies, such as in space conditioning and transportation, can represent a significant increase in electricity demand and should be included in future demand since these technologies are expected to be part of future living standards. The replacement of internal combustion engine (ICE) vehicles by electric vehicles (EVs) is growing as global commitments for GHG emission reductions are rising. Besides creating some stabilization issues on the power system, the GHG emissions avoided compared to ICE vehicles depend on the energy mix of the system [41]. However, the shift towards renewable energy sources might enhance EVs penetration due to environmental co-benefits. Although the system reliability can be threatened by the EVs penetration, the

impacts of climate change on dispatchable power plants (e.g. hydropower) to balance the supply and demand exposes a new opportunity for EVs. The EVs' batteries can act as energy buffers (vehicle-to-grid, V2G), charging and discharging as best for the system. As the power system increases its complexity and vulnerability to climate change and new electric loads, V2G can play a key role in helping with its management.

These discussions, from the electrification of heat loads to the introduction of EVs and V2G concepts, are mainly based on technology evolution and the addition of new loads. However, the future may entail more than the replacement of already existing elements for new ones with similar functions. It will also be highly dependent on people's behavior in different aspects of their lives and their consumption trends. One important driver for societal development is the cultural factor, which may suggest different reactions to new concepts or technologies, such as the introduction of autonomous vehicles or energy efficiency in cooking [14]. As society develops, new living standards arise, and new consumption patterns appear.

One of the most recent developments in the transportation sector has been the arising of the autonomous vehicle concept. This concept may change mobility, as autonomous vehicles may present a promising mobility option by improving comfort, security and driving efficiency [42]. The implementation of autonomous vehicles decreases the need for vehicle ownership, contributing to the decrease in the total number of vehicles. It changes the current driving patterns since these vehicles would be traveling for longer hours and would be parked for fewer hours. From a societal point-of-view, they would enable a higher autonomy for people, particularly for people with reduced mobility (e.g. elderly or impaired people). The first steps introducing this concept were in Singapore, where the *NuTonomy* was the first taxi company to test the use of autonomous vehicles in a real context [43]. Other large companies, such as *Uber*, *Google,* and *Tesla*, have also been mentioned to be testing autonomous cars [43]–[46].

The sharing economy is another concept that has the potential for social and economic change, and it is already a reality with online platforms such as *Uber* or *Airbnb* [47], [48]. Exchanging services or goods in a peer-to-peer framework can provide more convenience for both sides of the market [48]. High demand impacts should be expected from the dissemination of such business models. For instance, it could lead to lower transport demand in the case of deliveries of goods – several deliveries would be done at once in the same area, avoiding the commute of each customer to and from the store. On the other

hand, a peer-to-peer energy market – where each household generates its electricity (e.g. photovoltaics) and can sell/buy to/from neighbors – may change the overall electricity demand profile. Households with different demand profiles would complement each other with bi-directional energy exchange, avoiding the energy purchase from the utility and, consequently, decreasing its supply requirements.

The urban society is also envisioned as a changing concept with the population redistribution and socio-economic development. The reorganization of future cities may result in extremely different evolution paths for society, for instance leading to a horizontal or vertical spread of housing. The former increases the need for more efficient transportation (larger road distances), thus demanding higher energy for mobility. The latter may incentivize more densely populated cities; it would reduce road vehicles' use by promoting local services and commerce, but it would also entail higher energy demand due to the need to transport both people and objects to higher floors. Those two perspectives lead to changing and considerably different demand patterns, but new materials and technology innovation in buildings and transportation could mean decreasing demand needs compared to today's requirements. In addition, the growing internet usage may promote a stronger weight of teleworking, possibly resulting in lower transportation consumption by strongly decreasing commuting.

Currently, the exodus of a large fraction of the population towards the main cities and their reorganization to increase capacity may seem a probable scenario (mostly in developing regions), but this may change soon. Society may take a step back and reorganize unused land to create new urbanistic plans by building one-floor households spread across currently unused areas instead of high-rise buildings. Society evolution is also affected by policies often implemented after tragic events driven by social pressure to make drastic changes in some societal dimensions. One example is the recent interest in policies in Portugal to incentivize the exodus towards the interior to avoid its abandonment [49], [50]; these policies were accelerated following the 2017 fires.

All of these options are open and the uncertainty on the direction that social evolution might take is vast, and it will certainly be different across the globe. However, when trying to understand the future demand evolution it is crucial to consider that the living society will evolve. It may not have the same needs that it has now and those needs may be influenced by other aspects than economic factors, population numbers or climate

change. The uncertainty of societal evolution leads to the need for including a wide range of scenarios when assessing the evolution of power systems.

1.3. Research questions and general framework

The goal of this study is to address the role of climate variability on the future power system with a high share of renewable energy sources. As we shall see in Chapter 2, upon the literature revision on the impacts of climate change and climate variability on the power system, several gaps have been identified, prompting the following research questions. The driving research question is:

1. *How resilient will a renewables-based power system be?*

High penetration of variable renewables (mostly wind and photovoltaics) significantly increases the vulnerability of the power system to climate variability (i.e., heterogeneity of possible climate realizations) challenging its performance under highly different weather conditions. In this work, the resilience of a power system is defined as its ability to cope with different climate thresholds. In order to address this issue, it is important to assess the role of climate variability on the power system, including electricity demand, supply, and balance. Raising a second research question:

2. *What is the impact of climate variability on the power system?*

A realistic discussion of the impacts of climate variability on the power system requires scenarization of social evolution, including changes in power system configuration (e.g. introduction of stationary energy storage) and behaviors (e.g. increased electric mobility or adaptation to warmer environments). An emerging research question is thus,

3. *How will the power system respond to different society evolution scenarios?*

Accurately forecasting the evolution of society is not possible. Instead, five scenarios are developed to cover possible circumstances of the future that not only includes technology evolution but also societal changes, technology and non-technology related. To design the contrasting scenarios regarding demand evolution and availability of flexible mechanisms, for each sector, a Central scenario is built considering simple assumptions for two dimensions: electricity demand magnitude and system flexibility (e.g.

demand-side management, energy storage, etc.). Four additional scenarios are created using opposing assumptions for the evolution of those two dimensions.

These research questions are explored for the case study of the Portuguese power system in 2050. This choice is justified by several factors:

- Small case study – Portugal is a relatively small country.
- Access to data – The data available was also a major factor to choose Portugal as a case study. Data describing the current Portuguese power system (such as load diagrams, installed capacities, fossil primary consumption, etc.) is free of charge and easy to obtain.
- High share of renewable energy sources (RES) – Portugal already has a high share of RES in its electricity mix, including a wide range of RES from dispatchable sources (e.g. hydropower dams) to non-dispatchable (e.g. wind, photovoltaics and run-of-the-river) generation sources.
- Vulnerability to climate change – Portugal is located in an area that will likely be severely impacted by climate change (see section 3.2).
- Prior work – The Portuguese power system has been thoroughly addressed in the literature. Several published studies have shown that high RES share can be achieved for Portugal (see section 3.2).

For this particular case study, it is interesting to explore if, considering climate variability,

4. *Can Portugal be a resilient 100% renewables-based power system by the middle of the century?*

In this work, the power system is not required to operate in an island-mode. Instead, the power system may trade energy with the outside through cross-border interconnections. The full decarbonization of the power system depends on its net imports, i.e., a power system with null net imports (the difference between annual imports and annual exports) is assumed to be decarbonized. Different power system configurations are proposed according to the level of resilience to climate variability intended.

To answer these questions, the research focused on modelling the 2050 Portuguese power system under climate variability and different demand development scenarios. The power system is simulated using an energy planning tool (EnergyPLAN [51]), which performs hourly energy balances that prioritize the use of non-dispatchable renewable sources.

Highly renewables-based electricity mixes are proposed, considering two literature-based configurations and a fully decarbonized power system.

In this thesis, the concerns of planning future power systems are addressed by considering two major factors: 1) uncertainty; and 2) variability.

First, the uncertainty in future climate triggers strong concerns for policymakers to plan future power systems, since it entails higher risks for decision-taking. For instance, long-term investments in power systems (e.g. new power plants or reinforcement of transmission lines) may be risky due to the inherent climate uncertainty that might disprove their feasibility, such as building a dam in a region that might be affected by prolonged drought. Electricity demand uncertainty also adds to these concerns. Increasing demand might be expected and used to plan the power system but it may not be materialized. To mitigate the risk of decision-taking and consider several possible paths for climate, an ensemble of several climate models is used based on two representative concentration pathways: RCP4.5 and RCP8.5. As for electricity demand, five scenarios are built, aiming at representing different realities regarding the level of electricity demand and availability of mechanisms that provide demand and supply flexibility (e.g. demand-side management and energy storage).

Secondly, with increasing renewable penetration, the performance of power systems is more dependent on climate variability, since renewables-based systems are more vulnerable to weather (e.g. occurrence of wet, dry or windy weather conditions). Thus, instead of using a single year realization for each climate model, a period of eleven years (2045-2055) was used to extend the spectrum of climate realizations tested.

1.4. Outline of the manuscript

This manuscript is structured as follows. In Chapter 2, a summary of the literature review on the impacts of climate change and variability on the power system is provided, along with the research opportunities rising from literature gaps. Chapter 3 describes the case study today and provides a contextualization of existing literature on it. Chapter 4 presents all the methods applied and the assumptions used to model the power system and to create the demand-flexibility scenarios. Chapter 5 provides the results of the different layers of this work, showing the impacts of climate variability on the residential electricity demand,

the performance of the highly renewable power systems and the 100% renewable power system. Finally, Chapter 6 summarizes the conclusions and provides opportunities for further research.

This thesis has resulted in some original scientific publications in international peer-reviewed journals and oral presentations in international conferences, as follows in chronological order:

International peer-reviewed journals

- **R. Figueiredo**, P. Nunes, and M. C. Brito, "Multiyear calibration of simulations of energy systems," Energy, vol. 157, pp. 932–939, Aug. 2018. doi: 10.1016/j.energy.2018.05.188
- **R. Figueiredo**, P. Nunes, M. J. N. O. Panão, and M. C. Brito, "Country residential building stock electricity demand in future climate – Portuguese case study," Energy Build., vol. 209, 2020. doi: 10.1016/j.enbuild.2019.109694
- **Figueiredo, R.**, P. Nunes, M. C. Brito, **"**Resilience of a decarbonized power system to climate variability," 2020. **[under review in Applied Energy Journal]**

Conferences

- **R. Figueiredo**, P. Nunes, and M. C. Brito, "The role of climate variability on the assessment of roadmaps for power systems with high renewable penetration," Oral presentation/paper at *8th Solar Integration Workshop*, Stockholm, Sweden, 2018.
- **R. Figueiredo**, P. Nunes, M. J. N. O. Panão, and M. C. Brito, "Residential energy demand in a changing climate: Portuguese case study 2050," Oral presentation at *European Climate Change and Adaptation conference*, Lisbon, Portugal, 2019.

During the course of this research work, other authored or co-authored scientific papers and proceedings were also published:

International peer-reviewed journals

- P. Nunes, **R. Figueiredo**, and M. C. Brito, "The use of parking lots to solar-charge electric vehicles," *Renewable Sustainable Energy Reviews*, vol. 66, pp. 679–693, 2016. doi: 10.1016/j.rser.2016.08.015

- **R. Figueiredo**, P. Nunes, and M. C. Brito, "The feasibility of solar parking lots for electric vehicles," *Energy*, vol. 140, pp. 1182–1197, 2017. doi: 10.1016/j.energy.2017.09.024
- Â. Casaleiro, **R. Figueiredo**, D. Neves, M. C. Brito, and C. A. Silva, "Optimization of photovoltaic self-consumption using domestic hot water systems," *Journal Sustainable Development of Energy, Water and Environmental Systems*, vol. 6, pp. 291–304, 2018. doi: 10.13044/j.sdewes.d5.0178
- **R. Figueiredo**, P. Nunes, M. Meireles, M. Madaleno, and M. C. Brito, "Replacing coal-fired power plants by photovoltaics in the Portuguese electricity system," *Journal of Cleaner Production*, vol. 222, pp. 129–142, Jun. 2019. doi: 10.1016/j.jclepro.2019.02.217

Other publications

- **R. Figueiredo**, P. Nunes, and M. C. Brito, "The feasibility of solar parking lots for electric vehicles," Oral presentation/Poster at 2nd Annual Conference RedeMOV, Lisbon, Portugal, 2017.
- **R. Figueiredo**, P. Nunes, and M. C. Brito, "The feasibility of solar parking lots for electric vehicles," Poster at Encontro com a Ciência e Tecnologia 2017, Lisbon, Portugal, 2017.
- **R. Figueiredo**, P. Nunes, and M. C. Brito, "Simulation of power systems: proposal of an enhanced validation procedure," Poster at Encontro com a Ciência e Tecnologia 2018, Lisbon, Portugal, 2018.
- **R. Figueiredo**, P. Nunes, and M. C. Brito, "Simulation of power systems: proposal of an enhanced validation procedure," Poster at MIT Portugal 2018 Annual Conference, Lisbon, Portugal, 2018.
- **R. Figueiredo**, P. Nunes, and M. C. Brito, "On the Impacts of Removing Coal from the Portuguese Power System," *Proceedings of the 3rd APEEN & 5th ME3*, Braga, Portugal, 2019. doi: 10.21814/uminho.ed.3
- **R. Figueiredo**, P. Nunes, and M. C. Brito, "Residential market of heat pumps: present and future (in Portuguese)," *O Instalador*, Lisbon, Portugal, 2019.
- **R. Figueiredo**, P. Nunes, P. Soares, M.C. Brito, "The performance of a highly renewable-based power system in a changing climate - Portuguese case study," Oral presentation at IDL Annual Conference, Lisbon, Portugal, 2019.

- **R. Figueiredo**, P. Nunes, and M. C. Brito, "Future renewable-based power system under climate variability," Poster at MIT Portugal 2019 Annual Conference, Ponta Delgada (Azores), Portugal, 2019.

2. Literature review

In this chapter, a review of the existing literature on the impacts of climate change and variability on the power system is provided. The focus is given to the impacts of electricity demand (section 2.1) and supply (section 2.2) to highlight the challenges to be faced by future power systems (section 2.3). A brief revision of the main energy modelling tools is presented (section 2.4). A summary of some of the opportunities for future research that were found to be limitations of the current studies is presented at the end of this chapter (section 2.5).

2.1. Electricity demand

Even though the scientific community has done an effort to uniformize the assumptions made in climate impact studies (for example, by creating the RCPs), there are still several issues that make the studies hard to compare. In the specific case of the impacts of climate change on energy demand, those are strongly dependent on the region and socio-economic context. Also, the type of parameter that is used to measure such impacts varies significantly among the current literature. For these reasons, the comparison of results among climate impact studies might be challenging. Nevertheless, those impacts have been exhaustively explored in the literature.

Some literature can be found addressing the impact of climate change in all activity sectors. Usually, those studies explore the dependency of future electricity demand from socio-economic variables and climate separately. For example, Ahmed at al. [13] do it for the period 2040-2100 in Australia, while van Ruijven et al. [12] and Cian and Wing [52] cover all the globe for the year 2050. Other studies address more than one activity sector, such as Burillo et al. [17] that use two climate paths for 2040-2060 to understand the increase in peak electricity demand in Los Angeles, USA; and Dowling [15] who use Europe in 2050 as a case study to conclude about the changes on the energy system

performance. However, most studies addressing the impact of climate change on demand focus on a specific activity sector: Berger et al. [53] evaluate the changes in heating and cooling demand of service buildings in Austria in 2050, while Tettey et al. [16] explore climate impacts given different residential building design in Sweden in the decade of 2050 and 2090.

According to Apadula et al. [6], the methods used should be chosen according to time-horizon and data availability, to accurately assess the impacts of climate change on electricity demand. Among the gathered literature, the most common methods applied to determine electricity demand in the future use parametric, energy balance and degree-day models (HDD and CDD for heating and cooling degree days, respectively)[1]. Also, the majority of the studies consider the representative concentration pathways (RCPs) defined by the Intergovernmental Panel on Climate Change (IPCC).

The impacts of climate change throughout the globe are different between regions. The changes in electricity consumption, for example, are dependent on how climate changes in a given region but also on its socio-economic conditions, presently and in the future. For the sake of comprehensiveness, Table 2.1 shows some studies addressing the impact of climate change on the demand for several regions and with different focuses. The general trends are an increase in cooling demand and a decrease in heating demand.

[1] In this work, the residential electricity demand is explored in greater detail using a Monte Carlo-based approach from Panão and Brito [203], which is presented in subsection 4.4.

Table 2.1. Literature on the impacts of climate change and variability on demand
Summary of characteristics of reviewed literature on the impact of climate change and variability on the demand side of the power system (ordered by sectors and alphabetic order).

Literature	Geographic scope	Sector	Model type (demand)	Climate (IPCC scenarios)	Parameter analyzed	Results			
						2030-2040	2050-2060	2070-2080	2090-2100
Ahmed et al. [13]	Australia	Residential, commercial, industrial and agriculture	HDD and CDD; regression model	- (linear trend from historical data)	Electricity	-1% to +2%	-2% to +5%		-4% to +11%
Cian and Wing [52]	Global	Residential, commercial, industry, agriculture and transportation	econometric model	RCP4.5 RCP8.5	Heating		-4 to -3%		
					Cooling		+10 to +19%		
					Total demand		+7 to +17%		
van Ruijven et al. [12]	Global	Residential, commercial, industry and agriculture	econometric model	RCP4.5 RCP8.5	Total demand		+11 to +58%		
Burillo et al. [17]	USA	Commercial and residential	building simulation	RCP4.5 RCP8.5	Peak electricity	-4 to +31%	+2 to +51%		
Dowling [15]	Europe	Commercial and residential	HDD and CDD; partial equilibrium simulation	A1B E1B	Heating	-14% to -9%	-19% to -9%		
					Cooling	+14 to +53%	+41 to +85%		
Berger et al. [53]	Austria	Commercial	building simulation	A1B	Heating		-56% to -11%		
Sabunas and Kanapickas [54]	Lithuania	Residential	building simulation	RCP2.6 RCP8.5	Total demand		-19 to -9%	-30 to -15%	
Tettey et al. [16]	Sweden	Residential	building simulation	RCP2.6 RCP4.5 RCP8.5	Heating (RCP4.5)		-25 to -20%		-26 to -20%
					Cooling (RCP4.5)		+14 to +39%		+30 to +102%
					Total demand (all RCPs)		-4 to -0.3%		-3 to -0.1%
Wang et al. [55]	Switzerland	Residential	building simulation	RCP4.5 RCP8.5	Heating	-22 to -1%	-46 to -4%		
					Total demand	-33 to -17%	-51 to -25%		
Yi and Peng [56]	Seoul	Residential	parametric model	RCP4.5 RCP8.5	Peak electricity		+6 to +96%		

2.2. Electricity supply

The power system supply is affected by climate change and variability, moreover when future renewables-based power systems are considered. This issue has been thoroughly studied in the literature.

Literature reviews on the impacts of climate change on power systems supply, such as those of Solaun and Cerdá [28] and Cronin et al. [57], highlight the discrepancies on regional coverage (with Europe as the most studied region) and the predominance of studies on wind and hydro resources.

The impact of future climate on solar electricity potential has been studied for several locations. According to Jerez et al. [29], Ravestein et al. [34] and Müller et al. [58], climate change is not expected to significantly affect the solar electricity potential in Europe, especially in the Iberian Peninsula, as efficiency losses are outweighed by the increase on the solar resource. For Africa, Soares et al. [59] studied the potential of both photovoltaics and concentrated solar power (CSP) and found that PV potential would be unequally affected by climate showing pronounced increases in southern Africa, including Angola and Mozambique, but decreasing potential in parts of northern Africa. Wild et al. [30] expects a general increase in CSP potential across the globe in 2050. To address such impacts on the solar potential, the studies usually apply mathematical models that use irradiance and air temperature or use directly specific tools to calculate PV generation [9].

Extensive literature on the future wind power potential can be found for Europe. Ravestein et al. [34] explore the effect of climate change and climate variability on wind and photovoltaics in 2050 in Europe. They found that the impact of climate change in wind power is weaker than that of climate variability (triggered by changes in large-scale atmospheric circulation), which is responsible for a variation of up to 20-30% in renewable generation (enhanced by the changes in wind power). Karnauskas et al. [60] explore the potential changes in wind power across the globe up to 2100, showing a great spatial discrepancy of results. While at the north of the Equator, the study projects decreasing wind generation potential in the middle latitudes, at the Southern tropics it is expected to increase. As for offshore wind, Soares et al. [61] expect a small decrease in offshore wind generation for Iberia, except in summer. The methods applied to assess

wind power potential are mainly based on global climate models for future projections, often converting wind speed to wind generation using wind turbine models on the chosen turbine height [9], [60], [61].

The main impact of climate change on hydropower is precisely its increased variability [37], [38], [62]. Climate change impacts on hydropower resources are extremely site-dependent. Due to its critical role in power systems, future hydropower generation has also been the focus of several pieces of research. Studies focusing on the consequences of hydropower alterations for the power system performance found that increased dispatchable capacity is required to cope with the higher variability and uncertainty on hydropower generation. Such is concluded by Carvajal et al. [38], who explore the impact of different hydropower policies for the 2050 power system in Ecuador, and by Tarroja et al. [37] that studies the impact of hydropower changes on the power system from California, USA, in 2050. According to Teotónio et al. [63], exploring the consequences of future water availability in the Portuguese power system, hydropower generation will be impaired due to a more pronounced variability of precipitation caused by higher extremes of weather conditions (more accentuated droughts and stronger precipitation periods). Focusing on revenues from hydropower plants, Mendes et al. [64] study the impact of climate change in the Amazon, concluding that changes in river flows will result in fewer revenues in 2050, continuing to decline until 2100. Hydropower potential is commonly addressed through simulation models of hydropower plant operation or hydrological models [9], [37], [38].

As highlighted in Chapter 1, thermal power generation may suffer decreases in efficiency and shut-downs (for safety), due to water scarcity and increased water temperatures. This is supported by two studies for the mid-century in the USA addressing the thermal power plants' response to climate changes: the work of Miara et al. [65] and Liu et al. [66]. It is noteworthy to mention that this applies to all thermal power plants; those based on the combustion of fossil-based but also those based on other resources, such as nuclear or biomass. The operation of thermal power plants under climate change is assessed using specific thermal generation models and often considering water use models and hydrological models [9].

To assess the impacts of climate change on the supply side of the power system, several works are presented in Table 2.2, which differ on multiple dimensions. Time-horizon and regions are some of the most important factors that differ among the studies. Different

levels of complexity can be found across the literature, namely on the use of climate data [9]: whereas some authors base their work directly on the climate data, others feed these data to other models (e.g. economic, emission or energy planning simulation models) to explore the impacts on different background areas. Resource projects are generally addressed using Global Climate Models (GCMs) or Regional Climate Models (RCMs). Most of the studies use the representative concentration pathways defined by the IPCC.

Table 2.2. Literature on the impacts of climate change and variability on the supply
Summary of characteristics of reviewed literature on the impact of climate change and variability on the supply side of the power system (ordered by resource and alphabetic order).

Literature	Resource	Geographic scope	Model type (generation)	Climate (IPCC scenarios)	Parameter analyzed	Results	
						2050-2060	2070-2100
Carvajal et al. [38]	Hydro	Ecuador	hydrological model energy system simulation model	RCP4.5	Energy generation	-44 to +21%	
Tarroja et al. [37]	Hydro	USA	hydrological model grid dispatch model	RCP8.5	Energy generation	-20 to +15%	
Teotónio et al. [63]	Hydro	Portugal	hydrological model energy system simulation model	SRES A2c SRES B2a RCP4.5 RCP8.5	Energy generation	-17 to -41%	
Liu et al. [66]	Thermal	USA	hydrological-thermoelectric generation model	RCP4.5 RCP8.5	Available capacity	-12 to -2%	
Miara et al. [65]	Thermal	USA	hydrological-thermoelectric generation model	RCP2.6 RCP8.5	Available capacity (RCP8.5)	-31 to +6%	
Jerez et al. [29]	Solar (PV)	Europe	mathematical model	RCP4.5 RCP8.5	Energy generation		-12% to -3%
					Energy potential		-14% to +2%
Müller et al. [58]	Solar (PV)	Europe	mathematical model	RCP4.5 RCP8.5	Energy generation	-6 to +3%	
Soares et al. [59]	Solar (CSP and PV)	Africa	empirical model	RCP4.5 RCP8.5	CSP generation	-5 to +5%	
					PV generation	-3 to -2%	
Wild et al. [30]	Solar (CSP)	Global	empirical model	RCP8.5	CSP generation	-24 to +14%	
Karnauskas et al. [60]	Wind	Global	turbine power curve	RCP4.5 RCP8.5	Energy generation	-25 to +40%	-40 to +40%
Soares et al. [61]	Wind offshore	Iberia	turbine power curve	RCP4.5 RCP8.5	Power density		-10 to +5%

2.3. Performance of the power system

The performance of the power system may experience different consequences from a changing climate and climate variability. According to Ravestein et al. [34], climate variability represents a serious challenge for the performance of power systems, often affecting it more critically than climate change general trends. Nevertheless, they claim that both climate change trends and climate variability should be studied simultaneously, arguing that a power system prepared to face climate variability will be able to cope with general climate change.

Most of the reviewed studies focus on either the supply or demand side of the power system. The individual impacts of climate change and variability on these two sides are decisive to understand possible adaptation or mitigation measures. However, the performance of the power system under such impacts should be also addressed.

Commonly, works on the impact of climate change and variability on the performance of power systems focus also on the supply side. Within those, there are studies considering the climate impacts in only **one supply source**.

Considering solely wind variability, Weber et al. [67] focus on wind-based power systems to explore the requirements for backup and storage in the middle and end of the 21st century. Their results show that both backup and storage needs tend to increase in most of Europe by up to 24% (except in the South-Eastern and Baltic), due to potential longer periods of low wind generation and increased seasonal variability. Also focusing on wind generation changes, Rosende et al. [68] compare the optimization of the power system in Chile in the end-century considering a future with and without the influence of climate change. Under climate change, a higher decarbonized power system is achieved, with wind and solar additional capacities increasing up to 9% and natural gas decreasing up to 79%. Hydropower potential and uncertainty are the core focus of Guerra et al. [69], whose work aims at optimizing a power system in Colombia up to 2030. A decrease of up to 17% in hydro potential was found. It was also concluded that hydropower uncertainty was responsible for 79% of the variance in total system cost.

There are also studies focusing on the impact of climate change and variability in power systems that consider the impacts on **two supply sources**.

Zeyringer et al. [70] optimize the 2050 Great Britain power system with high renewable share and address climate variability by using different time-horizons of climate variability. It is found that planning using a shorter period would likely lead to an unfeasible power system under different weather conditions, while planning considering a longer period would lead to a more robust system but with overall higher emissions and costs. For Texas, Craig et al. [71] study the power system in the mid-21st century, finding that emissions could decrease up to 2% due to climate change. Such a result is achieved by the increase in wind and solar generation up to 3% combined with a decrease up to 7% in fossil and nuclear generation. Climate variability in the 2030 European power system is the focus of Collins et al. [72], whose work uses 30 years of historical data. The increasing introduction of variable renewables in the power system is found to significantly affect the performance of the European power system, with the inter-annual variability increasing 5-fold for the CO_2 emissions and total costs. Addressing the impact of climate change and variability in hydropower and thermal power plants, van Vliet et al. [73] explore the vulnerability of such supply sources in the middle and end of the 21st century worldwide. It is found that a higher fraction of the world's thermal power plants will be severely affected compared to hydropower. Moreover, thermal generation will be more affected by climate change than hydropower, potentially decreasing 7-12% of its capacity, compared to 1.2-3.6% for hydro.

Since the most important feature of the power system is the supply-demand balance, the overall consequences due to the simultaneous impacts of climate change on supply and demand should be further addressed [9]. Below, works focusing on the performance of the power system under the combined impact of climate change and variability on the **demand and supply-side** are summarized.

The impact of climate change and variability in Europe at the end of the 21st century is commonly addressed in the literature. Kozarcanin et al. [27] optimize wind-photovoltaic capacity to minimize dispatchable generation. Higher wind penetration does it but further exposes the system increasing 20% of the dispatchable generation requirements. Peter [74] compare the consequences of planning a power system neglecting climate change and considering climate change impacts on demand and all supply sources. While neglecting climate change shows 12% higher system costs (fuel costs and carbon permits), using it enables less expensive power systems with higher wind offshore

capacity to compensate for the reduction energy potential of wind onshore, solar and nuclear power plants (due to decreasing cooling water availability).

System costs are usually used in works to understand the economic feasibility of future power systems. Perera et al. [75] test different scenarios of demand and supply to optimize an energy-hub in Sweden for the end of the 21st century. The system cost is severely affected by limit conditions: overly high demand leads to an investment increase of up to 33%, while considering exceptionally high renewable energy generation potential may decrease the investment by up to 7%. Combining demand and weather extremes may require an investment increase by up to 25%. Emodi et al. [76] focus on the development of the 2050 Australian energy system under several policy strategies. Almost all scenarios lead to the decrease of fossil generation (mostly coal), while a strong increase in wind and solar penetration is observed. To plan an adequate power system, the authors stress the importance of considering climate change. Climate variability is also addressed in the work of Bloomfield et al. [77], who test the 2050 Great Britain power system in the mid-21st century. Even at current wind levels, climate variability significantly affects the power system: baseload generation decreases with the introduction of wind power, but its variability increases 11-fold; as for peak generation, it increases 46% and its variability range increases 30%.

Besides considering the climate impact on different supply sources (and on the demand), there are several other characteristics that differ between studies working on the performance of future power systems.

Time-horizon is one of them. The majority of the works point to the mid-21st century [70], [71], [76] and to the end of the 21st century [27], [74], [75], while others extend the work to several periods along the century [67], [68], [73]. Temporal resolution is also at most importance to address supply-demand balance in planning highly renewable power systems. The disregarding of renewable generation variability may underrate its curtailment, providing misleading results for decision-makers that may jeopardize renewable and emission targets achievement [78], [79]. Thus, a minimum of one-hour resolution should be considered. Several studies still use lower temporal resolutions: 3 to 4 hours are used in Refs. [27], [67], [68]; one day is used in Ref. [73]; and annual resolutions are considered in Refs. [69], [76].

Regarding climate data, some studies make use of historical data to simulate climate variability [70], [72], [77]. Others use data from global/regional climate models under

different IPCC scenarios. Usually, at least two RCPs are used (e.g. Refs. [67], [73], [75], [76] for two RCP and Refs. [27], [68], [69] for three or four RCPs), with some studies using solely one RCP [71], [74]. While some studies average an ensemble of climate models (discarding their divergent characteristics), Cronin et al. [57] propose the use of all the heterogeneity of an ensemble of climate models to address climate uncertainty.

To address the performance of power systems, several strategies may be applied using different indicators (e.g. installed power capacity, electricity generation, cross-border interconnection, energy curtailment, system costs, emissions, etc.). Most of the studies focus on the power and generation capacity and system costs (including investment and operation costs). Some also include the requirement for energy storage technologies and for cross-border interconnection [27], [67], [70] or potential energy curtailment needs [71], [72], [77].

Fully decarbonized power systems are often missing in the literature considering the impacts of climate change and variability on the power system. From the gathered literature, only Weber et al. [67] considers it. Finally, according to McCollum et al. [80], works focusing the future of energy systems tend to trace safe scenarios (including scenarios on demand, climate, demographics, etc.) based in well-known or widely accepted assumptions, disregarding extreme cases that may provide a whole new perspective over the object of study.

Table 2.3 summarizes the main characteristics of power systems addressing the performance of power systems under climate change and variability.

Table 2.3. Literature on the performance of power system under the impact of climate change and variability
Summary of characteristics of reviewed literature on the impact of climate change and variability on the power system (ordered by number and type of supply sources/demand impacted by climate and alphabetic order).

Literature	Geographic scope	Timestep	Time-horizon			Climate					Climate impact					Main indicators of performance									100% RES
							IPCC scenarios					Supply				Power capacity or energy							Others		
			Up to 2040	2040-2070	2070-2100	Historical data	RCP2.6	RCP4.5	RCP6.0	RCP8.5	Demand	Wind	Photovoltaics	Hydro	Thermal	Total capacity	Total generation	Dispatch./Backup	Var. renewables	Storage	Transmission	Curtailment	System/elect. cost	GHG emissions	
Rosende et al. [68]	Chile	4 hours	x	x	x			x	x	x		x				x		x	x		x		x		-
Weber et al. [67]	Europe	3 hours	x	x	x			x		x		x						x	x	x					x
Guerra et al. [69]	Colombia	annual	x				x	x	x	x				x		x	x	x	x				x		-
Collins et al. [72]	European	1 hour	x			x						x	x				x	x	x		x	x	x	x	-
Craig et al. [71]	Texas, USA	1 hour		x						x		x	x				x	x	x			x	x	x	-
Zeyringer et al. [70]	Great Britain	1 hour		x		x						x	x			x		x	x	x	x		x	x	-
van Vliet et al. [73]	Global	daily	x	x	x		x			x				x	x	x		x							-
Bloomfield et al. [77]	Great Britain	1 hour	x			x					x	x				x	x	x	x			x			-
Kozarcanin et al. [27]	Europe	3 hours			x		x	x		x	x	x	x			x		x		x	x				-
Perera et al. [75]	Lund, Sweden	1 hour			x			x		x	x	x	x								x		x		-
Emodi et al. [76]	Australia	annual		x				x		x	x	x	x		x	x	x	x	x		x		x	x	-
Peter [74]	Europe	1 hour			x					x	x	x	x	x	x	x	x	x	x				x		-

2.4. Energy modelling tools[2]

Planning and testing possible changes in the system can be addressed by modelling power system scenarios. A variety of methods and simulation tools are available, which recently have been reviewed. Debnath and Mourshed [81] summarized the methods used in energy planning tools. Collins et al. [82] reviewed different methodologies, using energy models, and analyzed their capability of considering short-term variations on the power system. Connolly et al. [83] reviewed modelling tools, presenting a thorough description of the characteristics of each one. A more recent review of energy models was made by Liu et al. [84], focusing on the challenges of modelling isolated regions.

Examples of tools that can be used to model energy systems are the MARKAL/TIMES [85], HOMER [86], LEAP [87], and EnergyPLAN [51]. Those present differ in the approach, e.g. bottom-up or top-down, and features and scope, e.g. timestep resolution and horizon and geographic scope. Table 2.4 presents the most representative energy modelling tools and some of their most relevant features.

Table 2.4. Examples of energy planning models
Summary of examples and features of energy models, including geographic scope, temporal resolution, and time-horizon.

	Geographic scope	Timestep	Time-horizon
BALMOREL [88]	International	Hourly	Max. of 50 years
EnergyPLAN [51]	National/ regional	Hourly	1 year
energyPRO [89]	Regional/Several locations	Minute	Max. of 40 years
HOMER [86]	Local	Minute	1 year
LEAP [87]	Global/National/ Regional/Local	Yearly	No limit
MARKAL/TIMES [85]	National/ regional	User defined	Max. 50 years
PLEXOS [90]	International	Hourly to minute	Max. of 10 years
RETScreen [91]	User defined	Monthly	Max. 50 years
WILMAR [92]	International	Hourly	1 year

[2] Adapted from Figueiredo et al., 2018 [224].

2.5. Research opportunities

The assessment of climate change impacts on the power system is not trivial. There are plenty of factors that contribute to the complexity of concluding these impacts. Comparable work is difficult to find because the impacts of climate change and variability on demand, supply or the performance of the power system (examples can be found in Table 2.1, Table 2.2 and Table 2.3) depend not only on the characteristics of each case study (e.g. region, activity sector, resource, energy mix, etc.) but also on the methods used (e.g. period, scenarios, models, assumptions, etc.).

Despite the difficulty in comparing studies, below, some of the main identified weaknesses in the literature are highlighted with the intent of summarizing research opportunities (see section 2.3, Table 2.3).

- Climate variability and uncertainty: One of the main drivers for the uncertainty in future power systems is the shift of power systems' operation from being based on dispatchable generation (e.g. fossil generation) to being based on weather-dependent generation (mainly variable renewables such as wind and solar). This makes future power systems highly dependent on climate variability. An increasing number of studies have been stressing the need for the introduction of climate variability on the planning of power systems to ensure their feasibility under a wide range of climate conditions [70], [72], [75], [76]. Recently, the literature on climate variability has been increasing. However, studies should draw more attention to it to better assess changes in generation, especially for variable renewables [24]. Climate variability should also be addressed within different scale periods, considering not only seasonality but also inter-annual and inter-decadal variations [9], [32], [93].
- Geographic scope: Many works simulate large regions (such as Europe or the world) leading to a broad conclusion for the region but lacking detailed information about the impacts on specific locations. Therefore, more detailed and specific studies are missing in the literature, so more work could focus on small scale case studies [9] to provide insightful information for policymakers to foment actions or policy implementation at a national/regional level.

- Temporal resolution of power system modelling: The modelling of power systems should consider at least an hourly resolution to better simulate the supply-demand balance, as in [70]–[72], [74], [77].
- Climate data: Some studies still use historical data to address climate variability. Instead, the consensually accepted IPCC scenarios under global/regional climate models to simulate future climate should be preferred. To emphasize the impact of variability and conclude about possible solutions to ensure a feasible power system (e.g. energy storage), a finer time-resolution (at least, hourly) should be applied both to the energy generation and power system modelling [24].
- Impact on supply sources: Most studies focus on a single supply source. Instead, further work should focus on the impacts of climate change and variability on more than one generation source.
- Future electricity demand: Future works should focus on the creation and simulation of scenarios that may help to envision how societal changes would affect the power systems' operation. In this regard, the studies on the impacts of climate change should be more quantitative and should consider different scenarios, not only concerning emissions but also socio-economic trends [1], [94].
- Combined impacts on electricity supply and demand: Rather than considering the impact of climate change and variability only partially, studies must include the combined consequences in all the supply sources as well as in the electricity demand [57].
- Fully decarbonized power systems: With the urgency to fight climate change, more studies on the modelling of future power systems must consider its full decarbonization, where higher importance should be given to variability in variable renewables' generation [24].
- Extreme conditions: There is still a lack of literature that aims at exploring extreme conditions for all the dimensions of their energy system's scientific work [80]. Those could be materialized in extreme scenarios for both demand projections or climate extremes.

3. Portuguese power system

This chapter aims to contextualize the case study used in this research – the Portuguese power system. A brief description of the current power system is provided (section 3.1), followed by a summary of the existing literature focusing on the future of the Portuguese power system (section 3.2).

3.1. Case study – The Portuguese power system[3]

During the last decade, the share of renewable energy has increased in the Portuguese power system. Focusing on the period 2011-2015 (the latest available data at the time of the analysis), the electricity demand was on average 49 TWh/year, 51% renewable – hydro (23.2%), wind (21.3%), biomass (5.5%) and photovoltaics (1%). Thermal power plants are mostly of condensing type (from coal, natural gas, biomass, and other non-renewables) but CHP (coming from natural gas, biomass, and other non-renewable fuels) are also part of the supply sources – mostly from industry, in which the heat produced is locally used.

The installed capacities of the Portuguese electricity mix are presented in Table 3.1.

[3] Part of this section was adapted from Figueiredo et al., 2018 [224].

Table 3.1. Portuguese power system in 2011-2015
Electricity demand and power plants installed capacity in the Portuguese power system between 2011 and 2015 [95], [96].

Portuguese power system					
Electricity demand [TWh]		49.1-50.6			
		Installed capacity [MW]			
Renewable power plants (excl. biomass)	Wind	4,081-4,826			
	Photovoltaic	155-429			
	Run-of-the-river	2,993-3,010			
	Dam hydro	2,397-3,136			
	Hydro pump	1,038-1,618			
	Large hydro storage cap. [GWh]	3,060-3,100			
		Installed capacity [MW]		Combined efficiency [%]	
		Condensing power plants	Industrial CHP	Condensing power plants	Industrial CHP
Thermal power plants	Coal	1,756	-	32.5-38.7	20.4-21.6
	Natural gas	3,829	858-929		
	Biomass	255-276	342-353		
	Other non-renewables	1,821-13[a]	407-52		

[a] Mainly fuel-oil based power plants that have been withdrawn from the power plants' fleet recently.

The only electricity interconnections are across the border with Spain, whose energy trades are market-driven through a ruled Iberian market (called MIBEL).

The Portuguese power system is highly sensitive to meteorological conditions due to the high share of renewables, in particular hydropower. A critical parameter for the performance of the system is the precipitation level: for years with high precipitation, the Portuguese system tends to be much less dependent on fossil fuels, while low precipitation levels lead to higher dependence on those supply sources, Figure 3.1.

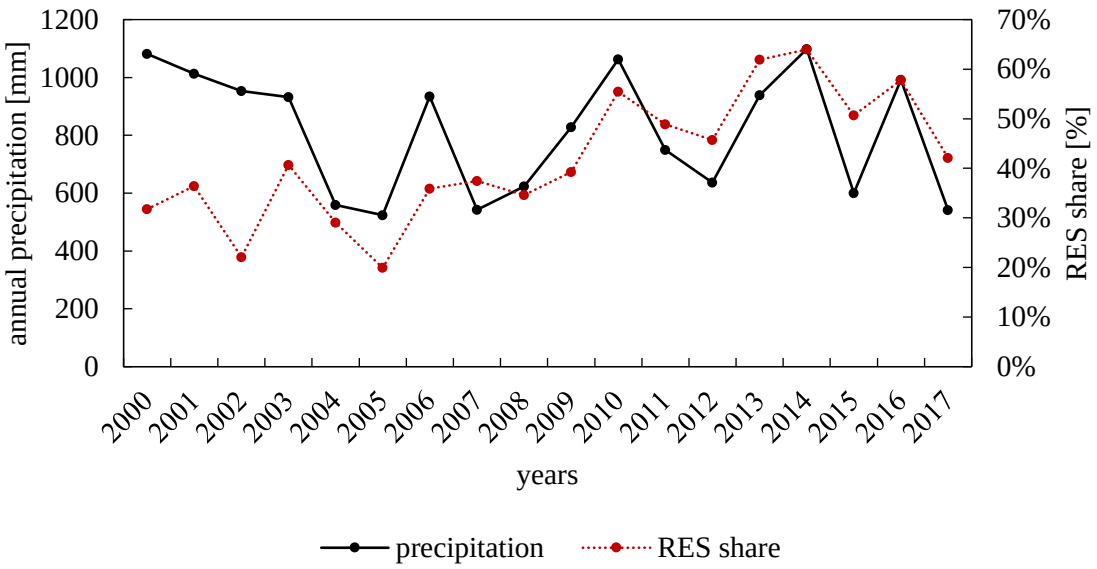

Figure 3.1. Historical annual precipitation
Annual precipitation and renewable electricity sources (RES) share from 2000 to 2017 in Portugal [97].

Hereafter, the most recent past five years with available data (2011-2015), at the time, are characterized in terms of weather, system performance and power capacity. Table 3.2 shows some weather characteristics for that period. It includes extremely wet years (2014) and dry years (2015).

Table 3.2. Historical weather characteristics
Summary of weather characteristics in Portugal for the standard calibration period from 2011 to 2015, compared to the historical mean for the period 1971-2000 [98].

Standard calibration period – Weather characteristics						
	1971-2000 mean	2011	2012	2013	2014	2015
T_{max} [°C]	20.5	21.7	20.9	20.9	21.0	21.9
T_{avg} [°C]	15.3	16.0	15.1	15.39	15.80	16.0
T_{min} [°C]	10.0	10.3	9.4	9.9	10.6	10.1
Precipitation [mm]	882	750	636	939	1,098	600

3.2. Future projections

The future of the Portuguese power system has been the focus of several scientific works. Several factors contribute to the interest in this case study. As highlighted in the previous section, Portugal has a wide range of endogenous resources that are available for

renewable generation. Adding to that, currently, the country has been consistently presenting high shares of renewable penetration in the power system. It paves the way for a future power system extremely based on renewables, which incentives its study under such conditions.

Hereafter, some of the works already developed about the Portuguese power system are addressed. From a governmental point-of-view, the power system is considered to be an important focus for future policies. Recently, the Portuguese 'Roadmap for Carbon Neutrality 2050' was presented, later referred to as 'RNC2050' [99]. It provides three visions for the future of the Portuguese energy system. From a scientific point-of-view, an extensive literature has also been focusing on Portugal, as follows. Nunes et al. [100], [101] explore a photovoltaics-based power system in Portugal in 2050 considering that electric vehicles would play a significant role in buffering the variable generation and supporting the grid. Fernandes and Ferreira [102] address renewables-based electricity mixes and the feasibility of a 100% renewable power system, without discarding the cost analysis of each solution presented. Krajačić et al. [103] aim at achieving a fully renewable Portuguese power system by testing a wide range of storage solutions. Pina et al. [104] explore the optimal electricity mix in Portugal in the 21st mid-century, focusing both in the future investment and assuming an hourly resolution for the power system operation. Santos et al. [105] study the 2030 Portuguese power system by testing several scenarios to achieve different targets regarding renewable share and emissions.

The location of Portugal exposes the country to a high level of vulnerability to changes in climate and weather conditions. Many works have explored the vulnerability of renewable generation to the future climate in the surrounding regions of Portugal.

Jerez et al. [29] study the future potential of photovoltaics' in Europe, and they found that Iberia is not expected to be suffering significant changes in its photovoltaics' potential, because lower efficiency, due to higher temperature, tends to be counterbalanced by the increase in solar radiation [29]. Carvalho et al. [25] draw its attention to wind potential alone for the short-, medium- and long-term future for the Mediterranean region. It expects a decrease in wind potential for Iberia. Similar projections are made by Soares et al. [61] for wind offshore up to the year 2100, except in the summer season. Teotónio et al. [63] simulate the Portuguese power system in 2050, assuming that hydropower generation is the most affected renewable supply source, and find a decline of up to 41% due to precipitation decrease. Also, they found that drier periods (especially in summer)

are expected, with increased rainfall in winter [63]. The higher temperatures in summer will lead to faster evaporation and therefore resource loss, aggravating potential droughts.

Besides electricity supply vulnerability, the Portuguese power system is likely to be challenged by a strong increase in electricity demand, which is confirmed by the literature. Table 3.3 summarizes the changes expected for the future electricity demand in Portugal in the year 2050 per activity sector.

Anjo et al. [106], without considering climate change, address the importance of demand response in the Portuguese power system in 2050, it projects an increase of about 30% in the mid-21st century. A study conducted by CENSE-UNL and APREN [107] uses also TIMES-PT to model the 2050 Portuguese power system, and it projects an increase in electricity demand from 25 to 58%. Fortes et al. [108] address the impact of different emission caps on the socio-economic sectors in Portugal in 2050 using TIMES-PT model. A potential increase of 27-94% on electricity demand is found. Using a similar model, the Portuguese roadmap for carbon neutrality, the RNC2050 [109], expects an increase in electricity demand between 23 and 92%. Following a broad work on worldwide roadmaps in 2050 for future energy systems, Jacobson et al. [110] estimate an increase of 18-58% for electricity demand. Finally, Pina et al. [104] consider an increase of about 59% of the Portuguese electricity demand for their target period 2005-2050.

A great discrepancy in the results can be observed among the different activity sectors. The residential and the transport sector are the ones whose the future development is the most consensual though with different magnitudes: the demand from the first is expected to range +6 to +71%, while the demand from the latter is expected to increase between +100% and 6-fold, compared to the present. For the remaining sectors, the studies are not in agreement in the signal of its future development, with some studies showing possibilities of decreasing or increasing trends and others focusing solely on the increasing tendencies.

Table 3.3. Literature on the future electricity demand in Portugal
Summary of the expected electricity demand in Portugal in the year 2050 (alphabetic order).

Summary of literature on future electricity demand for Portugal						
	Results (compared to present)					
	Total	Residential	Services	Industry	Agriculture	Transports
Anjo et al. [106]	+32%	+32%	+32%	+32%	-	-
CENSE & APREN, 2017 [107]	+25 to +58%	+4 to +7%	Up to +7%	+9 to +79%	-6 to +29%	+3,300 to +4,100%
Fortes et al. [108]	+27 to +94%	+6 to +18%	-4 to +4%	+24 to +119%	-	+3,187 to +4,428%
Jacobson et al. [110]	+16 to +56%	+25 to +63%	+50 to +93%	-21 to +20%	+182%	+87 to +100%
Pina et al. [104]	+59%	-	-	-	-	-
RNC2050 [109]	+23 to +92%	+15 to +71%	-7 to +1%	+10 to +112%	-7 to +4%	+2,865 to +5,949%

Besides the previous studies, it is worth mentioning the expected changes between heating and cooling demand in the residential sector in Portugal in the mid-century. Jakubcionis and Carlsson [111] use the cooling degree-days method to study the potential of space cooling residential demand in Europe; for Portugal, it expects total electricity demand to increase 35% while cooling demand is expected to 13- to 36-fold. Andrić et al. [112] address the impact of climate change on the heating needs of a neighborhood in Lisbon, using a Resistance-Capacitance model that considers the buildings' characteristics. It projects a decrease in heating needs of 7 to 52%.

Table 3.4 presents those results for the future residential demand for Portugal.

Table 3.4. Literature on the future residential demand in Portugal
Summary of the expected demand in Portugal in the year 2050 for the residential sector, including heating, cooling and total demand (alphabetic order).

Additional literature on future residential electricity demand for Portugal			
	Results (compared to the present)		
	Heating	Cooling	Total demand
Andrić et al. [112]	-7 to -52%	-	-
Jakubcionis and Carlsson [111]	-	+1,256 to +3,617%	+35%

4. Power system modelling

In this chapter, the methods applied to proceed to the modelling of the Portuguese power system in 2050 are described. It begins with a summary of the overall approach of modelling the power system by combining its essential elements (section 4.1). Then, the chapter proceeds presenting in detail the methods to assess each main part of the power system modelling. The climate data selected for this work is described, including the concentration paths and the climate models chosen (section 4.2). The modelling of the power system follows by describing the energy planning simulation tool used, along with the calibration performed and the methods to model the supply sources (section 4.3). A description of how the society development scenarios were built for each activity sector is presented, followed by the methods applied for projecting demand in each sector (section 4.4). After describing the methods to determine the CO_2 emissions (section 4.5), this chapter closes with a list of the main limitations of this work (section 4.6).

4.1. General approach

This section describes the approach taken to model the power system by combining the climate data, the supply sources and the electricity demand-flexibility scenarios.

Figure 4.1 summarizes the overall approach and corresponding sections where each item is detailed. First, the climate data is treated and is used to determine most of the renewable resource (except for biomass), while biomass and natural gas (when applicable) are used according to the requirements of the system and the resource constraints imposed. To ascertain some calibration parameters, the proposed multiyear approach is applied. On the demand-flexibility side, five scenarios are built for each activity sector and the energy storage availability. The electricity demand from the residential sector is determined using a Monte Carlo approach that takes into consideration the climate data. After ascertaining the supply, demand and the power system configuration (e.g. installed

capacities), the simulations in EnergyPLAN are performed. Each simulation regards one of almost 500 climate realizations (each corresponding to a single year with different weather conditions, commonly referred to as ‘years’ from now on) for each demand-flexibility scenario. Please refer to Annex I. for an illustration of the annual renewable generation for different ensemble years.

To analyze the performance of the power system under all climate realizations, boxplots are built for each demand-flexibility scenario and each chosen indicator of performance.

To highlight the need for including climate variability, the performance of the power system is analyzed according to different climate thresholds. Usually, the focus is given to the median climate realization (the year corresponding to the 50^{th} percentile of the calculated indicator) and the 95^{th} percentile (which, on average, is expected to occur once every 20 years) of the indicator of performance chosen. The climate thresholds above the 50^{th} percentile are considered to be unfavorable to the power system, since, for the same power system, they demand more from the system (e.g. higher imports, cross-border interconnection, etc.). For this reason, unfavorable years are also defined according to their determined indicator’s percentile, e.g. 95% unfavorable corresponds to the 95^{th} percentile of the calculated indicator of performance. The renewable electricity share is the exception, where the reverse is applied.

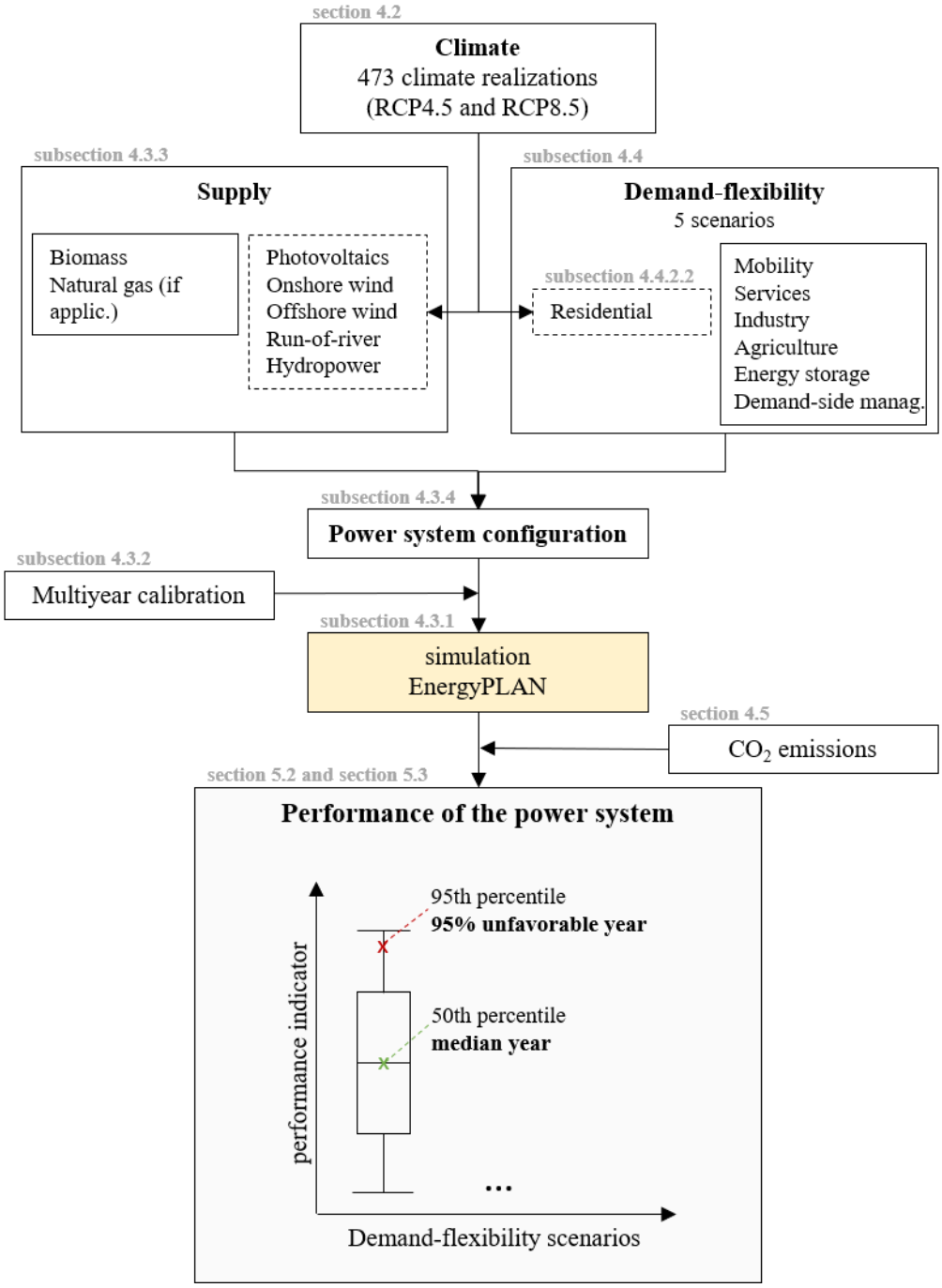

Figure 4.1. Scheme of modelling the power system
Summary of the overall approach to model and analyze the performance of the power system, including the combination of climate data, supply sources and demand-flexibility scenarios. The dashed boxes represent the supply sources and activity sectors considered to be affected by climate.

The main indicators to analyze the performance of each proposed power systems are:

- **Annual imports and exports** – *annual imports* and *annual exports* [TWh];
- **Net imports** – *net imports* [TWh] is determined as follows.

$$net\ imports = \ annual\ imports - annual\ exports \tag{4.1}$$

- **Cross-border interconnection requirements** – It is given by the 99th percentile of the hourly interconnection requirement observed for both import and export needs during each simulation. As it is common practice, the 99th percentile was chosen against the maximum value to avoid a misrepresentation of the system performance by the rare consumption peaks.
- **Potential energy curtailment** – It illustrates the fraction of excess generation that may be required to be curtailed, $f_{curtailment}$ [fraction]. It is obtained by the ratio between the annual exports and total electricity generation $AGen_{total}$ [TWh], according to Equation (4.2).

$$f_{curtailment} = \frac{annual\ exports}{AGen_{total}} \tag{4.2}$$

- **CO_2 emissions** – These include equivalent CO_2 emissions originated by the power system and by other energy uses (e.g. use of natural gas boilers in the residential sector). Section 4.5 aims at describing in detail this parameter.
- **Renewable electricity generation share** (only for HiRES and HiRES+UB power systems, see subsection 4.3.4) – It considers the annual generation of renewable supply sources and the total electricity generation $AGen_{total}$ [TWh], Equation (4.3).

$$RES_{share} = \frac{\sum_{ren} AGen_{ren}}{AGen_{total}} \tag{4.3}$$

  where *ren* represents each type of renewable: photovoltaics, wind onshore, wind offshore, run-of-the-river, hydro dams, and biomass power plants.

- **Dedicated stationary energy storage** (only in 100%RES configuration, see subsection 4.3.4) – To decrease the cross-border interconnection required, the sizing of a seasonal dedicated stationary energy storage is performed. Please refer to subsection 4.4.2.4 for more details.

4.2. Climate models

Climate change has been studied profusely in the literature. Its study is based on global climate models that simulate all the physical processes occurring in the atmosphere across the globe. The interactions between different components of climate are influenced by several factors including anthropogenic GHG emissions. To standardize studies on climate change impacts, the IPCC has compiled four scenarios regarding GHGs' concentration paths. Their aim was to provide a limited number of concentration pathways that could be used for the scientific community, facilitating the process of understanding scenarios used in different studies while making their results more easily comparable [113].

Bellow, a brief presentation of the representative concentration pathways defined by IPCC is presented (subsection 4.2.1). After describing concisely the ensemble of climate models used in this work (subsection 4.2.2), the approach taken regarding the treatment of climate data is explained (subsection 4.2.3). Lastly, an overview of the future variability of the climate variables considered is showed (subsection 4.2.4).

4.2.1. Representative Concentration Pathways (RCPs) scenarios

Energy studies about the future of power systems usually use models addressing the concentration scenarios defined by the IPCC for the future (the Representative Concentration Pathways – RCPs), so that their results can be comparable and consistent. A detailed description of the process of building these scenarios can be found in Ref. [114].

The RCPs define four pathways based on "*the change in the balance between incoming and outgoing radiation to the atmosphere caused by changes in atmospheric constituents, such as carbon dioxide*" relative to the pre-industrial period until the year 2100, where positive changes are directly related to the increase of temperature on Earth [115]. These changes are called radiative forcing and their values are used to name each scenario.

Each RCP is "*one of many possible scenarios that would lead to the specific radiative forcing characteristics*" [115] based on one documented scenario of the existing literature (considered as representative of the published scenarios for the future, regarding their

concentration and radiative forcing results), but it is not restricted to the socio-economic factors assumed on the document. The four RCPs do not derive from a unique scenario, they do not consider the same assumptions neither they use the same models to obtain their results. Thus, no RCP should be used as a reference to be compared against other RCPs [114].

Essentially, each RCP scenario defines the radiative forcing in 2100, which can be achieved by a wide range of frameworks combining different socio-economic conditions, technologies, and others [114]. The main characteristics of the four scenarios chosen are summarized in Table 4.1.

Table 4.1. Representative Concentration Pathways
Description of the main characteristics of each RCP scenario – adapted from [114].

IPCC scenarios	Radiative forcing in 2100 [W/m^2]	Concentration [ppm CO_2eq]	Pathways	Model providing RCP
RCP2.6	2.6	490	Peaks before 2100 at 3 W/m^2 and then declines	IMAGE [116], [117]
RCP4.5	4.5	650	Stabilizes after 2100	GCAM [118]
RCP6	6	850	Stabilizes after 2100	AIM [119], [120]
RCP8.5	8.5	>1370	Rising	MESSAGE [121]

Two RCPs were chosen to be analyzed in the present work: RCP4.5 and RCP8.5. The underlying reason for the RCP selection was to achieve good coverage of the possible pathways for concentration and radiative forcing; thus, one RCP with an intermediate radiative forcing (RCP4.5) and the worst-case scenario for the Earth warming (RCP8.5) were chosen. In the literature, RCP8.5 has often been used as a business-as-usual scenario, more likely to occur than other RCPs. Recently, this has been contested, since RCP8.5 was built to represent a very high emission scenario with no preference of occurrence over other RCPs [122], [123]. Even though a path towards RCP8.5 is not completely discarded, it has been seen as unlikely because it would require a strong global increase in coal consumption [123]. Lately, it has been suggested that RCP8.5 should not be the center of analyses [122], [123].

4.2.2. CORDEX climate models

Many climate models try to characterize the climate of the future, but as they depart from different assumptions and modelling approaches of atmospheric processes, each model has its own trace for the future. Thus, when studying the impact of climate change on the most diverse areas, several climate paths should be used to produce results that include a wider range of possible climate conditions. In this subsection, the description of the climate models used is provided.

Several climate data sets are freely available, and identifying its shortcomings is the first step to start using it. The spatial and temporal resolution are some of the key features of a data set, and they can easily be the limiting factor for the use of the data. A narrow temporal resolution is of major importance when studying energy systems, due to technical characteristics that deal with the system flexibility and variability. In this work, the aim was to use the models with the finest resolution since hourly data would be required for at least some of the variables.

Global climate models may provide highly informative data on a global scale, but they are characterized by a low spatial resolution that limits its use in smaller regions. To study smaller areas, a downscaling of the data is required, as is the case in this study.

The Coordinated Regional Climate Downscaling Experiment (CORDEX) project performs downscaling of climate data by using global climate models' results as forcing data to run regional climate models using a dynamical downscaling approach [124]. It includes a domain for Europe at a spatial resolution of 0.11º (approximately 12 km); its finest time resolution is three-hourly. The models of the database of CORDEX are run considering the IPCC scenarios, and they provide freely an acceptable range of climate variables. For those reasons, CORDEX data was the database chosen for all climate data used here. Besides the driving models, different climate outputs are generated by different ensemble members [125]. The climate models selected are all the available ones at the time of the data gathering (the year 2017), that presented the required following characteristics.

The data gathered corresponds to 11 years (from the year 2045 to 2055). To have a wider range of possible climate pathways, regarding the temporal resolution, three-hourly and daily resolution models were included. The models consider different time calendars: 1) the standard or Gregorian calendar, which considers normal and leap years; 2) the

365-days calendar, which assumes that all years have 365 days; and 3) 360-days calendar, which assumes 360 days in all years with all months having 30 days.

For this work, the relevant climate parameters are: 1) air temperature and solar radiation, which are crucial to determine the needs for space cooling and heating and to determine the photovoltaics' generation; 2) wind speed, essential to determine the wind power generation; and 3) precipitation, to ascertain hydropower and run-of-the-river generation.

The climate models with three-hourly data are shown in Table 4.2. The variables gathered included in these models are: precipitation [$kg.m^{-2}.s^{-1}$], surface downwelling shortwave radiation [W/m^2], near-surface wind speed [m/s] and near-surface air temperature [K].

Table 4.2. Three-hourly climate models
List of climate models from the CORDEX project with three-hourly timesteps under RCP4.5 and RCP8.5.

Three-hourly resolution climate models from the CORDEX project					
Institute	Model (RCM)	Driving model (GCM)	Ensemble members	Calendar	IPCC scenarios
SMHI	RCA4	CNRM-CERFACS-CNRM-CM5	r1i1p1	Standard	RCP4.5 and RCP8.5
SMHI	RCA4	ICHEC-EC-EARTH	r12i1p1	Standard	RCP4.5 and RCP8.5
SMHI	RCA4	IPSL-IPSL-CM5A-MR	r1i1p1	365-days	RCP4.5 and RCP8.5
SMHI	RCA4	MOHC-HadGEM2-ES	r1i1p1	360-days	RCP4.5 and RCP8.5
SMHI	RCA4	MPI-M-MPI-ESM-LR	r1i1p1	Standard	RCP4.5 and RCP8.5

In the case of daily data, more climate variables and climate models from the CORDEX project were available. The climate variables gathered from the daily resolution models were: precipitation [$kg.m^{-2}.s^{-1}$], surface downwelling shortwave radiation [W/m^2], near-surface wind speed [m/s], daily maximum near-surface wind speed [m/s], near-surface air temperature [K], daily maximum and daily minimum near-surface air temperature [K]. Table 4.3 presents the climate ensemble with daily resolution data for RCP4.5 and RCP8.5.

Table 4.3. Daily climate models
List of climate models with daily timesteps from the CORDEX project under RCP4.5 and RCP8.5.

Daily-hourly resolution climate models from the CORDEX project					
Institute	Model (RCM)	Driving model (GCM)	Ensemble members	Calendar	IPCC scenarios
CLMcom	CCLM4-8-17	CNRM-CERFACS-CNRM-CM5	r1i1p1	Standard	RCP4.5 and RCP8.5
CLMcom	CCLM4-8-17	ICHEC-EC-EARTH	r12i1p1	Standard	RCP4.5 and RCP8.5
CLMcom	CCLM4-8-17	MOHC-HadGEM2-ES	r1i1p1	360-days	RCP4.5 and RCP8.5
CLMcom	CCLM4-8-17	MPI-M-MPI-ESM-LR	r1i1p1	Standard	RCP4.5 and RCP8.5
DMI	HIRHAM5	ICHEC-EC-EARTH	r3i1p1	Standard	RCP4.5 and RCP8.5
DMI	HIRHAM5	NCC-NorESM1-M	r1i1p1	Standard	RCP4.5 and RCP8.5
IPSL-INERIS	WRF331F	IPSL-IPSL-CM5A-MR	r1i1p1	Standard	RCP4.5 and RCP8.5
KNMI	RACMO22E	ICHEC-EC-EARTH	r1i1p1	Standard	RCP4.5 and RCP8.5
KNMI	RACMO22E	ICHEC-EC-EARTH	r12i1p1	Standard	RCP8.5
KNMI	RACMO22E	MOHC-HadGEM2-ES	r1i1p1	360-days	RCP4.5 and RCP8.5
MPI-CSC	REMO2009	MPI-M-MPI-ESM-LR	r1i1p1	Standard	RCP4.5 and RCP8.5
MPI-CSC	REMO2009	MPI-M-MPI-ESM-LR	r2i1p1	Standard	RCP4.5 and RCP8.5
SMHI	RCA4	CNRM-CERFACS-CNRM-CM5	r1i1p1	Standard	RCP4.5 and RCP8.5
SMHI	RCA4	ICHEC-EC-EARTH	r12i1p1	Standard	RCP4.5 and RCP8.5
SMHI	RCA4	IPSL-IPSL-CM5A-MR	r1i1p1	365-days	RCP4.5 and RCP8.5
SMHI	RCA4	MOHC-HadGEM2-ES	r1i1p1	360-days	RCP4.5 and RCP8.5
SMHI	RCA4	MPI-M-MPI-ESM-LR	r1i1p1	Standard	RCP4.5 and RCP8.5

Figure 4.2. represents the summarized climate data gathered from the CORDEX project. This ensemble totalizes 473 climate realizations, each with a length of one year (below also referred to as ‘ensemble years’).

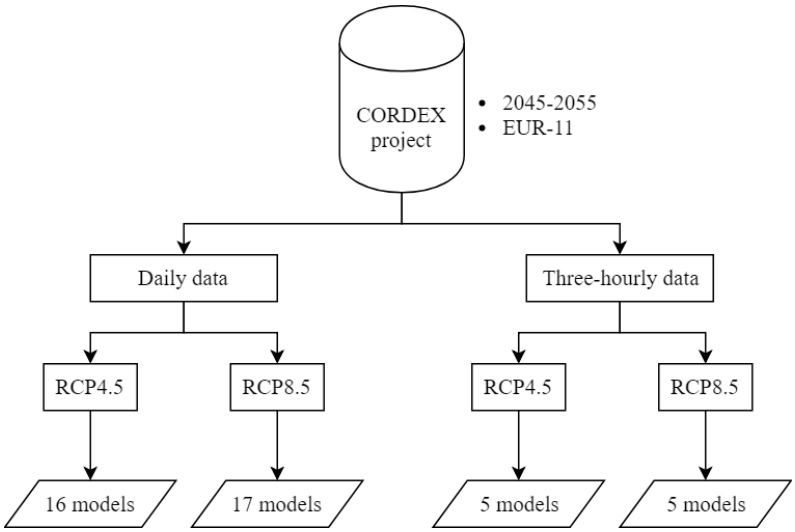

Figure 4.2. Scheme of climate ensemble
Summarized scheme of the gathering of the climate data from the CORDEX project, including the temporal resolution and number of climate models included in each RCP.

4.2.3. Data processing

Data processing is an essential initial step before starting using the data effectively. Climate data was gathered for Portugal mainland. After organizing the data, it was analyzed and errors such as repeated data were removed. As presented in Table 4.2 and Table 4.3, the calendar assumptions differ according to each climate model. Considering the energy planning tool chosen, EnergyPLAN [51] – which considers leap years only, see subsection 4.3.1 – the calendar models were uniformized to have 366 days per year, depending on the calendar different strategies were implemented. For months with missing days in the original dataset, those were introduced by replicating the last day of the month: 1) in the non-leap years of standard calendar models or the 365-days models, the missing February 29th was introduced by replicating February 28th; 2) in the 360-days models, where every month is considered to have 30 days, the 31-days months were completed by replicating its 30th day. Since the 360-days models consider 30 days for February, the last day was removed.

Regarding the temporal downscaling resolution, it was treated differently according to the required resolution for each climate parameter. Even though a minute-by-minute or even higher resolution could be of use in this type of study, here the finest resolution looked-for is hourly – in the case of air temperature, global horizontal irradiation and wind speed. Thus, a straightforward methodology to convert daily and three-hourly data

into hourly data for those variables is presented in the next subsections 4.2.3.1, 4.2.3.2 and 4.2.3.3. On the other hand, in the case of precipitation, an hourly resolution is not crucial for the final purpose. Thus, precipitation data were upscaled to monthly data, as detailed in subsection 4.2.3.4.

The validation of the different downscaling methods considered the following simple statistic parameters: the root mean square error (RMSE) and the mean absolute error (MAE) and their normalized values (NRMSE and NMAE, respectively); the maximum absolute difference (MAXAD) and the maximum relative difference (MAXRD). These parameters are described by Equations (4.4)-(4.8) [126].

$$\mathrm{RMSE} = \sqrt{\frac{1}{N}\sum_{t=1}^{N}(y_t - \hat{y}_t)^2} \tag{4.4}$$

$$\mathrm{NRMSE} = \frac{\sqrt{\frac{1}{N}\sum_{t=1}^{N}(y_t - \hat{y}_t)^2}}{\max(\hat{y}_t)} \times 100 \tag{4.5}$$

$$\mathrm{MAE} = \frac{1}{N}\sum_{t=1}^{N}|y_t - \hat{y}_t| \tag{4.6}$$

$$\mathrm{NMAE} = \frac{1}{N}\frac{\sum_{t=1}^{N}|y_t - \hat{y}_t|}{\max(\hat{y}_t)} \times 100 \tag{4.7}$$

$$\mathrm{MAXRD} = \max|(y_t - \hat{y}_t)/\hat{y}_t| \times 100 \tag{4.8}$$

where, y_t are the synthetized values of each downscaling method and $\hat{y}_t$ are the observations, both for each timestep *t* of an hour; *N* is the total number of observations.

In addition to the statistical parameters mentioned earlier, the percentage of timesteps in which the error is superior to a certain value defined for each case (e.g. for air temperature the limit value was 2ºC) was also considered, below it is defined by PTE (percentage of timesteps' error).

4.2.3.1. Air temperature

Temporal downscaling of air temperature has been studied for many authors. The focus has been on the downscale of daily data, using mainly the maximum and minimum temperature of the day, the most common data available. There are several methods to downscale hourly air temperature T_{air} [ºC] from daily data. However, the criteria here was to choose a straightforward approach that could be easily applied to any location and period, and that could be adapted also to a downscaling of three-hourly resolution.

To downscale temperature from daily data, the Erbs' method [127] was selected (see subsection Validation, below). "The Erbs' method" is based on Equation (4.9) and Equation (4.10) that were obtained from average daily temperature per month from nine cities across the USA.

$$T_{air}(t) = T_{avg} + (T_{max} - T_{min})[0.4632\cos(a - 3.805) + 0.0984\cos(2a - 0.360) + 0.0168\cos(3a - 0.822) + 0.0139\cos(4a - 3.513)] \quad (4.9)$$

with

$$a = 2\pi \times (t_{day} - 1)/24 \quad (4.10)$$

where T_{avg} is the average daily temperature [ºC], T_{max} is the maximum daily temperature [ºC], T_{min} is the minimum daily temperature [ºC] and t_{day} is the hour of the day.

Erbs' method was adapted to the present work context. First, instead of using the monthly-average day, here the data of each day of the year is used. Second, this method had to be adapted to the downscaling from three-hourly data. The same approach was applied, but the values of the mean/maximum/minimum temperature were selected using only the values available per day, i.e., from the eight values per day (three-hourly timesteps) the minimum/maximum temperature were chosen and the mean was determined.

Validation

The proposed methods were validated against hourly measured data from Lisbon in 2014, from the meteorological station of Instituto Dom Luiz (IDL).

Two downscaling methods were considered – Half-sin [128] and Erbs' [127]. They were already validated by their correspondent authors. However, the validation was not performed for Portugal, as it is here presented for the city of Lisbon. To perform such

validation, daily data was calculated (T_{avg}, $T_{min,}$ and T_{max}) from the hourly measured data, since daily data was the original input data used in the two methods tested. Table 4.4 shows the results obtained.

Table 4.4. Comparison of the temporal downscaling methods – Air temperature
Errors resulting from the temporal downscaling to hourly resolution and the observations using two different methods: Half-sin and Erbs' method.

Comparison of downscaling methods							
Downscaling methods	RMSE [°C]	NRMSE [%]	MAE [°C]	NMAE [%]	MAXAD [°C]	MAXRD [%]	PTE [%]>2°C
Half-Sin [128]	1.19	3.40	0.86	2.45	7.22	90.00	9.18
Erbs' [127]	1.10	3.15	0.83	2.37	5.83	117.24	6.93

As previously mentioned, the Erbs' method was chosen. Afterwards, the measured data was treated to be upscaled from hourly resolution to three-hourly resolution[4], since the final goal was to apply the described downscale methodology to the climate models which have daily and three-hourly resolution.

Figure 4.3 shows the original data and the synthetized data for both resolutions and a winter and spring week.

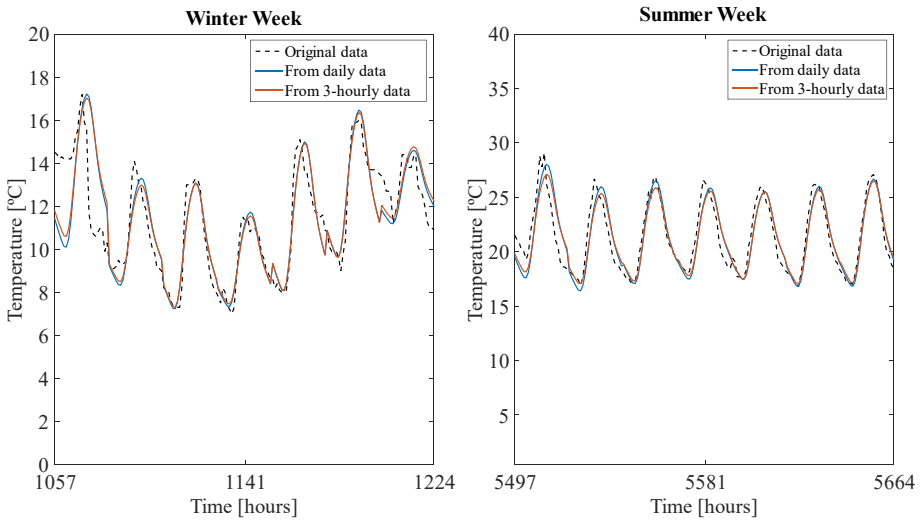

Figure 4.3 Validation of the temporal downscaling – Air temperature
The air temperature of a Winter week (left) and of a Summer week (right) - measured data and proposed methods.

[4] Starting at hour 0, a three-hourly timestep was considered and only the hourly values correspondent to the beginning of those steps were kept – i.e., the value of hour 0 was kept, the following two hourly values (from hour 1 and 2) were removed and the value after those was kept (hour 3), and so on. The resulting time-series has a three-hourly resolution.

The use of three-hourly data tends to overestimate/underestimate the daily limits of temperature (e.g. 1st day of Summer week, Figure 4.3), even though it does not differ significantly from the data obtained from the daily data. The statistic parameters comparing observations with the synthetized data are presented in Table 4.5.

Table 4.5. Temporal downscaling for daily and three-hourly data – Air temperature
Errors resulting from the temporal downscaling of air temperature to hourly resolution and the synthetized data obtained through daily and three-hourly resolution data.

Air temperature							
	RMSE [°C]	NRMSE [%]	MAE [°C]	NMAE [%]	MAXAD [°C]	MAXRD [%]	PTE (%) >2ºC
Daily data	1.10	3.15	0.83	2.37	5.82	117.24	6.93
Three-hourly data	1.06	3.02	0.79	2.27	5.55	114.39	6.27

The estimation method of air temperature that uses three-hourly data appears to better follow the observations' profile in terms of mean average error (0.79ºC against 0.83ºC) and of maximum absolute/relative errors. About 6-7% of the estimations showed an error above 2ºC for both approaches (daily and three-hourly).

Figure 4.4 shows when the differences between the synthetized data and the observations are higher. The air temperature estimation does not show a clear pattern of performance, but it seems to be underestimated at times when the temperature is naturally expected to be higher (in the middle of the day during the summer period) and it is overestimated at daytime along the rest of the year and in the late afternoon/night during the summer. For both under and overestimation, the maximum magnitude rounds 5.5ºC.

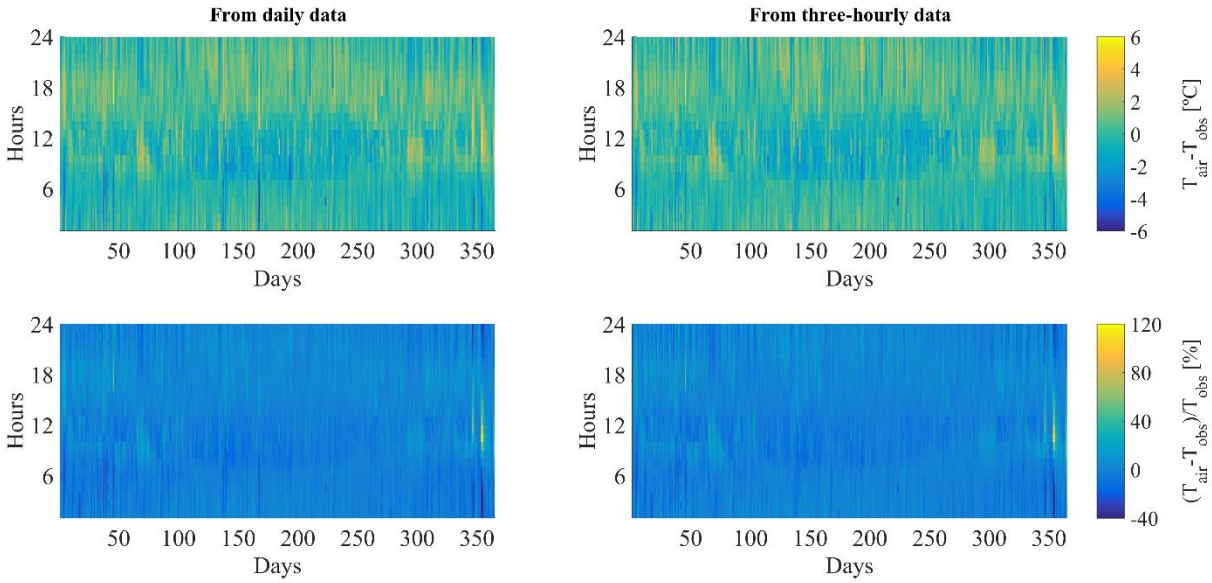

Figure 4.4. Absolute and relative errors for the temporal downscaling – Air temperature
Absolute error and relative error obtained when using the daily (left) and three-hourly data (right) of air temperature (T_{air}), compared to observations (T_{obs}).

4.2.3.2. Global horizontal irradiance

The global horizontal irradiance G_h [W/m^2] was downscaled using an approach based on solar geometry and atmosphere clearness, starting with two time-series with different time resolutions: 1) daily and 2) three-hourly. A summarized scheme of the methods is presented at the end of this subsection, Figure 4.5.

Firstly, for both temporal resolutions, the extraterrestrial global irradiance I [W/m^2] had to be calculated, which required the determination of several other parameters.

The equation of time EoT [hours] is used to correct the local time, Equation (4.11) and Equation (4.12) [129].

$$EoT(t) = \left[9.87\sin\left(4\pi \times d'(t)\right) - 7.53\cos\left(2\pi \times d'(t)\right) - 1.5\sin\left(2\pi \times d'(t)\right)\right]/60 \quad (4.11)$$

$$d'(t) = (d(t) - 81)/365 \quad (4.12)$$

where d is the Julian day and t is the hour of the year.

The correction of the time zone is applied to the hour angle ω [radians], according to Equation (4.13) [130].

$$\omega(t) = \frac{\pi}{12} \times \left(t_{solar}(t) - 12 + EoT(t)\right) + (\lambda - \lambda_{zone}) \quad (4.13)$$

where t_{solar} is the solar hour [hour], λ is the geographic longitude [radians] and λ_{zone} is the time zone of the location [radians].

Equation (4.14) shows the calculation of the declination angle δ [radians] [130].

$$\delta(t) = 0.4093 \times \sin\left(2\pi \times \frac{(284 + d(t))}{365}\right) \quad (4.14)$$

Equation (4.15) is used to calculate the cosine of the zenith angle θ_z [radians], whenever the solar altitude α [radians] is above zero [131].

$$\cos(\theta_z) = \sin\big(\delta(t)\big) \times \sin(\varphi) + \cos\big(\delta(t)\big) \times \cos(\varphi) \times \cos\big(\omega(t)\big) = \sin(\alpha) \quad (4.15)$$

where φ is the geographic latitude [radians].

Finally, the eccentricity correction factor of the Earth's orbit E_0 is calculated, Equation (4.16) [131].

$$E_0(t) = 1 + 0.0334\cos\left(2\pi \frac{d(t)}{365}\right) \quad (4.16)$$

The extraterrestrial irradiance I [W/m^2] could finally be calculated through Equation (4.17) [131].

$$I(t) = I_{SC}(t) \times E_0(t) \times \cos(\theta_z(t)) \quad (4.17)$$

where, I_{SC} is the solar constant [W/m^2] [131].

Secondly, the clearness index (K_t) was determined with the same temporal resolution of the original data (Equation (4.18)): 1) daily average index or 2) three-hourly resolution. For the first, the hourly k_t was determined using the hourly extraterrestrial irradiance profile and its corresponding daily average irradiance. For the latter, having a time-series of K_t with a three-hour timestep, a linear interpolation of the K_t was performed to obtain an hourly time-series k_t. Finally, for both temporal resolutions, using the hourly time-series of the extraterrestrial irradiance and the K_t (with daily resolution for the daily data and hourly resolution for the three-hourly data), the hourly global irradiation on the horizontal was determined.

$$G_{h_{original}}(t_{step\ resolution}) = K_t\big(t_{step\ resolution}\big) \times I(t_{step\ resolution}) \quad (4.18)$$

where $t_{step\ resolution}$ corresponds to the temporal resolution, i.e., is the day or the three-hour timestep; $G_{h\ original}$ is the original data of global irradiance on the horizontal [W/m^2].

Figure 4.5. summarizes and describes the methods applied to the daily and three-hourly global irradiance data to obtain hourly time-series.

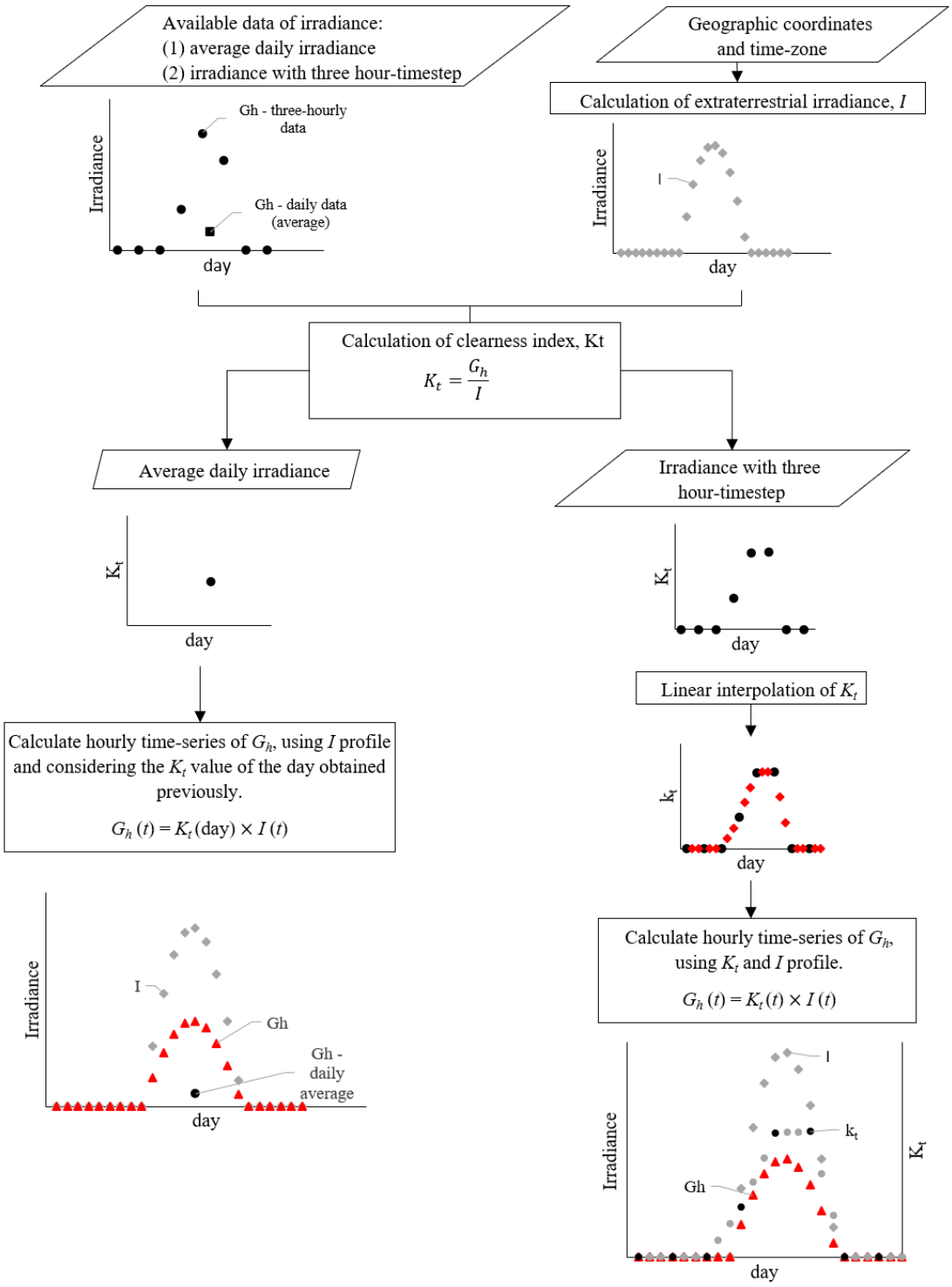

Figure 4.5. Scheme of temporal downscaling of global horizontal irradiance
Schematic of the methodology to downscale daily and three-hourly resolution data on global horizontal irradiance to hourly data.

Validation

For the global horizontal irradiance, hourly data from Lisbon airport was gathered, for 2014. As previously, the hourly data was converted to daily and three-hourly resolutions.

Figure 4.6. shows the measured global horizontal irradiance on two different weeks along with the synthetized data (daily and three-hourly).

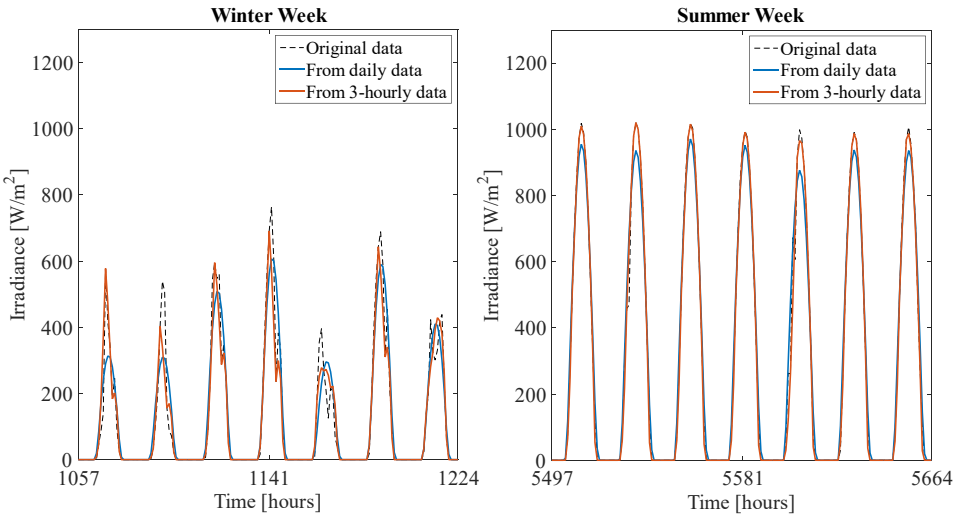

Figure 4.6. Validation of temporal downscaling – Global horizontal irradiance
Global horizontal irradiance of a Winter week (left) and of a Summer week (right) - measured data and proposed methods.

The most important factor responsible for the variability in global irradiance is cloud-related, i.e., the clearness of the sky. During the winter week (Figure 4.6.), the observed data shows significant variability due to the appearance of clouds in the sky. Since the methods here presented do not include any component for the stochastic appearance of clouds, the use of daily averages of irradiance tends to underestimate the actual irradiance in the middle of the day. Three-hourly resolution data provides more information about the sky clearness during the day. Thus, in this case, the method can get closer to reality mainly when a cloud appears at a time closer to one of the observations.

The comparison between observations and synthetized data are presented in Table 4.6.

Table 4.6. Temporal downscaling for daily and three-hourly data – Global horizontal irradiance
Errors resulting from the temporal downscaling of global horizontal irradiance to hourly resolution and the synthetized data obtained through daily and three-hourly resolution data.

Global horizontal irradiance							
	RMSE [W/m^2]	NRMSE [%]	MAE [W/m^2]	NMAE [%]	MAXAD [W/m^2]	MAXRD [%]	PTE (%) >100 W/m^2
Daily data	65.12	5.74	33.38	2.94	451.21	3322.10	10.23
Three-hourly data	50.31	4.43	19.62	1.73	574.29	730.20	5.82

The global horizontal irradiance estimation shows low accuracy, in part due to the absence of a cloudiness factor applied hourly. The maximum absolute error (MAXAD) is the only parameter that counters the best performance of the use of three-hourly input data, showing a higher value than for the case of daily data. However, that value could be an isolated case and may not be a representative observation, especially when observing the remaining parameters.

Figure 4.7 shows a clearer pattern of performance with overestimation of irradiance in the early morning and late afternoon periods.

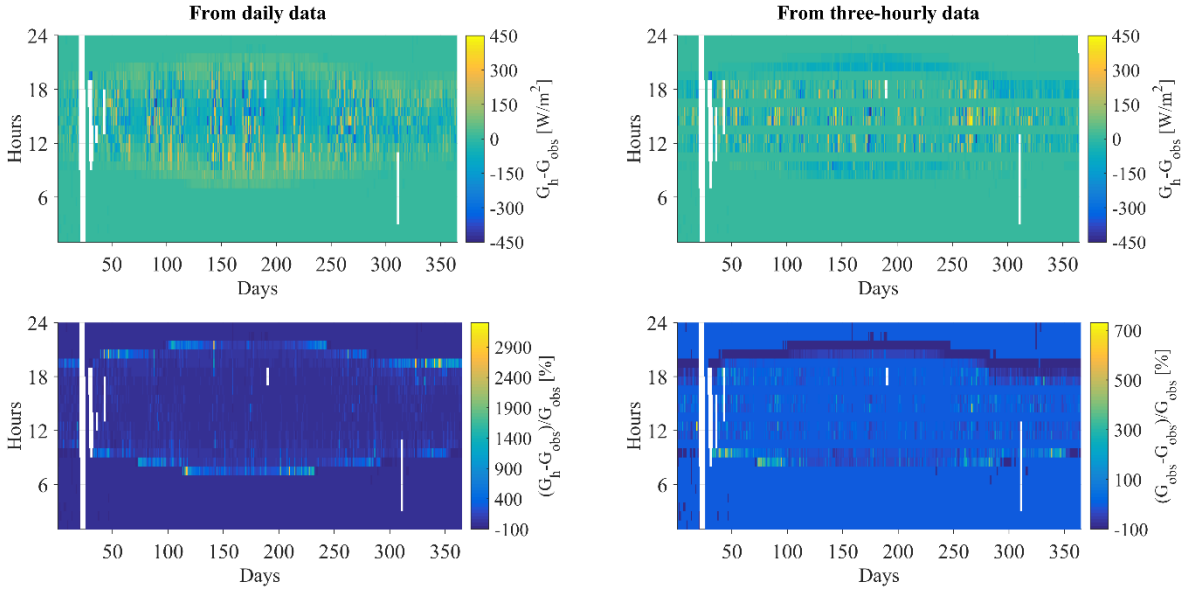

Figure 4.7. Absolute and relative errors for the temporal downscaling – Global horizontal irradiance
Absolute error and relative error obtained when using the daily (left) and three-hourly data (right) of global horizontal irradiance (G_h), compared to observations (G_{obs}).

4.2.3.3. Wind speed

Two different approaches to downscale wind speed from daily and three-hourly data were taken, after performing a comparison that resulted in selecting the most accurate method for each of the resolutions (see subsection Validation, below). The two approaches tested were: 1) a genetic-algorithm (GA) [132], and 2) a linear interpolation. Hereafter, a brief explanation of each approach is presented.

The genetic-algorithm approach is described in Ref. [132]. It implies the input of daily data, thus its validation for the three-hourly resolution data required the conversion of the three-hourly data into daily data (e.g. the mean/maximum daily temperature calculated from the eight three-hourly values available for each day). The range of some input parameters are defined, such as the shape factor of the Weibull distribution (k), the hour where the peak of wind speed normally occurs (h_p), the diurnal pattern strength (i_d) that indicates the behavior of wind during the day and an autoregressive coefficient (ac) used to generate random wind speed components. The ranges used match those described in Ref. [132]. Two objective functions are considered using the Euclidean distance method, one for the daily mean wind speed (OF_{mean}) and the other for the daily maximum wind speed (OF_{max}) – Equation (4.19).

$$OF_{mean/max} = \sqrt{\sum_{d=1}^{N} (y_d - \widehat{y_d})^2} \tag{4.19}$$

where d is the timestep of each day.

The second approach was based on a simple linear interpolation method applied to the original data to build the hourly time-series.

Validation

Hourly wind speed measurements from the meteorological station from IDL in 2014 were used for the validation of the proposed methods. Wind speed is a climate parameter characterized by strong variability. Thus, the validation of its downscaling is difficult to achieve.

To select the method to use for each resolution (daily data and three-hourly data) a comparison of the results was performed by applying both methods to both data resolutions. The results presented in Table 4.7 show that: 1) for daily data – the

genetic-algorithm performs slightly better, showing lower errors for some parameters (RMSE, NRMSE, MAXRD and mean hourly error) and it results in a mean wind speed closer to the measured data; and 2) for three-hourly data – the linear interpolation shows better performance for the comparison indicators selected. Consequently, to downscale the available data to an hourly resolution the methods used were: genetic-algorithm for the daily data and the linear interpolation for the three-hourly data.

Table 4.7. Comparison of the temporal downscaling methods – Wind speed
Errors resulting from the temporal downscaling to hourly resolution, compared to observations, for daily and three-hourly resolution data, using two different methods: genetic-algorithm and linear interpolation.

Wind speed											
	Method	RMSE [m/s]	NRMSE [%]	MAE [m/s]	NMAE [%]	MAXAD [m/s]	MAXRD [%]	PTE [%] >7m/s	Mean hourly error [%]	v_{mean} [m/s]	v_{max} [m/s]
Measured data		-	-	-	-	-	-	-	-	12.08	40.00
Daily data	GA	1.61	4.01	6.14	15.35	31.78	2280.7	35.38	40.62	12.07	42.97
	Linear interp.	5.47	13.66	5.58	13.95	31.58	2441.7	30.59	42.55	12.03	40.00
Three-hourly data	GA	1.57	3.93	5.87	14.69	31.95	2333.9	33.63	42.40	12.07	35.87
	Linear interp.	1.38	3.45	3.29	8.23	32.00	1766.7	15.89	23.71	12.07	40.00

The synthetized wind speed time-series shows an average value during the year very close to the observed one (which was of 12.08 m/s), for both resolution data. The maximum wind speed on the generated time-series was also similar to the one from the measured data (40 m/s). Comparing the performance of the synthetized time-series coming from the different resolutions datasets, it is possible to affirm that, as expected, the three-hourly data results on more accurate hourly data, having a mean hourly error of 23.71% against 40.62% from the daily data.

Figure 4.8 shows the measured data against the synthetized data for two weeks, one in winter and another in summer.

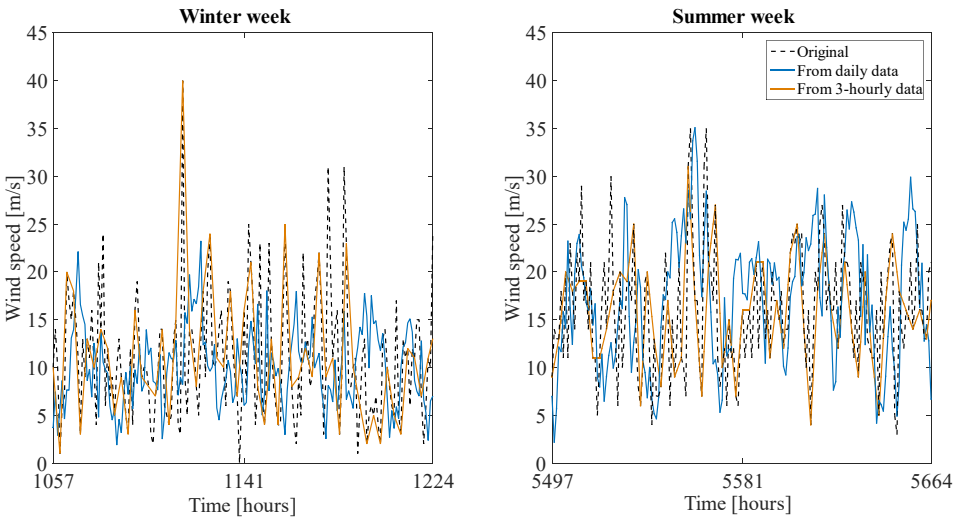

Figure 4.8. Validation of temporal downscaling – Wind speed
Wind speed of a Winter week (left) and of a Summer week (right) – measured data and proposed methods.

Observing the previous figure in a strict hourly comparison, one can easily perceive the strong differences between all the series. However, to better understand the results, Figure 4.9 shows the Weibull probability density function obtained from the results of this validation.

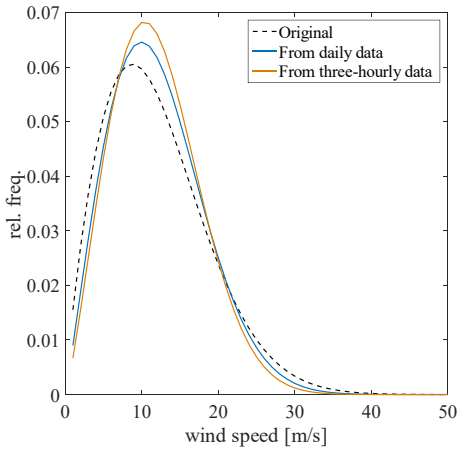

Figure 4.9. Distributions resulting from the temporal downscaling – Wind speed
Probability distribution functions for the hourly measured data and the hourly time-series generated from daily-resolution data and three-hourly data.

Figure 4.10 shows the occasions during the year when the generated wind speed differs the highest and the lowest from the measured data. For the daily data, the wind speed has higher errors during the daytime, and it seems to be more accurate in the middle of the

night. As for the three-hourly data, the errors appear lower and more uniformly distributed during the day and the year.

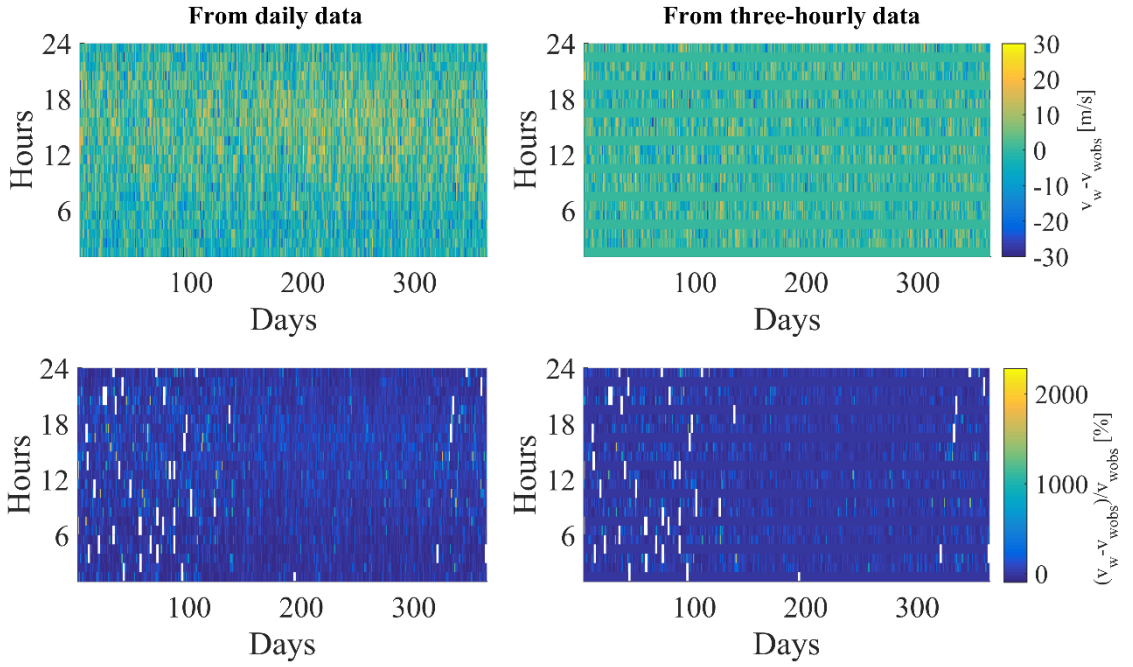

Figure 4.10. Absolute and relative errors for the temporal downscaling – Wind speed
Absolute error and relative error obtained when using the daily (left) and three-hourly data (right) of wind speed (v_w, in m/s), compared to observations (v_{wobs}, in m/s). White spaces correspond to periods when the measured wind speed was null.

From the previous results, it seems that the downscaling of wind speed results on acceptable and close general parameters – e.g. average and maximum values – that broadly characterizes the wind speed time-series (see Table 4.7), but it results in less accurate results when analyzing the results at a finer resolution.

4.2.3.4. Precipitation

The required time resolution for precipitation in this work is monthly data. For this reason, the daily/three-hourly data was aggregated into monthly data. Before aggregating to monthly data, the original precipitation $pr_{original}$ in [$kg.m^{-2}.s^{-1}$] was converted to millimeters of water per day or three-hour period [mm/time period] – pr_{mm}, depending on the resolution. As the time upscaling of precipitation is obtained by simply summing the daily values/three-hourly values to determine the monthly precipitation, no validation of the methodology was considered necessary.

4.2.4. Overview of future climate parameters

Climate variability is driven by the heterogeneous range of conditions that may occur over a certain period. The inter-annual variability of the main climate parameters is presented using all the climate models with daily resolution (before temporal downscaling to hourly data) and considering a spatial average of the whole country. Moreover, to contextualize such variability, the results from historical data are also presented. The historical climate data here presented results from the historical experiments from CORDEX project for the period 1990-2006 [133], including the same ensemble as the RCPs.

Figure 4.11 presents the probability density function for the average daily temperature per year. The distribution of future average temperatures is shifted to the right, showing a tendency for higher temperatures in the future, which is slightly more pronounced in the RCP8.5. Similar behavior is observed for future irradiance with a small decrease in the occurrence of lower irradiance and an increase of the higher values. As for average daily wind speed, the differences between the three cases studied (historical, RCP4.5 and RCP8.5) are negligible. Finally, lower rates of precipitation are expected for the future. For all of the climate parameters, the RCP8.5 shows more accentuated changes from the historical data, than the RCP4.5.

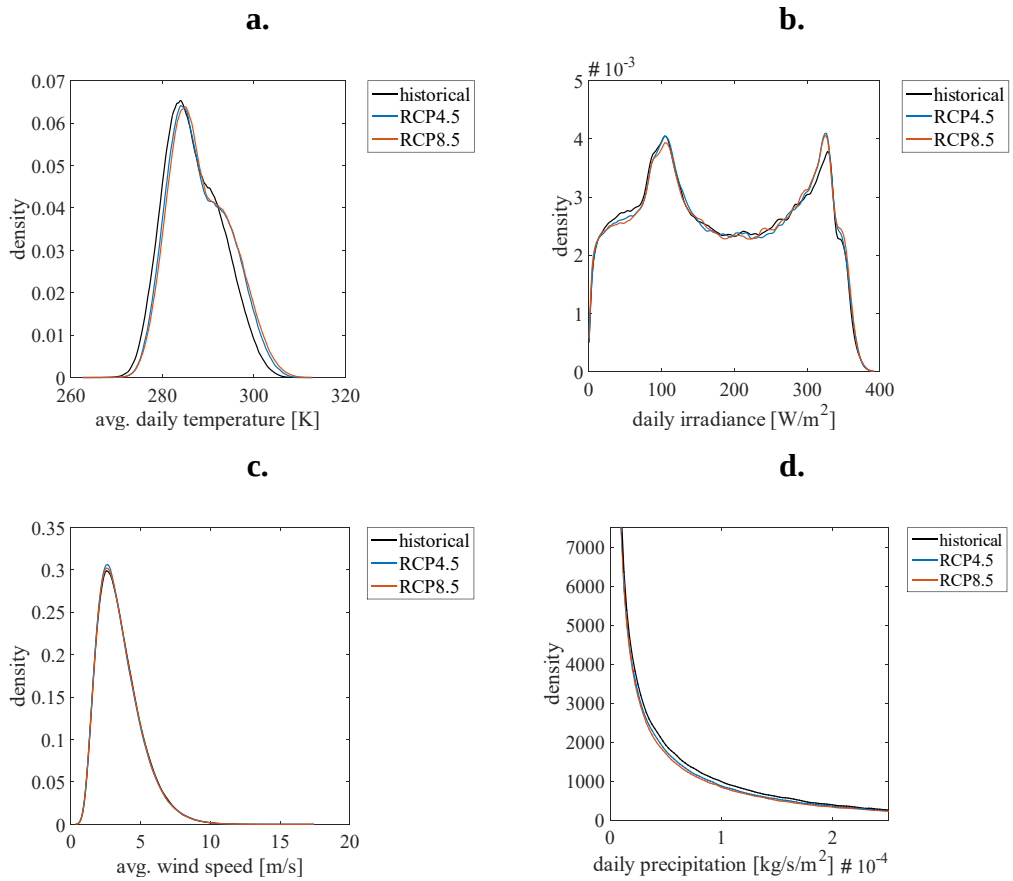

Figure 4.11. Probability density functions of climate parameters under historical and RCPs data
Probability density function for all the ensemble years with daily resolution for historical data (period 1990-2006) and RCP4.5 (blue) and RCP8.5 (red) for the period 2045-2055 for: a. average temperature; b. surface downwelling shortwave radiation; c. average daily wind speed; and d. daily precipitation (previous to temporal downscaling). Climate data gathered from CORDEX project [133].

After downscaling both the daily and three-hourly climate models to hourly resolution, the annual climate parameters may be presented as in Figure 4.12. for RCP4.5 and Figure 4.13 for RCP8.5. In those figures, it is presented the spatial average for the whole country. For temperature and wind speed, the average hourly value was chosen to be presented, while for precipitation and solar irradiation the chosen was the total annual values.

Some differences in future climate paths can be seen by comparing RCP4.5 with RCP8.5. Irradiation and temperature are expected to be higher for RCP8.5, while precipitation and wind speeds are likely to be slightly lower in RCP8.5, compared to RCP4.5.

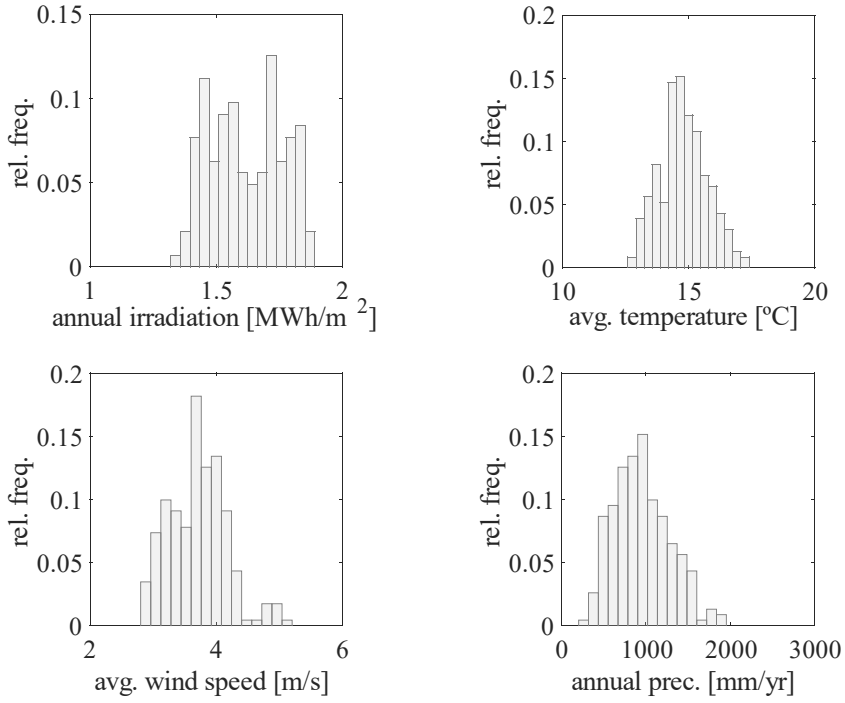

Figure 4.12. Histograms of annual climate parameters – RCP4.5
Histograms of annual precipitation, average air temperature, average wind speed and total annual global irradiation on the horizontal in Portugal for the period 2045-2055 of all the ensemble years under RCP4.5 (after temporal downscaling). Climate data gathered through CORDEX project [133].

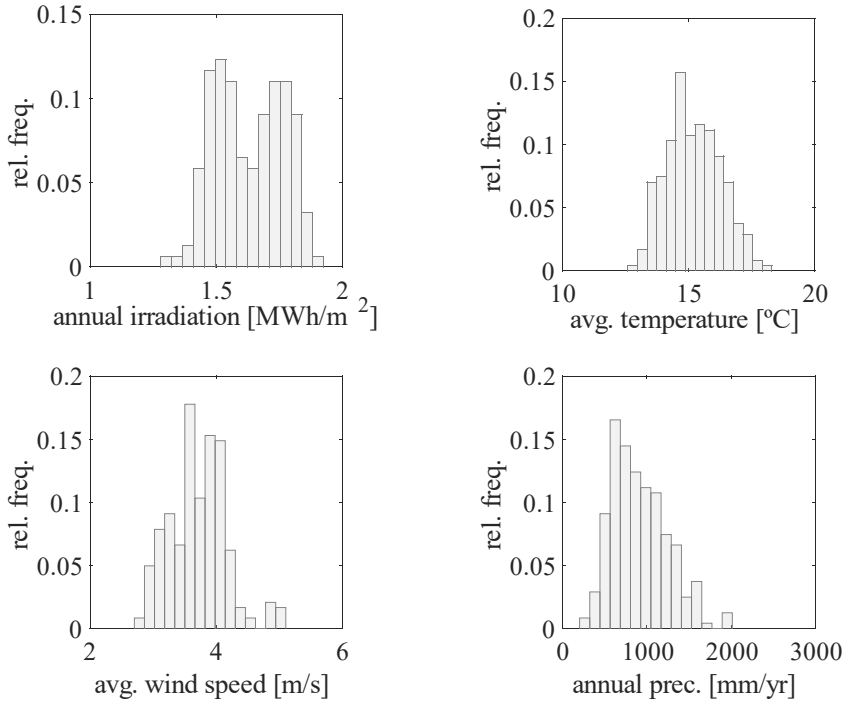

Figure 4.13. Histograms of annual climate parameters – RCP8.5
Histograms of annual precipitation, average air temperature, average wind speed and total annual global irradiation on the horizontal in Portugal for the period 2045-2055 of all the ensemble years under RCP8.5 (after temporal downscaling). Climate data gathered through CORDEX project [133].

4.3. Supply and power system modelling[5]

This section aims at describing the modelling of the power system and focusing the methods used to determine the supply sources. It starts with the description of the energy modelling tool applied in this work – EnergyPLAN (subsection 4.3.1). Then, the calibration method is described in detail (subsection 4.3.2). Finally, the methods used to model the generation of each supply source are explained (subsection 4.3.3).

4.3.1. Energy Modelling tool - EnergyPLAN

Upon the literature review of energy modelling tools presented in section 2.4, to perform the required simulations of the power system in this work, the EnergyPLAN tool (version 14.0) [51] was chosen. The main underlying reason for that was its fine time resolution of one hour, its time-horizon of one year, the light computation needs and quick time to perform one simulation, and the transparency and simplicity of the methodology used. A summary of the main framework used by EnergyPLAN to simulate the power system is hereafter explained.

The system operation is simulated using hourly energy balances of one complete leap year (8,784 hours). Priority is given to non-dispatchable renewable supply sources, then dispatchable renewable and fossil generation is adjusted accordingly (by this order) so that the generation matches the demand. The dispatchable generation includes thermal power plants (PPs) and the dam hydropower plants. Thermal power plants can be either condensing or combined heat and power (CHP).

When there is an excessive generation, the merit order to use the excess energy is (if the mechanism is available): 1) to pump water to the reservoirs; 2) to charge the electric vehicles' batteries; and 3) to charge the energy storage device. In case of a lack of supply, the system may use the stored energy by the same order. Only then, and if needed, imports/exports take place. If demand-side management is available, the scheduling of the flexible demand is performed to maximize the use of non-dispatchable renewables and to decrease the use of fossil-fueled generation and imports.

[5] Part of this section was adapted from Figueiredo et al., 2018 [224].

To avoid jeopardizing the balance of the grid, it is critical to guarantee a robust base and backup generation.

The minimum available power of condensing powerplants is implemented to preserve their technical constraints. Part of the condensing power plants, like coal- and biomass-fueled power plants, provide base generation, and they are not able to shut-down and turn-on suddenly. Thus, by establishing a bottom limit, these constraints ensure a more stable base generation. In this work, historical data (from the Portuguese power system in 2015 [134], which was of 580 MW) is used to limit the minimum of the simulated hourly distribution of thermal generation min_{PPs} [MW], Equation (4.20).

$$min_{PPs} = min(Gen_{PPs\ coal}(t) + Gen_{PPs\ NG}(t) + Gen_{PPs\ non-ren}(t) + Gen_{PPs\ biomass}(t)) \quad (4.20)$$

where $Gen_{PPs\ coal}$, $Gen_{PPs\ NG}$, $Gen_{PPs\ non\text{-}ren}$ and $Gen_{PPs\ biomass}$ are the generation power of thermal power plants supplied by coal, natural gas, other non-renewable fuels (mainly waste) and biomass [MW], respectively, at each hour *t*.

Moreover, a minimum stabilization share of dispatchable generation should be also considered. It ensures that there is a minimum of dispatchable generation operating at each hour that is able to follow the load by counteracting changes in other generation supply sources (e.g. variable renewables). This parameter is usually ensured by thermal power plants and dam hydropower plants. In this work, the minimum share of dispatchable generation min_{stab} [%] was considered to be the same as observed in historical data (from the Portuguese power system in 2015 [134], which was of 18.1%), Equation (4.21).

$$min_{stab} = min\left(\frac{Gen_{PPs\ total}(t) + Gen_{dam\ hydro}(t)}{Gen_{total}(t)}\right) \times 100 \quad (4.21)$$

where $Gen_{PPs\ total}$ and $Gen_{dam\ hydro}$ the generation of thermal power plants and dam hydro [MW], respectively, in each hour *t*; Gen_{total} is the total electricity generation in each hour *t* [MW].

EnergyPLAN offers two optimization strategies for the power system: technical and economical. During all this work, the technical optimization was chosen over a market optimization because the latter is highly sensitive to the economic conditions of the

country and its neighbors at a particular time, making the model less flexible to explore future energy scenarios.

The main inputs to the model are the installed power capacities of each supply source, the hourly distribution of dispatchable renewable generation and electricity demand, the annual values for electricity demand, fuel consumption and CHP electricity generation. Figure 4.14. summarizes the inputs and the outputs required for EnergyPLAN to model a power system with similar characteristics to this work's case study.

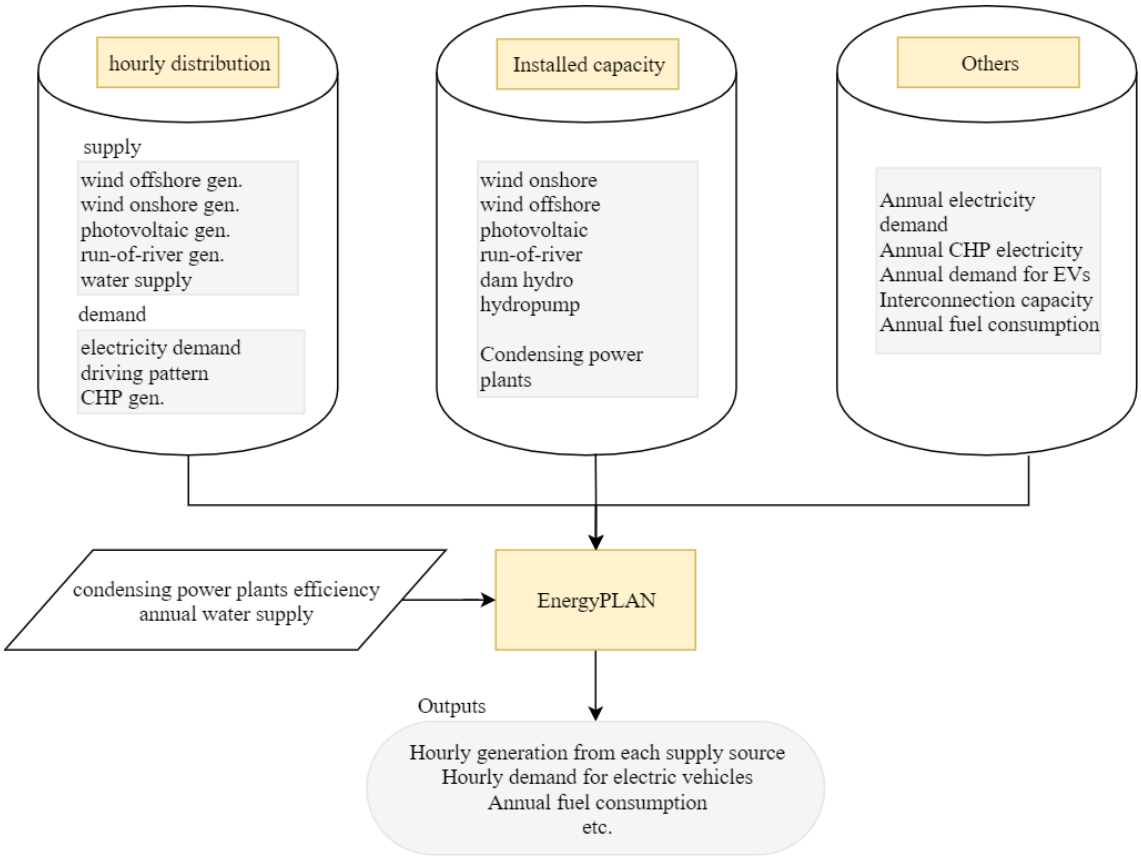

Figure 4.14. Outline of EnergyPLAN inputs and outputs
Summarized scheme of the inputs (e.g. installed capacities) required by EnergyPLAN, and its outputs (e.g. hourly generations).

An important feature from this tool is that it models thermal power plants as one large power plant, independently on the primary fuel distribution inputted. Thus, even though the model considers different fuel types and their primary fuel consumption to calculate emissions, it does not disaggregate thermal powerplants by its fuel type in the simulation. To differentiate between baseload and peak powerplants, in this work, two types of

thermal power plants are considered separately: 1) coal and biomass power plants; and 2) natural gas power plants. As for CHP, those power plants are mainly industrial in Portugal, thus they are also simulated separately.

4.3.2. Multiyear model calibration

In this subsection, the importance of calibrating a model is discussed and an innovative calibration methodology is proposed. It is based on a multiyear calibration, which is later used in this thesis to determine parameters for the future power system.

A scenario simulation should be preceded by a calibration of the model, to make sure it works accurately. "*Calibration is the estimation and adjustment of model parameters and constants to improve the agreement between model output and a data set*" [135]. It is performed by adjusting a set of not perfectly defined parameters to fit the simulation outputs to historical data [135]. The standard calibration of power systems' simulation considers a single year of historical data, regardless of the focus of the study or tool used [136]–[138].

Usually, the calibration parameters are kept constant in the simulation of new scenarios. In systems highly based on renewables, the choice of a meteorological year (usually the most recent or the typical one) to make the calibration can result in inaccuracies when simulating a dissimilar year, e.g. simulating a scenario where precipitation is above average, leading to underestimation of the hydro resource. Thus, single year calibrations will depend on the specific meteorological characteristics of that year. A well-calibrated model should be accurate within all the spectrum of conditions. This issue is particularly important in renewables-based systems with high inter-annual variabilities such as hydro [139] and wind power [140], [141]. In addition to inter-annual changes, climate change also has a significant impact on energy systems' modelling (see Chapter 2) [63], [64].

In this subsection, a proposal of a new calibration method using a multiyear approach, based on linear regressions of weather indicators to determine the calibration parameters is presented. It allows building a flexible simulation model, adjustable to different environmental conditions since the calibration period covers a wide spectrum of system operating conditions.

Before presenting the methods for the standard and multiyear calibration approaches (subsection 4.3.2.2), the specific characteristics of the Portuguese power system used for the calibrations are described (subsection 4.3.2.1). Using as the reference case the Portuguese power system during the period 2011-2015, the results obtained for both calibrations are provided (subsection 4.3.2.3). The subsection ends with the validation of the proposed multiyear calibration (subsection 4.3.2.4) – it addresses the accuracy of

single and multiyear calibrations by modelling two very different years as far as the weather was concerned, 2000 and 2005, and comparing the results.

4.3.2.1. Case study specifics

Portugal has a high share, with significant inter-annual variation, of renewable energy sources in its energy mix, and therefore it is particularly suitable to test the application of the multiyear calibration method.

However, some parameters of calibration are case study-specific, and they will be referred hereafter. For both calibration methods:

- The calibration period was 2011-2015 (in the case of single year calibration, each year of this period represents one different calibration);
- For each year of the calibration period, the correspondent demand and installed capacity were considered;
- The transmission line capacity was limited to its historical value for the year simulated (between 2,370 MW and 3,047 MW [142]);
- Biomass and coal powerplants were modelled together but separately from natural gas powerplants for two main reasons:
    - EnergyPLAN only allows two thermal powerplants to be modelled separately, thus it was not possible to model each type of powerplant individually; and
    - coal and biomass generation are the base generation for the power system, while a significant part of the natural gas powerplants is for backup or peak consumption periods. These powerplants' modelling division allowed a better simulation of the power system by scheduling the base generation first (coal and biomass) and the backup generation as the last resource (natural gas).
- The calibration parameters relevant for the case study are:
    - combined coal and biomass powerplant efficiency ($\eta_{PP,coal\ and\ biomass}$) – to calibrate the primary fuel consumption;
    - natural gas powerplant efficiency ($\eta_{PP,natural\ gas}$) – also to calibrate the primary fuel consumption;

- a dimensionless coefficient for run-of-the-river generation (C_{RoR}) – used to fit the water supply distribution to the run-of-the-river actual generation; and
- the annual water supply normalized to the installed capacity (WS_{norm}, in MWh/MW).

4.3.2.2. Methods

A period of n years of historical data is used to calibrate the model, by determining different calibration parameters Y_i^j , where $i = 1...m$ refers to the parameter (m parameters, such as power plants efficiency or run-of-the-river hydro generation, etc.) and $j = 1...n$ refers to the year. Linear regressions are applied to each calibration parameter using a wide range of weather and energy variables. The regression that best fits each calibration parameter is selected, defining $\widehat{Y}_i$, the calibrated parameter to be used in simulations.

The method is assessed by running energy system simulations for two past years, with very different weather conditions. For each, two approaches are used for the simulations:

(1) n single year calibrations using parameters Y_i^j, denoted *model year j*; and

(2) one linear regression, multiyear (*MY) model*, using $\widehat{Y}_i$.

Figure 4.15 shows a summarized scheme of the proposed methods.

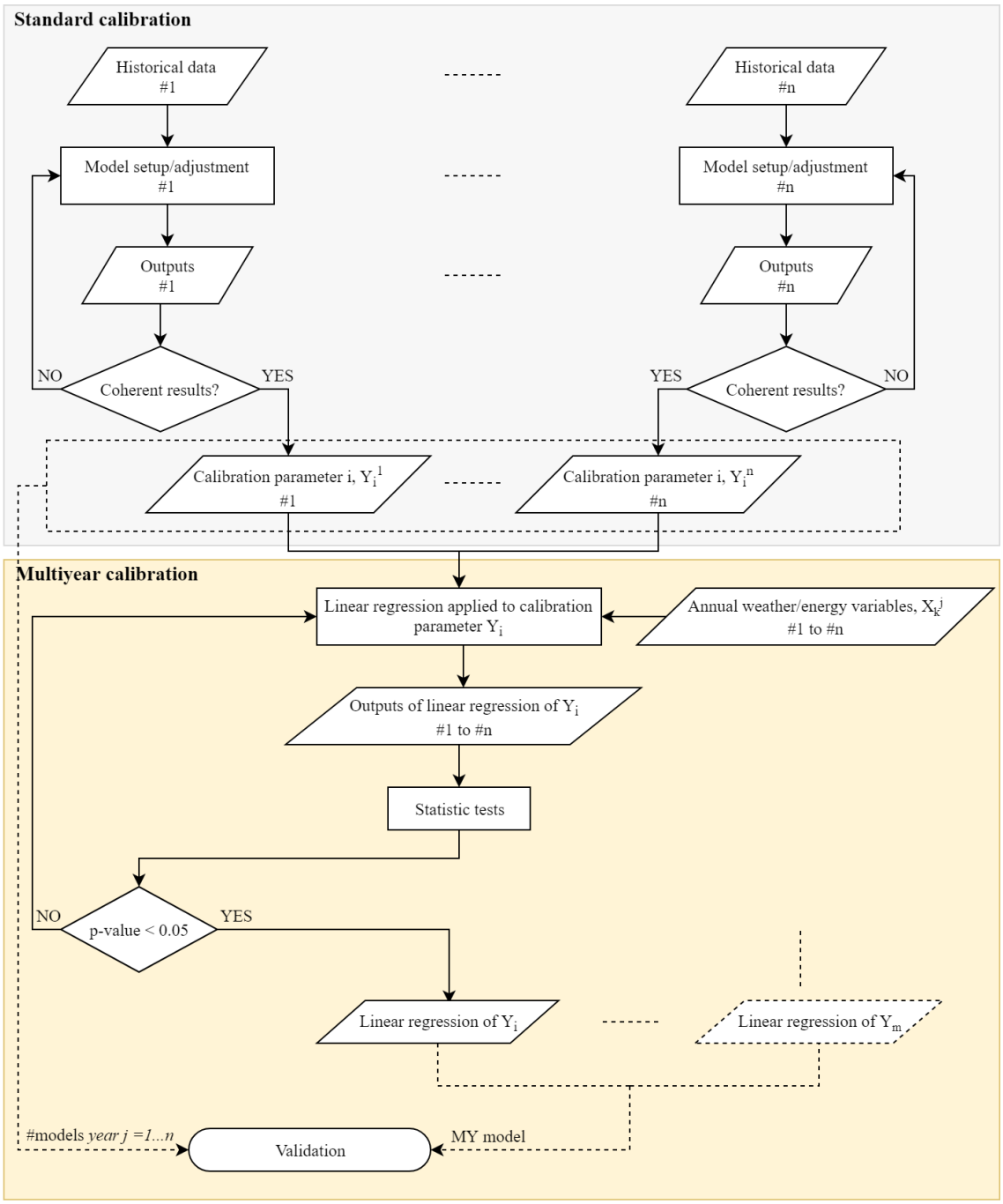

Figure 4.15. Scheme for the multiyear model calibration
Summarized schematic of the methods used to perform the multiyear calibration, using as a basis a standard calibration.

Standard calibrations

A calibration using a historical period should be performed before applying the model to other scenarios. A single year calibration – henceforth denoted *standard calibration* – begins with the input of all the historical data required by the energy system model. Then, it is performed a comparison between selected indicators, such as renewable energy share or annual CO_2 emissions, from historical data and simulation outputs. The calibration is done iteratively, changing model inputs not properly described in the historical data, the *calibration parameters*. It should be noticed that the number *m* of parameters will vary with the case study and/or simulation tool. In power system simulations, the calibration parameters are normally related to the performance of power plants and the available energy resources; these parameters may not be accurately described by the available data and/or may depend on the power plant fleet operating conditions and weather conditions. When an acceptable pre-established maximum difference between the historical and the simulation outputs is achieved, the calibration parameters are finally defined.

Multiyear calibration

The linear regression of standard calibrations results, Y_i^j, to meteorological and energy indicators for the *n* years are used to determine the multiyear calibration parameters. In general, a multivariable linear regression enables the prediction of a dependent variable *Y*, i.e., the calibration parameters Y_i^j, from independent variables X_k, their estimated coefficients $\hat{\beta}_k$, and error ε, as shown in Equation (4.22).

$$Y = \hat{\beta}_0 + \hat{\beta}_1 X_1 + \cdots + \hat{\beta}_k X_k + \varepsilon \tag{4.22}$$

When there is only one independent variable, the linear regression is called simple linear regression. The prediction of the dependent variable lies in testing its relation with different independent variables. Since calibration parameters can depend on the system operation and weather conditions, weather and energy variables were chosen to be tested for each regression, as listed in Table 4.8.

Table 4.8. Independent weather and energy variables
Independent variables tested in the linear regression models to perform a multiyear calibration.

	Independent variables
Weather	Average temperature, T_{avg} [°C]
	Maximum temperature, T_{max} [°C]
	Minimum temperature, T_{min} [°C]
	Precipitation [mm]
	Wind index [MWh/MW_{inst}]
Energy	Electricity consumption [TWh]
	Energy generation [TWh]
	Renewable energy sources' (RES) generation [TWh]

The number *n* of reference years is limited to five because structural changes in energy systems are occurring so fast that using longer periods for calibration would certainly lead to incoherent results. A restrictive set of reference years allows only simple and two independent variable regression models to be tested.

A preliminary analysis using the determination coefficient (R^2) to understand the relationship of the different independent variables with each dependent variable is performed. Independent variables showing an R^2 lower than 30% or without an explainable causal relationship with the dependent variable were discarded.

Then, simple and multivariable linear regressions are applied to the dependent variables. The causality of individual and combined independent variables on the dependent variables is assessed using the RMSE, the determination coefficient R^2 (Equation (4.23)), the p-value of F-statistics and the p-value of Wald-statistics.

$$R^2 = \sqrt{\frac{n \times \sum\left(Y^j \times \widehat{Y^j}\right) - \left(\sum Y^j\right) \times \left(\sum \widehat{Y^j}\right)}{\sqrt{\left[n \times \left(\sum {Y^j}^2\right) - \left(\sum Y^j\right)^2\right] \times \left[n \times \left(\sum \widehat{Y^j}^2\right) - \left(\sum \widehat{Y^j}\right)^2\right]}}} \quad (4.23)$$

In the equations, Y^j and $\widehat{Y^j}$ are the observed and estimated value of the dependent variable in year *j*, respectively.

The p-value serves as a criterion to evaluate which combinations of independent variables should enter in the regression model, using the significance level of 0.05. P-value is the

probability of obtaining a sample more extreme than the ones observed in the data, by assuming the null-hypothesis (Equation (4.24)). The F-statistics p-value of the model gives the significance of the combination of independent variables used, by testing the null hypothesis (H_0) of not using this combination. In the same fashion, the Wald-statistics p-value determines the significance of each individual independent variable. If p-value is higher than 0.05, the null-hypothesis is credible, thus that independent variable should be discarded. If the p-value is lower than 0.05, it is considered that the independent variable is significant and the alternative hypothesis (H_a – Equation (4.25)) should be considered.

$$H_0: \beta_k = 0 \tag{4.24}$$

$$H_a: \beta_k \neq 0 \tag{4.25}$$

It should be noted that the applicability of the multiyear calibration method does not depend on the geographic location or the specificities of the energy system in the study. Also, the choice of EnergyPLAN does not limit the suitability of the method, which could be adapted to any other simulation tool with distinctive characteristics regarding geographic scope, timestep resolution or others.

4.3.2.3. Calibration results

This subsection presents results for the standard calibrations followed by the results of the multiyear approach.

Standard calibration

The results for the five standard calibrations (2011-2015) are shown in Table II.1, Annex II. The simulated indicators differ little from historical data (on average they differ 0.61%). The highest discrepancies regard the import/export balances (9.1% on average), which are due to the fact that import/export trades are market-driven, as opposed to energy balance driven export, as the model considers. The monthly average power demand deviation from historical data is -0.02% on average.

The calibration parameters coal and biomass powerplant efficiency $\eta_{PP,coal\ and\ biomass}$, natural gas powerplant efficiency $\eta_{PP,natural\ gas}$, normalized water supply WS_{norm} and run-of-the-river coefficient C_{RoR} are shown in Table 4.9.

Table 4.9. Standard calibrations for the period 2011-2015
Values of calibration parameters obtained for each of the five standard calibrations from the period 2011-2015.

Standard calibrations – Calibration parameters				
Year	$\eta_{PP,coal\ and\ biomass}$	$\eta_{PP,natural\ gas}$	WS_{norm} [MWh/MW$_{inst}$]	C_{RoR}
2011	0.3049	0.5308	1,685.4	0.5375
2012	0.3175	0.5180	735.6	0.2555
2013	0.3153	0.4620	2,186.3	0.8400
2014	0.3167	0.4315	2,317.8	0.9555
2015	0.3269	0.5005	823.0	0.5615

Multiyear calibration

The effect of each independent variable (e.g. weather and energy variables) on the four calibration parameters is assessed using R^2 coefficient, presented in Figure 4.16. The data regarding the independent variables (in Table 4.8) was gathered from the Portuguese meteorological office and the transmission system operator [96], [98], [142].

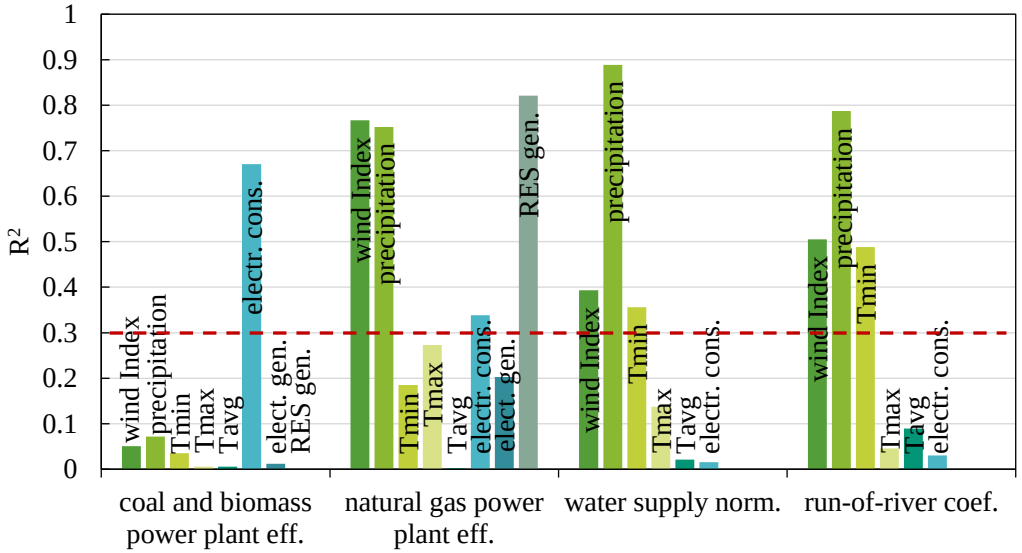

Figure 4.16. Correlation of calibration parameters and independent variables
Correlation results between calibration parameters (coal and biomass power plant efficiency, natural gas power plant efficiency, water supply normalized and run-of-the-river coefficient) and independent variables (wind index, precipitation, T_{min}, T_{max}, T_{avg}, electricity consumption, electricity generation, and RES generation, as Table 4.8 shows).

An assumed $R^2 > 0.3$ threshold associates electricity consumption to the coal and biomass power plant efficiency; wind index, precipitation, electricity consumption and RES

generation to natural gas power plant efficiency; wind index, precipitation, and T_{min} to water supply and run-of-the-river coefficient.

The results of the linear regressions tested to predict each of the calibration parameters are shown in Table III.1-4, in Annex III. The best regression models are presented in Figure 4.17, except for the biomass and coal power plant efficiency. For the latter, the electricity consumption is the only independent variable that leads to $R^2 > 0.3$, but it does not result in a model with statistical significance (p-value>0.05, Table III.1, in Annex III). For that reason, the standard and multiyear calibration consider the average of the efficiency of coal and biomass power plants in the period 2011-2015 (about 31.6%)[6].

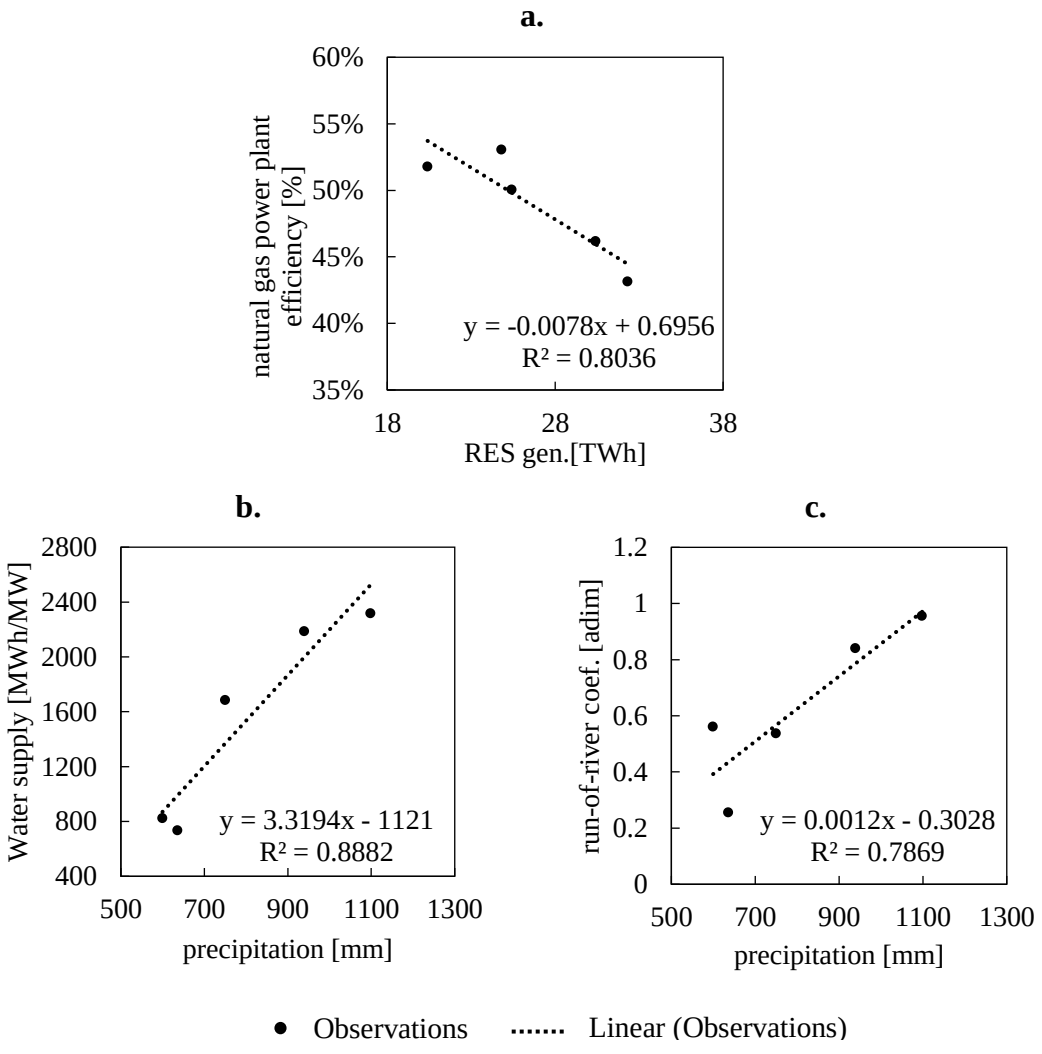

Figure 4.17. Linear regression models chosen for the multiyear calibration
Linear regression models, estimates and observations for each calibration parameter: a. – natural gas power plant efficiency (Model 5 in Table III.2, Annex III); b. – water supply normalized (Model 10 in Table III.3, Annex III); and c. – run-of-the-river coefficient (Model 15 in Table III.4, Annex III).

[6] Since in the future coal power plants are not considered, when simulating the future power system later in this document, this efficiency is solely from biomass power plants and it is assumed to be of 40% [144].

Within the single and multivariable models, the renewable energy generation is the only one that shows significance (F- and Wald p-values < 0.05) for all the considered independent variables when testing the models to predict $\eta_{PP,natural\ gas}$ (see Table III.2, Annex III). Hence, RES generation is the chosen independent variable to determine the natural gas power plant efficiency, as shown in Figure 4.17a. Since thermal power plants are more efficient operating close to the nominal capacity, when renewable generation increases, forcing them to operate at lower levels, their efficiency decreases. To avoid unreasonable efficiencies, those were bounded by a minimum of 40% and a maximum limit of 60%.

Regarding the water supply and the run-of-the-river coefficient (Table III.3 and Table III.4, in Annex III), the regression models showing significance are the simple regressions with rain as an independent variable, as Figure 4.17b and Figure 4.17c show. Thus, those are the chosen models to derive the normalized water supply and the run-of-the-river coefficient.

4.3.2.4. Validation

Using both the single year and the multiyear calibrations, energy system simulations were run for 2000 and 2005. The choice of validation years is determined by convenience, i.e., availability of input data for the simulations, and extreme climate conditions. Using these criteria, the years 2000 and 2005 were chosen: as shown in Table 4.10, 2000 had the second-highest annual precipitation in the past twenty years, while 2005 was the driest year since 1931 [98].

Table 4.10. Historical weather characteristics – Validation
Summary of weather characteristics in Portugal for the validation year 2000 and 2005, compared to the historical mean for the period 1971-2000 [98], [143].

Validation period – Weather characteristics			
	1971-2000 mean	2000	2005
T_{max} [°C]	20.5	21.3	21.6
T_{avg} [°C]	15.3	15.8	15.6
T_{min} [°C]	10.0	10.2	9.7
Precipitation [mm]	882	1082	524

The results for the relevant indicators are shown in Figure 4.18. The percentages indicate the variations of outputs to the historical data of each validation year.

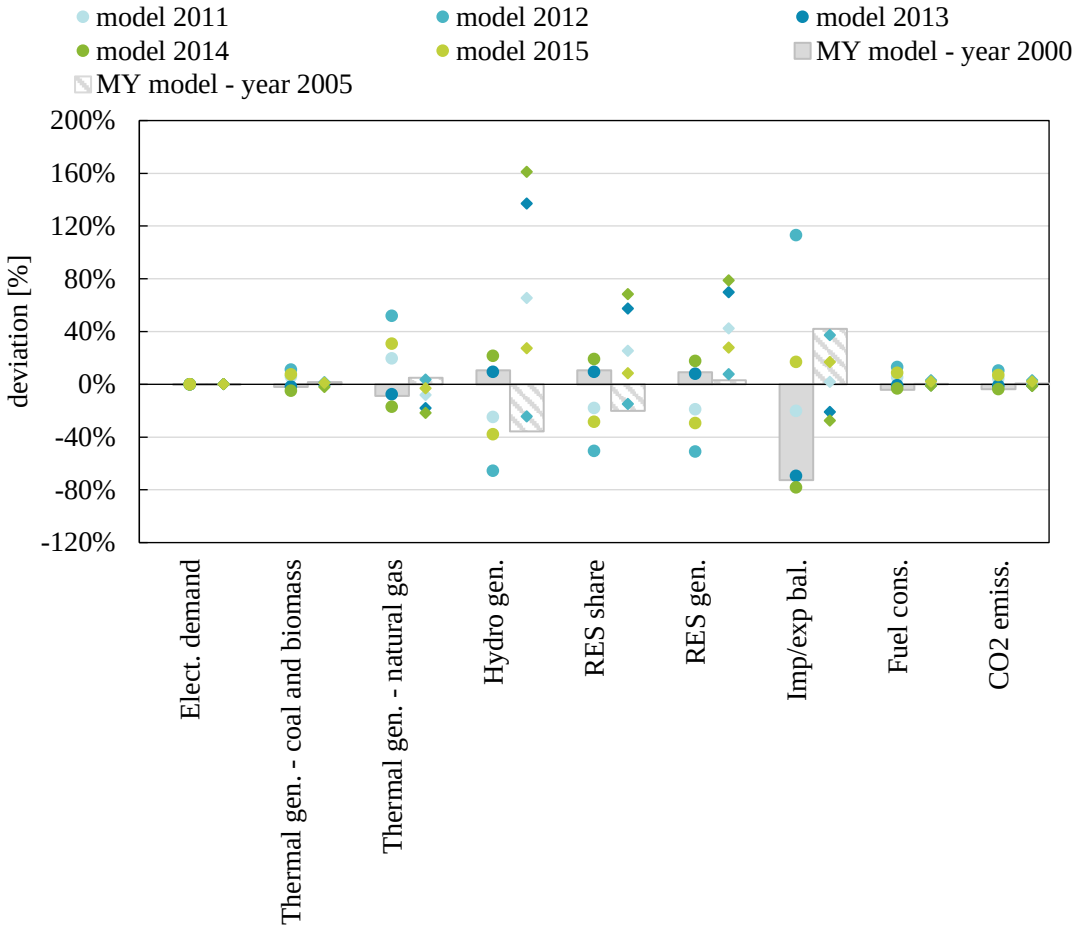

Figure 4.18. Comparison of standard and multiyear calibrations for the validation period
Validation and comparison of the two proposed calibration approaches: 1) dots/diamonds (for validation years 2000 and 2005, respectively) are results from using the inputs of standard calibrations in the validation period; and 2) columns are results from applying the linear regressions to each calibration parameter according to specific conditions of the validation years 2000 and 2005 (solid and dashed filling, respectively).

One can observe that regardless of the calibration used or the year considered, the thermal generation from biomass and coal power plants, the fuel consumption and the CO_2 emissions always present low errors, while the electricity demand shows no differences at all since it does not depend on the calibration parameters. On the other hand, the import/export balance is inaccurate in all the simulations because, as discussed above, international trade is usually market-driven, hence not well described by the technical scope of the simulations.

The importance of the calibration emerges in the large discrepancies in the hydropower generation and, therefore, the renewable and electricity generation. The standard single

year calibrations lead to higher inaccuracies because of the dependency on the weather observed in the respective reference years – the system under study strongly depends on inter-annual changes of available water supply, due to the high potential for hydropower. This resource dependency of hydropower makes its calibration more prone to errors than the abovementioned indicators, such as thermal generation. Model results considering the multiyear calibration for the year 2000 (wet) are slightly better reproduced than 2005 (dry), which may be because the calibration period does not include any year so dry. The wet year 2000 was better reproduced by model 2013 (2013 was also wet – see section 3.1) than when using the multiyear calibration. Model 2012 was the worst reproducing 2000, due to the large differences in precipitation between 2000 and 2012. The dry year, 2005, is better reproduced by the MY model, followed by model 2012 – which was expected, given the similarity between 2005 and 2012.

The average of the modules of the deviations presented in Table 4.11 shows that the multiyear calibration leads to between 2 and 5.8 times minor errors than using single year calibrations regarding hydropower generation, total renewable energy source generation, and share. In addition, the fuel-related indicators (i.e., thermal generation, fuel consumption, and CO_2 emissions) are also slightly better simulated using the MY calibration with about 2 times minor errors than the models 2011-2015.

The dispersion of the deviations obtained with the single year calibrations is well described by the standard deviations, also presented in Table 4.11. It shows that the multiyear calibration leads to between 1.1 and 1.5 times lower standard deviations for all the indicators analyzed.

Table 4.11. Deviations of standard and multiyear calibration for the validation period
Deviations of the simulation results from the observations of 2000 and 2005 using MY model and models 2011: the average of deviation modules, standard deviation and range. The average deviation modules correspond to the average of the module of the deviations. The range is from the minimum to maximum values of the deviation using each approach.

Deviation from historical data - Validation years 2000 and 2005								
	MY model				**models 2011-2015**			
	Avg. of deviation modules	Stand. Dev.	Range		Avg. of deviation modules	Stand. Dev.	Range	
			Min.	Max.			Min.	Max.
Elect. demand	0.0%	0.0%	0.0%	0.0%	0.0%	0.0%	0.0%	0.0%
Coal and biomass gen.	1.8%	3.7%	-1.9%	1.7%	3.8%	4.7%	-5.0%	11.2%
Natural gas gen.	6.9%	17.3%	-8.8%	5.0%	18.2%	22.8%	-21.8%	51.8%
Hydro gen.	23.1%	50.1%	-35.7%	10.6%	57.4%	70.7%	-65.5%	161.0%
RES share	15.3%	28.0%	-20.1%	10.5%	30.0%	35.3%	-50.5%	68.2%
RES gen.	6.1%	25.7%	3.1%	9.1%	35.1%	39.5%	-51.1%	78.8%
Fuel cons.	2.2%	3.8%	-4.1%	0.3%	3.9%	4.8%	-3.1%	13.0%
CO_2 emiss.	2.2%	3.4%	-3.8%	0.6%	3.4%	4.1%	-3.7%	10.5%

Model calibration is vital to trust the accuracy of the results of a simulation project when the operation of a power system is strongly affected by inter-annual changes (e.g. weather conditions), the single year calibration may not accurately reproduce dissimilar scenarios (e.g. different systems' and weather conditions). The multiyear calibration has proven to be much more robust than single year calibration, leading to acceptable results regardless of the characteristics of the simulated year. For this reason, the multiyear calibration is a useful approach to build a more flexible and broad energy model, enabling the study of different scenarios to be less dependent on weather conditions, providing more dependable results.

In this work, the multiyear calibration approach was used, and its results were applied for the inputs required in the future scenarios for the water supply and run-of-the-river coefficient regressions.

Since coal power plants are absent from future scenarios, the efficiency of biomass power plants was set to 40% [144].

For the case of natural gas power plant efficiency, the regression model obtained correlates negatively the renewable generation with efficiency. As mentioned above, a minimum limit of 40% was implemented to avoid the use of unrealistic values. Because the future scenarios considered in this work are highly renewable, the regression model obtained was not applied, and 40% was considered as the efficiency of natural gas power plants.

4.3.3. Modelling the supply sources

In this subsection, the focus will be given to the calculation of the energy generation of the different supply sources included in the system. The methods applied here are the result of the requirements asked by the simulation tool used, EnergyPLAN.

4.3.3.1. Thermal power plants

To simulate the current Portuguese power system, thermal power plants were simulated separately as two big condensing powerplants and one big CHP power plant. For the two condensing power plants (one fueled by coal and biomass, and another by natural gas), the installed capacity, the distribution of its primary fuel consumption, its efficiency and the minimum power capacity were the required inputs, which were based on the historical data provided by the Portuguese Department of Energy and Geology (DGEG) and by the Portuguese Energy Networks (REN) [145], [146].

Using the same sources, for CHP power plants, the electricity generated and the distribution of the primary consumption were introduced; and it was considered that industrial CHP has a constant generation distribution during the year. To ensure a solid base generation for reliability and operational reasons, the minimum dispatchable stabilization share and the thermal generation capacity (see subsection 4.3.1) are defined according to the historical data available [134].

While the simulation of the current system includes all existing powerplants at the moment, the future system only includes natural gas[7] and biomass[8] as supply. In that case, it is given priority to the use of biomass before the consumption of natural gas.

Higher biomass generation is limited by the energy and economic cost of the fuel collection, which can decrease in the future with technology evolution such as process automation. However, more biomass generation would lead to more powerful plants requiring much higher fuel consumption, which would lead to an increasing need for biomass that may no longer be supported by local sources. It would result in the need to import biomass from more and farther locations, which may result in unprofitable and, consequently, unviable businesses. Moreover, the desertification of the territory

[7] When considering a fully renewable power system, natural gas-fueled power plants are not considered.
[8] It also includes residues and waste.

(aggravated by climate change) could also contribute to a lower biomass availability [147]. On the other hand, the strong fires of 2017 (and possibly future fires that may occur due to the migration towards urban areas and climate change) triggered a forest valorization strategy, which can promote biomass use for electricity generation [148].

But carbon-neutrality of biomass is being contested: 1) biomass is, in fact, renewable since the organic material consumed can be generated again (e.g. harvested trees can grow again), but the growth time of, for example, trees should be weighted; 2) biomass burning process is carbon-neutral since the captured CO_2 during the trees' lifetime compensates the emitted emissions, but the time required for the capture of the emitted CO_2 can be of decades, and it is relevant to add that the biomass might burn in fires or be cut down before it sequesters the CO_2 that would compensate its burning; 3) the additional emissions from the biomass generation/collection or even transportation, the land-use changes, and others are not being contemplated in some carbon-neutrality calculations, turning the carbon-neutrality of biomass a debated issue [147], [149].

Biomass use in the future is an issue with a high level of uncertainty as demonstrated by the previous reasons. Therefore, when considering also non-renewable resources, this work considers two frameworks for biomass availability (see subsection 4.3.4): 1) a conservative approach that assumes the same amount of available biomass for the future, as it was in the year 2015; and 2) considering unlimited biomass resources, where natural gas is solely used when the biomass power plants are already using its maximum power capacity.

Besides biomass to some extent, generation from the other renewable sources is much more closely related to weather and climate conditions. The supply generation of those sources is determined by EnergyPLAN with their installed capacity and the normalized hourly distribution of the generation. Hereafter, the methods used to calculate the generation of each type of renewable is explained.

4.3.3.2. *Photovoltaic generation*

The photovoltaic generation was determined for each NUTS III[9] region of the country. The total country generation assumed a weight for each region considering their current photovoltaics' installed capacities.

Photovoltaic energy generation PV_{gen} [W/m^2] is determined by multiplying the irradiance incident on the photovoltaic panels G_i [W/m^2] by the overall efficiency of the system (η_{syst}, in fraction) in each hour t, Equation (4.26).

$$PV_{gen}(t) = G_i(t) \times \eta_{syst}(t) \tag{4.26}$$

The incident irradiance on the photovoltaic panels depends on several factors, including their orientation ψ_{module} and tilt β_{module}. For simplicity, the orientation was always assumed to be South (180º) and the tilt was assumed to be equal to the mean latitude of the region. The incident irradiance is the sum of the beam irradiance on the tilted surface B_i [W/m^2] and the diffuse irradiance on that same surface D_i [W/m^2], Equation (4.27).

$$G_i(t) = B_i(t) + D_i(t) \tag{4.27}$$

The beam irradiance on the tilted surface is obtained as follows.

$$B_i(t) = B_h(t) \times \frac{\cos\left(AOI(t)\right)}{sen(\alpha(t))} \tag{4.28}$$

where B_h is the beam irradiance on the horizontal surface [W/m^2] and *AOI* is the angle-of-incidence [radians]. The sun altitude α is determined according to the Equation (4.15) (subsection 4.2.3.2).

The angle-of-incidence is the angle comprised between the normal to the tilted surface and the beam irradiance on the surface, its cosine is determined by Equation (4.29).

$$\cos\big(AOI(t)\big) = \cos(\alpha(t)) \times sen(\beta_{module}) \times \cos(\psi(t) - \psi_{module}) + sen(\alpha(t)) \times cos(\beta_{module}) \tag{4.29}$$

The sun position along the day can be calculated through the following expression.

$$\psi_a(t) = acos\left(\frac{sen\big(\delta(t)\big) \times \cos(\varphi) - \cos\left(\delta(t)\right) \times sen(\varphi) \times \cos\left(\omega(t)\right)}{\cos\left(\alpha(t)\right)}\right) \tag{4.30}$$

[9] Nomenclature of Territorial Units for Statistical Purposes (NUTS) is a system developed by Eurostat that divides the territory hierarchically for the purpose of statistical studies. NUTS III defines "small regions for specific diagnosis" and include, in the case of Portugal, 30 regions [225], [226].

However, this real azimuth ψ_a must be converted to the corrected azimuth, ψ, according to the time of the day (morning and afternoon). In the morning (when $\omega < 0$), ψ_a is equal to ψ, while in the afternoon ($\omega \geq 0$) ψ is equal to $2\pi - \psi_a$.

In order to ensure that when the beam irradiance does not intersect the panels the beam irradiance on the tilted surface (i.e., on the panels) is null, *cos(AOI(t))* is considered null when the sun altitude is too low (less than 5° from the horizon) and when the beam irradiance coming from the sun intersects the back of the panel. These two conditions are described by the following:

$$\alpha(t) < 5 \times \frac{\pi}{180} \tag{4.31}$$

$$\cos\left(\psi_{module} - \psi\right) < 0 \tag{4.32}$$

Regarding the diffuse irradiance on the tilted surface, it is determined according to Equation (4.33).

$$D_i(t) = D_h(t) \times \frac{1 + \cos\left(\beta_{module}\right)}{2} \tag{4.33}$$

where D_h is the diffuse irradiance on the horizontal [W/m^2], which is calculated following the method CLIMED2 described in [150], Equation (4.34).

$$D_h(t) = G_h(t) \times f_h(t) \tag{4.34}$$

G_h is the global irradiance on the horizontal surface calculated through the climate data available (see subsection 4.2.3.2). The factor f_h varies with the global clearness index, K_t, previously described in subsection 4.2.3.2. Still following [150], f_h is calculated according to the following Equation (4.35).

$$f_h(t) = \begin{cases} 0.995 - 0.081 \times K_t(t) & K_t(t) \leq 0.21 \\ 0.724 + 2.738 \times K_t(t) - 8.32 \times K_t(t)^2 + 4.967 \times K_t(t)^3 & 0.21 < K_t(t) \leq 0.76 \\ 0.180 & K_t(t) > 0.76 \end{cases} \tag{4.35}$$

Having the components of irradiance on the tilted surface calculated, the G_i is easily obtained by their sum, Equation (4.27). To determine the PV generation, the efficiency of the overall system has to be ascertained – it should include the total efficiency of the modules (η_{module}), the efficiency of the inverters ($\eta_{inverters}$) and the cables (η_{cables}).

$$\eta_{syst}(t) = \eta_{module}(t) \times \eta_{inverters} \times \eta_{cables} \tag{4.36}$$

The modules' efficiency is obtained by multiplying two different efficiencies: the nominal efficiency of the modules ($\eta_{nominal}$) and their thermal efficiency ($\eta_{thermal}$, Equation (4.37)).

$$\eta_{thermal}(t) = 1 - TC_{MPP} \times |NOCT - T_{module}(t)| \quad (4.37)$$

The thermal efficiency includes the loss of efficiency according to the increase of the modules' temperature T_{module} [^{0}C], given the temperature coefficient at the maximum point TC_{MPP} [%/°C] and the Normal Operating Cell Temperature $NOCT$ [^{0}C] of a given photovoltaic module. The temperature of the modules is calculated through Equation (4.38).

$$T_{modules}(t) = \frac{NOCT - 20}{800} \times G_i(t) + T_{amb}(t) \quad (4.38)$$

The features of all the system components are presented in Table 4.12.

Table 4.12. Photovoltaic system
Main characteristics assumed for the components of a common photovoltaic system [151]–[153].

Features of photovoltaic system components	
$NOCT$	46°C
TC_{MPP}	0.41%/K
$\eta_{nominal}$	17%
$\eta_{inverters}$	98.8%
η_{cables}	95%

Finally, using the first equation presented in this subsection, Equation (4.26), the photovoltaic generation can be determined.

4.3.3.3. Wind generation

The wind resource is very heterogeneous due to its high sensitivity to rugosity and altimetry of the territory. For this reason, wind farms are normally located in places where the terrain is more favorable to higher wind speeds. In Portugal, wind farms are mostly located in the North and Central regions. Moreover, according to the study performed by Couto et al. [154], the region where the wind speed is better correlated with the Portuguese wind generation is also around the Centre of Portugal. Thus, here, wind data

from the Centre region of Portugal was considered to determine the national wind generation.

In Portugal, one of the most common wind turbines is the Enercon E-82 2MW [155]. For this reason, the power curve of the mentioned turbine was used to characterize the wind generation profile in Portugal, Figure 4.19. This turbine has a rotor diameter of 82 m, maximum power of 2,050 kW and a wind-rated speed of 13 m/s (i.e., its maximum power is achieved at 13 m/s, and for higher wind speeds this maximum power is kept constant) [156].

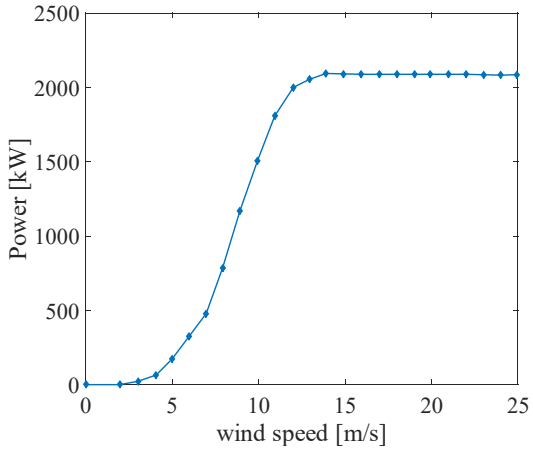

Figure 4.19. Power curve of wind turbine
The Enercon E-82 2MW turbine was considered as a reference – Adapted from [156].

Before applying the power curve to the hourly wind speed data, the wind speed data at the hub height was extrapolated. The original wind speed data is modelled at 10 m above the surface $h_{near\text{-}surface}$ [m], while the average hub height was considered 80 m h_{hub} [m], which is considered a typical value. The following equation was applied to the near-surface wind speed $v_{near\text{-}surface}$ [m/s] to extrapolate the wind speed at the hub height v_{hub} [m/s], Equation (4.39) [157].

$$v_{hub}(t) = v_{near-surface}(t) \times \frac{\ln\left(\frac{h_{hub}}{z_0}\right)}{\ln\left(\frac{h_{near-surface}}{z_0}\right)} \tag{4.39}$$

where z_0 is the mean roughness parameter [m], considered to be of 0.45 m for the Centre of Portugal [158].

Having the wind speed at the hub height, the hourly distribution of wind power generation $Gen_{wind\ on}$ [MW] is determined by applying the power curve at each hour and normalizing the values according to the rated power of the turbine.

The hourly wind offshore generation $Gen_{wind\ off}$ [MW] is obtained by adjusting onshore wind power with a 30% higher capacity factor [101], [159]. The resulting generation can be described by [51]:

$$Gen_{wind\ off}(t) = Gen_{wind\ on}(t) \times \frac{1}{1 - \mathrm{f_{corr}} \times (1 - Gen_{wind\ on}(t))} \tag{4.40}$$

4.3.3.4. Hydropower and run-of-the-river generation

Regarding hydropower generation, EnergyPLAN requires the installed capacity, the annual water supply, its hourly distribution during the year and its efficiency. As stated before, the focus of this work is to establish a methodology that can be applied for the future, where a limited number of variables are available. Since, water supply will not be available for the future, here a simple approach to build an hourly time-series for water supply is presented.

For the annual water supply, an efficiency of 90% [160] was applied to the dam hydro generation. Even though the dam hydro generation will not be available in the future, the annual water supply is one of the calibration parameters which will be characterized through a linear regression with the use of precipitation, an available climate variable for the future (see subsection 4.2.2).

As for the hourly distribution, the approach taken is described hereafter. On the one hand, the water supply is mainly driven by precipitation, since part of the precipitated water runoffs directly into the reservoirs and the other part takes longer to get into the reservoir due to the infiltration on the ground, but it eventually reaches them. On the other hand, the relationship between precipitation and water supply varies with seasons. For example, in a dry season, the amount of precipitation is lower and, usually, the temperatures are higher, which can lead to higher evaporation of water, resulting in lower water availability. Hence, to better describe the relationship between precipitation and water supply, a wet and a dry season have been defined (October to March and April to September, respectively). Using monthly values from 2011 to 2015, two linear regressions (accounting for wet and dry seasons) were created to determine the water supply in function of precipitation, Figure 4.20.

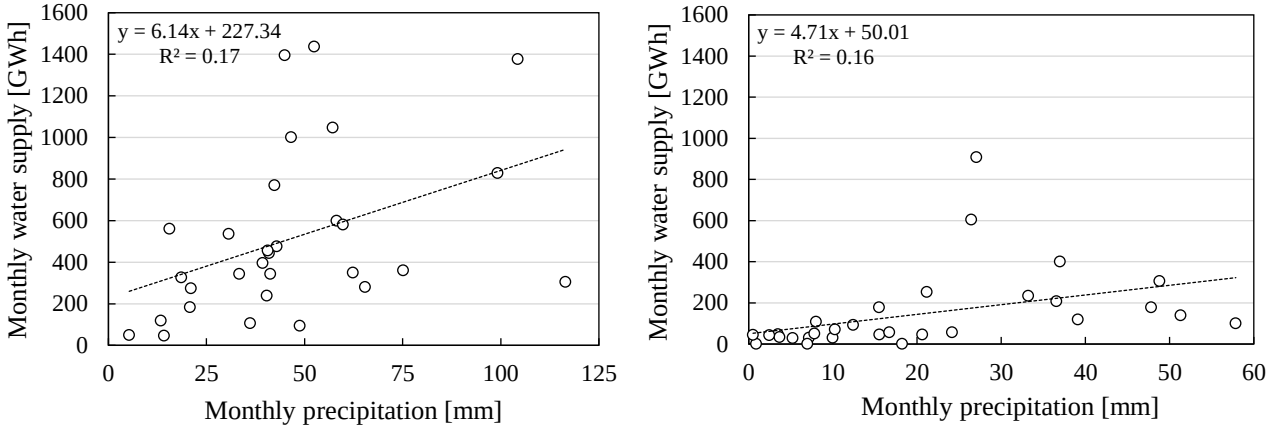

Figure 4.20. Monthly water supply and precipitation in Portugal
Water supply in function of the monthly average precipitation in wet and dry seasons (left and right, respectively) in Portugal, considering data from the period 2011-2015. The wet season was considered from October to March and dry season was from April to September.

The resulting determination coefficients shown in Figure 4.20 are low, indicating the need for a deeper study, which is beyond the scope of this work.

Using the resulting trendlines and the precipitation, the water supply of each month and year was calculated and was then normalized with the highest monthly water supply for each year. Considering the same water supply availability within each month, the monthly values were converted to hourly values, resulting in an hourly vector of 8,784 values. To avoid abrupt discontinuities, a three-days wide moving average filter was applied. The hourly distribution of water supply (*WS*) is represented in Figure 4.21. The close-up figure below clearly shows the effect of the filter.

It is worth noting that the water supply is used to determine the water availability existing during the year for dam hydro generation. Dam hydro operates as a giant buffer of energy, i.e., it can store a large amount of energy (in this case, in the form of gravitational potential energy) and use it whenever it is necessary, as it is a dispatchable generation source. Hence, a fine and highly accurate resolution is not of major importance.

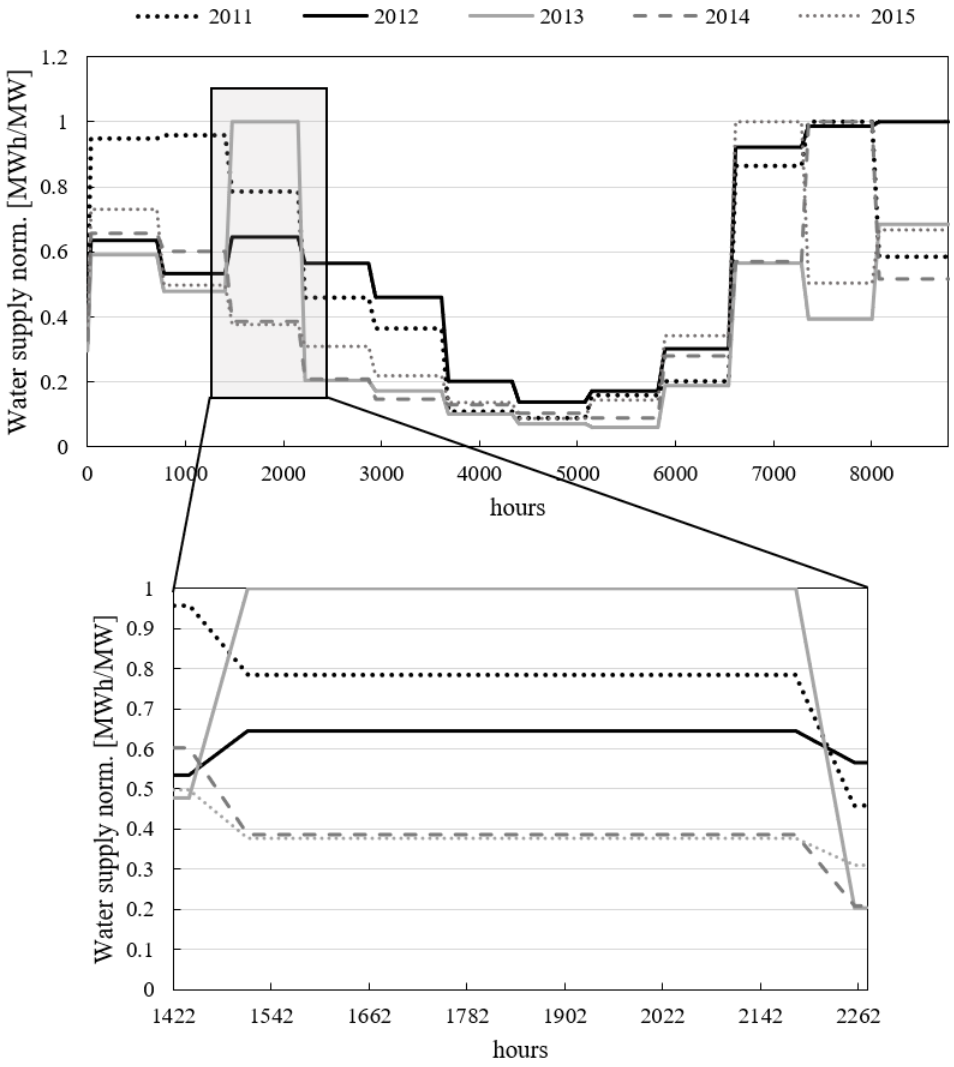

Figure 4.21. Yearly distribution of water supply
Hourly distribution of normalized water supply from 2011 to 2015 and for March (above and below, respectively).

For modelling run-of-the-river generation, precipitation is expected to be the ideal proxy, in a first approach. However, the direct linking from precipitation to run-of-the-river generation raises some critical issues. First, some run-of-the-rivers powerplants have small reservoirs that provide some generation. Secondly, the Spanish operation of their own hydropower plants also influences the Portuguese river flow, which will therefore also depend on the precipitation in Spain. Hence, run-of-the-river is assumed to be solely driven by the water supply distribution. Even though the water supply is not the only variable to the run-of-the-river generation, it generally represents the energy that should be available to generation. Thus, the run-of-the-river generation distribution Gen_{RoR} [MW] took into account the water supply hourly distribution described above, multiplied

by a dimensionless coefficient (which is called run-of-the-river coefficient, C_{RoR}, see subsection 4.3.2) and by the installed capacity P_{RoR} [MW], to fit the annual run-of-the-river generation, Equation (4.41).

$$Gen_{RoR}(t) = WS(t) \times P_{RoR} \times C_{RoR} \tag{4.41}$$

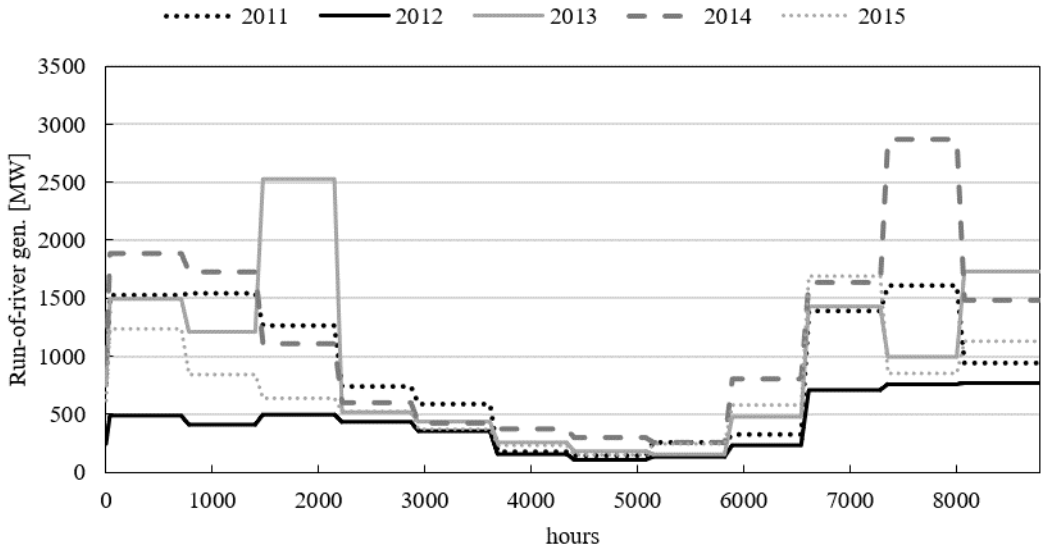

Figure 4.22. Yearly distribution of run-of-the-river generation
Run-of-the-river generation obtained through the water supply distribution, installed capacity and calibration parameter C_{RoR}.

4.3.4. Future power system

In this subsection, a detailed description of the Portuguese power system configuration in 2050 is suggested. Two major configurations are proposed:

1) Highly renewable power system (HiRES)

The power system with high penetration of renewable energy sources (HiRES) includes 20 GW of photovoltaics and 10 GW of onshore wind, reflecting a projection for Portugal in 2050, which is in line with the literature found and summarized in Table 4.13. Although those capacities may seem hard to achieve considering the current Portuguese power fleet, the fast deployment of photovoltaics and wind power has already been proven to be attainable [161].

Table 4.13. Photovoltaic and wind onshore power in literature
Summary of literature on photovoltaics and onshore wind capacities in Portugal in 2050.

Summary of literature on photovoltaic and wind onshore capacities in Portugal in 2050		
	Photovoltaic [GW]	Wind onshore [GW]
Anjo et al. [106]	9.3	7.8
Jacobson et al. [110]	34.9	8.1
Nunes et al. [101]	10.3-16.7	7.6
RNC2050 [162]	19-26	7.1-13

Other installed capacities are adapted from the work of Nunes et al. [100]. About 88% of the installed capacity uses renewable energy sources. It still has a considerable amount of natural gas power plants; those are mainly used to face peak consumption periods when biomass power is not enough or when biomass resource has run out. Table 4.14 shows the configuration of the highly renewable power system.

Table 4.14. Proposed high renewable penetration power system
Configuration of the Portuguese power system considered in the high renewable penetration power system (HiRES) in 2050 [100], [163].

Configuration of future power system – HiRES	
	Installed capacity [GW]
Photovoltaics	20.0
Onshore Wind	10.0
Offshore Wind	1.4
Run-of-the-River	2.9
Dams	5.7
Thermal power plants	
Biomass and others[a]	1.0
Natural gas	4.9
Industrial CHP	
Biomass	0.4
Natural gas[b]	0.8
Hydropump	4.0

[a] It is considered thermal power plants fueled by biomass, residues, and waste.
[b] For HiRES+UB, natural gas-fueled industrial CHP power plants are replaced by biomass-fueled CHP.

The biomass resource available to electricity generation in thermal power plants is the same as in the year 2015, about 5.4 TWh [145]. As mentioned in subsection 4.3.3.1, when this limited biomass runs out, the power plants may continue to operate (within its power capacity) but fueled by non-renewable residues or waste. While in the calibration exercise the minimum thermal power plant capacity was the one observed in historical years (still considering coal-fueled power plants), here a minimum power of 50% of the biomass power capacity is considered due to its flexibility constraints [164], [165].

The primary energy consumption and electricity generation from industrial CHP is also considered to be similar to the year 2015; the consumption was 13.1 TWh of biomass and 14.3 TWh of natural gas and its corresponding electricity generation was about 6.1 TWh [145], [146].

To address the impact of renewable resource limitation, a variation of the HiRES scenario was tested: a high renewable penetration power system with unlimited biomass resources

(HiRES+UB). The main difference between HiRES and HiRES+UB is the unlimited biomass resource available for thermal power plants and CHP (for the latter, the primary energy consumption of biomass is the sum of the biomass and natural gas resource considered previously).

Even though the spatial distribution of supply and demand is not considered in the simulation tool used, here, the transmission and distribution power losses are contemplated in a simplified manner. Such losses were applied to the electricity demand included in the simulation tool. The suggested power system has 6.5% of power losses. In 2050, about 4.9% of transmission and distribution power losses are expected on average for Europe [166]. Although Portugal has been constantly showing higher losses [167], a similar development should be expected for the country. It was assumed that the difference between the European and Portuguese average losses (in the period 2010-2014 [167]) would be reduced by half, resulting in losses of about 6.5% in 2050.

A cross-border interconnection capacity of 5 GW is proposed for 2050, as per the literature (Table 4.15).

Table 4.15. Future cross-border interconnection in Portugal
Summary of literature on the future interconnection capacity for the Portuguese power system.

Summary of literature on future cross-border interconnection capacity for Portugal		
	Time-horizon	Interconnection [GW]
PDIRT 2018-2027 [168]	2027	3.2-3.6 GW
PNEC [169]	2030 | 2040	3.2-4.2 GW | 3.5-4.7 GW
APREN & POYRY [170]	2040	5-8 GW

2) 100% renewable power system (100%RES):

Here, all the non-renewable energy sources are discarded. The industrial CHP is also discarded to avoid a prohibitive requirement for biomass; thus it is assumed that the industries using CHP: 1) will absorb a higher fraction of their electricity generation due to the electrification of other processes that are not heat-intensive; and 2) new technologies may arise allowing electrification of such industries.

This proposed 100% renewable power system entails a significantly smaller fraction of dispatchable generation comparing to the present one, which may lead to grid stabilization issues. To avoid this, considering expectable technology developments, it is assumed that energy storage technologies and about 15% of the capacity of non-dispatchable

renewables are able to provide grid stabilization, complementing the one provided by dispatchable generation.

4.4. Power system model – Demand-flexibility [10]

In this section, the description of electricity demand of each sector (mobility, residential, services, industry and agriculture) is presented. First, a detailed description of the methods for creating the social evolution scenarios is provided for each sector (subsection 4.4.1). Then, the methods used to calculate the electricity demand and flexibility for the different sectors are presented (subsection 4.4.2).

4.4.1. Scenarios for the evolution of society

It is incredibly hard to speculate how the future of society will be, but different paths can be explored to have an unbiased wide range of options. Ideally, distinct qualitative visions provided by stakeholders should aid the quantitative description of more robust scenarios for the development of economic sectors [171]. In this work, that was not feasible, thus a quantitative approach for scenario building was implemented. However, to make the analysis wider, five scenarios were built for each sector of society, focusing mainly on two indicators: impact on the overall electricity demand and power system flexibility – e.g. the grid-support provided by EVs, using smart charging, V2G, battery capacity, and others.

First, a Central scenario was designed considering conservative assumptions – the reference scenario. Then, four other scenarios were designed around the reference according to the previously mentioned indicators – i.e., two scenarios where both indicators increase/decrease and two others where one indicator increases and the other decreases, always keeping the comparison to the Central scenario.

In order to facilitate the process, two paths were created for the electricity demand (Low demand – LoDe, and High demand – HiDe) and the other two for the system flexibility (Low flexibility – LoFlex, and High flexibility – HiFlex). Then, the four scenarios were built by a combination of the paths – e.g. scenario LoDeLoFlex considers the path LoDe for electricity demand and path LoFlex for the system flexibility. The relation between the five scenarios is qualitatively represented in the scheme of Figure 4.23.

[10] Part of this section is adapted from Figueiredo et al., 2019 [227] and Figueiredo et al., 2020 [under review in Applied Energy Journal].

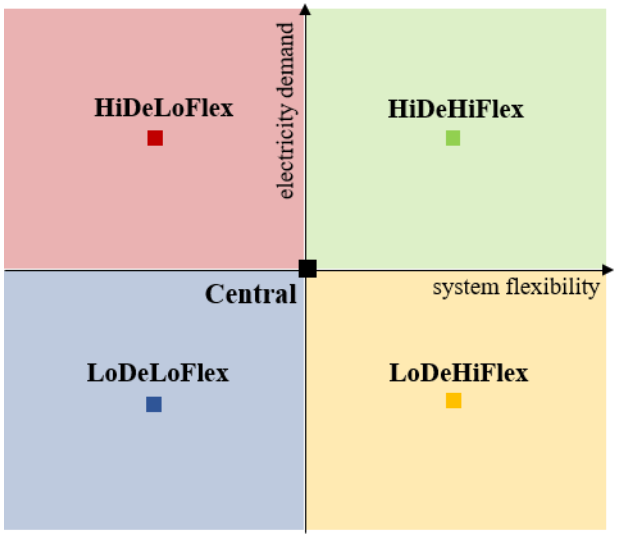

Figure 4.23. Demand-flexibility scenarios
Qualitative scheme of the relative position of four scenarios in comparison to the Central scenario, in terms of the electricity demand and the power system flexibility.

It should be underlined that many parameters determine each pathway for a particular sector. For instance, for the mobility sector, higher electricity demand (relative to the Central scenario) might be due to higher penetration of electric vehicles or more and/or longer trips. The pathway that represents higher electricity demand in mobility is built considering strong (but reasonable) assumptions on all these parameters. A similar approach is performed for the remaining economic sectors.

In the following subsections, the paths considered for each sector are described.

4.4.1.1. Mobility

Nowadays, strongly supplied by fossil fuels, mobility is a sector with relevant CO_2 emissions. Transportation is witnessing a transition in supply sources from fossil fuels to electricity. With renewables as the main source of electricity supply, transport electrification has a high potential for decreasing significantly CO_2 emissions.

A consensual projection for the future of transportation is that it will suffer significant electrification. However, several questions with neither simple nor consensual answers arise. Will people shift to shared transports? Will vehicle batteries have bigger energy capacities? Will people travel more or less? Will people adhere to the smart charging of their vehicles and help grid stabilization? In this work, the focus is given to light

passenger transportation and to the road transportation of goods[11]. In addition, biofuels' vehicles were considered in detriment of hydrogen-propelled vehicles (see section 4.5).

Central scenario

The electricity demand for electrified transportation depends on parameters such as EV penetration, the number of light passenger privately-owned vehicles (referred below as private vehicles), electricity consumption per kilometer, daily travelled distance per vehicle, etc. The assumptions taken for the reference – Central scenario – are presented in Table 4.16.

For this scenario, two types of privately-owned light passenger electric vehicles are assumed: PEV (Pure Electric Vehicles) and PHEV (Plug-in Hybrid Electric Vehicles). The daily distance travelled by a PEV was assumed as 35 km/vehicle/day [172]. For the PHEV, the daily distance travelled on electric mode was assumed to be 95% of the distance travelled by a PEV (i.e., about 33 km/vehicle/day), since most of the car trips in Europe are shorter than the 85 km electric-mode autonomy of a PHEV [173] (only 20% of the trips are longer than 25 km) [101], [172]. To prevent significant damage to the vehicle's battery, it was assumed that only a fraction of the battery capacity (about 85% [174]) would be available for smart charging.

The electricity consumption from freight transportation is bounded by the results of RNC2050 [175], assuming only battery electric vehicles. In the Central scenario, the electricity consumption of freight transports is considered half of the highest value assumed in the Portuguese roadmap RNC2050 [12]. Thus, electrification of 50% and about 30% is considered for light- and heavy-duty vehicles, respectively. The charging characteristics of this type of transport are similar to the ones from the private vehicle's fleet, e.g. the fraction of vehicles available to smart charge and V2G are equal to the values assumed for the private fleet.

[11] The electrification of heavy-duty passenger vehicles was not considered, since they represent a small fraction of the total national electricity consumption with about 0.16-0.38 TWh [109].

[12] The highest EV penetration shown in RNC2050 assumes 100% and 63% of electrification of light- and heavy-duty freight vehicles, respectively [175].

Table 4.16. Central scenario – Mobility
Characteristics considered for the vehicles' fleet in the Central scenario, including electric vehicle penetration, number of private light passenger vehicles, vehicle characteristics, etc.

Central scenario – Mobility	
Light passenger vehicle	
EV penetration	61.4% [100]
PEV	33.7% [100]
PHEV	27.6% [100]
Nº of private vehicles	4.175 million [172]
Nº of shared AeVs	-
Electricity consumption	0.17 kWh/km [176]
Daily distance of private vehicles	
PEV	35 km/vehicle/day [172]
PHEV	33 km/vehicle/day [101], [172]
Vehicle characteristics	
Efficiency grid-to-battery and battery-to-grid	90% [177]
Battery capacity	
PEV	41 kWh/vehicle [178]
PHEV	18 kWh/vehicle [173]
Capacity of grid-connection	
PEV	22 kW/vehicle [178]
PHEV	3.6 kW/vehicle [173]
Freight transportation	
EV penetration	
Light-duty vehicles	50%
Heavy-duty vehicles	31.5%
Charging characteristics (similar to both fleets)	
Driver patterns	
max. share of cars driving during rush hours	20% [177]
% of parked vehicles grid-connected	70% [177]
Charging behavior	
% of vehicles available to smart charge	80%
% of vehicles available to V2G	40%
% of battery capacity available	85% [174]

Paths for electricity demand

Paths Low and High electricity demand represent two alternative and opposite paths that shift away from the Central scenario:

Path Low Demand (LoDe) – a significant decrease in electricity demand is considered due to an 80% decrease in privately-owned vehicles, replaced by shared autonomous electric vehicles (AeVs). An autonomous vehicle is assumed to be able to substitute 5.25 private vehicles [179]. The electricity consumption [kWh/km] of the private vehicles decreases 20% due to technical efficiency gains whilst for shared AeVs it decreases 45% [180], due to usage efficiency gains (optimized velocity and vehicles' distance). On the other side, since a significant part of non-drivers (elderly, disabled, teenagers, etc.) is expected to do more trips due to the easy use of shared vehicles, the daily distance per vehicle increases 14% for the AeVs [181]. Besides those additional car users, the increasing travelled distance of AeVs can also be representative of the shifting from public transport users to car-sharing users and of the last-mile travelled through car-sharing (without such option, the last-mile would be probably completed by walking or riding a bicycle). It is assumed that there is no electrification of freight transportation[13].

Path High Demand (HiDe) – assumes that light-duty passenger vehicles are all privately-owned with 100% EV penetration. EV consumption and distance travelled are assumed constant. The freight transport is assumed to be partially electrified with an electricity consumption equal to the highest electrification consumption of road freight transports assumed in the Portuguese roadmap [175]. It results in total electrification of the light-duty freight vehicles and a 63% electrification of the heavy-duty freight vehicles.

The relative differences between paths Low and High electricity demand to the Central scenario are presented in Table 4.17.

[13] As is in the least electrified scenario of RNC2050 [175].

Table 4.17. Relative differences between Low and High electricity demand paths – Mobility
Characteristics considered for the vehicle's fleet for the Central scenario and the relative differences assumed for the Low and High electricity demand paths.

Relative differences between Low and High demand paths – Mobility			
	Central	LoDe	HiDe
Light-duty passenger vehicles			
EV penetration	61.4%[a]	-50%	+63%
PEV	33.7%[a]	-50%	+63%
PHEV	27.6%[a]	-50%	+63%
Nº of private vehicles	4.175 million	-81%	-
Electricity consumption			
Private vehicles	0.17 kWh/km	-20%	-
Shared AeVs		-45%	-
Daily distance of private vehicles			
PEV	35 km/vehicle/day	-	-
PHEV	33 km/vehicle/day	-	-
Daily distance of shared AeVs	35 km/vehicle/day	+14%	-
Freight transportation			
EV penetration			
Light-duty vehicles	50%	-100%	+100%
Heavy-duty vehicles	31.5%	-100%	+100%

[a] Penetration on the overall light passenger vehicle fleet.

The number of private/shared EVs, the travelled distances, the distinguished consumptions and travelled distances for the demand evolution paths (LoDe and HiDe) are shown in Table 4.18.

Table 4.18 Electricity demand paths – Mobility
Characteristics considered for the vehicles' fleet in the Central, Low and High demand paths, including electric vehicle penetration, number of private light-duty vehicles, vehicle characteristics, etc.

Electricity demand paths – Mobility			
	Central	LoDe	HiDe
Light-duty passenger vehicles			
EV penetration	61.4%	30.7%	100.0%
PEV[a]	33.7%	16.9%	55.0%
PHEV[a]	27.6%	13.8%	45.0%
Shared AeV penetration	-	76.2%	-
Number of light-duty passenger vehicles [million]			
Private vehicles	4.175	0.835	4.175
Shared AeVs	-	0.636	-
Total number of light passenger EVs	2.563	0.893	4.175
Electricity consumption [kWh/km]			
Private vehicles	0.17	0.13	0.17
Shared AeVs		0.09	
Daily distance [km/vehicle/day]			
Private vehicles			
PEV	35.0	35.0	35.0
PHEV	33.0	33.0	33.0
Shared AeVs	35.0	39.9	35.0
Freight transportation			
EV penetration			
Light-duty vehicles	50%	-	100%
Heavy-duty vehicles	31.5%	-	63%

[a] PEV and PHEV penetration on the overall light passenger vehicle fleet.

The availability of EV batteries to support the power system, via storage and/or demand response, depends on the driving patterns, which determine the parking patterns. Pathway HiDe assumes that driving patterns of all vehicles will be as those from today's light

passenger vehicles, as in Ref. [182]. Pathway LoDe, on the other hand, considers changes in urban mobility which are expected to have an impact on driving patterns, and thus the patterns of EVs connected to the power grid. It was assumed that the shared mobility pattern corresponds to today's pattern of public transportation added to 10% of the ones of bike and walking trips. The LoDe driving pattern is obtained weighting the patterns of light passenger and shared mobility vehicles (see Table 4.18). Figure 4.24 presents the assumed impact for workdays and weekends for both pathways.

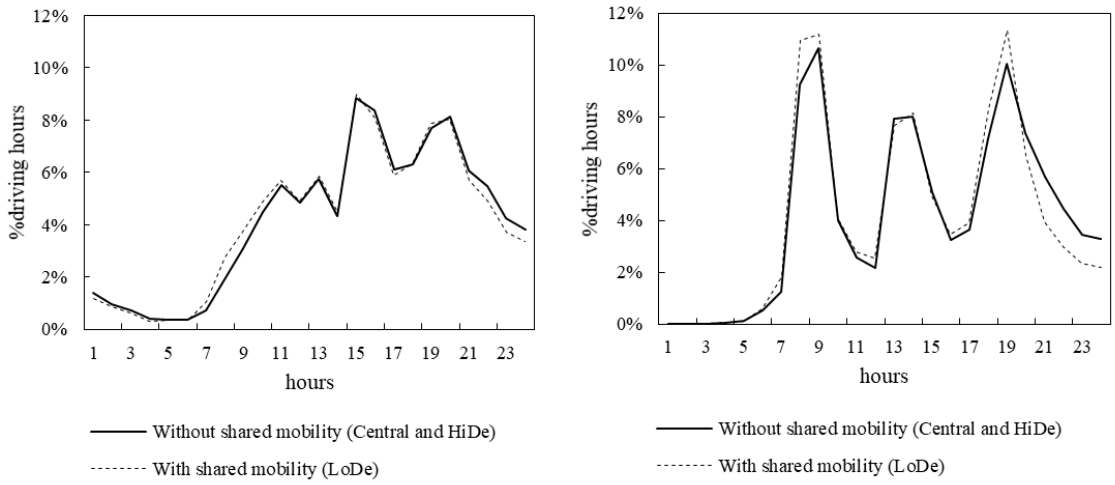

Figure 4.24. Driving patterns
Driving profiles for the electric vehicle's fleet for a weekend day (left) and working day (right) [182].

Paths for power system flexibility

The impact of mobility sector on the power grid flexibility is determined by the parking characteristics, the charging behavior, and vehicle characteristics.

Private vehicles are parked most of the time (c.a. 90%) and only a maximum of 20% is driving during rush hours. Shared AeVs spend more time on the road, being parked only 60% of the time [183]. Assuming a direct proportion between driving time and the cars driving in rush hours, the maximum share of AeVs driving during rush hours is 80%. It is assumed that 80% of private vehicles are smart charged, while the remaining are charged whenever plugged in (i.e., dumb or rigid charging). About 40% of the vehicles are available to V2G. Similar assumptions are considered for the freight fleet.

Central assumes as a typical PEV a 41 kWh battery capacity and a 22 kW power connection capacity, which are both characteristics of the current Renault Zoe [178]. For the PHEV, the Chevy Volt is used with a typical battery capacity of 18 kWh and a power capacity of 3.6 kW [173]. The AeVs are assumed with the same characteristics as PEVs

(i.e., same battery and power capacity). The summary of the assumptions of Central path for the power system flexibility is shown in Table 4.19.

Again, the alternative paths to explore contrary evolutions on the system flexibility are hereafter described.

Path Low Flexibility (LoFlex) – this path considers a limited contribution to the power system flexibility, including a 20% decrease in parking availability and smart charging adoption. It also considers a 50% decrease in the availability of vehicles to V2G. The power and battery capacity are assumed to remain the same as in Central, i.e., of 22 kW and 41 kWh for PEV and 3.6 kW and 18 kWh for PHEV, respectively. The charging features are similar for light-duty passengers and freight fleet.

Path High Flexibility (HiFlex) – electric vehicles provide some system flexibility in this path. The parking and smart charging adoption increase 20%, V2G availability and the battery capacity increased 50% in comparison to Central. Power capacity is assumed as 43 kW for PEV and 7 kW for PHEV, resulting in a capacity improvement of 95% compared to the Central scenario. The flexibility characteristics are considered to be similar for private passenger and freight vehicles.

The relative differences described previously are summarized in Table 4.19.

Table 4.19. Relative differences between Low and High flexibility paths – Mobility
Characteristics considered for the vehicle's fleet for the Central scenario and the relative differences assumed for the Low and High flexibility paths.

Relative differences between Low and High flexibility paths – Mobility			
	Central	LoFlex	HiFlex
Light-duty passenger vehicles			
Vehicle characteristics			
Battery capacity			
PEV	41 kWh/vehicle	-	+50%
PHEV	18 kWh/vehicle	-	+50%
Capacity of grid-connection			
PEV	22 kW/vehicle	-	+95%
PHEV	3.6 kW/vehicle	-	+95%
Charging characteristics (similar to both fleets)			
Parking characteristics			
max. share of cars driving during rush hours			
Private vehicles	20%	+20%	-20%
Shared AeVs	80%	+20%	-20%
% parked vehicles grid-connected	70%	-20%	+20%
Charging behavior			
% of vehicles available to smart charge	80%	-20%	+20%
% of vehicles available to V2G	40%	-50%	+50%

The assumptions taken for each flexibility path are described in the following Table 4.20.

Table 4.20. Flexibility paths – Mobility
Characteristics considered for the vehicles' fleet in the Central, Low and High flexibility paths, including electric vehicle penetration, number of private light-duty vehicles, vehicle characteristics, etc.

Flexibility paths – Mobility			
	Central	LoFlex	HiFlex
Light-duty passenger vehicles			
Vehicle characteristics			
Battery capacity [kWh/vehicle]			
PEV	41	41	62
PHEV	18	18	27
Capacity of grid-connection [kW]			
PEV	22	22	43
PHEV	3.6	3.6	7
Charging characteristics (similar to both fleets)			
Parking characteristics			
max. share of cars parked during rush hours			
Private vehicles	20%	24%	16%
Shared AeVs	80%	96%	64%
% parked vehicles grid-connected	70%	56%	84%
Charging behavior			
% of vehicles available to smart charge	80%	64%	96%
% of vehicles available to V2G	40%	20%	60%

4.4.1.2. Residential sector

The residential electricity demand represents a significant fraction of the total final electricity demand, about 30% in the European Union [184]. As climate changes and the electrification of heating and cooling devices increases, the electricity consumption of a residential building may also change. Such changes may also be enhanced by the electrification of other domestic equipment. As for any other economic sector, the residential electricity demand depends on the assumptions made for the evolution of social behavior and choices.

Central scenario

The residential electricity demand depends mainly on the electricity consumption of residential buildings, which in turn depends on location, weather, its own characteristics (construction materials), its purpose, occupation, type, etc. The energy performance of a building is generally determined through its heat balances. Heat gains and losses both change significantly with the density of people, building insulation, solar exposure, appliances, outside air infiltration, etc.

The Central scenario considers 2.5 people per dwelling[14], assuming 9.2 million inhabitants in Portugal in 2050 [185]. The behavior of occupants is crucial to understand the profile of consumption on weekdays and weekend days, which is considered to remain the same as today's [186].

According to the Buildings Performance Institute Europe (BPIE), European countries should increase their renovation rate of old constructions up to 3% per year to meet international commitments [187]. However, Europe is still far from this goal, with a current yearly average rate of 1.2% [187], whilst in Portugal, it is lower, 0.06% [188], [189]. Regarding new residential buildings per year, Europe presents a rate of 0.5% according to the EU Buildings Database (2014) [190], while in Portugal is 0.13% (2016) [188], [189]. To keep reasonable retrofitting/new buildings' rates for all scenarios, the Central scenario assumes a retrofitting rate of 2% per year and one of 0.75% for new buildings. It is also assumed that older buildings are replaced/retrofitted first. The retrofitting and new buildings' rates were assumed to have a linear development until 2050, assuming the previously mentioned values for Portugal in 2016 as their starting point.

The characteristics of the new or retrofitted buildings follow the evolutions below, depending on the nature of the parameter:

- Distributions without significant changes in the future housing stock: overall thermal transmittance of the internal envelope (i.e., envelope in contact with non-usable areas), linear thermal bridges, normalized overall opaque area, ceiling-to-floor height, etc. Their distributions were kept constant and equal to the values assumed in Ref. [191], Table 4.21;

[14] According to the Portuguese Census 2011, the average number of people per dwelling was of 2.6 [213].

Table 4.21. Housing stock characteristics remaining constant
Probability distribution functions considered and their parameters for the housing stock, which are assumed to be the same in the future housing stock [191].

Probability distribution functions considered and their parameters		
	Type	Parameters
Overall thermal transmittance of the internal envelope, U_i	Weibull	$\lambda = 1.411$ $Wm^{-2}K^{-1}$; $\kappa = 2.914$
Length of linear thermal bridges, l_ψ/A_{op}	Weibull	$\lambda = 1.169$ m^{-1}; $\kappa = 1.756$
Internal-to-opaque envelope area, A_i/A_{op}	Weibull	$\lambda = 0.343$; $\kappa = 1.835$
Ceiling-to-floor height, h	Burr	$\lambda = 2.567$ m; $\kappa = 36.864$; $\nu = 0.560$

- No further changes from today's standards: external envelope thermal transmittance, linear thermal transmittance, normalized window area, shading g-value for windows, air infiltration rate and glazed surface g-value for normal incidence. It considers that future buildings keep the average values of modern buildings, i.e., buildings built in the present (taken from the updated database of ADENE – Portuguese Energy Agency [192], Table 4.22);

Table 4.22. Average characteristics of new dwelling as of 2017
Average values of characteristics of new dwellings in 2017, including thermal transmittance, shading g-value, etc. [192].

Characteristics of modern buildings in 2017	
	Average value
External envelope thermal transmittance, U_e	0.45 $Wm^{-2}K^{-1}$
Linear thermal transmittance, ψ	0.4 $Wm^{-1}K^{-1}$
Window-to-floor area, A_{window}/A_{floor}	0.25
Shading g-value for windows, g_{shaded}	0.1
Glazed surface g-value for normal incidence, $g_{gl\perp}$	0.56
Air infiltration rate, ACH	0.65 ACH

- Linear development towards the projected values in 2050: windows thermal transmittance (from an average of 2.2 $Wm^{-2}K^{-1}$ in 2017 to 1.2 $Wm^{-2}K^{-1}$ in 2050)[15].

[15] Even though windows with lower thermal transmittance may be available (e.g. triple glazing windows with 0.75 $Wm^{-2}K^{-1}$ [228]), it is believe that, given the expected future climate in Portugal, such windows would not be required or economically feasible to install.

The floor area of a dwelling also impacts its consumption, influencing lighting and space heating/cooling needs. In general, bigger dwellings would demand higher energy consumption. GDP is commonly used to project future socio-economic factors, such as dwellings' floor area. In the past, the Portuguese size of dwellings per capita has increased with GDP per capita [192], [193]. However, diverging tendencies may be put in place for the future.

In this regard, the creation of scenarios aims at covering different trends for the future of dwellings' size. For the evolution trend of dwellings' size, literature diverges: for 2050, Gouveia et al. [194] considered a 20% increase in floor area of dwellings, while the Portuguese 'Roadmap for Carbon Neutrality' [162] considers it constant or smaller. In the Central scenario, dwellings to be built in 2050 keep the average area observed in current new dwellings, about 136 m^2. The floor area of other dwellings, undergone or not major renovations, was considered to stay the same.

Besides the housing stock characteristics, the electrification of domestic devices also impacts strongly the consumption trends of the residential sector. According to the studies, in Portugal, electric domestic hot water was present in 6% of households in 2008 (EcoFamílias project [195]), in 14% in 2010 (EcoFamílias II project [196]), and in about 26% in 2015 (FROnT project [197], [198]). As for electric ovens and cooking hobs, in 2008 about 69 and 18% of households had them, respectively (EcoFamílias project [195]), which is about 6% more than in 2006 (EcoFamílias 30 project [199]). Thus, for the domestic hot water (DHW) and cooking needs, it was assumed a level of electrification of 75%.

The electrification of heating and cooling technologies is also increasing in the residential sector. Based on past records of sales of heat pumps for the residential sector (from Ref. [184], using data provided by APIRAC – Portuguese Association of the Refrigeration and Air Conditioning Industry), the current penetration of heat pumps was estimated to be about 7 to 9% in the dwellings existing in 2017, following a linear trend since 1999 [200]. Maintaining the tendency, it is to expect heat pumps in 27% of all the existing houses[16] by 2050.

[16] It is worth highlighting that the heat pump penetration of 27% is applied to all existing houses, which means that the value increases when considering solely occupied houses, as can be seen below in subsection 4.4.2.2.

Regarding demand-side management, it is considered that a fraction of the residential electricity demand may be flexible and may contribute to grid stabilization, e.g. the use of a washing machine can be delayed if the grid requires it. In the Central scenario, about 8% of the residential electricity demand is available to be shifted within a 24h-period [106].

Table 4.23 shows the main assumptions taken for the Central scenario for the case of the residential sector.

Table 4.23. Central scenario – Residential sector
Characteristics considered for residential sector characteristics in the Central scenario, including space heating/cooling and demand-side management.

Central scenario – Residential sector		
Household market	Housing stock development	Middle
	Retrofitting rate	2%/year
	New buildings rate	0.75%/year
	Replacement strategy	Replace older buildings
	People/household	2.5
Floor area of new dwellings	Dwellings built in 2050	current avg. (136 m^2)
Electrification of DHW and cooking	% electrification	75%
Space heating/cooling	% heat pumps	27%
Demand-side management	% annual demand (24h-period)	8%

Paths for electricity demand

Two significantly different paths are considered for the evolution of electricity consumption in the residential sector:

Path Low Demand (LoDe) – an improved housing stock is considered with higher retrofitting/new building rates: since Portuguese retrofitting rates are still behind the European average (see Central scenario, above), and even more from the European goal, it is assumed that the country will meet this goal in 2050 – 3% per year. As for new buildings, based on several European countries with a rate of about 1% of new residential buildings per year (Austria, Belgium, France, Finland, etc. [190]), it is assumed that Portugal will achieve this value in 2050. Similar to Central scenario, it is considered that

new buildings are replacing the older ones first and it is also assumed an average density of 2.5 people per dwelling.

In this scenario, future dwellings are 20% smaller than the current new ones [162]. Regarding electrification rates, it considers 50% and 17% penetration for domestic hot water/cooking and heating/cooling electric devices, respectively.

Path High Demand (HiDe) – an older housing stock is considered for this path, assuming a retrofitting rate of 1% and a new building rate of 0.5%. Here, it is considered 2 people per dwelling and that new buildings replace equally existing buildings of all ages. These assumptions lead to a higher number of houses and a more aged housing stock.

Electrification of 100% and 37% are considered for domestic hot water/cooking and heating/cooling devices, respectively. In this path, the new dwellings are assumed to be 20% bigger than the current average today, contributing to higher electricity consumption.

Table 4.24 presents the relative differences from the Low and High demand paths to the Central scenario for the residential sector.

Table 4.24. Relative differences between Low and High electricity demand paths – Residential sector
Characteristics considered for residential sector characteristics for the Central scenario and the relative differences assumed for the Low and High electricity demand paths.

Relative differences between Low and High demand paths – Residential sector				
		Central	LoDe	HiDe
Household market	Housing stock development	Middle	New	Old
	Retrofitting rate	2%/year	+1 p.p./year	-1 p.p./year
	New buildings rate	0.75%/year	+0.25 p.p./year	-0.25 p.p./year
	Replacement strategy	Replace older buildings	Replace older buildings	Replace all buildings
	People/household	2.5	-	-20%
Floor area of new dwellings	Dwellings built in 2050	current average (136 m^2)	-20%	+20%
Electrification of DHW and cooking	% electrification	75%	-33%	+33%
Space heating/cooling	% heat pumps	27%	-37%	+37%

Table 4.25 summarizes second-order assumptions about the scenarios resulting from the previous assumptions.

Table 4.25. Electricity demand paths – Residential sector
Characteristics considered for the residential sector characteristics in the Central, Low and High demand scenario, including space heating/cooling and demand-side management.

Electricity demand paths – Residential sector				
		LoDe	Central	HiDe
Housing stock	Houses in 2050 [#]	7,230,004	6,952,410	6,627,432
	Occupied houses in 2050 [#]	3,687,200	3,687,200	4,609,000
	% old houses	34%	52%	72%
	% retrofitted houses	49%	33%	18%
	% new houses	18%	14%	10%
	Occupation factor	51%	53%	70%
Floor area per dwelling	New buildings in 2050 [m^2]	109	136	163
	Avg. of housing stock in 2050 [m^2]	88	96	118
Electrification of DHW and cooking		50%	75%	100%
Space heating system (occupied houses)	Heat pump	26%	40%	41%
	Electric resistance	34%	27%	27%
	Others	32%	26%	25%
	No system	8%	7%	7%
Space cooling system (occupied houses)	Heat pump	37%	51%	52%
	No system	63%	49%	48%

Figure 4.25 compares the distribution of old, retrofitted and new dwellings of the housing stock for each demand scenario, and presents the correspondent average area of dwellings. The average area of dwellings shows a strong increase of 26% in the High demand scenario, while it does not change significantly for the remaining scenarios. The number of occupied dwellings decreases slightly for Low and Central scenario compared to the present, because of the lower number of inhabitants. Improved building stock is expected for the Low scenario with more than two-thirds of the dwellings being new or renovated, whilst for the Central scenario, the value is slightly below half. It is the result of higher rates of retrofitting and new buildings. The High demand scenario reflects the

most critical housing stock, i.e., the biggest and oldest. This is due to less people living in each dwelling and less retrofitting and new buildings.

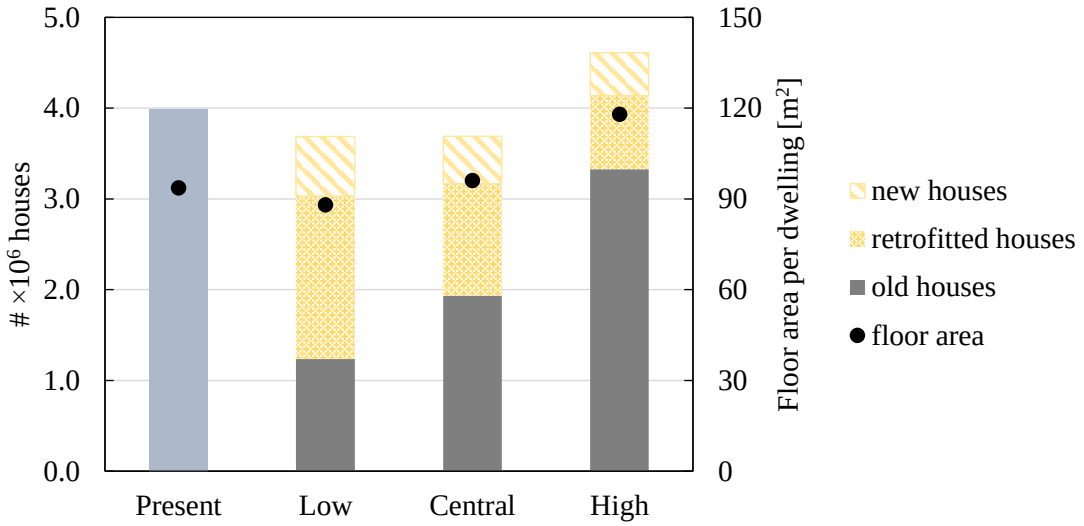

Figure 4.25. Area and age distribution of occupied housing stock
Distribution of the occupied housing stock for each electricity demand scenario according to the construction type (old, retrofitted or new) (left axis) and the average area of each dwelling (right axis).

Figure 4.26 presents the distribution of space heating and cooling systems according to their type. For every scenario, higher electrification of both space cooling and heating is expected. A significant increase in dwellings equipped with cooling devices is observed, from 11% in the present to 52% in the High demand scenario. For space heating, the major differences are seen in the distribution of the type of systems. Heat pumps for heating play a critical role in the future, increasing from 3% of presence in dwellings today to 41% in the High demand scenario. As expected, for every indicator, the fraction of electrified equipment increases with the increasing level of the electricity demand of the scenarios.

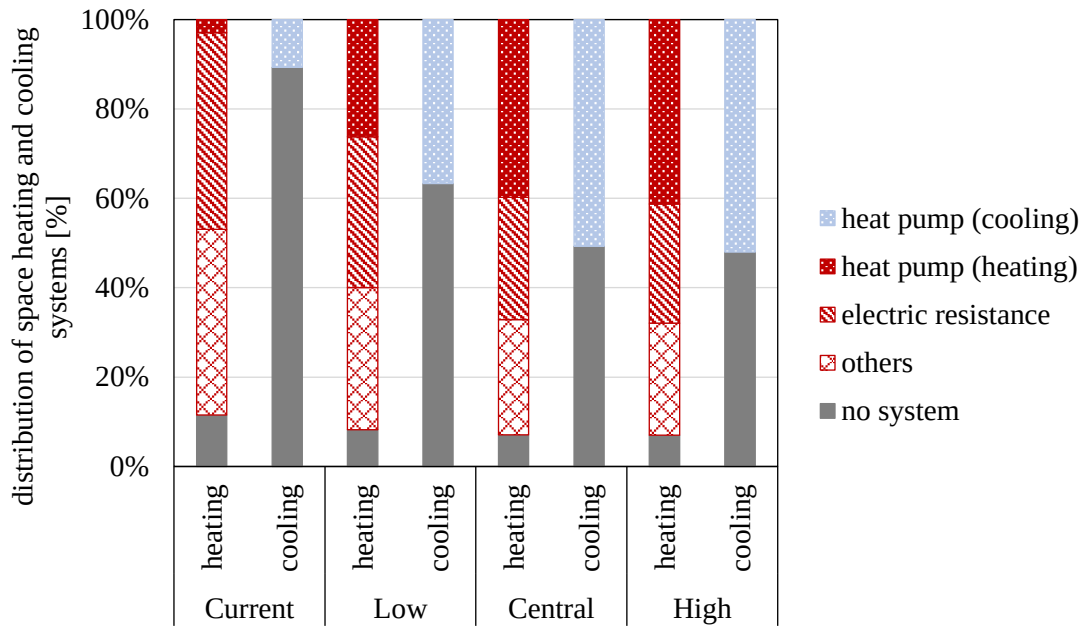

Figure 4.26. Space heating and cooling
Distribution of space heating and cooling devices currently and for each electricity demand scenario, including the absence of systems.

Paths for power system flexibility

The contribution for demand-side management from the residential sector differs for each path, Table 4.27:

Path Low Flexibility (LoFlex) – It is considered half the value considered for the Central scenario, i.e., about 4% of the annual residential electricity demand is flexible.

Path High Flexibility (HiFlex) – About 12% of the residential electricity demand is flexible.

Table 4.26. Relative differences between Low and High flexibility paths – Residential
Characteristics considered for the residential sector characteristics for the Central scenario and the relative differences assumed for the Low and High flexibility paths.

Relative differences between Low and High flexibility paths – Residential sector				
		Central	LoFlex	HiFlex
Demand-side management	% annual demand (24h-period)	8%	-50%	+50%

Table 4.27. Flexibility paths – Residential sector
Characteristics considered for the residential sector characteristics in the Central, Low and High flexibility paths.

Flexibility paths – Residential sector				
		Central	LoFlex	HiFlex
Demand-side management	% annual demand (24h-period)	8%	4%	12%

4.4.1.3. Services, Industry and Agriculture sector

The services, industry and agriculture sectors represent almost 70% of the final electricity demand in the European Union. For this reason, the evolution of the consumption in those sectors will dominate the evolution of the overall consumption.

Results from the literature are not consensual when projecting the future electricity demand in the different demand sectors, Figure 4.27. Among other factors, the future electricity demand depends mainly on socio-economic scenarios. The gathered information presented is uniformized by the population assumed in each study.

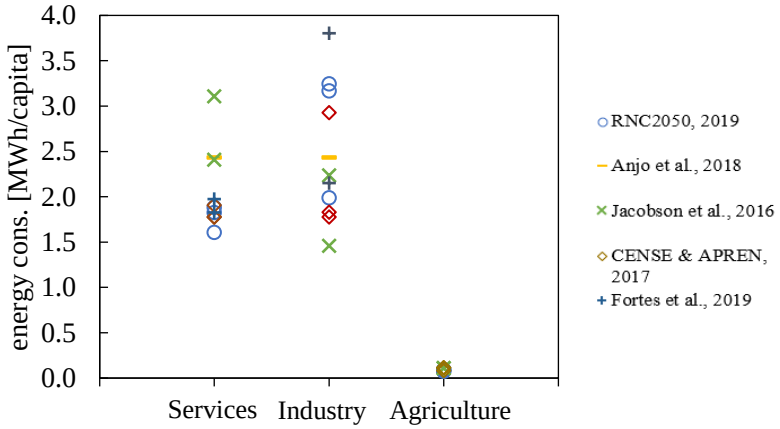

Figure 4.27. Literature on energy consumption of services, industry, and agriculture
Summary of different projections found in the literature for the future electricity demand for the services, industry and agriculture sectors in Portugal in 2050 – some values were obtained from graphs and maybe not perfectly accurate [106]–[110].

Central scenario

In the Central scenario, the consumption of each sector considers the middle values found in the literature (Figure 4.27). For the service sector, consumption was set at 2.36 MWh/capita, just below the 2.63 MWh/capita for the industry sector. Finally, with a much lower weight on the overall electricity consumption, electricity demand in agriculture represents about 0.10 MWh/capita.

Demand-side management was also considered for services and industry. In the services, about 6.5% of annual demand is available for flexible usage within one day, while in the industry it is 5%, also for a time-horizon of one day [106].

As for the electricity consumption profile of these three sectors, it was considered to be the same as in 2015. The assumptions are summarized in Table 4.28.

Table 4.28. Central scenario – Services, Industry and Agriculture
Characteristics considered for the electricity consumption in the Central scenario for Services, Industry and Agriculture, including demand-side management.

Central scenario – Services, Industry and Agriculture			
Electricity consumption [MWh/capita]		Services	2.36
		Industry	2.63
		Agriculture	0.10
Demand-side management	% annual demand (24h-period)	Services	6.5%
		Industry	5%
		Agriculture	-

Paths for electricity demand

The evolution of electricity demand assumes two diverging trajectories (Table 4.29):

Path Low Demand (LoDe) – this path considers a lower electricity demand, thus, the lower limits of the values summarized in Figure 4.27 were considered. The values assumed were 1.61 MWh/capita for the services sector, 1.57 MWh/capita for the industry sector and 0.08 MWh/capita for agriculture.

Path High Demand (HiDe) – assuming a higher demand, this path considers 3.11 MWh/capita for the services, 3.80 MWh/capita for the industry and 0.12 MWh/capita for agriculture.

Table 4.29. Electricity demand paths – Services, Industry and Agriculture
Electricity consumption considered for electricity consumption in the Central, Low and High demand paths for Services, Industry and Agriculture.

Electricity demand paths – Services, Industry and Agriculture				
		Central	LoDe	HiDe
Electricity consumption [MWh/capita]	Services	2.36	1.61	3.11
	Industry	2.63	1.46	3.80
	Agriculture	0.10	0.08	0.12

Paths for power system flexibility

Different levels of contribution for demand-side management are used:

Path Low Flexibility (LoFlex) – a less flexible system is considered where the service and industry sectors allow a demand shift of half the value of the Central scenario, i.e., 2.5% of the services annual demand and 3.25% of the annual industry demand is available for grid services.

Path High Flexibility (HiFlex) – on the contrary, this path provides higher flexibility on demand-side management. It considers 7.5% and 9.75% of the annual electricity demand available for demand-side management for a time-horizon of one day for services and industry, respectively.

Table 4.30. Relative differences between Low and High flexibility paths – Services, Industry and Agriculture
Demand-side management considered in the Central scenario and the relative differences assumed for the Low and High flexibility paths for Services, Industry and Agriculture.

Relative differences between Low and High flexibility paths – Services, Industry and Agriculture					
			Central	LoFlex	HiFlex
Demand-side management	% annual demand (24h-period)	Services	5%	-50%	+50%
		Industry	6.5%	-50%	+50%
		Agriculture	-	-	0%

Table 4.31. Flexibility paths – Services, Industry and Agriculture
Demand-side management considered in the Central, Low and High flexibility paths for Services, Industry and Agriculture.

Flexibility paths – Services, Industry and Agriculture					
			Central	LoFlex	HiFlex
Demand-side management	% annual demand (24h-period)	Services	5%	2.5%	7.5%
		Industry	6.5%	3.25%	9.75%
		Agriculture	-	-	-

4.4.1.4. Energy storage – Second-life batteries

Energy storage plays an important role in power systems with high penetration of variable renewables. It may enable higher renewable energy use by storing excess generation to later use in times of need. Energy storage is assumed to be provided by large hydro with pump-back capacity and batteries of electric vehicles supplemented by stationary energy storage in batteries. Other technologies such as compressed air energy storage or hydrogen [201] were not considered, but they could be an option (both cases would entail higher electricity demand due to lower energy efficiency).

The stationary energy storage includes 1) electric vehicles' second-life batteries; and 2) dedicated stationary storage.

The **dedicated stationary energy storage** will only be considered for the 100% renewable power system (see subsection 4.4.2.4) to accommodate imports that surpass a given cross-border interconnection limit. Therefore, the dedicated stationary storage is only presented in the results from section 5.3.

The **second-life batteries** are available in every demand-flexibility scenario and they are modelled as a large buffer of energy, similar to on-board batteries. Since second-life batteries are present in all demand-flexibility scenarios and power system configurations (unlike the dedicated stationary energy storage), during this work, 'energy storage' refers to 'second-life batteries' unless otherwise stated.

Different levels of energy storage are available depending on the system flexibility of each scenario (discarding changes in electricity demand).

Following the work of Almeida and Nunes [202], the Central scenario considers an energy capacity of 38 GWh, with an efficiency of charging and discharging of 90%. Then, the paths for power system flexibility were considered the following:

Path Low Flexibility (LoFlex) – it shows a significant decrease in the second-life battery capacity, i.e., half of the capacity of the Central scenario.

Path High Flexibility (HiFlex) – here, the power system has a higher level of flexibility, showing a 50% increase in the energy storage capacity of the Central scenario.

Table 4.32 and Table 4.33 summarize the energy storage characteristics considered for each path.

Table 4.32. Relative differences between Low and High flexibility paths – Second-life batteries
Characteristics considered for the second-life batteries for the Central scenario and the relative differences assumed for the Low and High flexibility paths.

Relative differences between Low and High flexibility paths – Second-life batteries			
	Central	LoFlex	HiFlex
Energy capacity [GWh]	38.32	-50%	+50%
c_{rate}	0.1C	-	-

Table 4.33. Flexibility paths – Second-life batteries
Characteristics considered for the second-life batteries in the Central, Low and High flexibility scenario, including energy and power capacity.

Flexibility paths – Second-life batteries			
	Central	LoFlex	HiFlex
Energy capacity [GWh]	38.32	19.16	57.48
Power capacity [MW]	3,832	1,916	5,748
c_{rate}	0.1C	0.1C	0.1C

4.4.2. Modelling the demand sectors

In this subsection, the methods used to calculate the electricity demand in each of the considered sectors will be described.

4.4.2.1. Mobility

The paths defined for electricity demand and power system flexibility were combined to define five different scenarios. Hereafter, the main parameters to be considered for the EnergyPLAN model are briefly described.

Dumb and smart charging require as input the parking and driving patterns, respectively – as presented in subsection 4.4.1.1 and Figure 4.24.

The energy consumption of light passenger vehicles is determined in Equation (4.42) separately for dumb and smart charging $C_{dumb/smart,\ light\ pass.}$ [TWh].

$$C_{dumb/smart,light\ pass} = n_{days} \times S_{dumb/smart} \times \left(N_{pr.veh.} \times c_{pr.veh.,electric}(S_{PEV} \times D_{PEV} + S_{PHEV} \times D_{PHEV}) + N_{AeV} \times c_{AeV} \times D_{AeV}\right) \times 10^{-9} \quad (4.42)$$

where $N_{pr.veh}$, N_{AeV} and N_{EV} are the numbers of private light passenger vehicles, shared autonomous vehicles and the total number of light passenger electric vehicles, respectively; D_{PEV}, $D_{PHEV,\ electric}$ and D_{AeV} are the daily distance travelled by the PEV private vehicles, PHEV private vehicles in electric mode and the autonomous vehicles, respectively [km]; $c_{pr.veh.,electric}$ and c_{AeV} are the electricity consumption of private and autonomous vehicles, respectively [kWh/km]; n_{days} is the number of days in the year; S_{PEV} and S_{PHEV} is the share of private PEV and PHEV, respectively [fraction] and $S_{dumb/smart}$ is the share of dumb or smart charged vehicles [fraction]; the multiplying factor '10^{-9}' is used to adjust units.

For freight transportation, the electricity consumption of battery electric vehicles is based in RNC2050 $C_{freight,electric,RNC2050}$ [TWh], Equation (4.43).

$$C_{dumb/smart,freight} = S_{dumb/smart} \times C_{freight,electric,RNC2050} \quad (4.43)$$

In the case of smart charging, several other parameters have to be described. The share of parked cars that are grid-connected is assumed as 70% for Central with a variation of 50%

for the other paths, as mentioned above. The maximum share of vehicles driving during rush hours $S_{max\ EV\ rush}$ [fraction] is a weighted average of the fleet parked accordingly to the fleet type (considering that for AeVs the number is 80% and for private vehicles, it is of 20% – $S_{max\ AeV\ rush}$ and $S_{max\ pr.veh.\ rush}$, respectively), Equation (4.44). Freight transports are assumed to behave similarly to the obtained $S_{max\ EV\ rush}$.

$$S_{max\ EV_{rush}} = \frac{N_{pr.veh.} \times S_{max\ pr.veh._{rush}} + N_{AeV} \times S_{\max AeV_{rush}}}{N_{EV}} \quad (4.44)$$

The total capacity of the light passenger battery storage $Storage_{smart,light\ pass.}$ [GWh] accounts for all the EVs available for smart charging and for the maximum available fraction of energy capacity for smart charging purposes $S_{SOCavail.}$ [fraction], Equation (4.45).

$$Storage_{smart,light\ pass.} = S_{smart} \times S_{SOCavail.} \times \quad (4.45)$$
$$(N_{PEV} \times B_{PEV} + N_{PHEV} \times B_{PHEV} + N_{AeV} \times B_{PEV}) \times 10^{-6}$$

where B_{PEV} is the battery capacity of one PEV [kWh] and B_{PHEV} is the battery capacity of one PHEV [kWh]; the multiplying factor '10^{-6}' is used to adjust units.

The battery capacity of freight vehicles is determined considering a similar ratio between energy capacity/consumption as in light passenger vehicles.

$$Storage_{smart,freight} = \frac{Storage_{smart,light\ pass.}}{C_{smart,light\ pass.}} \times C_{smart,freight} \quad (4.46)$$

Ideally, the power capacity for grid-connection would be determined according to the number of vehicles of each type on the fleet and their corresponding power capacity. Such an approach was not followed, due to the modelling features of the simulation tool used.

EnergyPLAN schedules the charging and discharging of the storage energy options, such as EV batteries, according to the electricity generation and consumption in each hour. After using all the hydro pump capacity, EnergyPLAN will store the excess of generation in EVs at the maximum possible power, if there is enough energy capacity available in their batteries. At times of high generation excess, it results in a rapid full charge of the batteries. On the other hand, when consumption is higher than electricity generation, the scheduling is done using all the electricity stored in the EV batteries at the maximum available power, which results in huge ramps to completely discharge the batteries.

Besides the increased degradation of batteries due to this charging and discharging with accentuated ramps, the simulation tool performs limited scheduling for the battery usage that does not account for later periods with critical needs for a stored energy device, e.g. during peaks of electricity consumption. To overcome this limitation and prevent a significantly higher battery degradation, a 10-hour discharging/charging rate (c_{rate} of $0.1h^{-1}$) was considered to force a slower charging and discharging of the batteries. Thus, the total capacity for grid-connection P_{G2V} [MW] is calculated using the total energy storage capacity of all the electric fleet (light-duty passenger vehicles and freight vehicles – $Storage_{smart}$ [GWh]) and applying Equation (4.47).

$$P_{G2V} = Storage_{smart} \times c_{rate} \times 10^3 \quad (4.47)$$

Following the same approach, the V2G grid-connection capacity P_{V2G} [MW] is determined using the available share of EVs for V2G – S_{V2G} [fraction], Equation (4.48).

$$P_{V2G} = S_{V2G} \times Storage_{smart} \times c_{rate} \times 10^3 \quad (4.48)$$

In the latter two equations, where the multiplying factor '10^3' is used to adjust units.

Finally, the assumptions for each combined scenario are shown in Table 4.34.

Table 4.34. Electricity consumption and flexibility – Mobility
Summary of all characteristics of the vehicles' fleet that are required to be inputted in EnergyPLAN.

Electricity consumption and flexibility – Mobility					
	Central	LoDe LoFlex	LoDe HiFlex	HiDe LoFlex	HiDe HiFlex
Light-duty passenger vehicles					
Dumb charge					
Consumption [TWh]	1.1	0.5	0.1	3.1	0.3
Parking pattern	w/o shared vehicles	w/ shared vehicles		w/o shared vehicles	
Smart charge					
Consumption [TWh]	4.3	0.8	1.2	5.5	8.3
Electricity consumption [km/kWh]	6.0	10.0	10.0	6.0	6.0
Driving pattern	w/o shared vehicles	w/ shared vehicles		w/o shared vehicles	
Specifications of smart charge					
max. share of vehicles during rush hours [%]	20%	75%	50%	24%	16%
Capacity of grid connection [MW]	5,341	1,846	4,154	6,959	15,657
Share of parked vehicles grid connected [%]	70%	56%	84%	56%	84%
Battery storage capacity [GWh]	53.4	18.5	41.5	69.6	156.6
V2G					
Capacity of grid connection [MW]	2,136	369	2,492	1,392	9,394
Freight transportation					
Dumb charge					
Consumption [TWh]	0.7	-	-	2.4	0.3
Smart charge					
Consumption [TWh]	2.6	-	-	4.2	6.3
Specifications of smart charge					
Capacity of grid connection [MW]	3,294	-	-	5,270	11,858
Battery storage capacity [GWh]	32.9	-	-	52.7	118.6
V2G					
Capacity of grid connection [MW]	1,318	-	-	1,054	7,115

4.4.2.2. Residential sector

In this work, the residential sector is the only activity sector whose demand is considered to vary with climate projections. The reasons for this are: 1) residential sector is considered to be one of the most affected by climate [1]; 2) a higher potential for improving electrification of equipment in the residential sector is expected, especially in Portugal, where still a low electrification is seen – e.g. a penetration of 26%, 18%, and 8% was recently observed for electrified domestic hot water, cooking hobs and heat pumps' penetration [197], [199], [200].

The residential electric demand was determined using the methodology presented and validated in Ref. [203]. It uses the Portuguese housing stock firstly characterized using a Monte Carlo approach described in Ref. [191], which uses data based on Energy Performance Certificates provided by ADENE [192] and creates probability distribution functions (PDFs) for several characteristics of the buildings – e.g. building year, building thermal characteristics, floor area, glazing, etc. People's behavior regarding the use of electric equipment, heating, and cooling devices during the days and week is also taken into consideration, based on a survey developed in Portugal [186].

A brief description of the process to achieve the hourly electric demand of the residential sector in Portugal is here presented, already including the values assumed in this study.

First, the model randomly generates one batch with 100 dwellings, characterized by random combinations of the different parameters of the building features (e.g. heating/cooling areas, floor area, type of heating system, etc.) according to their statistical distributions and user profiles (considering the probability of occupants being at home and of using space heating/cooling appliances). Then, it calculates the average hourly profile for the total electricity and heating demand for that batch. The model generates successive random batches until the total electricity and heating demand of the new batch does not change the average of the previous batches, i.e., when it is aligned, within a given tolerance (<0.5%) and ensuring a minimum number of iterations (N=20), with the average demand of the previous batches. Figure 4.28 exemplifies the application of the process.

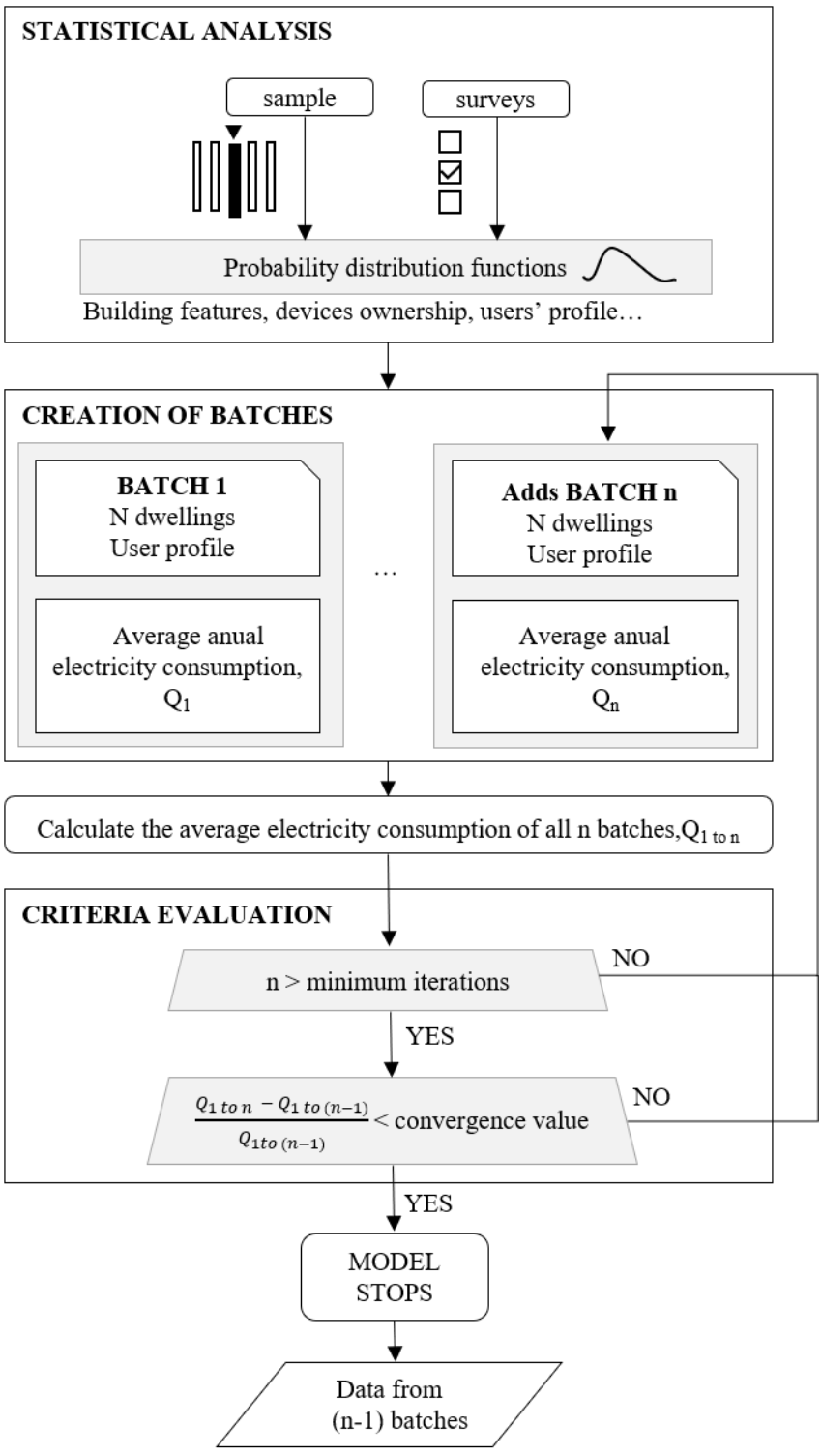

Figure 4.28. Schematic of the Monte Carlo approach
Summary of the Monte Carlo approach used: first a statistical analysis is made to get the probability distributions required to create representative batches and, finally, an evaluation of the batches compared to the previously generated batches is performed. Some elements adapted from [191].

Space heating and cooling demand are based on hourly energy balances considering losses and heat gains. It uses as inputs hourly air temperature, solar irradiation, electric devices, occupancy and building features to determine both the heat gains and losses. The efficiency of space heating and cooling was assumed constant over time: 1) electric resistance has a 100% efficiency; and 2) the heat pumps' efficiencies are described by Weibull probability distribution functions (describing the present situation [191]: for space heating, the parameters are $\lambda = 2.76$; $\kappa = 2.20$, while for space cooling, the Weibull parameters are $\lambda = 2.80$; $\kappa = 3.83$).

The heating and cooling seasons are dynamic, i.e., their first and last days change according to the climate data. The heating season starts on the day that precedes a period of more than 10 consecutive days with an average daily temperature below 15ºC and ends on the day preceding a correspondent period warmer than 15ºC. The cooling season is determined analogously, considering a temperature above or below 20ºC.

The original Monte Carlo model did not include electric DHW needs, which was added in this work. This is of major importance for this study, given the expected increase in this type of energy consumption. Equation (4.49) describes the calculation of the DHW energy needs per day per household. It considers 40 litres of hot water per person per day V_{H2O} [m^3], the final temperature of 60ºC T_{final} [ºC] and an initial temperature of 15ºC $T_{initial}$ [ºC] [204], [205]. It also depends on the number of occupants N_{occup}. The assumed water density (ρ_{H_2O}) is 1,000 kg/m^3 and thermal capacity (c_{H2O}) is 4,186 $J.kg^{-1}K^{-1}$.

$$DHW_{day} = c_{H2O} \times \rho_{H_2O} \times V_{H_2O} \times (T_{final} - T_{initial}) \times N_{occup} \quad (4.49)$$

A typical hourly profile for domestic hot water consumption was also assumed, which considers the larger peak in the morning, small hot water usage at lunch and the second peak of hot water usage in the late afternoon and dinner time [206]. Houses with electric DHW feature an equal distribution between electric hot water tanks (efficiency of 93% [207]) and heat pumps with a coefficient of performance (COP) of 3 [208], since these are well-established technologies its efficiency were considered constant over time.

Regarding cooking electricity demand, the model considers that cooking appliances usage follows the same typical profile of hourly lighting use in kitchens in Portugal [209], and that cooking electric demand corresponds to 7.6% of total electricity consumption in households having electric cooking appliances (excluding electric DHW) [210],[211].

Besides space heating/cooling and DHW/cooking electric loads, the model also assumes a baseload profile dependent on the floor area of the dwelling, representing other typical electric devices in use, mentioned below as 'sockets', e.g. television, fridge, washing machine, etc. The 'sockets' profile is the same for all dwellings and corresponds to the average mid-season electric profile (since the use of heating and cooling devices is unlikely at this time of the year); the data was obtained from a smart metering project [212] and used in the validation of the original model by Panão and Brito [203]. Since lighting needs are dependent on natural light, which changes according to the time of day and year, following Ref. [203] it is considered that when the global solar radiation is below 100 W/m^2, during the early morning and late afternoon, the 'sockets' electric profile increases 10%. The 'sockets' profile is also adapted according to the occupancy of the dwelling.

The space heating/cooling, DHW and cooking loads are summed to this typical profile to calculate the aggregate one. All electric loads (including space heating and cooling, DHW and cooking) consider the occupancy profile of the houses, i.e., at a given hour the loads are adapted according to the occupancy and probability of using the appliances.

The climate data required by this Monte Carlo-based model includes hourly data for the air temperature and global solar irradiance incident on a vertical surface facing each of the eight main orientations (North, Northeast, East, Southeast, South, Southwest, West, Northwest). These data were obtained by applying the same methodology described in subsection 4.3.3.2, with the tilt changed to 90° (vertical surface) and the surface orientation was changed to each of the previously mentioned orientations.

As residential demand changes with several factors such as the climate and socio-economic conditions, the computation of the hourly residential demand were done separately for each NUTS III region (based on the 2002 version), excluding the archipelagos – this is, the previously described Monte-Carlo process was applied for each region separately. Thus, not only climate data (derived from the climate ensemble – see section 4.2) but also several other indicators required for the calculations were gathered for each of the region (such as number of houses, percentage of apartments, average area per dwelling, average number of inhabitants per dwelling, percentage of existence of each type of heating and cooling system, etc. [213]). While it is considered that some regional factors are kept constant such as the percentage of apartments or the windows' orientation, other regional parameters are adapted to correspond to the new assumptions

made at a national level, such as regional population, number of houses, average floor area, density of people per house, heating/cooling ownership and its distribution by type, etc. After calculating the electricity demand in the residential sector for each region, a weighted sum according to the number of houses of each region was done to obtain the Portuguese residential demand.

In this work, the validation of the Monte-Carlo approach was performed using the climate data provided by DGEG [214] by region and the current housing stock. The average annual electricity demand per household was found to be about 3,028 kWh, while the official value presented in the Portuguese national survey of 2011 was 3,673 kWh [211].

Housing stock

The housing stock plays a critical role in residential electricity demand. Its energy performance may enhance the impact of temperature changes, mainly due to its thermal characteristics, e.g. higher insulation may lead to lower heating/cooling needs. Thus, to address the changes in residential consumption in 2050, an evolution of the housing stock was considered.

The starting point to characterize the Portuguese housing stock considers the distribution of dwellings per decade of construction presented in the Portuguese national census in 2011 [213], the new dwellings built [215] and the retrofitted dwellings [216] – the latter two between 2012 and 2017. The expected total number of dwellings existing in the year 2017 was determined by summing the dwellings being built in each decade up to 2017. However, the resulting number of dwellings differ slightly from the Portuguese national statistics from the year 2017, since it considers more 0.06% of dwellings [215]. Therefore, the distribution of dwellings was adapted to the 2017 statistics by considering that the extra dwellings were demolished or suffered renovations in equal weight in the decades before 1980 since they were all considered older than 40 years (about the average age of buildings in 2011). It resulted in the distribution presented in Figure 4.29.

The housing stock in 2050 is determined by taking the current housing stock age distribution and applying a linear evolution of the annual rates of new buildings' construction and retrofitting. It is assumed that the new or retrofitted dwellings replace existing dwellings.

The level of renovation and construction determines the total number of existing dwellings N_{dwell}. However, the number of occupied houses $N_{occupied\ dwell}$ is given by the

population and the average number of people living in each dwelling d_{dwell}, Equation (4.50). The ratio between these two numbers gives the occupation factor of residential dwellings $f_{occupation}$ [fraction], Equation (4.51).

$$N_{occupied\ dwell} = \frac{population}{d_{dwell}} \tag{4.50}$$

$$f_{occupation} = \frac{N_{occupied\ dwell}}{N_{dwell}} \tag{4.51}$$

In the year 2011, the occupation factor was about 68% according to the Portuguese census (the same was considered for 2017) [213], [215]. Following the assumptions described in subsection 4.4.1.2, the housing stocks built show an occupation factor of 51%, 53% and 70% for the new, middle-age and old housing stock, respectively.

The distribution of occupied dwellings across the decades is presented in Figure 4.29 for the year 2017 and the different evolution possibilities presented in subsection 4.4.1.2.

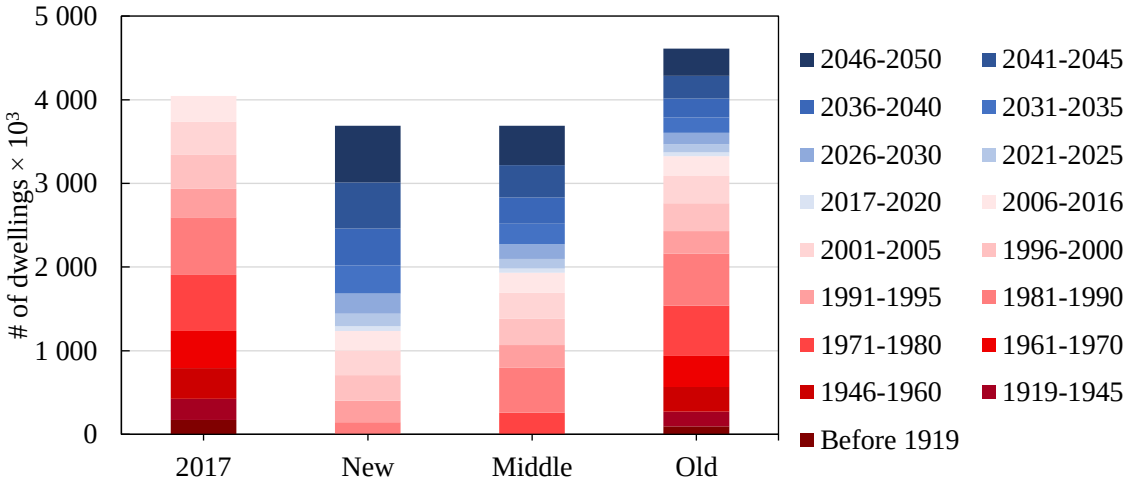

Figure 4.29. Age of housing stock
Distribution of occupied dwellings per decade for the year 2017 and the different possible developments of the housing stock.

The probability distribution functions that characterize the future housing stock consider that dwellings built or renovated in the same 5-year period show the same main design characteristics (e.g. windows thermal transmittance). As mentioned previously, the evolution of the building parameters changes according to their nature. The distribution of some parameters does not suffer any changes in the future. For several parameters, it is considered that dwellings built today present state-of-the-art characteristics that will be

kept constant until 2050; thus, their distributions change with the introduction of the new dwellings with the same performance levels as of today. For the windows' thermal transmittance, a linear improvement is considered until 2050 and its distribution is altered accordingly.

4.4.2.3. Services, Industry and Agriculture sector

Several socio-economic factors affect the sectors addressed in this subsection: services, industry, and agriculture. Even though the hourly profiles may change in the future, for lack of insight on what these changes could be, it was considered that the profiles would remain similar to the ones observed in 2015 [134].

Using the Portuguese hourly load diagram from 2015 $demand_{2015}$ [MW], the normalized hourly profile of services, industry, and agriculture sectors (SIA_{norm}) was obtained by the subtraction of the residential hourly demand obtained in the validation process $demand_{resid.,valid.}$ [MW], Equation (4.52).

$$SIA_{norm}(t) = \frac{demand_{2015}(t) - demand_{resid.,valid.}(t)}{\max\left(demand_{2015} - demand_{resid.,valid.}\right)} \quad (4.52)$$

The final hourly electricity demand from the services, industry and agriculture sectors $demand_{SIA}$ [MW] was determined through Equation (4.53), considering the total annual electricity demand of those three sectors C_{SIA} [TWh]. The multiplying factor '10^{-6}' is used to adjust units.

$$demand_{SIA}(t) = \frac{SIA_{norm}(t)}{sum(SIA_{norm})} \times C_{SIA} \times 10^{-6} \quad (4.53)$$

4.4.2.4. *System flexibility strategies: Demand-side management and energy storage*

The future of power systems faces a higher supply variability than the current and past framework shows, due to the expected high penetration of renewables. To keep the energy balance required, the accommodation of variable generation requires different types of strategies that make the system more responsive to supply and demand dynamics. Two of the most common techniques to accommodate variable renewables without compromising the security of supply are demand-side management and the use of energy storage devices.

The role of **demand-side management (DSM)** may be significant for the power system because it enables the shifting of loads from consumption peaks to periods with lower consumption needs. The activity sectors, depending on their level of flexibility, may place at the grid disposal a fraction of their energy consumption to be used at a given maximum power if required, in exchange of, for example, an economic compensation.

In this work, the demand-side management is modelled with EnergyPLAN. Defining annual energy, a power capacity for DSM and a time-horizon for load shifting, the model uniformly divides the flexible demand within the time-horizon and manages it to minimize fossil generation, imports and exports.

To define the annual energy consumption available to demand-side management, the fraction of demand available for DSM in each sector $f_{DSM,\ sector}$ [fraction] and their own demand C_{sector} [TWh] was considered. The sum of availability of all sectors for DSM gives the total annual energy consumption availability C_{DSM} [TWh].

$$C_{DSM} = \sum_{sector} f_{DSM,sector} \times C_{sector} \tag{4.54}$$

A time-horizon of one day was considered for demand-side management, i.e., the load could only be shifted within the period of one day. One-day shifting was selected to avoid the unrealistic shifting of activities on all the sectors considered. Residential, services and industry were the sectors selected to provide this type of service since agriculture does not have great flexibility for its activities, and mobility already provides flexibility with smart charging and V2G.

The power capacity available for DSM P_{DSM} [MW] is determined from the maximum power of the total hourly demand *demand* [MW] (including residential, services, industry and agriculture), the relative weight of each sector in the annual consumption w_{sector} [fraction] and the corresponding fraction available to DSM, as in Equation (4.55).

$$P_{DSM} = \sum_{sector} f_{DSM,sector} \times w_{sector} \times \max(demand) \quad (4.55)$$

The use of energy storage may be used to satisfy consumption with a lag from energy generation. It is able to store energy when it is in excess and use it later.

Besides large hydro with pumping and electric vehicles, this work considers as stationary energy storage repurposed automotive batteries (second-life batteries) and dedicated stationary storage devices (stationary batteries). While the capacity of second-life batteries available are defined according to the demand-flexibility scenario and are considered in all scenarios and power systems, the dedicated stationary energy storage is only introduced to decrease the need of cross-border interconnection observed in the reference 100% renewable power system and its sizing is determined for each climate realization and each photovoltaics-wind power configuration.

The **second-life batteries** were also modelled as a large buffer of energy, similarly to on-board batteries, also limited to a charging/discharging rate of 0.1C for the same reasons. Similarly to mobility, EnergyPLAN uses the whole potential of charging and discharging of the technology. As mentioned above, it may accelerate the storage technology's degradation and, by using the maximum available power capacity in each hour, it does not properly manage the energy stored, e.g. save the energy stored for periods with higher consumption peaks. To limit the charging/discharging rates, the power capacity was determined by assuming a ten-hour discharging and charging rate (c_{rate} of $0.1h^{-1}$). Hence, the power capacity available for the charging and discharging of the energy storage $P_{2nd\ life\ bat}$ [MW] is determined by its energy capacity $Storage_{2nd\ life\ bat}$ [GWh] and the c_{rate}, Equation (4.56). A multiplying factor '10^3' is used to adjust units.

$$P_{2nd\ life\ bat} = Storage_{2nd\ life\ bat} \times c_{rate} \times 10^3 \quad (4.56)$$

In the case of **dedicated stationary energy storage**, the following strategy was used to determine the energy storage capacity to decrease the cross-border power transmission

capacity needs. To achieve that, firstly, the imports and exports that surpass a given limit are calculated ($imports_{residual}$ and $exports_{residual}$ [GW]) by subtracting the cross-border interconnection limit. Then, for each hour t the net import balance for the residuals $net\ imp_{residual}$ [GW] is calculated, according to Equation (4.57).

$$net\ imp_{residual}(t) = imports_{residual}(t) - exports_{residual}\ (t) \qquad (4.57)$$

To ascertain the accumulated import needs, an accumulated balance of the $net\ imp_{residual}$ is created. The highest increase in this accumulated balance shows the most critical period of import needs, which is finally used to size the battery capacity. This process is repeated for every ensemble year in each of the power systems tested. A schematic example for sizing of the dedicated stationary energy storage is shown in Figure 4.30.

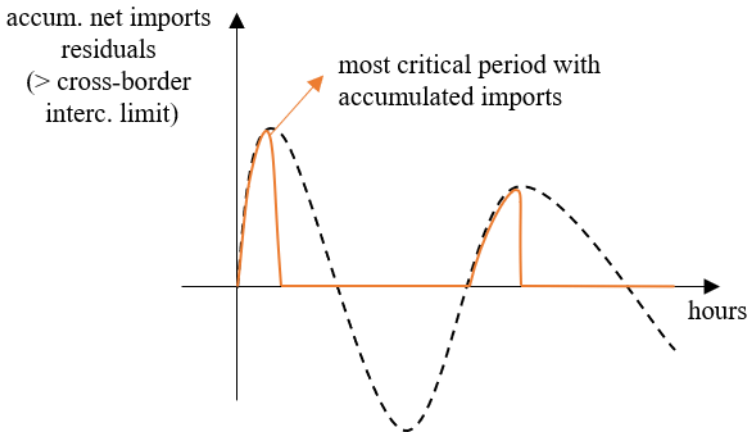

Figure 4.30. Sizing of the dedicated stationary energy storage
The dedicated stationary energy storage is sized for each ensemble year with the highest increase in the accumulated import needs above the cross-border interconnection limit. The dashed black line shows the accumulated net imports balance above the interconnection limit defined (residuals) and the solid orange line shows the critical periods with accumulated import needs.

4.4.3. Summary of electricity demand-flexibility scenarios

A summary of the electricity demand-flexibility scenarios considered is provided in Table 4.35.

Table 4.35. Electricity demand-flexibility scenarios
Summary of assumptions taken for the electricity demand-flexibility scenarios.

Assumptions for electricity demand-flexibility scenarios					
Electricity demand					
	LoDe LoFlex	LoDe HiFlex	Central	HiDe LoFlex	HiDe HiFlex
avg. total[17] [TWh]	42.4	42.4	69.4	98.5	98.5
System Flexibility					
	LoDe LoFlex	LoDe HiFlex	Central	HiDe LoFlex	HiDe HiFlex
Demand-side management (% annual demand available)					
Services	2.5%	7.5%	5%	2.5%	7.5%
Industry	3.25%	9.75%	6.5%	3.25%	9.75%
Residential	4%	12%	8%	4%	12%
Mobility					
Energy battery cap. [GWh]	18.5	41.5	86.3	122.3	275.2
Cap. grid connec. [GW]					
Smart charge	1.8	4.1	8.6	12.2	27.5
V2G	0.4	2.5	3.4	2.4	16.5
Second-life batteries					
Energy battery cap. [GWh]	19.2	57.5	38.3	19.2	57.5
Power cap. [GW]	1.9	5.7	3.8	1.9	5.7

[17] Because residential electricity demand varies with climate conditions, the average total electricity demand is presented.

4.5. CO_2 emissions

The CO_2 equivalent emissions result from the electricity generation in the power system $CO_{2electric}$ [Mton] and from other energy uses $CO_{2\ nonelectric}$ [Mton], Equation (4.58).

$$CO_2 emissions = CO_{2_{electric}} + CO_{2_{nonelectric}} \quad (4.58)$$

4.5.1. Power system

The $CO_{2\ electric}$ depends on the electricity mix of the power system. It is determined by summing the emissions from burning natural gas and other non-renewable resources to supply the power system demand, according to the specified emission factor for each type of fuel fe_{fuel} [kgCO_2/GJ], Table 4.36 and Equation (4.59).

Table 4.36. CO_2 emission factor for each type of fuel
Emission factor to determine the CO_2 emissions relative to the use of fossil fuels like natural gas [217].

	Emission factor [kgCO_2/GJ]
Natural Gas	56.6
Other non-renewable[c]	78.9

[a]The non-renewable fuel was considered to have the same emissions as fuel-oil.

$$CO_{2_{electric}} = \sum_{fossil\ fuel} Cons_{fossil\ fuel,gen} \times fe_{fossil\ fuel} \times 3.6 \times 10^{-3} \quad (4.59)$$

where $Cons_{fossil\ fuel,gen}$ corresponds to the annual consumption of fossil fuel resource to electricity generation [TWh] and *fossil fuel* represents each fossil fuel resource considered; a multiplying factor '3.6×10^{-3}' is used to adjust the units.

For simplicity, CO_2 emissions exclude any embodied emissions related to equipment or power plants.

4.5.2. Non-electric uses of energy

The combustion of fossil fuels provides the required energy for a variety of end-uses in all activity sectors. The emissions related to non-electric uses of energy are here determined for each sector. The CO_2 emissions from non-electric uses of energy ($CO_{2non\text{-}electric}$) will commonly be referred to as 'non-electric emissions' since they result from uses of energy other than electricity. The determination of non-electric emissions depends on the electricity demand-flexibility scenario.

The **residential sector** is expected to strongly shift a significant part of its energy usage towards electricity. However, the use of natural gas will still be significant in the future to supply part of the domestic hot water, cooking, and heating needs. To ascertain the residential non-electric emissions, the natural gas consumption was determined for each end-use.

The non-electric emissions were determined similarly for the domestic hot water, cooking, and heating needs, considering the Portuguese average consumptions. The final natural gas consumption is calculated according to the useful energy required to satisfy the households that is not supplied by electricity for each end-use.

First, the final electricity consumption previously determined (see subsection 4.4.2.2) is split by the type of electric system, according to their distribution. The useful energy is determined using the efficiency of each type of system considered ($\eta_{system,electric}$). DHW and heating consider electric resistances and heat pumps as the systems used, while for cooking no specific equipment is used and only an overall efficiency is assumed.

Using the electrification rate, the useful energy required for the natural gas appliances (e.g. boilers) is determined. Finally, the natural gas equipment efficiency ($\eta_{system,NG}$) is applied to determine the primary consumption of natural gas. This process is repeated for each residential end-use (DHW, cooking, and heating) and each demand-flexibility scenario and each ensemble year.

A summarized scheme of the approach is presented in Figure 4.31 and the efficiency of the appliances is presented in Table 4.37.

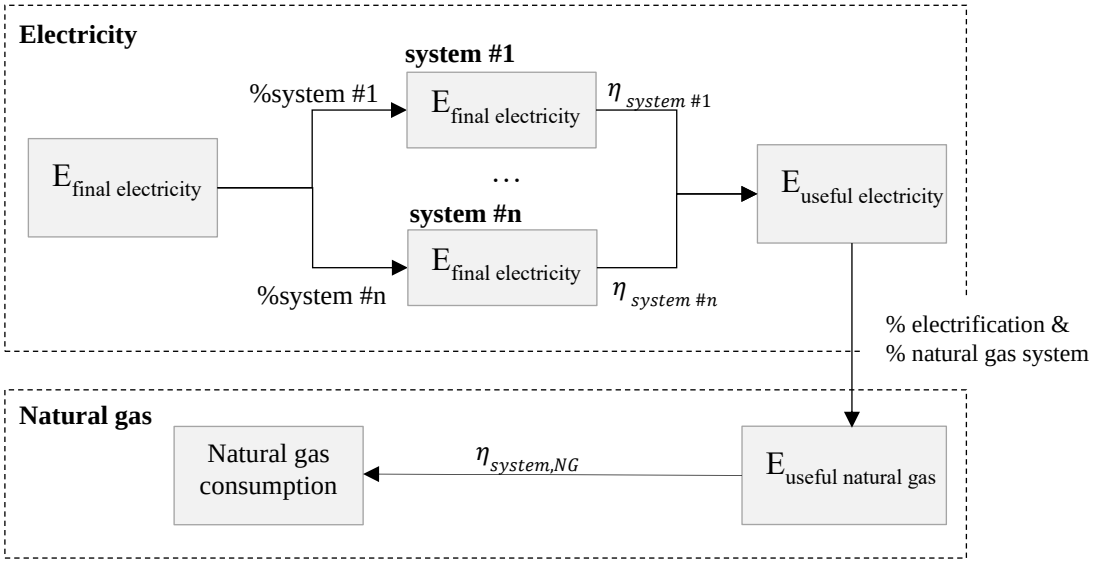

Figure 4.31. Final energy needs for domestic hot water and cooking
Summary of the approach taken to determine the final energy needs for natural gas for domestic hot water and cooking needs.

Table 4.37. Efficiency of electric and natural gas systems
Efficiency of electric and natural gas equipment for domestic hot water and cooking appliances.

Efficiency of electric and natural gas systems			
	Domestic hot water	Cooking[a]	Space heating
$\eta_{system,electric}$	Heat pumps - COP of 3 [208] Resistance - 93% [207]	77% [218], [219]	Heat pumps - COP of 2.5 [204] Resistance - 100% [204]
$\eta_{system,NG}$	92% [220]	38% [218], [219]	92% [220]

[a] It was considered a 7% improvement in technology efficiency, compared to present.

Having the total energy consumption of natural gas required to satisfy the residential sector $Cons_{NG}$ [TWh], the emission factor of natural gas (Table 4.36) is applied to ascertain the non-electric CO_2 emissions resulting from this sector, Equation (4.60).

$$CO_{2_{nonelectric,resid.}} = (Cons_{NG,DHW} + Cons_{NG,cooking} + Cons_{NG,heating}) \times fe_{NG} \quad (4.60)$$

The non-electric emissions from the **services, industry and agriculture sectors** rely on the Portuguese RNC2050.

For industry and agriculture, a linear regression between electricity consumption and the non-electric emissions per capita is traced using the three scenarios considered in the

RNC2050 [109] (as shown in Figure 4.32). Using those regressions and the electricity consumption considered in this work for each electricity demand scenario, the non-electric emissions are determined.

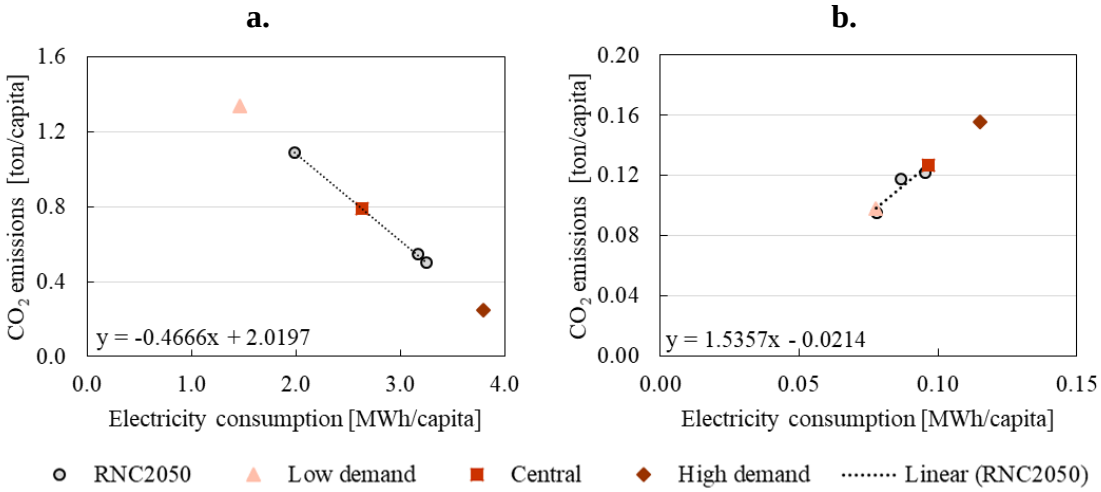

Figure 4.32. CO_2 emissions and electricity demand for industry and agriculture
Linear regressions for electricity demand and CO_2 emissions from RNC2050 for: a. industry; and b. agriculture. The CO_2 emissions assumed in this work for the electricity consumption are also shown: light red triangle – Low demand scenario; red square – Central demand; and dark red diamond – High demand scenario. The grey circles represent the CO_2 emissions for the three scenarios considered in RNC2050 [109].

In the case of **services**, the RNC2050 assumes that two of their scenarios have undergone complete electrification of the sector. For this reason, here, it is assumed that the scenarios with higher electricity demand (Central and High demand) are also completely dependent on electricity, thus they are free from non-electric emission originated in the services.

The less electrified scenarios (i.e., Low demand) are considered to still rely on natural gas for other energy uses, e.g. for space heating. In RNC2050, the only scenario that is not completely electrified considers an electricity demand of 1.83 MWh/capita and 0.07 tCO_2/capita. Since less electrification leads to the displacement of energy to natural gas, resulting in higher non-electric emissions, the non-electric emissions were considered to be inversely proportional to electricity demand. Thus, the non-electric CO_2 emissions for the services is of 0.08 tCO_2/capita for the Low demand scenarios.

For **mobility**, different approaches were taken. Non-electric light passenger vehicles were assumed to use gasoline ($fe_{gasoline}$ of 73.7 $kgCO_2/GJ$ [217]) and to travel the same daily distance as EVs. PHEV gasoline consumption was also considered since about 5% of its distance is travelled using conventional fuels. Equation (4.61) describes the calculation required to determine the CO_2 emissions originated by light passengers.

$$CO_{2_{nonelectric,light\ pass.}} = n_{days} \times N_{pr.veh.} \times c_{pr.veh.,\ gasoline}[(1 - S_{EV}) \times D_{pr.veh.,gasoline} + S_{PHEV} \times D_{PHEV,gasoline}] \times fe_{gasoline} \times 10^{-12} \quad (4.61)$$

where n_{days} is the number of days in the year; $N_{pr.veh.}$ is the number of private light passenger vehicles; $c_{pr.veh.,\ gasoline}$ is the energy consumption of private light passenger vehicles, assumed as 2.05 MJ/km [18]; S_{EV} and S_{PHEV} is the share of electric vehicles and light plug-in hybrid electric vehicles (PHEV) in the light passenger fleet, respectively [fraction]; $D_{pr.veh.,gasoline}$ and $D_{PHEV,gasoline}$ are the daily distance travelled by the gasoline private vehicles and the daily distance travelled by PHEV private vehicles in non-electric mode, respectively [km]; finally, the multiplying factor '10^{-12}' is used to adjust units.

The Portuguese roadmap RNC2050 was used as a reference for the remaining fuel consumption, with some adaptations [175]. For freight vehicles, the vehicles propelled by hydrogen in the roadmap were shifted to biofuels, while the consumption from diesel-fueled vehicles is taken directly from the roadmap (fe_{diesel} of 74.1 kgCO_2/GJ [217]). To replace hydrogen consumption by biodiesel, a 48% [221] and 22.5% [222] efficiency of hydrogen and biodiesel were assumed, respectively. Heavy passenger vehicles were assumed to be completely fueled by diesel and biofuels. The roadmap includes a small fraction of electricity, that was converted to biofuel consumption (assuming also 22.5% efficiency for biofuel consumption).

[18] A 20% improvement in efficiency was applied to the current energy consumption of 2.56 MJ/km [229], as in Ref. [101].

Table 4.38. Fuel consumption from freight and heavy-duty passenger vehicles
Assumptions for the fuel consumption from freight and heavy-duty passenger vehicles, according to adapted results from the RNC2050 [175].

Freight and Heavy-duty passenger vehicles – Fuel consumption [GJ]					
			Low demand	Central demand	High demand
Freight	Light-duty	Diesel	6.6	-	-
		Biofuels	2.9	-	-
	Heavy-duty	Diesel	25.2	-	-
		Biofuels	28.4	17.9	35.8
Passenger	Heavy-duty	Diesel	2.68	0.02	0.05
		Biofuels	3.78	5.64	11.3

CO_2 emissions from railways, navigation and aviation were not considered in this work.

The resulting non-electric emissions are shown in Table 4.39.

Table 4.39. Non-electric CO_2 emissions
Summary of non-electric CO_2 emissions for residential, services, industry, agriculture and mobility.

Non-electric CO_2 emissions [Mton]					
			Low demand	Central demand	High demand
Residential			0.7-0.9	0.4-0.6	0.1-0.3
Services			0.8	-	-
Industry			12.3	7.3	2.3
Agriculture			0.9	1.2	1.4
Mobility	Passenger	Light-duty (private)	1.3	3.2	0.2
		Heavy-duty[a]	0.2	~0	~0
	Freight	Light-duty	1.9	-	-
		Heavy-duty	0.5	-	-
Total non-electric CO_2 emissions			18.6-18.8	12.1-12.3	4.0-4.2

[a] In Central and High demand scenarios, the heavy passenger vehicles are assumed to be mostly from biofuels.

4.6. Approach limitations

For the sake of comprehensiveness, some simplifications have been made during this research. This section summarizes the main simplifications of this work.

In regards to climate parameters, some limitations may be pointed. Daily and three-hourly data of temperature, irradiance and wind speed were interpolated to hourly data using simple methods. Those interpolations could be significantly improved by implementing more complex approaches that may more accurately describe the behavior of the climate parameters. Even though the water supply was addressed using a multiyear calibration, it is only driven by monthly precipitation. Hydrological models could be applied to better simulate the available water supply.

The spatial resolution of the climate parameters used to ascertain the energy supply was considerably large. Photovoltaics' generation was determined using temperature and irradiance averaged per NUTS III, while for wind power the driving factor was wind speed averaged for the Centre region. Water supply was averaged at a national level, driving the hydropower and run-of-the-river generation. The renewable sources of energy generation were then averaged to deliver a single time-series to introduce in the energy modelling tool. Ideally, the spatial resolution to determine those generations should be finer in order to include differences in the resource availability and behavior.

Power system modelling also shows significant shortcomings. One of the biggest limitations is the use of a single point in space to simulate the power system. It neglects the power constraints in the national transmission lines by ignoring the spatial distribution of supply and demand. Due to the same constraint, each supply source is modelled as one large power plant, discarding the individual characteristics of each power plant. Thermal power plants are great examples of this limitation: only two may be modelled, implying that the model does not allow to simulate condensing power plants using different fuels with different kinds of operation and characteristics. Hydro dam storage capacity is also a good example, the model considers a single reservoir that does not include geographical distribution of both the water supply and of the dams.

The modelling of hydro pump also raises two issues: 1) there are no limitations of the water availability in the downstream, i.e., while excess electricity is being generated and

while the reservoir is not at its full capacity, the downstream water is pumped to the reservoir, independently on the level of river flow in that downside of the dam; and 2) the water supply is completely used for electricity generation, ignoring other uses of water (e.g. irrigation). Another limitation in the power system modelling is the hourly resolution: it is not enough to explore grid stabilization issues; for that, a thinner resolution is required.

Focusing on electricity demand, some simplifications were implemented. Even though a wide range of possible demand evolutions was provided to cover divergent paths, they still might be debatable. The assumptions taken for the services, industry, and agriculture sectors were simply gathered according to the literature. The electricity demand for the mobility sector was built in a detailed bottom-up manner for the light vehicles, e.g. the number of vehicles and respective driving patterns, and the same approach could be extended to heavy-duty freight vehicles. Also, some of the mobility players were not taken into account, such as it is the case for heavy-duty passenger vehicles, railways, navigation, and aviation.

The main limitation in the modelling of the electricity demand was that solely the residential electricity demand was assumed to depend on climate. Below, the limitations from the approach taken to model the residential demand are listed.

Residential electricity demand depends on socio-economic context, signal prices, user's behavior, climate, etc. The projection of its development is strongly dependent on the assumptions and on the chosen approach to model it. Thus, as for any complex framework, the method proposed to model residential electricity demand in the future has some limitations, which are discussed below.

To determine the residential electricity demand, several sets of dwellings are created and characterized by their building characteristics, the existence of space heating and cooling systems, etc. Each parameter of a dwelling is selected according to its probability distribution function, without considering possible correlations with other characteristics besides age (e.g. a dwelling with double glazing windows may be more likely to be well insulated). One of the limitations of this method is not considering possible correlations among variables. For example, more efficient equipment is expected in houses with improved thermal performance.

A future energy efficiency improvement of heat pumps was disregarded. The residential space heating and cooling needs were determined considering several sources for internal gains (e.g. occupants, electric appliances, lighting, etc.), excluding non-electric appliances. One significant limitation is the disregard of economic factors such as price-driven mechanisms that may change consumer's behavior, and economic growth that may affect ownership of electric appliances.

Energy storage in batteries was considered under two alternatives. First, due to a model limitation, electric vehicles and second-life batteries assume a charging/discharging rate of 0.1C (see subsections 4.4.2.1 and subsection 4.4.2.4); also, they are modelled as a single large battery, emphasizing the limited spatial resolution of the model. Second, the capacity of the dedicated energy storage was determined by applying a simple algorithm to calculate the imports energy need above the defined cross-border interconnection capacity defined. It does not take into account charging/discharging efficiency rates as it aims at illustrating the potential requirement for additional storage capacity.

In what regards overall emissions, the results aims at illustrating the differences in CO_2 emissions between demand-flexibility scenarios. It considers a basic approach that neglects emissions from other activities not focused on this work (e.g. aviation).

Finally, hydrogen or electricity for its production was not included in this work, for any sector. In mobility, biofueled-vehicles were considered as opposed to hydrogen-fueled vehicles. For energy storage, second-life electrochemical batteries were assumed as opposed to hydrogen (or other storage technologies such as compressed air energy storage). Also, other uses could consider hydrogen, such as in industrial processes. Its implementation would require an adjustment of electricity demand due to different efficiencies of the technologies, for example, compared to electrochemical batteries. The introduction of hydrogen would add more complexity to the built system, but it is one of the most interesting follow-ups for this work.

5. Results

This research work led to results that address three main topics, as can be seen in the following sections. It begins by exploring the residential electricity demand in the future (section 5.1), followed by the results from the performance of highly renewable power systems (section 5.2) and of 100% renewable power system (section 5.3). In this chapter, the results from RCP8.5 are provided in the Supplementary Material, see the end of subsection 4.2.1.

5.1. Residential electricity demand[19]

In this section, the residential electricity demand is analyzed in detail. Then, to understand the sensitivity of the results to some of the assumptions taken, a sensitivity analysis is performed to the housing stock, floor area of new dwellings, electrification of cooking and domestic hot water and penetration of heat pumps (subsection 5.1.1). Finally, the section ends with a small discussion on the results.

As described in detail in subsection 4.4.1.2, the residential sector was modelled by considering three scenarios according to their level of electricity demand. The Central scenario assumes 75% of electrified cooking and domestic hot water, 27% of heat pumps' penetration, retrofitting and new buildings' rate of 2 and 0.75% per year, respectively. The Low and High scenarios exacerbate particular features of the Central scenario such as the electrification of equipment, the age of the housing stock and the average area of dwellings.

The average load profiles of the total electricity demand in households are shown by the lines in Figure 5.1. Their ranges, due to the different ensemble years, are represented by the shaded areas. As expected, the Low demand scenario is the one with the lowest load

[19] Part of this section is adapted from Figueiredo et al., 2019 [227].

profile, while High demand scenario shows the highest, resulting from the high electrification levels assumed but also from the older housing stock, which, being less efficient, contributes to higher needs of space heating and cooling.

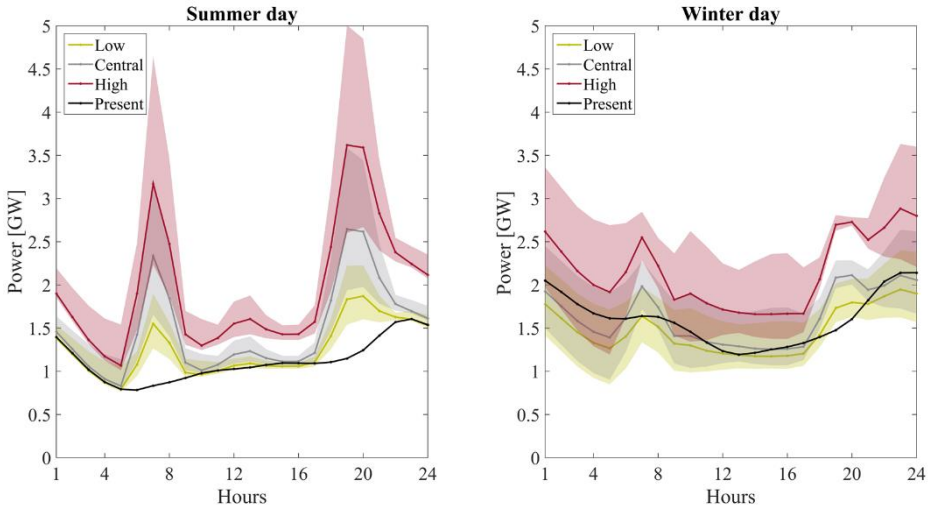

Figure 5.1. Residential load profiles
Average load diagram for a summer day (left) and a winter day (right). The shaded area represents the range of the results (between the maximum and minimum observed).

The High demand scenario also shows a higher dispersion of results, due to its higher electrification of space heating/cooling, making electricity consumption more sensitive to climate. Scenarios with lower electrification of space heating/cooling, or higher energy performance buildings (e.g. higher insulation), or both, are much less sensitive to the ensemble year used.

In summer, the pronounced peaks at times of leaving/arriving home are observed for future consumption but not for present consumption. This is mainly due to the higher usage of electric appliances (for cooking, DHW and space cooling) compared to the present.

In Figure 5.2 the discriminated histograms for the consumption in each scenario are presented for the climate path RCP4.5. The present level of demand is also shown by the dashed vertical line. It may be noted that climate impacts only heating and cooling demands. The remaining loads are mainly dependent on the society development considered for each scenario, such as the floor area of dwellings and the electrification of cooking and DHW loads.

The High scenario shows always higher levels for the different types of demands. As previously mentioned, the high electrification rates for space heating/cooling makes this scenario highly dependent on climate, increasing significantly its space heating/cooling needs. Bigger new dwellings also help to increase the plug loads and space heating/cooling.

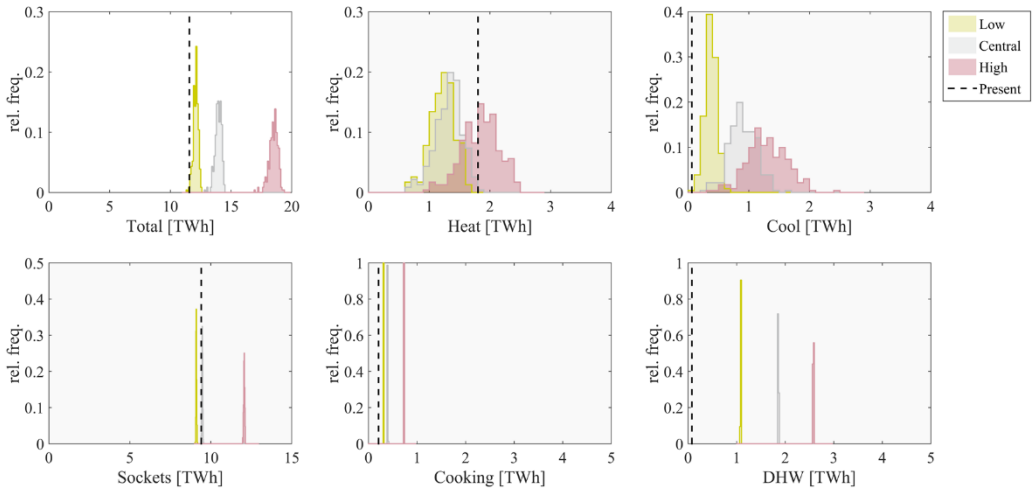

Figure 5.2. Residential electricity consumption per type of demand – RCP4.5
Histograms for the electricity consumption of the different types of demand (total, heat, cool, sockets, cooking and DHW) in the mid-century under RCP4.5 according to the Low, Central, and High demand scenarios. The black dashed line shows the present electricity consumption.

The results for the two climate paths (RCP4.5 and RCP8.5) are qualitatively similar, and those for RCP8.5 are only shown in Annex IV. RCP8.5 shows slightly higher cooling needs and slightly lower heating needs, both explained by the higher temperature increase considered in this climate path.

Table 5.1 shows the average electricity consumption per type of consumption and scenario, for both RCP paths.

Table 5.1. Metrics for residential electricity consumption per type of demand
Average electricity consumption for every scenario considered, including RCP4.5 and RCP8.5. The minimum and maximum values obtained in the simulation are shown below the average value as: '(minimum/maximum)'.

Average, minimum and maximum electricity consumption [TWh/year]						
	Total	Heat	Cool	Sockets	Kitchen	DHW
Present	11.56	1.80	0.06	9.42	0.21	0.08
Low	12.07 (11.31/12.51)	1.17 (0.57/1.72)	0.38 (0.09/0.70)	9.11 (9.03/9.17)	0.32 (0.31/0.32)	1.08 (1.08/1.09)
Central	13.92 (12.83/14.48)	1.28 (0.64/1.81)	0.91 (0.21/1.65)	9.47 (9.40/9.55)	0.40 (0.39/0.40)	1.86 (1.85/1.87)
High	18.46 (16.92/19.31)	1.79 (0.90/2.51)	1.31 (0.30/2.42)	12.06 (11.96/12.16)	0.73 (0.73/0.74)	2.58 (2.57/2.59)

In the future, residential electricity demand may increase from 4 to 60% on average for the Low and High demand scenarios, respectively. The heating demand tendency differs between the High demand scenario and the remaining ones: in the High scenario, the average heating demand remains at the present value, while in the Low and Central scenarios it may decrease 35 and 30%, respectively. For the cooling needs, it is expected an increase from 5 to 20-fold.

The decrease in heating electricity consumption is the result of three main factors: 1) increase on average temperature; 2) better insulated houses; and 3) wider adoption of more efficient heating devices (heat pumps). The High scenario maintains the magnitude of current consumption mainly because it considers not only more occupied houses but also an aged housing stock.

As for the increase in cooling needs, it results from higher temperatures and from wider adoption of cooling electric devices. The electrification rate for domestic hot water and cooking is also a driver for the increase in demand. Demand attributed to socket loads is mainly determined by assumptions on the dwelling floor areas.

This work assumes that the final electricity consumption is directly dependent on the assumptions made for each scenario, ignoring two-way dynamics such as 1) price-driven mechanisms conditioning end-user behavior, such as the use of air-conditioning, which may affect and be affected by the investment need in the electrification of buildings; and 2) societal factors, such as economic growth, migration fluxes, and changes in the age structure of the population, which may affect investment in buildings.

Regarding the impact of different climate conditions on the variability of demand, it is clearly observed in the spread of the histograms presented in Figure 5.2. One can observe that changes in building stock, electrification rates of cooking and DHW and adoption of heat pumps have a stronger effect on residential demand than climate variability, i.e., the range of demand for each scenario driven by the different ensemble years is smaller than the range of demand across different scenarios. Hence, future residential demand is primarily driven by policies and market choices regarding the development of the building stock and technologies used.

Increasing electrification (High demand scenario) leads to a higher sensitivity to climate. That is, the variability on the demand (i.e., the range between minimum and maximum values) increases with the electrification of space heating/cooling devices, as shown in Table 5.1. For heating, the range goes from low electrification with 1.2 TWh to 1.6 TWh for high electrification – which corresponds to 2.4% and 3.2% of the overall Portuguese consumption in 2017 [163], respectively. It also means that heating demand oscillates between -51 to +47% of the average value around it. For cooling, the variation between maximum and minimum observations is wider, starting at 0.6 TWh (Low) to 2.1 TWh (High), meaning that cooling demand fluctuates between -77 to +85% around its average. Variability of the total demand hence ranges between 1.2 and 2.4 TWh (corresponding to an oscillation around the average of -8 to +5%), for the Low and High demand scenarios, respectively.

By observing the extreme values of demand, total residential demand may change from -2.2% to +67.0%, compared to current levels. The range of change for heating electricity demand goes from a slight increase of 0.6% to a decrease down to -68.3%. Cooling electricity demand is expected to increase in every case, from a minimum of +50.0% to a maximum of +3,933.3%. For the remaining loads, the development of demand depends mainly on the future electrification levels (e.g. DHW demand can increase 31-fold due to the low level of DHW electrification existing today).

5.1.1. Sensitivity analysis

A sensitivity analysis is performed to understand the impact of the assumptions taken regarding the development of the housing stock, floor area of new houses, electrification of cooking and domestic hot water and penetration of heat pumps. The Central scenario is used as the basis for these sensitivity analyses. Then, each assumption at a time is changed from the values assumed in the Central to the values taken in the Low and in the High demand scenarios, keeping all the remaining unchanged. By taking such an approach, it is possible to understand the individual impact of each assumption.

Figure 5.3 shows the effect of the household market, floor area of new dwellings, electrification of DHW and cooking and space heating and cooling on the total residential demand for the RCP 4.5 pathway.

For the household market, the changes to the Central scenario are associated with energy demand for space heating and cooling. A newer housing stock results in less heating but more cooling, due to better thermal insulation. Also, with less inhabited houses, penetration of heat pumps in occupied buildings is higher (to keep the level of penetration on the overall existing houses, see subsection 4.4.1.2). This higher adoption of heat pumps can contribute to lower heating needs (due to higher efficiency of heat pumps compared to electric resistances), while also contributing to higher cooling energy consumption due to the availability of heat pumps (heat pumps are the only cooling devices considered in this work).

An older housing stock with more houses, and thus fewer people per house, lead to more heating but less cooling, due to less efficient houses and fewer people per house, respectively. Even though the average dwellings' floor area is smaller in older houses, more dwellings lead to demand associated with general electric appliances and cooking, which are related to the floor area. The existence of fewer heat pumps, given the higher number of occupied houses (fewer heat pumps), also contribute to the heating/cooling results obtained.

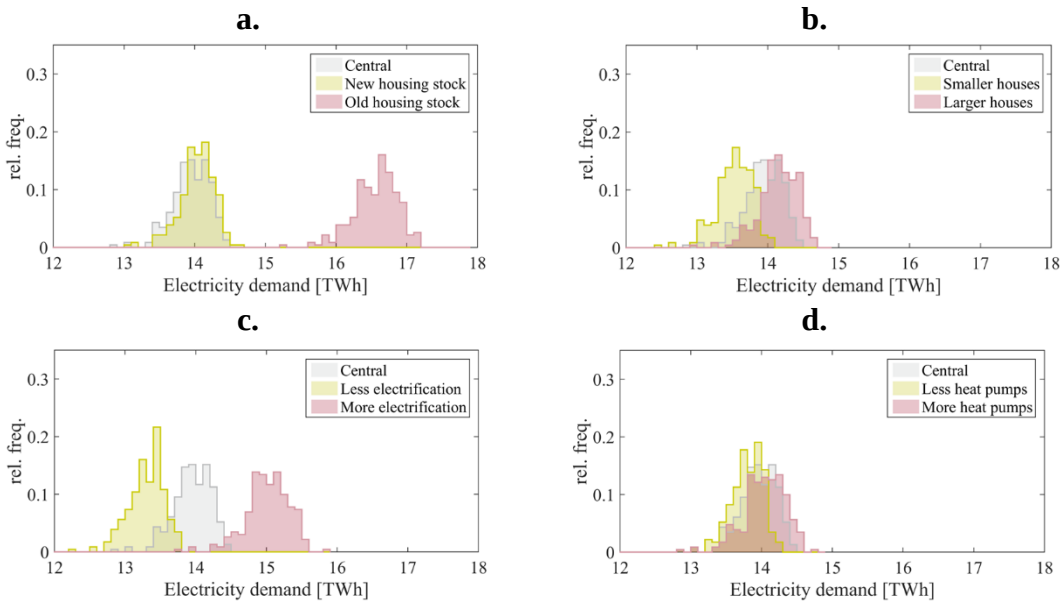

Figure 5.3. Sensitivity analysis on different housing stock development characteristics RCP4.5 – Histograms
Histograms for the sensitivity analysis performed under RCP4.5: a. Household market; b. Floor area of new dwellings; c. Electrification of cooking and DHW; and d. Space heating and cooling.

As for the floor area of new dwellings, as expected, smaller homes lead to lower electricity consumption due to lower heating, cooling, cooking and general electric appliances needs (all assumed to be area dependent). In contrast, larger homes lead to higher electricity needs mainly for heating, cooling, and general appliances. Since the use of general electric appliances represents heat gains, they may also contribute to increasing cooling needs in dwellings.

The cooking and DHW rates of electrification correlate positively with electricity consumption. As a second-order effect, lower electrification rates lead to lower internal heat gains (less electric DHW and cooking devices), which leads to higher needs of heating and lower needs of cooling. The opposite happens in the case of higher electrification rates. It is noteworthy mentioning that the use of non-electric appliances may also contribute to the increase of internal gains. However, non-electric appliances' energy demand or their contribution to internal gains are not taken into account in this study.

Finally, regarding the adoption of heat pumps, one may observe a positive correlation with electricity consumption but with a very slight expression of changes compared to the Central scenario. Fewer heat pumps available result in an increase of non-electric heating, although there is only a small decrease in heating demand because there is also an increase in electric resistance usage. The decrease in cooling energy consumption is

explained by the fact that cooling is only provided by heat pumps. More heat pumps result only on a slightly higher heating electricity demand because of their high efficiency. The increase in cooling consumption is directly due to the increase in the availability of heat pumps. Even though it is not considered in this study, the operation of heat pumps may aggravate the urban heat island effect, contributing potentially to increase cooling needs.

Figure 5.4 summarizes the averaged numerical effect of the changing parameters on the demand per sector. One can observe that total electricity demand is more sensitive to an old housing stock (+19%), due to increased heating and cooking demand, followed by electrification rate of DHW and cooking (+8%), which has an obvious strong effect on cooking and DHW needs but also cooling demand. Floor area and penetration of heat pumps are shown to have a lower impact on residential demand.

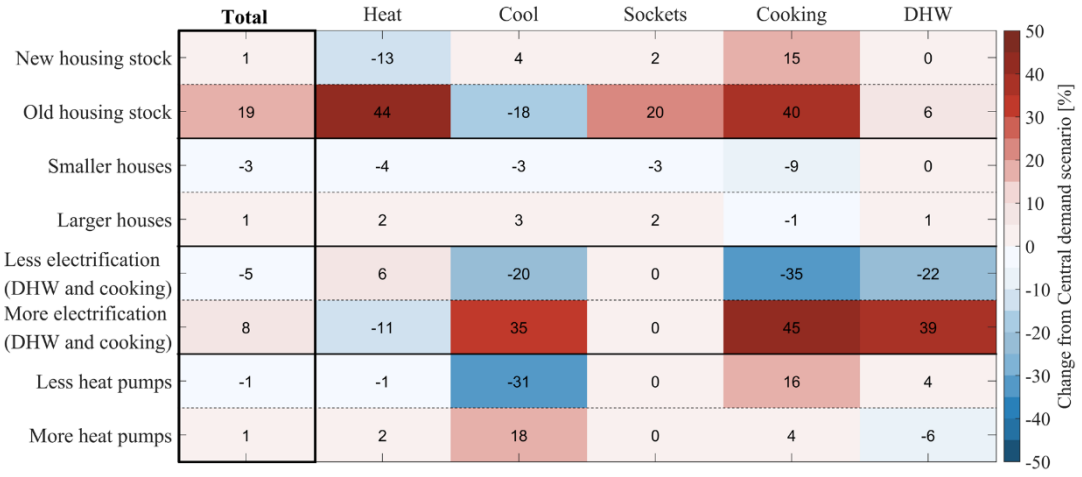

Figure 5.4. Sensitivity analysis on different housing stock development characteristics RCP4.5 – Average
Change in the average electricity consumption relative to the Central scenario for each type of consumption under RCP4.5.

In this study, the average residential electricity demand in the future is expected to increase more or less, depending on the scenario (4, 20 and 60%, for the Low, Central, and High demand scenarios, respectively). The heating needs tend to decrease by 35 and 30% in the Low and Central scenarios, respectively, remaining at the present level in the High scenario. Cooling needs increase in every scenario: 20-fold in the most extreme case. Such results are in line with the existing literature (see section 3.2) [106], [108], [111].

5.2. Highly renewables-based power system

In this section, the high renewables-based power systems proposed above are analyzed. The results for RCP4.5 are presented in the main text, the results from RCP8.5 do not differ significantly and they may be consulted in Annex V and Annex VI.

5.2.1. Reference Power Systems[20]

In the highly renewable power system, the HiRES, about 88% of the power capacity is renewable and the biomass resource is limited to the present values, while in the HiRES+UB power system an unlimited availability of biomass is considered. Since the power capacity fleet is the same and the only difference is biomass availability, which influences solely the renewable generation and emissions, most performance indicators of the power system are the same.

Figure 5.5 shows the performance of the power systems under several variants of climate conditions and different demand-flexibility scenarios for electricity demand, annual net imports, cross-border interconnections, and curtailment rates.

[20] A fraction of this subsection is adapted from Figueiredo et al., 2020 [under review in Applied Energy Journal].

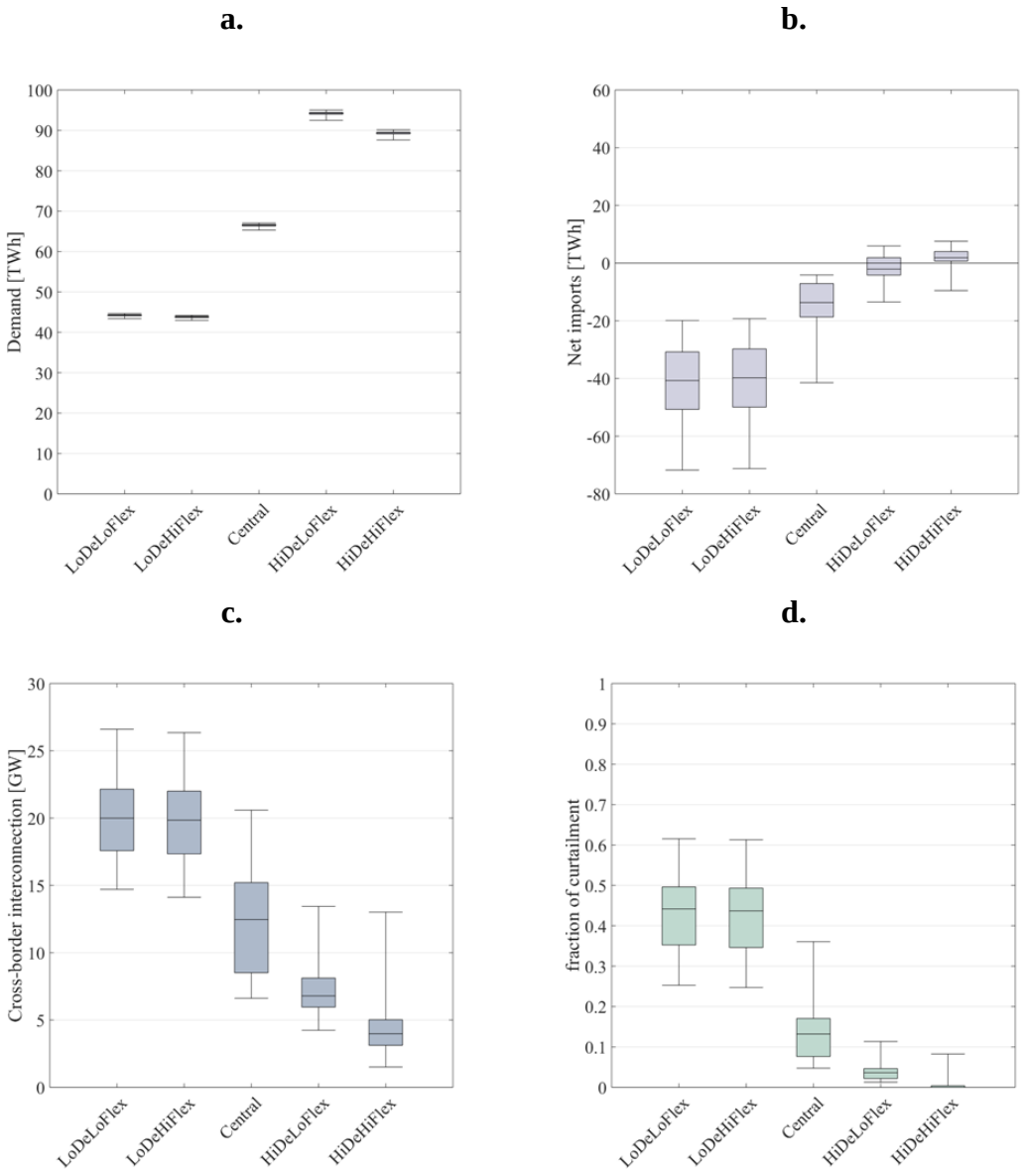

Figure 5.5. Highly renewable power systems – RCP4.5
Performance of the proposed highly-renewable power systems for all ensemble years and each demand-flexibility scenario under RCP4.5 in terms of: a. electricity demand; b. annual net imports (resulting from the difference between annual imports and exports); c. cross-border interconnection requirements; and d. potential energy curtailment (relative to generation). Each boxplot represents the results obtained for all the ensemble years tested.

The total electricity demand may decrease up to 15% in the Low demand scenarios, while it may double in High demand scenarios, compared to current values (about 50 TWh, see section 3.1). It can be seen that climate does not impact significantly total electricity demand since it is assumed that only residential demand, accounting for 19-28.5% of total demand depending on the demand-flexibility scenario, is affected by it. Due to climate variability, residential demand fluctuates between -8.3 and +4.6% of its average demand.

However, since renewable energy generation is mostly driven by climate, energy trade across the border strongly depends on climate. Low electricity demand scenarios have large energy exports (negative values in Figure 5.5b.), while high demand leads to more balanced energy trading (values around zero in Figure 5.5b.). For the same reason, the required cross-border interconnection capacity and the curtailment rates are higher for the Low demand scenarios due to higher power in excess.

One may also observe that the flexibility of the system does not affect significantly the median nor the scattering of import needs or the required cross-border interconnection capacity. In the High demand scenarios, the weak role of flexibility may be caused by the great dominance of imports, reducing the importance of the system capability to match demand with generation. Conversely, the same is true for the Low demand scenarios, where exports are dominant.

In most ensemble years, all demand-flexibility scenarios lead to cross-border interconnection needs well above 5 GW, which is what is expected to be put in place in 2050 (see Table 4.15 in subsection 4.3.4). For the Low demand scenarios, this may lead to a high curtailment of up to 61%, hence increasing costs.

Figure 5.6 shows the biomass consumption for HiRES (dashed line) and HiRES+UB (boxplots). Independently on the climate conditions and demand-flexibility scenarios, the HiRES+UB power system more than doubles the biomass consumption of HiRES. Even though the aim is to reduce fossil usage, a framework considering an unlimited use of biomass resources leads to serious concerns about the sustainable use of natural resources. Thus, this configuration of the power system should be addressed cautiously. More than half of the biomass consumption in the HiRES comes from industrial CHP power plants. The reduction of CHP consumption may be supported by higher electrification of processes that are not heat-intensive.

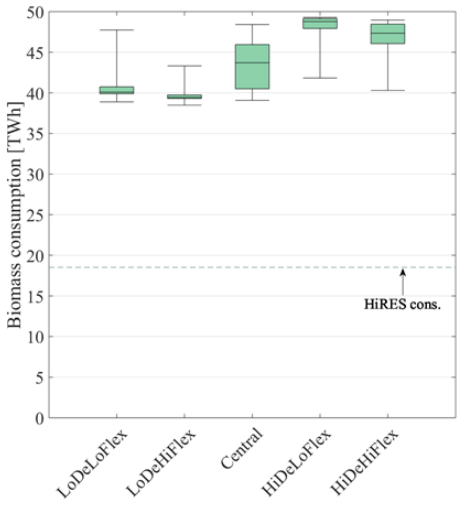

Figure 5.6. Biomass consumption in highly renewable power systems – RCP4.5
Comparison between the biomass consumption for all ensemble and each demand-flexibility scenario under RCP4.5 for HiRES (highly renewable power system) and HiRES+UB (same with unlimited biomass resource) configurations. HiRES is represented in a single dashed line since its biomass consumption is limited to current values and it is always fully needed. For HiRES+UB, each boxplot represents the results obtained for all the ensemble years tested.

Figure 5.7 shows the renewable generation share and the CO_2 electric emissions from both HiRES and HiRES+UB power systems.

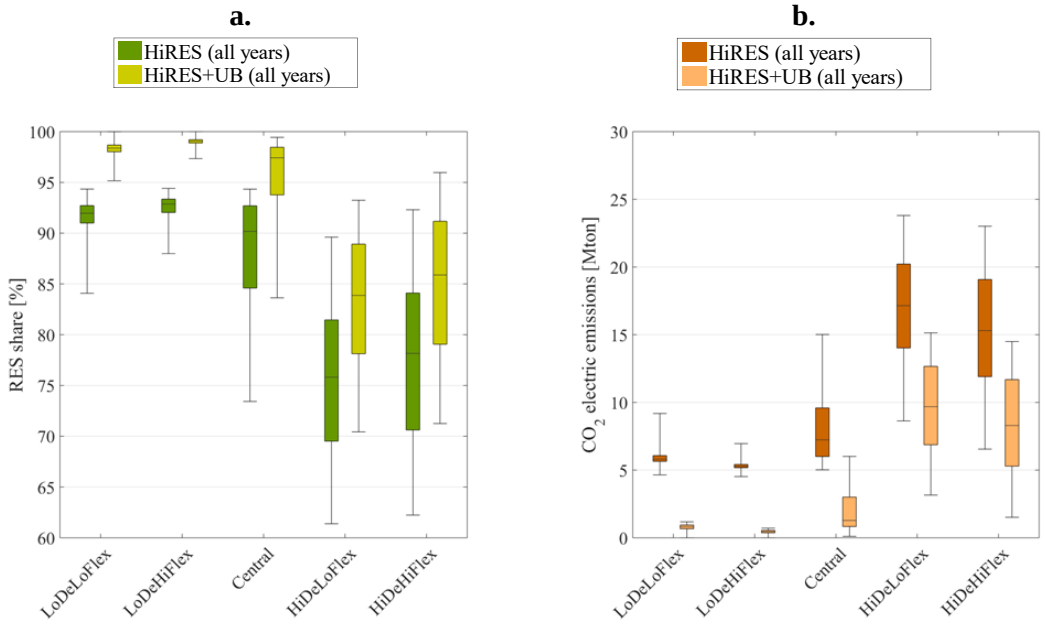

Figure 5.7. Renewable share and CO_2 emissions from the power systems HiRES and HiRES+UB – RCP4.5
Comparison between the performance of HiRES (highly renewable power system) and HiRES+UB (same with unlimited biomass resource) configurations for all ensemble years and each demand-flexibility scenario under RCP4.5 in terms of: a. generation share of renewable energy; and b. CO_2 emissions from the power system. Each boxplot represents the results obtained for all the ensemble years tested.

As expected, when unlimited biomass is considered, the natural gas power plants are only used in periods of peak demand when the full power capacity of biomass is not enough. Thus, HiRES+UB shows better indicators of renewable share and emissions: for the median year, it shows on average +7 p.p. of renewable share (84-99%, compared to 76-93% for HiRES) and -70% of CO_2 electric emissions (0.5-9.7 Mton, compared to 5.3-17.1 Mton for HiRES).

As expected, the higher demand scenarios lead to lower renewable shares since they require higher energy generation. For HiRES and HiRES+UB, the maximum renewable share achieved is of 92.3 and 96.0%. In the Low demand scenarios, the HiRES+UB power system shows considerably high shares of renewable shares with a minimum of 95.2%, while the same value for HiRES is 84.1%.

For the renewable generation share, the impact of flexibility is relatively small for both power systems. In the Low and High demand scenarios, flexibility increases the median renewable share on less than 1 and 2 p.p., respectively. As for CO_2 electric emissions, the impact of flexibility is more pronounced for HiRES+UB: Low demand scenarios decrease 43% their electric emissions and a 14% decrease is expected for high demand. The same numbers for HiRES are about 10% decrease in electric emissions. It should be highlighted that the more critical relative decreases in HiRES+UB are mainly driven by the very low absolute emissions originated.

In all demand-flexibility scenarios, the impact of climate variability is visible. Higher electricity demand combined with the same power capacity increases the chances that renewable generation may not be enough to satisfy all electricity demand. It leads to higher variability in High demand scenarios, while Low demand scenarios have a narrower variation of renewable generation share. Therefore, the most affected are the High demand scenarios, where a fluctuation around the median values of the renewable share goes from -16 to +14 p.p. and -15 to +10 p.p. for HiRES and HiRES+UB, respectively. As for electric CO_2 emissions, the oscillation around the median is of -60 to +50% and -82 to +75% for HiRES and HiRES+UB, respectively.

Looking at the CO_2 electric emissions, one could be led to conclude that lower electricity demand would be the easy option to fight climate change due to their much lower emissions. However, CO_2 emissions are not only originated in the power system. In fact, other uses of energy may emit a larger amount of CO_2. Figure 5.8 shows the total CO_2

emissions (see section 4.5), which include the emissions originated in the power system and the remaining activity sectors.

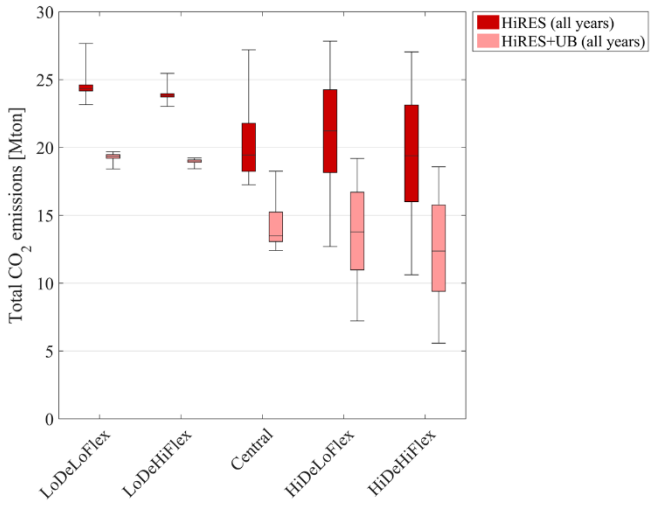

Figure 5.8. Total CO_2 emissions – RCP4.5
Comparison between the performance of HiRES (highly renewable power system) and HiRES+UB (same with unlimited biomass resource) configurations for all ensemble years and each demand-flexibility scenario under RCP4.5 in terms of: a. generation share of renewable energy; and b. CO_2 emissions from the power system. Each boxplot represents the results obtained for all the ensemble years tested.

When including other emissions besides the electricity-related emissions, the trend changes considerably. The most critical changes are seen in the Low electricity demand scenarios, where the emissions increase up to 4.5 and 41-fold in the HiRES and HiRES+UB, respectively. The High demand scenarios increase up to 27 and 49% for HiRES and HiRES+UB, respectively. Accounting for other emissions shows that higher electricity demand may provide a less pollutant alternative (when considering highly decarbonized power systems).

Again, the High demand scenarios show the highest oscillations of CO_2 emissions with climate variability, showing a fluctuation around the median value of -44 to +40% and -53 to +51% for HiRES and HiRES+UB. Such results highlight the need to consider climate variability in the performance of the power system to more realistically establish the impact of policies and other measures under different climate conditions.

5.2.2. Solar-wind power capacity

To achieve power system targets, such as renewable energy share and CO_2 emissions, for all the years present in the ensemble, one needs to increase the renewable energy installed capacity. Since hydropower and biomass are already constrained in these future power system configurations, the solution seems to be to adjust the installed capacity of photovoltaic and onshore wind. Below, the photovoltaic and onshore wind installed capacities are varied keeping a 2:1 ratio as in the reference power systems (which consider 20 GW of solar and 10 GW of onshore wind, see subsection 4.3.4). The impact of installed capacities differs among the power systems tested (HiRES and HiRES+UB), the demand-flexibility scenarios and the performance indicators. To self-contain this analysis, four indicators were chosen: net imports, cross-border interconnection for imports, renewable share generation and total CO_2 emissions. Also, for comprehensiveness reasoning, three demand-flexibility scenarios are chosen to bound the results: Low demand + High flexibility (LoDeHiFlex), Central and High demand + Low flexibility (HiDeLoFlex). The remaining results may be consulted in Annex VI. To better contextualize the results, one goal for each indicator was selected, as follows

- Annual net imports – To ensure a balanced power system that is not under- or over-generating electricity, the cancellation of the annual net imports was considered.
- Cross-border interconnection for imports – A 5 GW limit for interconnection was assumed, supported by literature (see subsection 4.3.4).
- Renewable generation share – A fully decarbonized power system (i.e., 100% renewable generation) was settled as the goal for this indicator. It is also the goal of the Portuguese roadmap RNC2050 [99].
- Total CO_2 emissions – The goal was defined as 6.3 Mton of CO_2 emissions [109]. It is the value for the most optimistic vision of RNC2050, excluding emissions that are not taken into account in this work: fluorinated gases, refining, and fugitive emissions, aviation, navigation and railways.

Figure 5.9 shows the annual net imports and cross-border imports' interconnection for the three chosen demand-flexibility scenarios given different photovoltaics and onshore wind (PV+Wind) power capacities. Similarly to above, the HiRES and HiRES+UB power systems result in the same annual net imports and cross-border interconnection for imports, since those power systems differ only in biomass and natural gas availability.

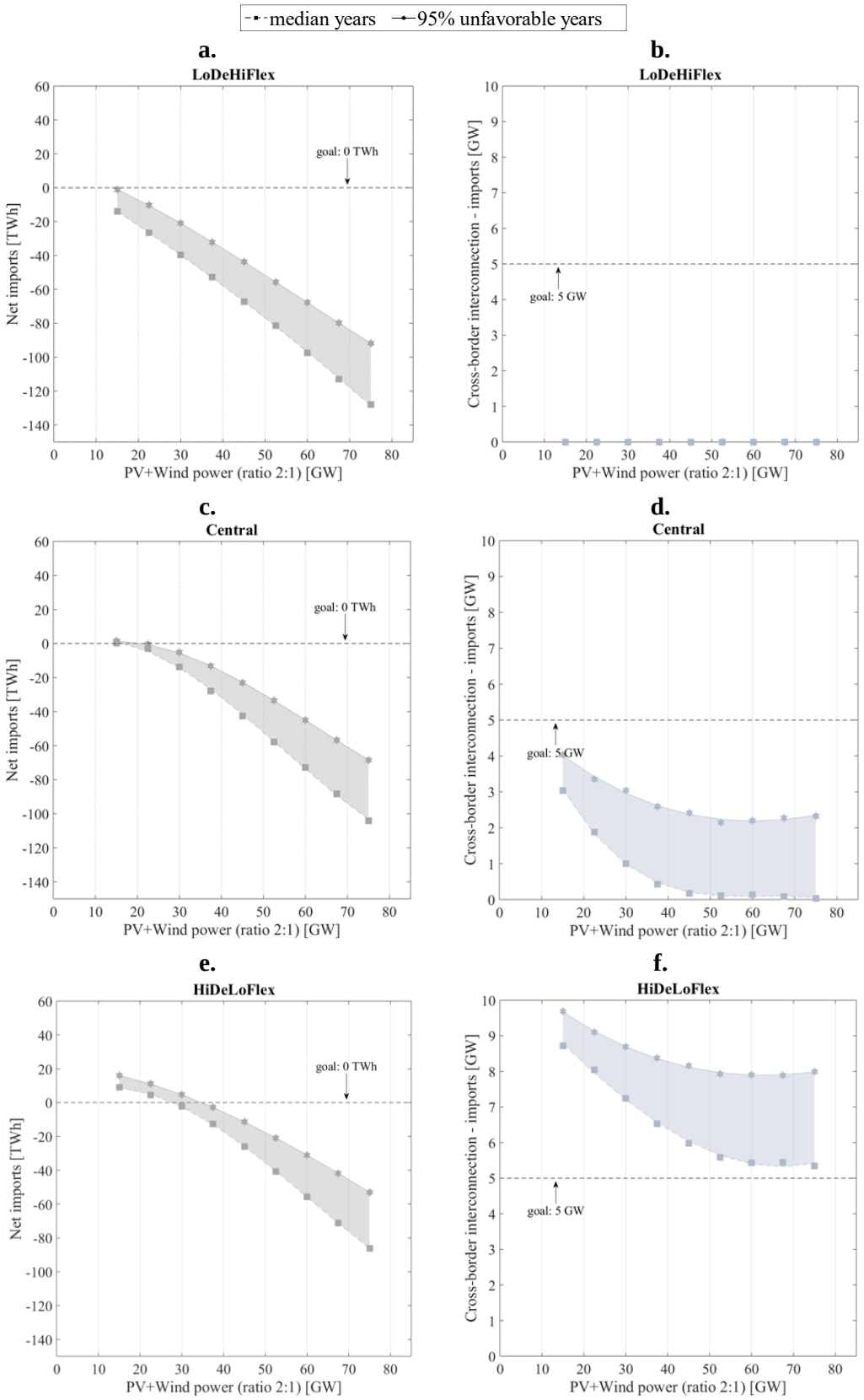

Figure 5.9. Annual net imports and cross-border interconnection in varying PV+Wind capacities – RCP4.5
Annual net imports and cross-border interconnection for imports for different PV+Wind installed capacities (ratio 2:1) for different climate conditions and three demand-flexibility scenarios under RCP4.5: a/b. Low demand + High flexibility (LoDeHiFlex); c/d. Central; and d/e. High demand + Low flexibility (HiDeLoFlex), respectively. Each marker represents different percentiles of net imports/cross-border interconnection: square with a dashed line – 50th percentile and hexagram with a solid line – 95th percentile.

Null net imports show that the power system is able to generate the same amount of energy that it consumes. In the Low demand scenarios, a strong bias towards exports is observed for all PV+Wind capacities tested, leading to high curtailment rates. To achieve null net imports in median years, in the Central scenario a 45% decrease below the reference power system capacities is required, while for higher levels of demand a decrease of 7% of the PV+Wind reference power is needed resulting in about 16.5 and 28 GW, respectively. For unfavorable years (95^{th} percentile), the High demand scenarios require 35 GW of PV+Wind power, corresponding to a 25% increase compared to the requirements for the median year (and 16% above the reference PV+Wind power).

Cross-border interconnections are extremely important to ensure the feasibility of a power system that is not prepared to operate in an island-mode. While export interconnection requirements may be diminished by curtailing energy generation, the need for imports interconnection is more complex to solve. For this reason, the focus here is given to the behavior of the power system in terms of import interconnection. The import needs in Low demand scenarios are negligible. The Central scenario shows reasonable cross-border interconnection requirements, but always below 5 GW, both for median and unfavorable years. On the contrary, the High demand scenario with low flexibility (HiDeLoFlex) is not able to decrease the import cross-border interconnection. But when high flexibility is added (HiDeHiFlex, see Annex VI), an 83% increase in PV+Wind power (corresponding to 55 GW) enables the decrease of the interconnection to values below 5 GW under the median climate year.

Figure 5.10 shows the renewable generation share and the total CO_2 emissions under different PV+Wind power capacities for HiRES and HiRES+UB.

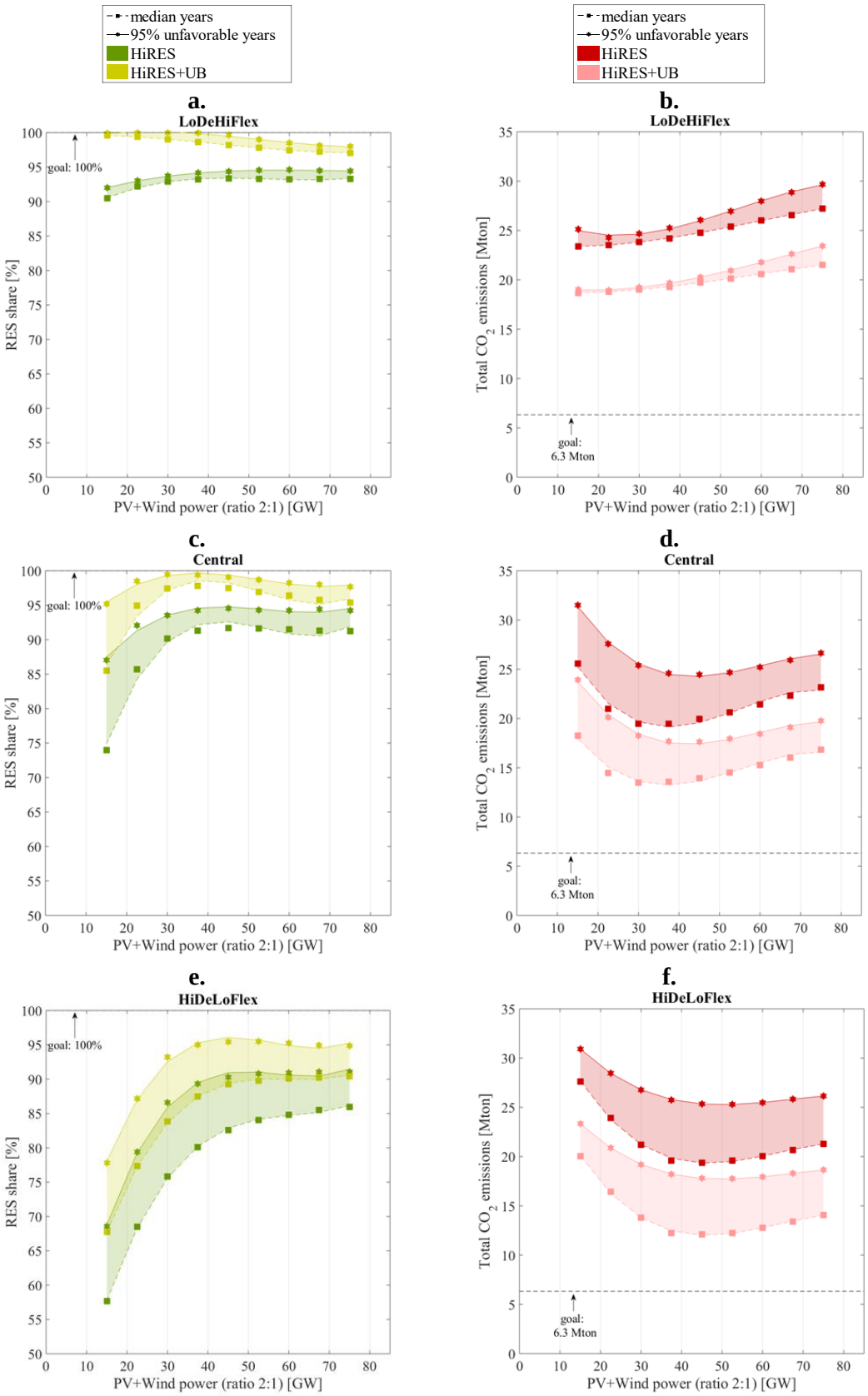

Figure 5.10. Annual net imports and cross-border interconnection in varying PV+Wind capacities – RCP4.5
Annual net imports and cross-border interconnection for imports for different PV+Wind installed capacities (ratio 2:1) for different climate conditions and three demand-flexibility scenarios under RCP4.5: a/b. Low demand + High flexibility (LoDeHiFlex); c/d. Central; and d/e. High demand + Low flexibility (HiDeLoFlex), respectively. Each marker represents different percentiles of net imports/cross-border interconnection: square with dashed line– 50th percentile and hexagram with a solid line – 95th percentile.

Considerably different behaviors can be seen among the demand-flexibility scenarios. In the LoDeHiFlex, the renewable generation share decreases or shows small increases with the introduction of variable renewable power capacity. It results from the increasing need for stabilization share provided by dispatchable generation, i.e., the increase of variable renewable generation leads to the need for increasing dispatchable generation which may be provided by natural gas powerplants. The total CO_2 emissions increase for the same reasons for both power systems.

In the Central scenario, a strong increase in the renewable share is observed, peaking at 37.5 GW (i.e., 25 GW of photovoltaic and 12.5 GW of onshore wind, an increase of 25% over the reference) with 91.3 and 97.8 % for HiRES and HiRES+UB under the median year, respectively. The total CO_2 emissions are minimized at 30 GW (precisely, the reference power system proposed with 20 GW of photovoltaic and 10 GW of onshore wind) with 19.6 and 13.6 Mton of CO_2 emissions for HiRES and HiRES+UB under median year conditions, respectively. The change in the trend towards a more sustainable system is the result of the increase in fossil dispatchable generation to compensate the variable generation while keeping the defined stabilization share.

Finally, under the median year, the HiDeLoFlex scenario requires an increase of 50% in the PV+Wind capacities to maximize the renewable generation share (82.6 and 89.4% for HiRES and HiRES+UB, respectively) and minimize the total CO_2 emissions (19.4 and 12.0 Mton for HiRES and HiRES+UB, respectively).

5.3. Fully renewable power system

In this section, the 100% renewable power system (100%RES) is analyzed in detail. It shows only the results for RCP4.5. The results for RCP8.5 are analogous and are included as Annex VII-VIII.

5.3.1. Approach

In the highly renewable power systems (HiRES and HiRES+UB) configuration described in the previous section, natural gas power plants were available to meet peak demand. In the 100% renewable power system this is not true. Since the risk of not complying with the system needs is higher in the 100%RES, the level of resilience of the power system is here introduced.

Required power configurations for wind onshore and photovoltaics are proposed to achieve zero net annual imports for each demand-flexibility scenario. These configurations of installed capacity are defined according to the chosen climate variability threshold, used to define the level of resilience. In this context, the term resilience is used to characterize the level of national independence from outside energy trades, assuming null net imports.

Thus, the required installed power for the median year (50% resilient) will be lower than the required installed power for a more conservative approach of using the year that corresponds to the 95^{th} percentile (95% resilient power system). As before, unfavorable conditions are represented by the climate thresholds above the 50^{th} percentile, since, for the same power system, they require higher net imports. Hence, the 95^{th} percentile of net imports is considered as a 95% unfavorable year's threshold.

Figure 5.1 schematizes the level of resilience of a power system and the corresponding thresholds.

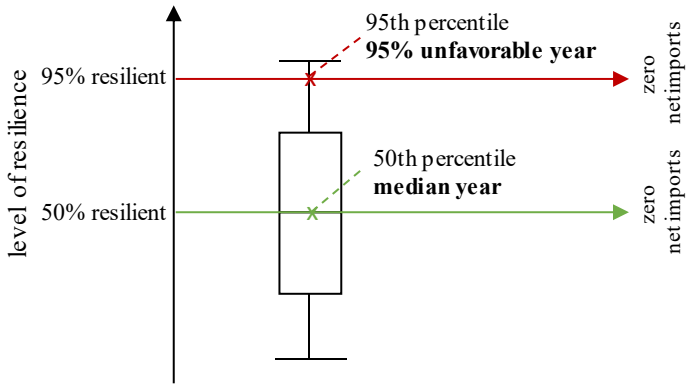

Figure 5.11. Level of resilience of the power system
Schematic of the level of resilience of the power system and the definition of unfavorable/median years, according to the net imports.

The cross-border interconnection and dedicated stationary energy storage requirements are then explored for those power systems with the required photovoltaics-wind onshore capacities. The dedicated stationary storage aims at decreasing the cross-border interconnection to 5 GW (see subsection 4.3.4 and subsection 4.4.2.4). Figure 5.12 summarizes the approach taken here.

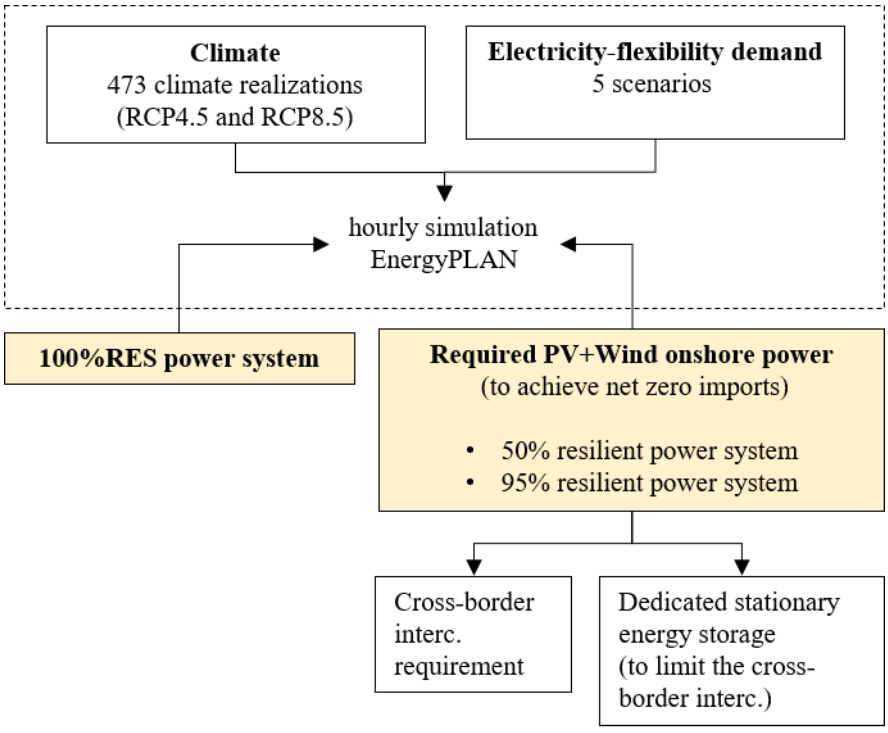

Figure 5.12. General approach for the fully renewable power system
Summarized scheme describing the approach taken to analyze the performance of the 100% renewable power system.

5.3.2. Reference Power System

Figure 5.13 shows, for the reference power system under all ensemble years, the electricity demand, the cross-border interconnection requirements, the net annual imports and the curtailment fraction for each demand-flexibility scenario.

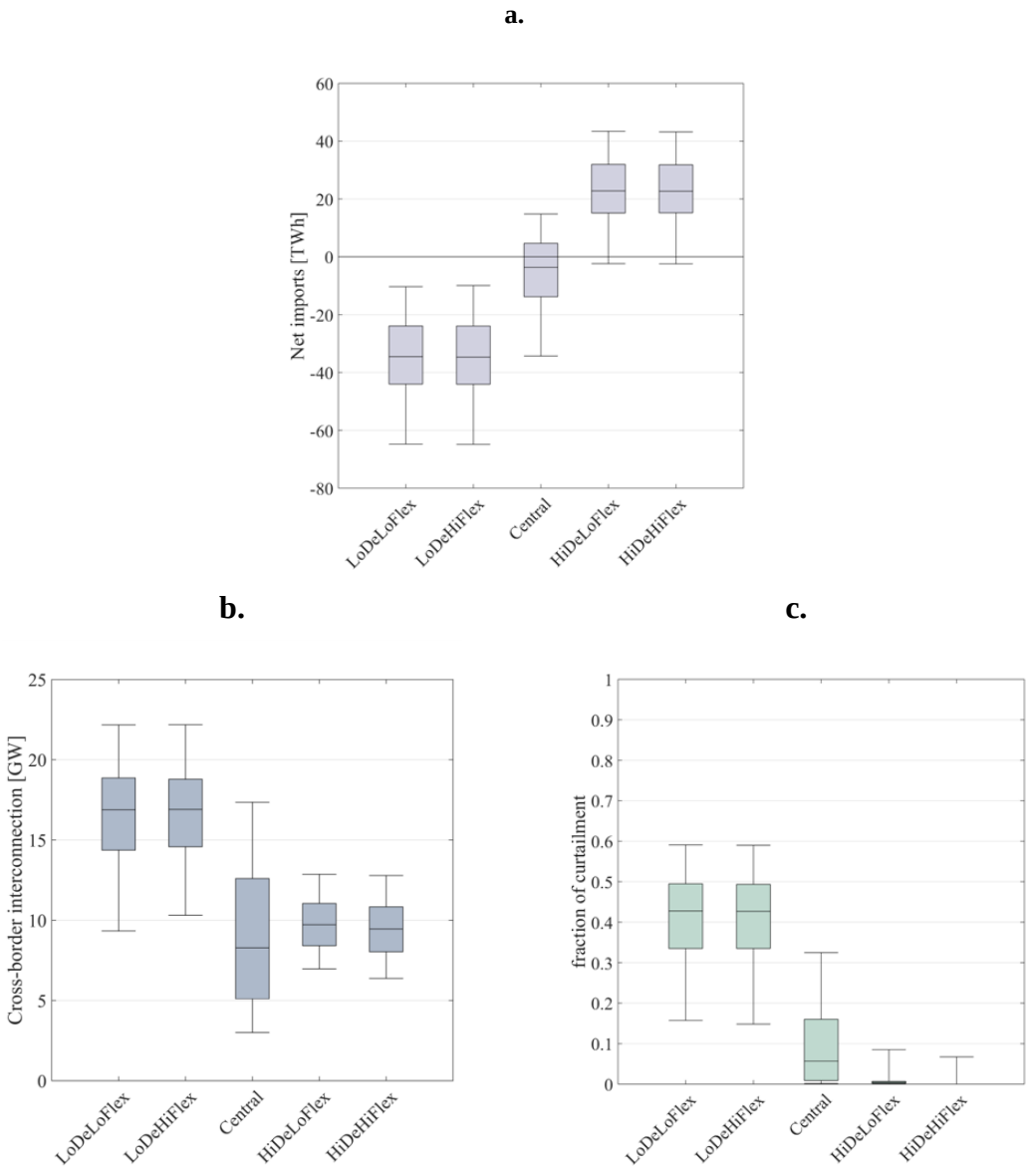

Figure 5.13. Fully renewable power system – RCP4.5
Performance of the proposed 100%RES power system for all ensemble years and each demand-flexibility scenario under RCP4.5 in terms of: a. electricity demand; b. annual net imports (resulting from the difference between annual imports and exports); c. cross-border interconnection requirements; and d. potential energy curtailment (relative to generation). Each boxplot represents the results obtained for all the ensemble years tested.

Higher exports are expected for Low demand scenarios whereas higher imports are required for High demand scenarios. The Central scenario seems to be a more balanced

alternative since its distribution is centered on zero net imports. This is also supported by the cross-border interconnection needs.

The Central scenario shows a wider range of cross-border interconnection needs but with lower median values, mainly because it is a more balanced scenario. It shows that the reference power system is better suited for the Central scenario demand, i.e., installed capacities are better adjusted to the electricity demand. With a better adjusted power system, the cross-border interconnection capacity is less critical because the number of hours with high interconnection requirements decreases (for both exports and imports). Despite the decrease of the median cross-border interconnection, the Central scenario still shows significant export needs that surpass the highest interconnections from the High demand scenarios, which may be explained by the exporting needs that are still significant. As for curtailment, it is expected to be higher in Low demand scenarios due to excess generation.

Overall, the highly-renewable power systems (HiRES and HiRES+UB), presented in section 5.2, show higher annual exports (lower annual net imports), higher cross-border interconnection and similar curtailment rates. The higher exports may be explained by:

1) the industrial CHP generation, which is removed in this 100%RES (see subsection 4.3.4);

2) stabilization share – In HiRES and HiRES+UB, it was only provided by dispatchable generation. Hence, with high variable renewable the system requires higher dispatchable generation, consequently increasing the total generation and the exports. With the introduction of variable generation stabilization (15% of variable generation, see subsection 4.3.4), the required dispatchable generation decreases so does the total generation and exports. The higher cross-border interconnection may be explained with the same rationale since the highest values presented in HiRES and HiRES+UB are due to exports.

Figure 5.14 shows the biomass consumption in all ensemble years and demand-flexibility scenarios. With the removal of industrial CHP and the increase of available generation for stabilization, the use of biomass decreases compared to the HiRES+UB scenario. While for the Low and Central demand scenarios the biomass consumption is mostly under the present consumption, in the High demand scenarios it may increase 3-5% under the median years' conditions and about 12% at maximum.

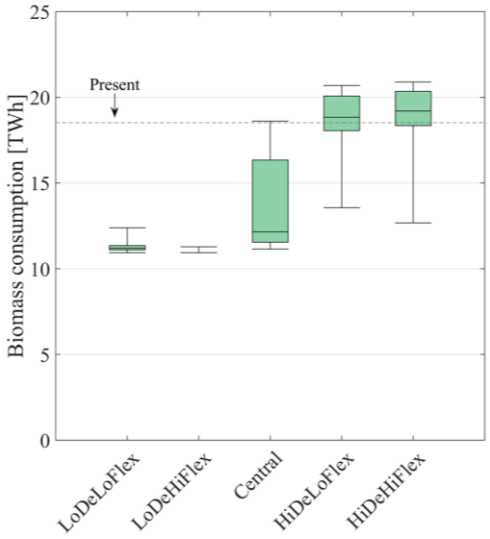

Figure 5.14. Biomass consumption in the fully renewable power system – RCP4.5
Comparison between the biomass consumption for all ensemble years and each demand-flexibility scenario under RCP4.5 for 100%RES (100% renewable power system) and the present consumption. The dashed line represents the present consumption of biomass and each boxplot represents the results obtained for all the ensemble years tested in the 100% RES.

5.3.3. Required solar-wind power capacity

Different scenarios implying different levels of external energy dependency raise an issue, which is how to define the required power fleet assumed as installed in such scenarios. In order to do this, a zero annual import/export balance was imposed, i.e., total annual demand must be met by the endogenous total renewable annual generation. This to identify system portfolios conducive to that result.

The installed capacity required to achieve zero net imports for each demand-flexibility scenario was determined by adjusting the solar and onshore wind power capacity preserving a 2:1 power ratio present in the reference 100%RES power system (e.g. 20 GW of solar for 10 GW of onshore wind, see subsection 4.3.4). The required power system was determined for different climate conditions, e.g. a median year will require less installed capacity than a 95% unfavorable year (the 95th percentile).

Figure 5.15 exemplifies the analysis performed for the Central scenario. The details of the analysis for the remaining demand-flexibility scenario are presented in Annex VIII.

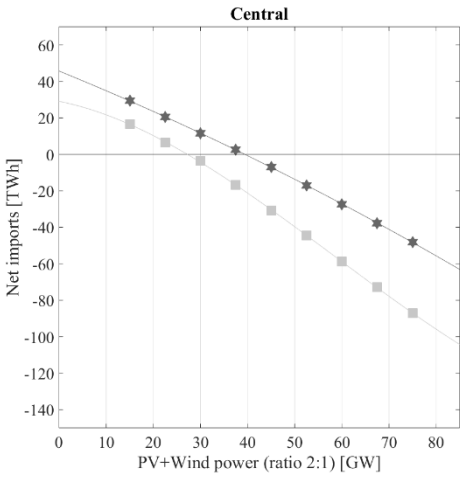

Figure 5.15. Analysis of the required photovoltaics and onshore wind capacity in Central scenario – RCP4.5
Analysis of the required photovoltaics and onshore wind capacity for different levels of resilience under RCP4.5 Central scenario. Each marker represents different percentiles of net imports: square – 50th percentile and hexagram – 95th percentile (95% unfavorable year).

Figure 5.16 shows the PV+Wind power capacity required to achieve zero net imports for the different demand-flexibility scenarios for a 50 and 95% level of resilience (i.e., for the median and the 95% unfavorable year, respectively). For each of the demand-flexibility scenarios, different climate conditions imply different PV+Wind capacities. It is noteworthy to highlight that these power systems are only guaranteeing zero net imports within the climate they were designed for.

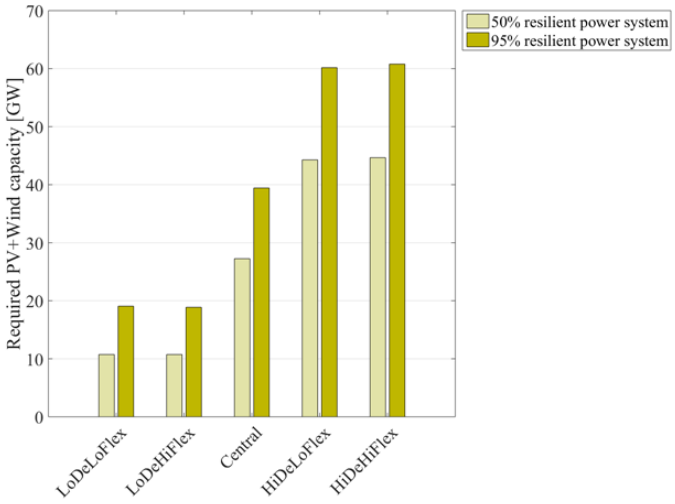

Figure 5.16. Required photovoltaic and wind capacity – RCP4.5
Combined photovoltaics and onshore wind capacities required for having null net imports for the different demand-flexibility scenarios with 50 and 95% resilience under RCP4.5.

The impact of demand-flexibility is clearly represented in these results: the required solar-wind capacity for a fully decarbonized power system may increase 3-fold from a Low to a High demand scenario (from 50 to 80% of the total installed capacity for the 50% resilient system), assuming that marginal demand is fully satisfied by these technologies.

To achieve a very resilient power system with zero net imports, *ceteris paribus* one should increase the installed capacity. Within the Low demand scenarios, a 95% resilient power system needs 77% more PV+Wind (about more 8 GW) than a 50% resilient one. For the High demand scenarios, the corresponding increase is 36%, from 44 to 60 GW.

Under the median years' conditions, the HiRES and HiRES+UB power systems achieved null net imports around 16.5 GW and 28 GW for the Central and High demand scenarios (see section 5.2). The higher requirements shown by the 100%RES (27 and 44 GW for Central and High demand scenarios) are translated into an increasing vulnerability to climate, explained by the lower generation (e.g. industrial CHP and natural gas power plants).

Figure 5.17 shows the import cross-border interconnection requirements for the 50 and 95% resilient power system (defined for each scenario), highlighting the important variations depending on demand and climate.

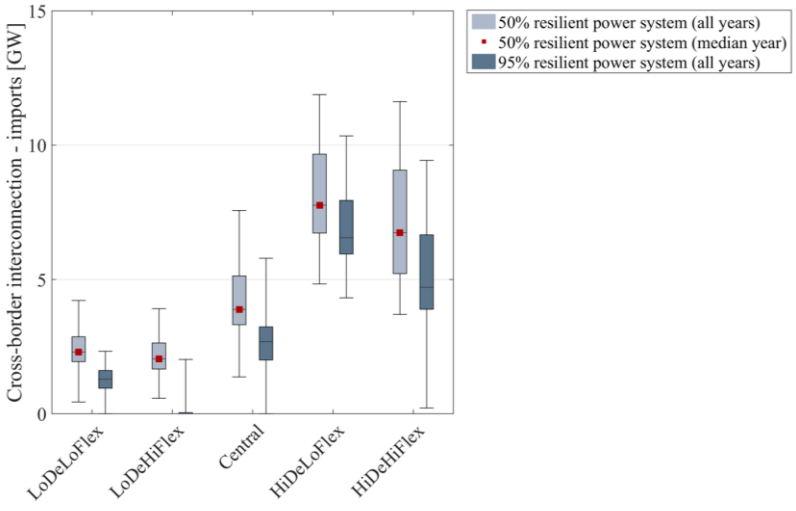

Figure 5.17. Cross-border interconnection requirements – RCP4.5
Cross-border interconnection required for imports for the power systems designed with a level of resilience of 50 and 95% under RCP4.5. Each boxplot represents the results obtained for all the ensemble years tested. The dark red square highlights the median of the 50% resilient power system.

For the 50% resilient power system, the higher flexibility in the system allows for slightly lower cross-border interconnection needs, on average -5% for the extreme years, due to the mechanisms shifting demand to off-peak periods. For the median year (zero import-export balance), this power system requires an interconnection between 2.0 and 7.8 GW, mostly depending on demand. A power system should be prepared for different weather conditions possible of occurring during its lifetime, ensuring always a reliable performance. In this sense, to become a resilient power system, the cross-border interconnection corresponding to the 50% resilience level should increase by 53-95%. The most critical increase is in the Central scenario, where the 3.9 GW interconnection, enough for the median year, should increase to 7.6 GW to meet the needs under the most extreme years.

The 95% resilient power system shows an average decrease in the required cross-border interconnection needs for imports of 30% compared to the 50% resilient system. This significant decrease is observed in every flexibility-demand scenario; it is mainly caused by a substantial increase in energy generation, avoiding import needs. Flexibility plays an important role within this power system: more potential to export energy allows better use of load shifting mechanisms, leading to an average decrease of 11% of the maximum cross-border interconnection required.

These results point to the critical role of high cross-border interconnection capacity, particularly for the High demand scenarios, whose requirement is about 10-12 GW, significantly above the 5 GW assumed as a sensible interconnection capacity for the Portuguese power system.

An alternative to the (expensive) expansion of the cross-border interconnection required would be the introduction of dedicated stationary energy storage. For the Low demand scenarios, there is no need for additional energy storage, as Figure 5.18 shows, since the need for interconnection is always below 5 GW.

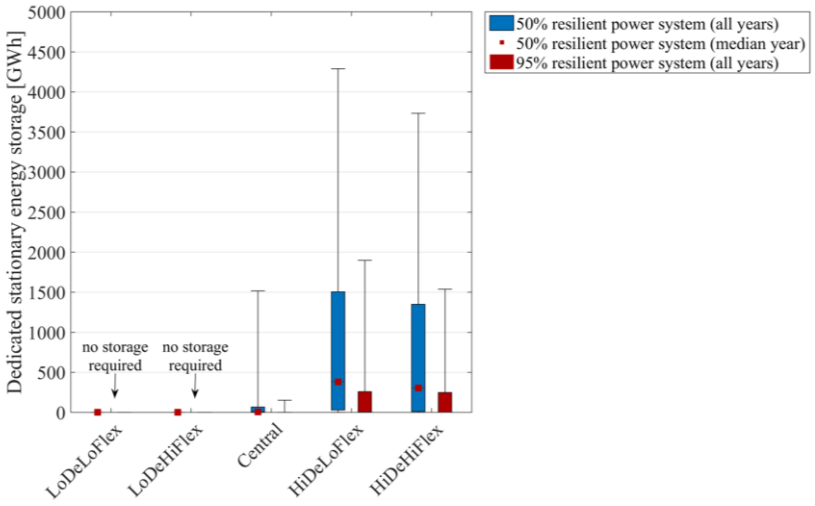

Figure 5.18. Dedicated stationary energy storage – RCP4.5
Dedicated stationary energy storage required for the power system designed with a level of resilience of 50 and 95% under RCP4.5, to limit the cross-border interconnection to 5 GW. Each boxplot represents the results obtained for all ensemble years tested. The dark red square highlights the median of the 50% resilient power system.

For the remaining, in the case of the 50% resilient system, an increase up to 200-fold is required, which is the case of the Central scenario, where a limited additional energy capacity of 7.6 GWh is needed for the median year increasing up to 1.5 TWh under extreme climate. Correspondingly, a 10-fold increase (0.4 to 4.3 TWh) in storage needs is observed for the HiDeLoFlex scenario. Considering that the initial storage included in the model ranges from 3.1 to 3.4 TWh (mostly from hydro reservoir storage capacity), this additional stationary storage is considerably relevant. Depending on the demand-flexibility scenario and climate, it may entail a doubling of the initial storage. For the power system with the resilience of 95%, the need for additional storage decreases significantly, becoming null for most of the weather conditions tested. The flexibility plays an important role in the High demand scenarios as it reduces the maximum additional storage required by 13 and 19% for the 50 and 95% resilient power systems, respectively.

A sensitivity analysis on the cross-border interconnection was performed for the demand-flexibility scenario with higher storage needs (HiDeLoFlex) for both the 50 and 95% resilient power systems, Figure 5.19.

The present cross-border interconnection is about 3 GW; if it remains constant until 2050, the power system may require a dedicated storage capacity equivalent of up to 8 and 2.6% of total demand for the 50 and 95% resilient power system, respectively. Considering the

European Union target for 2030 of 15% interconnection capacity (as per the ENTSO-E [223]), which is also the target for Portugal [169], the cross-border interconnection for the power system required in the HiDeLoFlex scenario is of 10 and 13 GW for a 50 and a 95% level of resilience, respectively. With those interconnection levels, the required dedicated energy storage for a 95% unfavorable year decreases significantly: 240 GWh (0.2% of total demand) for the 50% resilient power system, and none for the 95% resilient system. One should highlight that such high cross-border interconnection needs are very ambitious and would require a significant investment in both the Portugal-Spain and the Spain-France interconnections.

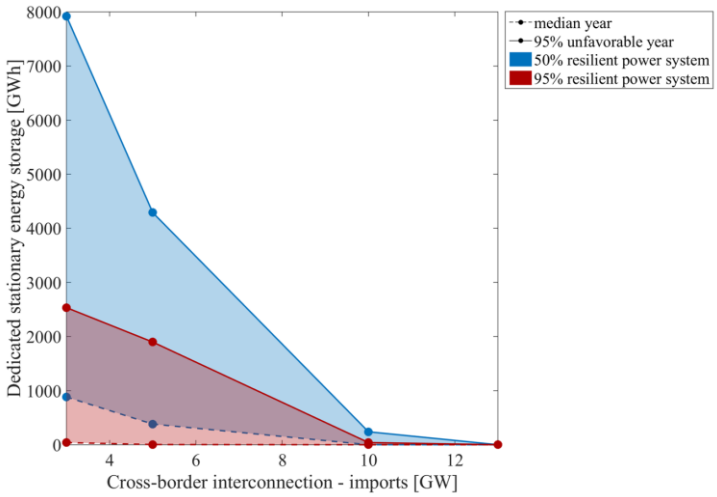

Figure 5.19. Sensitivity analysis on the cross-border interconnection for High demand + Low flexibility – RCP4.5 Dedicated stationary energy storage required according to the cross-border interconnection for the power system designed with a level of resilience of 50 and 95% under RCP4.5. The required dedicated stationary energy storage requirement for different cross-border interconnection capacities is represented in: dashed line– 50th percentile and solid line – 95th percentile.

Planning for a power system based on a 95% unfavorable year makes it more resilient, but it may also entail higher energy costs. Figure 5.20 shows the fraction of generated energy potentially curtailed according to the level of resilience. Power systems with higher resilience lead to high export needs for most of the ensemble years, because they are prepared for rare climate conditions that otherwise would result in import needs. Thus, some curtailment may be required for a higher fraction of the ensemble years tested, resulting in up to 48% of curtailment, compared to 35% within the 50% resilient power system. Regarding system flexibility, when more is available it is expected a decrease of up to 3% on potential curtailment for a 95% resilient system, and up to 7% for a 50% resilient system.

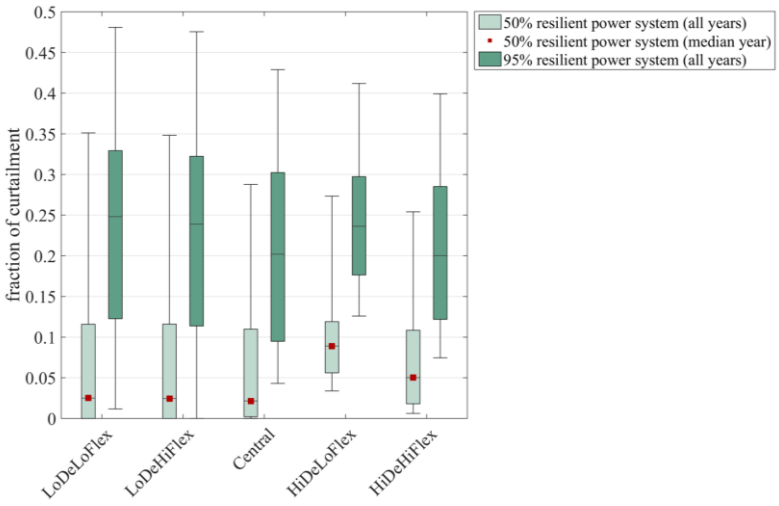

Figure 5.20. Potential energy curtailment – RCP4.5
Generation potentially curtailed for the power systems designed with a level of resilience of 50 and 95% under RCP4.5. Each boxplot represents the results obtained for all the ensemble years tested. The dark red square highlights the median of the 50% resilient power system.

As to a comparison between the 50% resilient power system for a median year, and the 95% resilient one for all weather conditions (a red dark square is presented in Figure 5.17, Figure 5.18 and Figure 5.20 to highlight the performance of a power system planned for and subjected to a median year), the cross-border interconnection requirements for the median year are always higher for the less resilient configuration, as Figure 5.17 shows, because it assumes less capacity installed. For the median year, a 95% resilient system requires less 1-2 GW of cross-border capacity. To cover all climate conditions in the HiDeLoFlex scenario, the most critical, the 95% resilient power system needs 10 GW of interconnection, 13% less than the 12 GW required by the 50% resilient power system.

Similar trends can be seen in Figure 5.18 for the dedicated energy stationary storage that is required: the power system with a lower level of resilience also presents higher storage needs than the more resilient one. In this case, for the median year, no stationary storage is required when considering the 95% resilient power system. Regarding the maximum storage required in the HiDeLoFlex scenario, the 95% resilient power system needs 1.9 TWh while the 50% resilient one needs twice this value. Following the same rationale, the median potentially curtailed energy of the 95% resilient system increases on average 6-fold compared to the median of the 50% resilient system, due to the lower generation rates.

6. Conclusions and final remarks

To fight climate change, nations worldwide are coming together to urge the need for an energy transition. Part of their attention is turned to power systems and their corresponding emissions. For this reason, power systems will become fully renewable. Critical challenges arise for future power systems highly dependent on renewables. From one point-of-view, the high penetration of renewables is augmenting the power systems' sensitivity to climate conditions, since most renewable resources are directly dependent on climate. From another angle, the development of future electricity demand is subject to a high level of uncertainty. The high sensitivity of future power systems to climate and future society development builds up the need to further study them under different combined outcomes in demand and supply dimensions.

This thesis aims to fulfill that need by studying the performance of highly renewable power systems under climate variability and different demand development scenarios. The case study is the Portuguese power system in the mid-21st century. It uses an hourly-based modelling tool to simulate the power system. A multiyear calibration is proposed, validated and implemented. Climate variability is addressed by applying an ensemble containing the equivalent to almost 500 years of climate data, provided by an ensemble based on two representative concentration pathways (RCP4.5 and RCP8.5) for the period 2045-2055. Five demand-flexibility scenarios are built to address uncertainty in the development of electricity demand. Diverging paths for electricity demand and system flexibility are applied to create those scenarios. Three power fleet configurations are proposed: a highly renewable power system with the current biomass availability, a highly renewable power system with unlimited biomass availability and 100% renewable power system. This work has focused on the Portuguese power system, but its qualitative results may be applied to other regions with similar characteristics.

The main question that motivates this research work is: *How resilient will a renewables-based power system be?* Its answer may be divided into two main dimensions

of the power system: climate variability and future demand. The first emerging question is about the impact of climate variability:

What is the impact of climate variability on the power system?

First, the focus is given to the impact on residential electricity demand. Climate variability is more relevant within scenarios of increased electrification, because of increased needs for electric space heating and cooling. The demand varies between -77 and +85% for space cooling and between -51 and +47% for space heating, around their average values. Due to climate variability, the total residential electricity demand oscillates between -8 and +5% around its average value. Those results may entail significant consequences for the power system.

The impact of climate variability on the performance of a highly renewables-based power system can be noticed in different aspects. Potential curtailment shows high variability in Low demand scenarios, decreasing its value and variability with increasing demand. Its median goes from 44% to none from the Low to High demand scenarios, and its variability ranges from 36 to 8 p.p. Cross-border interconnection needs oscillates between -62 and +226% around the median. For High demand scenarios, the renewable generation share varies 15 p.p. around its median value, while CO_2 emissions fluctuate 40-50% around the median value. Regarding the PV+Wind power capacity variation, increasing renewable penetration leads to higher variability in the performance indicators. Considering, for example, the balance between annual imports and exports, the required capacity to achieve null net imports may suffer an increase of 25% for high demand from the median to unfavorable year. These results are supported by the results obtained using RCP4.5; RCP8.5 shows similar but slightly more pronounced results, which is also true for the discussion presented below.

Besides climate variability, the development of electricity demand comprises significant changes to the performance of the power system. This triggers the following research question:

How will the power system respond to different society evolution scenarios?

The impact of different society evolution scenarios is primarily seen directly in the magnitude of demand and system flexibility. However, its inclusion in the power system modelling also changes its performance.

For the residential demand, the demand-flexibility scenarios are driven by demand magnitude only. The total residential demand is expected to increase on average from 4 to 60%, depending on the scenario considered. Space heating is expected to decrease on average between 1 and 35%, whereas space cooling tends to increase from 5 to 21-fold. As for the total electricity demand, it may decrease up to 15% in the Low demand and double in High demand scenarios, compared to the present.

The performance of the highly renewable power system is seriously affected by society's evolution scenarios. Potential curtailment may go up to 61% for Low demand scenarios, while it does not exceed 10% for high demand. Cross-border interconnection needs are mainly driven by export needs, thus Low demand scenarios show a median cross-border requirement four times higher than High demand scenarios. Under the median years' conditions, a decrease of 16 p.p. may be observed for the renewable share from Low to High demand scenarios. A decrease of 20 to 36% of total CO_2 emissions is observed from the Low to High demand scenarios. When looking at the changes in PV+Wind power capacities, the main differences across demand-flexibility scenarios are their ability to comply with the established goals. The Low demand scenarios are able to achieve almost 100% renewable electricity generation while showing almost no need for imports capacity.

Finally, the impact of the system flexibility differs among the performance indicators. While it almost does not affect the import needs or cross-border interconnection needs, a small impact may be observed for the renewable generation share, where an increase of 1-2 p.p. is due to system flexibility improvement. The impact of different society evolution scenarios (i.e., demand-flexibility scenarios) is noteworthy and often higher than that from climate variability.

The study of the impact of both climate variability and different demand-flexibility scenarios under a 100% renewable power system is of utmost importance to determine its resilience. This leads to the following and final research question:

Can Portugal be a resilient 100% renewables-based power system by the middle of the century?

The answer to this question depends on the path taken from now until the year 2050 in the power system and demand development. Portugal may choose to be in the far front of renewable power systems, but that must entail the careful planning of the power system

that should be iteratively adapted with changes in the electricity demand trend along the coming years. Below, the impact of climate variability and demand in a 100% renewable power system is summarized.

The 100% renewable power system was defined by removing any fossil-based generation present in the previous highly renewable power systems. For this reason, it lost a great amount of dispatchable generation, making it rather vulnerable to climate variability.

Planning a 100% renewable power system for all climate conditions requires doubling the cross-border interconnection than when it is planned for the median year. Instead of adding cross-border interconnections, additional energy storage may be included. In this case, to be resilient under extremely unfavorable years it may be required to double all the energy storage present in the reference system. However, the cross-border interconnection required (without additional energy storage) does not surpass Europe's 2030 15% interconnection capacity target (regarding the total power capacity) defined for any of the demand-flexibility scenarios. Thus, if that target is to be met, there would be no need for the implementation of energy additional storage.

A resilient power system should be planned based on unfavorable years. If so, an increase of 36 to 77% of PV+Wind power capacity is required to face the unfavorable year, compared to a power system planned for the median year. With that high level of resilience, such power system ensures null net imports for the unfavorable years while requiring less 2 GW of cross-border imports interconnection. As expected, when planning a more resilient power system the high installed capacities are being oversized to comply with the unfavorable years. For this reason, it increases the curtailment from 35 to 48%.

This thesis has shown the role of climate variability, electricity demand and system flexibility in the performance of highly renewable power systems. The future of the power system is highly uncertain, which is even more critical if its planning does not take into account climate variability and different societal development paths. By considering these factors, the planning of power systems may be dynamically adjusted with updated information, considerably reducing the risks related to uncertainty. In addition, the dependency of the power system planning from societal development was also shown to be important. This reveals the strong role that policies might have to properly drive society towards sustainability. It may include policies directed to new technologies, energy efficiency, buildings' refurbishment, new mobility solutions, and the deployment of demand-side management and energy storage.

6.1. Opportunities for further research

There are still plenty of opportunities to further explore the planning of the power system under climate variability and considering diverging electricity demand development paths. Future work may build upon some of the limitations of methods developed in this thesis. Hereafter, some suggestions are presented.

In this work, one single economic sector (residential sector) was considered to be dependent on climate. Thus, more elegant approaches to determine the future hourly and annual electricity demand linked with climate should be applied for the remaining sectors, essentially in services, industry and agriculture sectors. The role of heavy passenger, aviation, navigation, and railways in a decarbonized framework of society could also be further explored since here little attention was given to it. Hydrogen could also be included as an energy vector in different activity sectors.

Regarding the supply side, temporal interpolation of temperature, irradiance and wind speeds was based in simplified methods, but other more sophisticated methods could be adopted. The water supply availability and the determination of the run-of-the-river generation also deserve further attention, e.g. by implementing hydrological models. One of the biggest limitations of this work is the spatial resolution for the power system modelling. While here a single point in space is assumed for the total supply-demand balance, a significant improvement would be to consider the decentralization of generation and demand. It could include a more precise representation of the power system with transmission lines connecting different regions with endogenous generation and electricity demand. In this sense, the congestion of transmission lines could be a focal point for future research. For example, a finer temporal resolution could be applied to further explore the feasibility of highly renewable power systems under a more refined simulation that considers in more detail security of supply and grid stabilization issues.

References

[1] Y. H. Yau and S. Hasbi, “A review of climate change impacts on commercial buildings and their technical services in the tropics,” *Renew. Sustain. Energy Rev.*, vol. 18, pp. 430–441, 2013.

[2] S. Vijayavenkataraman, S. Iniyan, and R. Goic, “A review of climate change, mitigation and adaptation,” *Renew. Sustain. Energy Rev.*, vol. 16, no. 1, pp. 878–897, 2012.

[3] M. J. Santos, P. Ferreira, and M. Araújo, “A methodology to incorporate risk and uncertainty in electricity power planning,” *Energy*, vol. 115, pp. 1400–1411, Nov. 2016.

[4] P. Frankl, “Energy system debate: What lies ahead for the future,” *IEEE Power and Energy Magazine*, vol. 17, no. 2. Institute of Electrical and Electronics Engineers Inc., 01-Mar-2019.

[5] R. Schaeffer *et al.*, “Energy sector vulnerability to climate change: A review,” *Energy*, vol. 38, no. 1, pp. 1–12, 2012.

[6] F. Apadula, A. Bassini, A. Elli, and S. Scapin, “Relationships between meteorological variables and monthly electricity demand,” *Appl. Energy*, vol. 98, pp. 346–356, 2012.

[7] J. Shi and S. Oren, “Stochastic Unit Commitment with Topology Control Recourse for Power Systems with Large-Scale Renewable Integration,” *IEEE Trans. Power Syst.*, vol. 8950, no. c, pp. 1–1, 2017.

[8] J. P. Gouveia, L. Dias, I. Martins, and J. Seixas, “Effects of renewables penetration on the security of Portuguese electricity supply,” *Appl. Energy*, vol. 123, pp. 438–447, Jun. 2014.

[9] M. C. B. Stanton, S. Dessai, and J. Paavola, “A systematic review of the impacts of climate variability and change on electricity systems in Europe,” *Energy*, vol. 109, no. 95, p. 64, 2016.

[10] A. Levesque, R. C. Pietzcker, L. Baumstark, S. De Stercke, A. Grübler, and G. Luderer, “How much energy will buildings consume in 2100? A global perspective within a scenario framework,” *Energy*, vol. 148, pp. 514–527, 2018.

[11] J. Pérez-García and J. Moral-Carcedo, “Analysis and long term forecasting of electricity demand trough a decomposition model: A case study for Spain,” *Energy*, vol. 97, pp. 127–143, 2016.

[12] B. J. van Ruijven, E. De Cian, and I. Sue Wing, “Amplification of future energy demand growth due to climate change,” *Nat. Commun.*, vol. 10, no. 1, Dec. 2019.

[13] T. Ahmed, K. M. Muttaqi, and A. P. Agalgaonkar, “Climate change impacts on electricity demand in the State of New South Wales, Australia,” *Appl. Energy*, vol. 98, pp. 376–383, 2012.

[14] B. K. Sovacool and S. Griffiths, “The cultural barriers to a low-carbon future: A review of six mobility and energy transitions across 28 countries,” *Renewable and Sustainable Energy Reviews*, vol. 119. Elsevier Ltd, p. 109569, 01-Mar-2019.

[15] P. Dowling, “The impact of climate change on the European energy system,” *Energy Policy*, vol. 60, pp. 406–417, 2013.

[16] U. Y. A. Tettey, A. Dodoo, and L. Gustavsson, “Energy use implications of different design strategies for multi-storey residential buildings under future climates,” *Energy*, vol. 138, pp. 846–860, 2017.

[17] D. Burillo, M. V. Chester, S. Pincetl, E. D. Fournier, and J. Reyna, “Forecasting peak electricity demand for Los Angeles considering higher air temperatures due to climate change,” *Appl. Energy*, vol. 236, pp. 1–9, Feb. 2019.

[18] J. Goggins, P. Moran, A. Armstrong, and M. Hajdukiewicz, “Lifecycle environmental and economic performance of nearly zero energy buildings (NZEB) in Ireland,” *Energy Build.*, vol. 116, pp. 622–637, Mar. 2016.

[19] R. Gomes, A. Ferreira, L. Azevedo, R. Costa Neto, L. Aelenei, and C. Silva, “Retrofit measures evaluation considering thermal comfort using building energy simulation: two Lisbon households,” *Adv. Build. Energy Res.*, pp. 1–24, Sep. 2018.

[20] Z. J. Zhai and J. M. Helman, “Implications of climate changes to building energy and design,” *Sustain. Cities Soc.*, vol. 44, pp. 511–519, Jan. 2019.

[21] D. H. W. Li, L. Yang, and J. C. Lam, “Impact of climate change on energy use in the built environment in different climate zones - A review,” *Energy*, vol. 42, no. 1, pp. 103–112, 2012.

[22] K. K. W. Wan, D. H. W. Li, W. Pan, and J. C. Lam, “Impact of climate change on building energy use in different climate zones and mitigation and adaptation implications,” *Appl. Energy*, vol. 97, pp. 274–282, 2012.

[23] M. Auffhammer and E. T. Mansur, “Measuring climatic impacts on energy consumption: A review of the empirical literature,” *Energy Econ.*, vol. 46, pp. 522–530, 2014.

[24] M. T. Craig *et al.*, “A review of the potential impacts of climate change on bulk power system planning and operations in the United States,” *Renewable and Sustainable Energy Reviews*, vol. 98. Elsevier Ltd, pp. 255–267, 01-Dec-2018.

[25] D. Carvalho, A. Rocha, M. Gómez-Gesteira, and C. Silva Santos, “Potential impacts of climate change on European wind energy resource under the CMIP5 future climate projections,” *Renew. Energy*, vol. 101, pp. 29–40, Feb. 2017.

[26] B. Tarroja, A. AghaKouchak, and S. Samuelsen, “Quantifying climate change impacts on hydropower generation and implications on electric grid greenhouse gas emissions and operation,” *Energy*, vol. 111, pp. 295–305, 2016.

[27] S. Kozarcanin, H. Liu, and G. B. Andresen, “21st Century Climate Change Impacts on Key Properties of a Large-Scale Renewable-Based Electricity System,” *Joule*, vol. 3, pp. 992–1005, 2019.

[28] K. Solaun and E. Cerdá, “Climate change impacts on renewable energy generation. A review of quantitative projections,” *Renewable and Sustainable Energy Reviews*, vol. 116. Elsevier Ltd, 01-Dec-2019.

[29] S. Jerez *et al.*, “The impact of climate change on photovoltaic power generation in Europe,” *Nat. Commun.*, vol. 6, no. 10014, 2015.

[30] M. Wild, D. Folini, and F. Henschel, “Impact of climate change on future concentrated solar power (CSP) production,” *AIP Conf. Proc.*, vol. 1810, no. February, 2017.

[31] J.-C. Ciscar and P. Dowling, “Integrated assessment of climate impacts and adaptation in the energy sector,” *Energy Econ.*, vol. 46, pp. 531–538, 2014.

[32] N. Kirchner-Bossi, R. García-Herrera, L. Prieto, and R. M. Trigo, “A long-term perspective of wind power output variability,” *Int. J. Climatol.*, vol. 35, no. 9, pp. 2635–2646, 2015.

[33] J. A. Santos, C. Rochinha, M. L. R. Liberato, M. Reyers, and J. G. Pinto, “Projected changes in wind energy potentials over Iberia,” *Renew. Energy*, vol. 75, no. 2015, pp. 68–80, 2015.

[34] P. Ravestein, G. van der Schrier, R. Haarsma, R. Scheele, and M. van den Broek, “Vulnerability of European intermittent renewable energy supply to climate change and climate variability,” *Renew. Sustain. Energy Rev.*, vol. 97, pp. 497–508, Dec. 2018.

[35] D. J. Brayshaw, A. Troccoli, R. Fordham, and J. Methven, “The impact of large scale atmospheric circulation patterns on wind power generation and its potential predictability: A case study over the UK,” *Renew. Energy*, vol. 36, no. 8, pp. 2087–2096, Aug. 2011.

[36] J. A. Santos, C. Rochinha, M. L. R. Liberato, M. Reyers, and J. G. Pinto, “Projected changes in wind energy potentials over Iberia,” *Renew. Energy*, vol. 75, no. July 2016, pp. 68–80, 2015.

[37] B. Tarroja, K. Forrest, F. Chiang, A. AghaKouchak, and S. Samuelsen, “Implications of hydropower variability from climate change for a future, highly-renewable electric grid in California,” *Appl. Energy*, vol. 237, pp. 353–366, Mar. 2019.

[38] P. E. Carvajal, F. G. N. Li, R. Soria, J. Cronin, G. Anandarajah, and Y. Mulugetta, “Large hydropower, decarbonisation and climate change uncertainty: Modelling power sector pathways for Ecuador,” *Energy Strateg. Rev.*, vol. 23, pp. 86–99, Jan. 2019.

[39] D. Rübbelke and S. Vögele, “Short-term distributional consequences of climate change impacts on the power sector: Who gains and who loses?,” *Clim. Change*, vol. 116, no. 2, pp. 191–206, 2013.

[40] S. Spiecker and C. Weber, “The future of the European electricity system and the impact of fluctuating renewable energy – A scenario analysis,” *Energy Policy*, vol. 65, pp. 185–197, 2014.

[41] Maarten Messagie, “Life Cycle Analysis of the Climate Impact of Electric Vehicles,” *Transp. Environ.*, 2017.

[42] A. Talebpour and H. S. Mahmassani, “Influence of connected and autonomous vehicles on traffic flow stability and throughput,” *Transp. Res. Part C Emerg. Technol.*, vol. 71, pp. 143–163, 2016.

[43] J. Gallego, “The World’s First Autonomous Taxis Just Started Driving in Singapore,” *Futurism*, 2016.

[44] B. Vlasic and M. Isaac, “Uber Aims for an Edge in the Race for a Self-Driving Future,” *The New york Times*, 2016.

[45] “Google Self-Driving Car Project,” *Google*, 2016. [Online]. Available: https://www.google.com/selfdrivingcar/.

[46] J. Gallego, “Elon Musk Hints That Tesla Updates Will Soon Lead To Level 4 Autonomy,” *Futurism*, 2016.

[47] G. Zervas, D. Proserpio, and J. W. Byers, “The Rise of the Sharing Economy: Estimating the Impact of Airbnb on the Hotel Industry,” *J. Mark. Res.*, vol. LIV, no. October, pp. 687–705, 2017.

[48] C. Codagnone and B. Martens, “Scoping the Sharing Economy: Origins, Definitions, Impact and Regulatory Issues,” 2016.

[49] “OE/2018: Portuguese Government admits to give fiscal incentives and to review tolls for the Interior development (in Portuguese),” *Diário de Notícias*, 2017.

[50] M. Prado, “Workers who move to the interior of the country will receive a finantial support of up to 4,827 euros,” *Expresso - Economia*, 2020. .

[51] Aalborg University, “EnergyPLAN: advanced energy system analysis computer model,” 2017. [Online]. Available: http://www.energyplan.eu/.

[52] E. De Cian, I. S. Wing, and E. Mattei, “Global Energy Consumption in a Warming Climate Centro Euro-Mediterraneo sui Cambiamenti Climatici and Fondazione Eni,” *Env. Resour. Econ*, vol. 72, pp. 365–410, 2019.

[53] T. Berger *et al.*, “Impacts of climate change upon cooling and heating energy demand of office buildings in Vienna, Austria,” *Energy Build.*, vol. 80, pp. 517–530, 2014.

[54] A. Sabunas and A. Kanapickas, “Estimation of climate change impact on energy consumption in a residential building in Kaunas, Lithuania, using HEED Software,” *Energy Procedia*, vol. 128, pp. 92–99, Sep. 2017.

[55] D. Wang, J. Landolt, G. Mavromatidis, K. Orehounig, and J. Carmeliet, “CESAR: A bottom-up building stock modelling tool for Switzerland to address sustainable energy transformation strategies,” *Energy Build.*, vol. 169, pp. 9–26, Jun. 2018.

[56] C. Y. Yi and C. Peng, “Correlating cooling energy use with urban microclimate data for projecting future peak cooling energy demands: Residential neighbourhoods in Seoul,” *Sustain. Cities Soc.*, vol. 35, pp. 645–659, Nov. 2017.

[57] J. Cronin, G. Anandarajah, and O. Dessens, “Climate change impacts on the energy system: a review of trends and gaps,” *Clim. Change*, vol. 151, no. 2, pp. 79–93, Nov. 2018.

[58] J. Müller, D. Folini, M. Wild, and S. Pfenninger, “CMIP-5 models project photovoltaics are a no-regrets investment in Europe irrespective of climate change,” *Energy*, vol. 171, pp. 135–148, Mar. 2019.

[59] P. M. M. Soares, M. C. Brito, and J. A. M. Careto, “Persistence of the high solar potential in Africa in a changing climate,” *Environ. Res. Lett. Press*, 2019.

[60] K. B. Karnauskas, J. K. Lundquist, and L. Zhang, “Southward shift of the global

wind energy resource under high carbon dioxide emissions," *Nat. Geosci.*, vol. 11, no. 1, pp. 38–43, 2018.

[61] P. M. M. Soares, D. C. A. Lima, R. M. Cardoso, M. L. Nascimento, and A. Semedo, "Western Iberian offshore wind resources: More or less in a global warming climate?," *Appl. Energy*, vol. 203, pp. 72–90, 2017.

[62] G. Oyerinde *et al.*, "Quantifying Uncertainties in Modeling Climate Change Impacts on Hydropower Production," *Climate*, vol. 4, no. 3, 2016.

[63] C. Teotónio, P. Fortes, P. Roebeling, M. Rodriguez, and M. Robaina-Alves, "Assessing the impacts of climate change on hydropower generation and the power sector in Portugal: A partial equilibrium approach," *Renew. Sustain. Energy Rev.*, vol. 74, pp. 788–799, Jul. 2017.

[64] C. A. B. Mendes, A. Beluco, and F. A. Canales, "Some important uncertainties related to climate change in projections for the Brazilian hydropower expansion in the Amazon," *Energy*, vol. 141, pp. 123–138, Dec. 2017.

[65] A. Miara, J. E. Macknick, C. J. Vörösmarty, V. C. Tidwell, R. Newmark, and B. Fekete, "Climate and water resource change impacts and adaptation potential for US power supply," 2017.

[66] L. Liu, M. Hejazi, H. Li, B. Forman, and X. Zhang, "Vulnerability of US thermoelectric power generation to climate change when incorporating state-level environmental regulations," vol. 2, p. 17109, 2017.

[67] J. Weber *et al.*, "Impact of climate change on backup energy and storage needs in wind-dominated power systems in Europe," 2018.

[68] C. Rosende, E. Sauma, and G. P. Harrison, "Effect of Climate Change on wind speed and its impact on optimal power system expansion planning: The case of Chile," *Energy Econ.*, vol. 80, pp. 434–451, May 2019.

[69] O. J. Guerra, D. A. Tejada, and G. V. Reklaitis, "Climate change impacts and adaptation strategies for a hydro-dominated power system via stochastic optimization," *Appl. Energy*, vol. 233–234, pp. 584–598, Jan. 2019.

[70] M. Zeyringer, J. Price, B. Fais, P. H. Li, and E. Sharp, "Designing low-carbon power systems for Great Britain in 2050 that are robust to the spatiotemporal and inter-annual variability of weather," *Nat. Energy*, vol. 3, no. 5, pp. 395–403, 2018.

[71] M. T. Craig, I. Losada Carreño, M. Rossol, B. M. Hodge, and C. Brancucci, "Effects on power system operations of potential changes in wind and solar generation potential under climate change," *Environ. Res. Lett.*, vol. 14, no. 3, 2019.

[72] S. Collins, P. Deane, B. Ó Gallachóir, S. Pfenninger, and I. Staffell, "Impacts of Inter-annual Wind and Solar Variations on the European Power System," *Joule*, vol. 2, no. 10, pp. 2076–2090, Oct. 2018.

[73] M. T. H. Van Vliet, D. Wiberg, S. Leduc, and K. Riahi, "Power-generation system vulnerability and adaptation to changes in climate and water resources," *Nat. Clim. Chang.*, vol. 6, no. 4, pp. 375–380, 2016.

[74] J. Peter, "How does climate change affect electricity system planning and optimal

allocation of variable renewable energy?," *Appl. Energy*, vol. 252, Oct. 2019.

[75] A. T. D. Perera, V. M. Nik, and J. L. Scartezzini, "Impacts of extreme climate conditions due to climate change on the energy system design and operation," in *Energy Procedia*, 2019, vol. 159, pp. 358–363.

[76] N. V. Emodi, T. Chaiechi, and A. B. M. R. Alam Beg, "A techno-economic and environmental assessment of long-term energy policies and climate variability impact on the energy system," *Energy Policy*, vol. 128, pp. 329–346, May 2019.

[77] H. C. Bloomfield, D. J. Brayshaw, L. C. Shaffrey, P. J. Coker, and H. E. Thornton, "Quantifying the increasing sensitivity of power systems to climate variability," *Environ. Res. Lett.*, vol. 11, no. 12, 2016.

[78] G. Haydt, V. Leal, A. Pina, and C. A. Silva, "The relevance of the energy resource dynamics in the mid/long-term energy planning models," *Renew. Energy*, vol. 36, no. 11, pp. 3068–3074, Nov. 2011.

[79] A. Pina, C. Silva, and P. Ferrão, "Modeling hourly electricity dynamics for policy making in long-term scenarios," *Energy Policy*, vol. 39, no. 9, pp. 4692–4702, Sep. 2011.

[80] D. L. McCollum, A. Gambhir, J. Rogelj, and C. Wilson, "Energy modellers should explore extremes more," *Nat. Energy*.

[81] K. B. Debnath and M. Mourshed, "Forecasting methods in energy planning models," *Renew. Sustain. Energy Rev.*, vol. 88, pp. 297–325, May 2018.

[82] S. Collins *et al.*, "Integrating short term variations of the power system into integrated energy system models: A methodological review," *Renew. Sustain. Energy Rev.*, vol. 76, no. January, pp. 839–856, 2017.

[83] D. Connolly, H. Lund, B. V. Mathiesen, and M. Leahy, "A review of computer tools for analysing the integration of renewable energy into various energy systems," *Appl. Energy*, vol. 87, no. 4, pp. 1059–1082, 2010.

[84] Y. Liu, S. Yu, Y. Zhu, D. Wang, and J. Liu, "Modeling, planning, application and management of energy systems for isolated areas: A review," *Renew. Sustain. Energy Rev.*, vol. 82, pp. 460–470, 2018.

[85] International Energy Agency, "MARKAL/TIMES." [Online]. Available: https://iea-etsap.org/index.php/etsap-tools. [Accessed: 27-Nov-2017].

[86] HOMER Energy LLC, "HOMER Energy," 2015. [Online]. Available: https://www.homerenergy.com/. [Accessed: 27-Nov-2017].

[87] Stockholm Environment Institute, "Long-range Energy Alternatives Planning (LEAP) system," 2016. [Online]. Available: https://www.energycommunity.org. [Accessed: 27-Nov-2017].

[88] Hans Ravn, "Balmorel," 2018. [Online]. Available: http://www.balmorel.com/index.php. [Accessed: 27-Nov-2017].

[89] EMD International A/S, "energyPRO," 2018. [Online]. Available: https://www.emd.dk/energypro/. [Accessed: 27-Nov-2017].

[90] Energy Exemplar, "PLEXOS," 2018. [Online]. Available:

https://energyexemplar.com/software/plexos-desktop-edition/. [Accessed: 27-Nov-2017].

[91] Natural Resources Canada, "RETScreen," 2017. [Online]. Available: http://www.nrcan.gc.ca/energy/software-tools/7465. [Accessed: 27-Nov-2017].

[92] Risoe National Laboratory, "WILMAR - Wind Power Integration in Liberalised Electricity Markets," 2012. [Online]. Available: http://www.wilmar.risoe.dk/. [Accessed: 27-Nov-2017].

[93] S. Jerez *et al.*, "The impact of the north atlantic oscillation on renewable energy resources in Southwestern Europe," *J. Appl. Meteorol. Climatol.*, vol. 52, no. 10, pp. 2204–2225, 2013.

[94] V. Taseska, N. Markovska, and J. M. Callaway, "Evaluation of climate change impacts on energy demand," *Energy*, vol. 48, no. 1, pp. 88–95, 2012.

[95] Portuguese Department of Energy and Geology (DGEG), "Energy Balance, 2011-2015 (in Portuguese)."

[96] Portuguese Energy Networks (REN), "Technical data - Electricity: 2011 to 2015," Lisbon.

[97] "Production - Evolution of the Electricity Generation in Mainland Portugal (2000-2017)," *APREN*, 2018. [Online]. Available: http://www.apren.pt/en/renewable-energies/production/. [Accessed: 28-Mar-2018].

[98] Portuguese Institute of Sea and Atmosphere (IPMA), "Climatological bulletin, 2000/2005/2011-2015 (in Portuguese)."

[99] Presidency of the Council of Ministers, *Decree-Law n.º 85/2019 (in Portuguese)*, vol. 132. Portugal, 2019, pp. 3208–3299.

[100] P. Nunes, T. Farias, and M. C. Brito, "Enabling solar electricity with electric vehicles smart charging," *Energy*, 2015.

[101] P. Nunes, T. Farias, and M. C. Brito, "Day charging electric vehicles with excess solar electricity for a sustainable energy system," *Energy*, vol. 80, no. February, pp. 263–274, 2014.

[102] L. Fernandes and P. Ferreira, "Renewable energy scenarios in the Portuguese electricity system," *Energy*, vol. 69, pp. 51–57, 2014.

[103] G. Krajačić, N. Duić, and M. da G. Carvalho, "How to achieve a 100% RES electricity supply for Portugal?," *Appl. Energy*, vol. 88, no. 2, pp. 508–517, 2011.

[104] A. Pina, C. A. Silva, and P. Ferrão, "High-resolution modeling framework for planning electricity systems with high penetration of renewables," *Appl. Energy*, vol. 112, pp. 215–223, Dec. 2013.

[105] M. J. Santos, P. Ferreira, and M. Araújo, "A Multi-Criteria Analysis of Low Carbon Scenarios in Portuguese Electricity Systems," *Int. Conf. Proj. Eval.*, no. June, pp. 183–190, 2014.

[106] J. Anjo, D. Neves, C. Silva, A. Shivakumar, and M. Howells, "Modeling the long-term impact of demand response in energy planning: The Portuguese electric system case study," *Energy*, vol. 165, pp. 456–468, Dec. 2018.

[107] P. Fortes, S. G. Simoes, F. Monteiro, and J. Seixas, “Renewable electricity in the Portuguese energy system 2015-2050 - Global report (in Portuguese),” 2017.

[108] P. Fortes, S. G. Simoes, J. P. Gouveia, and J. Seixas, “Electricity, the silver bullet for the deep decarbonisation of the energy system? Cost-effectiveness analysis for Portugal,” *Appl. Energy*, vol. 237, pp. 292–303, Mar. 2019.

[109] P. Fortes *et al.*, “National Energy System compatible with carbon neutral economy by 2050: Results from the TIMES_PT model for the RNC2050 (in Portuguese).” CENSE. Faculdade de Ciência e Tecnologia da Universidade Nova de Lisboa., 2019.

[110] M. Z. Jacobson *et al.*, “100% Clean and Renewable Wind, Water, and Sunlight All-Sector Energy Roadmaps for 139 Countries of the World,” *Joule*, vol. 1, no. 1, pp. 108–121, 2017.

[111] M. Jakubcionis and J. Carlsson, “Estimation of European Union residential sector space cooling potential,” *Energy Policy*, vol. 101, pp. 225–235, Feb. 2017.

[112] I. Andrić *et al.*, “Modeling the long-term effect of climate change on building heat demand: Case study on a district level,” *Energy Build.*, vol. 126, pp. 77–93, Aug. 2016.

[113] D. P. van Vuuren *et al.*, “The representative concentration pathways: an overview,” *Clim. Change*, vol. 109, no. 1–2, pp. 5–31, 2011.

[114] R. Moss *et al.*, “Towards new scenarios for analysis of emissions, climate change, and response strategies - IPCC Expert Meeting Report,” Geneva, 2008.

[115] R. H. Moss *et al.*, “The next generation of scenarios for climate change research and assessment,” *Nature*, vol. 463, no. 11, 2010.

[116] D. P. van Vuuren *et al.*, “Stabilizing greenhouse gas concentrations at low levels: an assessment of reduction strategies and costs,” *Clim. Change*, vol. 81, no. 2, pp. 119–159, 2007.

[117] D. P. van Vuuren, B. Eickhout, P. L. Lucas, and M. G. J. den Elzen, “Long-Term Multi-Gas Scenarios to Stabilise Radiative Forcing — Exploring Costs and Benefits Within an Integrated Assessment Framework,” *Energy J.*, vol. 27, no. Multi-Greenhouse Gas Mitigation and Climate Policy, pp. 201–233, 2006.

[118] L. E. Clarke, J. a Edmonds, H. D. Jacoby, H. M. Pitcher, J. M. Reilly, and R. G. Richels, “Scenarios of Greenhouse Gas Emissions and Atmospheric Concentrations,” Washington DC, 2007.

[119] T. M. and Y. M. Junichi Fujino, Rajesh Nair, Mikiko Kainuma, “Multigas mitigation analysis on stabilization scenarios using aim global model,” *Energy J.*, vol. 27, no. Multi-Greenhouse Gas Mitigation and Climate Policy (2006), 2006.

[120] H. Yasuaki, M. Yuzuru, N. Hiromi, M. Toshihiko, and K. Mikiko, “Global GHG Emission Scenarios Under GHG Concentration Stabilization Targets,” *J. Glob. Environ. Eng.*, vol. 13, no. March, pp. 91–108, 2008.

[121] K. Riahi, A. Grübler, and N. Nakicenovic, “Scenarios of long-term socio-economic and environmental development under climate stabilization,” *Technol. Forecast. Soc. Change*, vol. 74, no. 7, pp. 887–935, 2007.

[122] Z. Hausfather and G. P. Peters, “Emissions – the ‘business as usual’ story is misleading,” *Nature*, vol. 577, no. 7792. Nature Research, pp. 618–620, 30-Jan-2020.

[123] Z. Hausfather, “Explainer: The high-emissions ‘RCP8.5’ global warming scenario,” *Carbon Brief - Clean on Climate*, 2019.

[124] “CORDEX Data Structure,” *European Network for Earth System Modelling*, 2016. [Online]. Available: https://portal.enes.org/data/enes-model-data/cordex/datastructure. [Accessed: 22-May-2018].

[125] “CERA project information for RCM forcing data from MPI-ESM (ECHAM6/JSBACH/MPIOM/HAMOCC) CMIP5 experiments,” *WDC Climate - DKRZ*. [Online]. Available: https://cera-www.dkrz.de/WDCC/ui/cerasearch/project?acronym=CMIP5_RCM_forcing_MPI-ESM.

[126] C. Magarreiro, M. C. Brito, and P. M. M. Soares, “Assessment of diffuse radiation models for cloudy atmospheric conditions in the Azores region,” *Sol. Energy*, vol. 108, pp. 538–547, 2014.

[127] D. Erbs, S. Klien, and W. Beckman, “Estimation of Degree-Days And Ambient Temperature Bin Data From Monthly-Average Temperatures,” *Ashrae*, no. June. p. 6, 1983.

[128] D. Chow and G. J. Levermore, “New algorithm for generating hourly temperature values using daily maximum, minimum and average values from climate models,” *Build. Serv. Eng. Res. Technol.*, vol. 28, no. 3, pp. 237–248, 2007.

[129] “The Sun’s Position | PVEducation,” 2017. [Online]. Available: http://pveducation.org/pvcdrom/2-properties-sunlight/suns-position. [Accessed: 11-Oct-2017].

[130] R. Ehrlich, *Renewable Energy - A first course*. Boca Raton: CRC Press - Taylor & Francis Group, 2013.

[131] M. Iqbal, *An Introduction to Solar Radiation*. Ontario, Canada: Academic Press Canada, 1983.

[132] R. Carapellucci and L. Giordano, “A methodology for the synthetic generation of hourly wind speed time series based on some known aggregate input data,” *Appl. Energy*, vol. 101, pp. 541–550, 2013.

[133] “Coordinated Regional Climate Downscaling Experiment (CORDEX) Project.” [Online]. Available: http://www.cordex.org/.

[134] Portuguese Energy Networks (REN), “Load Diagram.” 2015.

[135] J. E. J. Rykiel, “Testing ecological models: the meaning of validation,” *Ecol. Modell.*, vol. 90, pp. 229–244, 1996.

[136] B. Cleary, A. Duffy, B. Bach, A. Vitina, A. O’Connor, and M. Conlon, “Estimating the electricity prices, generation costs and CO2 emissions of large scale wind energy exports from Ireland to Great Britain,” *Energy Policy*, vol. 91, pp. 38–48, 2016.

[137] G. Zhao, J. M. Guerrero, K. Jiang, and S. Chen, “Energy modelling towards low

carbon development of Beijing in 2030," *Energy*, vol. 121, pp. 107–113, 2017.

[138] A. Hast, S. Rinne, S. Syri, and J. Kiviluoma, "The role of heat storages in facilitating the adaptation of district heating systems to large amount of variable renewable electricity," *Energy*, vol. 137, pp. 775–788, Oct. 2017.

[139] U. Bhaskar Gunturu, "Asynchrony of wind and hydropower resources in Australia," *Sci. Reports*, vol. 7, no. 8818, 2017.

[140] I. Staffell and S. Pfenninger, "Using bias-corrected reanalysis to simulate current and future wind power output," *Energy*, vol. 114, pp. 1224–1239, 2016.

[141] J. M. Correia, A. Bastos, M. C. Brito, and R. M. Trigo, "The influence of the main large-scale circulation patterns on wind power production in Portugal," *Renew. Energy*, vol. 102, pp. 214–223, 2017.

[142] Portuguese Energy Networks (REN), "Load diagram - 2011-2015."

[143] Portuguese Institute of Sea and Atmosphere (IPMA); FCUL (Faculdade de Ciências da Universidade de Lisboa), "Climate Portal - Climate Change in Portugal."

[144] G. A. Ekama, S. W. Sötemann, M. C. Wentzel, G. A. Ekama, and Eurelectric, "Efficiency in Electricity Generation," *Water Res.*, vol. 32, no. 3, pp. 297–306, 2003.

[145] Portuguese Department of Energy and Geology (DGEG), "Energy Balance - 2015 (in Portuguese)," 2015.

[146] Portuguese Energy Networks (REN), "Technical data - 2015," Lisboa, 2015.

[147] W. H. Schlesinger, "Are wood pellets a green fuel?," *Science (80-.).*, vol. 359, no. 6382, pp. 1328–1329, 2018.

[148] "Government creates working group to valorize and protect forest resources and stands (in Portuguese)," *Público*, 07-Oct-2017.

[149] E. Johnson, "Goodbye to carbon neutral: Getting biomass footprints right," *Environ. Impact Assess. Rev.*, vol. 29, no. 3, pp. 165–168, Apr. 2009.

[150] A. De Miguel, J. Bilbao, R. Aguiar, H. Kambezidis, and E. Negro, "Diffuse solar irradiation model evaluation in the North Mediterranean Belt area," *Sol. energy*, vol. 70, no. 2, pp. 143–153, 2001.

[151] R. M. Mayrbaurl and S. Camo, "Guidelines for inspection and strength evaluation of suspension bridge parallel-wire cables," Washington, 2004.

[152] "Sunny Tripower Inverters," *Wind & Sun Powering the future*. [Online]. Available: http://www.windandsun.co.uk/products/Inverters/SMA-Inverters/Sunny-Tripower-Inverters#10066. [Accessed: 22-Jul-2015].

[153] SolarWorld AG, "Sunmodule Plus - SW285 MONO - Technical sheet." pp. 3–4.

[154] A. Couto, P. Costa, L. Rodrigues, V. V. Lopes, and A. Estanqueiro, "Impact of Weather Regimes on the Wind Power Ramp Forecast in Portugal," *IEEE Trans. Sustain. Energy*, vol. 6, no. 3, pp. 934–942, 2015.

[155] Portuguese endogenous energies (e2p) and Institute of Mechanical Engineering

and Industrial Management (INEGI) Portuguese Renewable Energy Association (APREN), “Wind Farms in Portugal - December 2017,” 2018.

[156] ENERCON, “ENERCON product overview.”

[157] I. González-Aparicio *et al.*, “Simulating European wind power generation applying statistical downscaling to reanalysis data,” *Appl. Energy*, vol. 199, pp. 155–168, 2017.

[158] P. Costa, P. Miranda, and A. Estanqueiro, “Development and Validation of the Portuguese Wind Atlas,” in *Proceedings of the European Wind Energy Conference 2006*, 2006, p. 9.

[159] P. Costa, T. Simões, and A. Estanqueiro, “Sustainable offshore wind potentital in continental Portugal,” 2010.

[160] International Energy Agency (IEA) and Ministry of Mines and Energy of the Federative Republic of Brazil, “Technology Roadmap - Hydropower,” Paris, 2012.

[161] A. Blakers, M. Stocks, B. Lu, C. Cheng, and R. Stocks, “Pathway to 100% Renewable Electricity,” *IEEE J. Photovoltaics*, vol. 9, no. 6, pp. 1828–1833, Sep. 2019.

[162] GET2C, FCT, AGROGES, Lasting Values, and J. Walter Thompson, “Roadmap For Carbon Neutrality 2050,” 2018.

[163] Portuguese Energy Networks (REN), “Technical data - 2017,” 2017.

[164] A. Purkus *et al.*, “Contributions of flexible power generation from biomass to a secure and cost-effective electricity supply - a review of potentials, incentives and obstacles in Germany,” *Energy. Sustain. Soc.*, vol. 8, no. 1, p. 18, Dec. 2018.

[165] D. Thrän, M. Dotzauer, V. Lenz, J. Liebetrau, and A. Ortwein, “Flexible bioenergy supply for balancing fluctuating renewables in the heat and power sector—a review of technologies and concepts,” *Energy. Sustain. Soc.*, vol. 5, no. 1, pp. 1–15, 2015.

[166] K. Sadovskaia, D. Bogdanov, S. Honkapuro, and C. Breyer, “Power transmission and distribution losses – A model based on available empirical data and future trends for all countries globally,” *Int. J. Electr. Power Energy Syst.*, vol. 107, pp. 98–109, May 2019.

[167] IEA Statistics, “Electric power transmission and distribution losses (% of output).” The World Bank, 2018.

[168] Portuguese Energy Networks (REN), “Development and investment plan of the national transport network (PDIRT) 2018-2017,” 2017.

[169] National Department of Energy and Geology (DGEG), Portuguese Environmental Agency (APA), National Laboratory of Energy and Geology (LNEG), and Portuguese Energy Agency (ADENE), “National Energy Climate Plan 2021-2030 - PNEC (in Portuguese),” 2018.

[170] Portuguese Renewable Energy Association (APREN);Pöyry, “Portuguese Market Outlook up to 2040 - POYRY: A report to APREN.” 2018.

[171] P. Fortes, A. Alvarenga, J. Seixas, and S. Rodrigues, “Long-term energy scenarios:

Bridging the gap between socio-economic storylines and energy modeling," *Technol. Forecast. Soc. Change*, vol. 91, pp. 161–178, Feb. 2015.

[172] P. Nunes, "Enabling solar electricity with electric vehicles in future energy systems," Universidade de Lisboa, 2015.

[173] "The Chevy Volt | PluginCars.com," *plugincars*, 2018. [Online]. Available: http://www.plugincars.com/chevrolet-volt. [Accessed: 29-May-2018].

[174] F. Nemry and M. Brons, "Plug-in Hybrid and Battery Electric Vehicles Market penetration scenarios of electric drive vehicles," *Jrc-Ipts*, pp. 1–36, 2010.

[175] Portuguese Ministry of Environment and Energy Transition, "Roadmap For Carbon Neutrality 2050 - Technical Appendix - Mobility and Transportation (in Portuguese)." 2019.

[176] R. Gough, C. Dickerson, P. Rowley, and C. Walsh, "Vehicle-to-grid feasibility: A techno-economic analysis of EV-based energy storage," *Appl. Energy*, vol. 192, pp. 12–23, 2017.

[177] H. Lund and W. Kempton, "Integration of renewable energy into the transport and electricity sectors through V2G," *Energy Policy*, vol. 36, pp. 3578–3587, 2008.

[178] Renault UK, "Renault ZOE Brochure," no. April. 2017.

[179] T. D. Chen, K. M. Kockelman, and J. P. Hanna, "Operations of a shared, autonomous, electric vehicle fleet: Implications of vehicle & charging infrastructure decisions," *Transp. Res. Part A*, vol. 94, pp. 243–254, 2016.

[180] L. Bertoni, J. Guanetti, M. Basso, M. Masoero, S. Cetinkunt, and F. Borrelli, "An adaptive cruise control for connected energy-saving electric vehicle," *IFAC Pap.*, vol. 50, no. 1, pp. 2359–2364, 2017.

[181] C. D. Harper, C. T. Hendrickson, S. Mangones, and C. Samaras, "Estimating potential increases in travel with autonomous vehicles for the non-driving, elderly and people with travel-restrictive medical conditions," *Transp. Res. Part C*, vol. 72, pp. 1–9, 2016.

[182] Statistics Portugal (INE) and National Department for Land Transports, "Survey for residents' mobility: 2000 (in Portuguese)," Porto, 2002.

[183] G. Gardner, "Why most self-driving cars will be electric." USA Today, 2016.

[184] "Simplified balance electricity heat ktoe EU-28 - Statistics Explained," *Eurostat*, 2016. [Online]. Available: https://ec.europa.eu/eurostat/statistics-explained/index.php?title=File:Simplified-balance-electricity-heat-ktoe-EU-28-2016.png. [Accessed: 02-Apr-2019].

[185] "Population of Portugal," *PopulationOf*, 2019. [Online]. Available: https://www.populationof.net/portugal/. [Accessed: 29-Mar-2019].

[186] M. Ferreira and M. J. O. Panão, "The role of inhabitants behaviour in the pre-bound effect of housing energy consumption," in *BEHAVE 2016, 4th European Conference on Behaviour and Energy Efficiency*, 2016.

[187] Mariangiola Fabbri, Maarten De Groote, and Oliver Rapf, "Building Renovation Passports - Customised roadmaps towards deep renovation and better homes,"

2016.

[188] Statistics Portugal (INE), “Completed buildings (No.) by Geographic localization (NUTS - 2002), Type of work and Destination of the work,” 2017. [Online]. Available: https://www.ine.pt/xportal/xmain?xpid=INE&xpgid=ine_indicadores&indOcorrCod=0000075&contexto=bd&selTab=tab2.

[189] Statistics Portugal (INE), “Construction and housing statistics - 2016 - Board 1: Buildings - Classic Family Housing, by NUTS III (2001-2016),” *Construction and housing statistics - 2016*, 2016. .

[190] European Comission, “Annual share of new dwellings in total residential stock,” *EU Buildings Database*. [Online]. Available: https://ec.europa.eu/energy/en/eu-buildings-database.

[191] J. N. B. Fonseca and M. J. N. Oliveira Panão, “Monte Carlo housing stock model to predict the energy performance indicators,” *Energy Build.*, vol. 152, pp. 503–515, 2017.

[192] Portuguese Energy Agency (ADENE), “Energy Performance Certificates Database.” 2018.

[193] “GDP - Portugal,” *PORDATA*, 2017. [Online]. Available: http://www.pordata.pt/Portugal/Produto+Interno+Bruto+na+óptica+da+despesa+(base+2011)-2283. [Accessed: 21-Jun-2017].

[194] J. P. Gouveia, P. Fortes, and J. Seixas, “Projections of energy services demand for residential buildings: Insights from a bottom-up methodology,” *Energy*, vol. 47, no. 1, pp. 430–442, Nov. 2012.

[195] Portuguese Association for the Conservation of Nature (Quercus), “EcoFamílias Project - Final Report (in Portuguese),” 2008.

[196] Portuguese Association for the Conservation of Nature (Quercus), “EcoFamílias II Project (in Portuguese),” 2011.

[197] “FROnT - Fair Renewable Heating and Cooling Options and Trade.” [Online]. Available: http://www.front-rhc.eu/about/countries/portugal/.

[198] S. Fonseca, “Characterization of the Energy Consumption in the Residential sector in Portugal (in Portuguese),” Instituto Superior técnico, Universidade de Lisboa, 2015.

[199] Portuguese Association for the Conservation of Nature (Quercus), “EcoFamílias 30 Project - Final Report (in Portuguese),” p. 77, 2007.

[200] R. Figueiredo, P. Nunes, and M. C. Brito, “Residential market of heat pumps: present and future (in Portuguese),” *O Instalador*, Lisbon, 2019.

[201] C. R.Matos, J. F.Carneiro, and P. P.Silva, “Overview of Large-Scale Underground Energy Storage Technologies for Integration of Renewable Energies and Criteria for Reservoir Identification,” *J. Energy Storage*, vol. 21, no. February, pp. 241–258, 2019.

[202] A. Almeida and P. Nunes, “The role of second-life batteries on renewable based power systems,” in *13th Conference on Sustainable Development of Energy, Water*

and environment Systemsnvironment Systems (SDEWES), 2018.

[203] M. J. N. O. Panão and M. C. Brito, "Modelling aggregate hourly electricity consumption based on bottom-up building stock," *Energy Build.*, vol. 170, pp. 170–182, 2018.

[204] Presidency of the Council of Ministers, *Decree-Law 118/2013 - Order No 15793-I/2013 - Regulation for Energy Performance of Residential Buildings (in Portuguese)*. Portugal, 2013, pp. 41–54.

[205] Government of Portugal - Ministry of Economy, Portuguese Quality Institute, and Portuguese Company of Free Waters (EPAL), "Prevention and Control of Legionella in Water Systems (in Portuguese)," Lisbon, 2014.

[206] Â. Casaleiro, R. Figueiredo, D. Neves, M. C. Brito, and C. A. Silva, "Optimization of photovoltaic self-consumption using domestic hot water systems," *J. Sustain. Dev. Energy, Water Environ. Syst.*, vol. 6, no. 2, pp. 291–304, 2018.

[207] E. C. Balke, W. M. Healy, and T. Ullah, "An assessment of efficient water heating options for an all-electric single family residence in a mixed-humid climate," *Energy Build.*, vol. 133, pp. 371–380, Dec. 2016.

[208] G. Martinopoulos, K. T. Papakostas, and A. M. Papadopoulos, "A comparative review of heating systems in EU countries, based on efficiency and fuel cost," *Renew. Sustain. Energy Rev.*, vol. 90, pp. 687–699, Jul. 2018.

[209] ADEME *et al.*, "Demand-side Management - End-use metering campaign in 400 households of the European Community - Assessment of the Potential Electricity Savings (Project EURECO)," 2002.

[210] Portuguese Energy Agency (ADENE), Portuguese Institute of Industrial Engineering and Technology, National Laboratory of Civil Engineering, and Portuguese Quality Institute, "Energy efficiency in electrical equipment and systems in the residential sector (in Portuguese)," 2004.

[211] Statistics Portugal (INE) and Portuguese Department of Energy and Geology (DGEG), "2010 Household Consumption Survey (in Portuguese)," 2011.

[212] L. E-Nova, "Intelligent monitor for efficient decisions, 2011–2012, (funded by ERSE under the National PPEC - Plan for Promoting Efficiency in Electricity Consumption)." .

[213] Statistics Portugal (INE), "Census 2011," 2011. [Online]. Available: http://censos.ine.pt/xportal/xmain?xpid=CENSOS&xpgid=ine_censos_indicadores.

[214] Portuguese Department of Energy and Geology (DGEG), "SCE.CLIMA 1.0 - Portuguese Reference Meteorological Years." 2016.

[215] Statistics Portugal (INE), "Construction and Housing Statistics 2017 (in Portuguese)," Lisbon, 2018.

[216] Statistics Portugal (INE), "Construction and Housing Statistics 2012-2017 (in Portuguese)," Lisbon.

[217] Portuguese Environmental Agency (APA), "Low Calorific Power, Emission Factor and Oxidation Factor - European Emission Trading Scheme (ETS) - 2013-

2020 (in Portuguese),” 2013.

[218] H. Im and Y. Kim, “The Electrification of Cooking Methods in Korea — Impact on Energy Use and Greenhouse,” 2020.

[219] M. Griffin, T. Ramsson, and G. Gibson, “Cooking Appliances- Technology Brief,” 2012.

[220] Presidency of the Council of Ministers, *Decree-Law 118/2013 - Order No 349-B/2013 - Regulation for Energy Performance of Residential Buildings (in Portuguese)*, vol. 232. Portugal, 2013, pp. 18–29.

[221] “E-storage : Shifting from cost to value. Wind and solar applications.,” London, United Kingdom, 2016.

[222] Portuguese Ministry of Environment and Energy Transition, “Long-Term Strategy for Carbon Neutrality of the Portuguese Economy by 2050 - Roadmap to Carbon Neutrality 2050,” vol. R 262/2019. 2019.

[223] European Network of Transmission System Operators for Electricity (ENTSO-E), “Scenario Outlook and Adequacy Forecast 2030,” Brussels, 2014.

[224] R. Figueiredo, P. Nunes, and M. C. Brito, “Multiyear calibration of simulations of energy systems,” *Energy*, vol. 157, pp. 932–939, Aug. 2018.

[225] “Background,” *Eurostat*, 2018. [Online]. Available: http://ec.europa.eu/eurostat/web/nuts/background.

[226] “What are the NUTS?,” *PORDATA*, 2018. [Online]. Available: https://www.pordata.pt/O+que+sao+NUTS.

[227] R. Figueiredo, P. Nunes, M. J. N. O. Panão, and M. C. Brito, “Country residential building stock electricity demand in future climate – Portuguese case study,” *Energy Build.*, vol. 209, 2020.

[228] “Windows Technical Background Report Windows, Glazed Doors and Skylights,” Brussels, 2010.

[229] T. C. Pereira *et al.*, “Portuguese National Inventory Report on Greenhouse Gases, 1990 - 2015,” 2015.

Supplementary Material

This supplementary material aims to complete the results before presented. It contains Annex I to VIII, presented in the same order as referred to in the main body of this thesis.

Annex I. Renewable energy generation

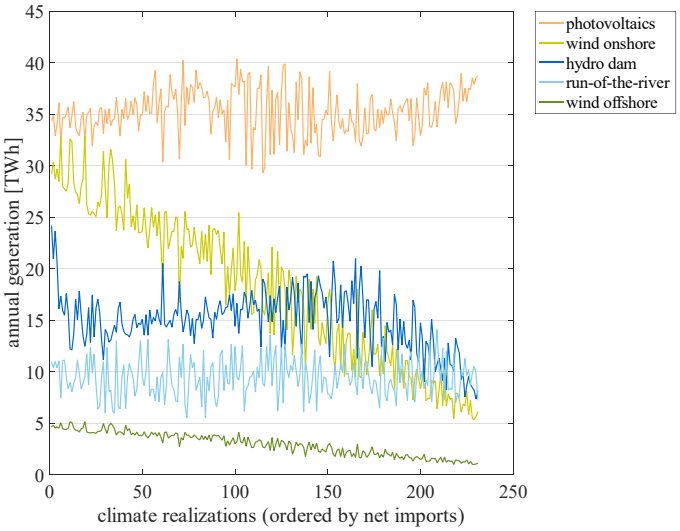

Figure I.1. Annual generation of renewable energy – RCP4.5
Annual renewable generation for each of the climate realizations (ordered by net imports, with the first climate realizations corresponding to situations with high exports) under RCP4.5. The hydro dam generation corresponds to the one observed in Central scenario for the 100% renewable power system (100%RES).

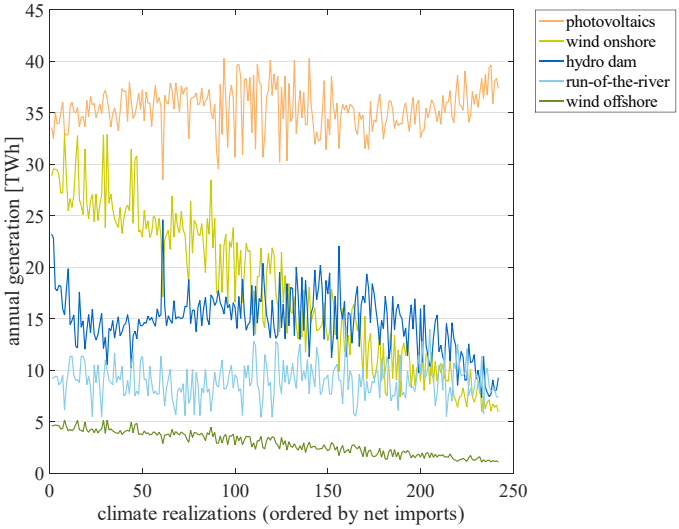

Figure I.2 Annual generation of renewable energy – RCP8.5
Annual renewable generation for each of the climate realizations (ordered by net imports, with the first climate realizations corresponding to situations with high exports) under RCP8.5. The hydro dam generation corresponds to the one observed in Central scenario for the 100% renewable power system (100%RES).

Annex II. Standard calibration

Table II.1. Standard model calibration in the period 2011-2015
Model results using single year calibration for corresponding calibrating year [95], [96], [142].

Model results [differences in %]					
	2011	2012	2013	2014	2015
Electricity demand	0.00	0.00	0.00	0.00	-0.01
Average monthly demand differences	-0.03	-0.02	0.01	-0.01	-0.03
Electricity generation					
Thermal power plant					
CHP	-0.02	-0.02	0.00	+0.03	+0.02
Condensing power plant	-0.02	-0.02	0.00	0.03	0.02
Coal and biomass	0.01	0.04	0.02	0.02	-0.02
Natural gas	-0.05	-0.02	-0.07	0.36	-0.02
Dammed hydro	-0.11	-0.32	-0.70	-0.58	+0.31
Run-of-the-river	-0.03	+0.11	-0.36	-0.05	-0.07
Wind	+0.03	-0.01	-0.03	-0.06	+0.02
PV	-1.00	+0.73	-0.61	-0.69	+0.25
RES share	-0.89	-2.19	-0.88	-0.4	-1.54
Primary fuel consumption					
Coal	-0.03	0.02	-0.01	0.01	0.00
Natural gas	-0.01	0.00	0.04	0.04	-0.03
Biomass	-0.01	0.01	0.01	0.01	0.00
Other non-renewable	-0.03	0.00	0.00	-0.01	0.00
Total consumption	-0.02	0.01	-0.06	-0.03	-0.01
Import/Export balance	-4.57	-4.87	-8.53	-16.60	-11.36
CO_2 emissions	-0.02	0.01	0.01	0.00	-0.01

Annex III. Multiyear calibration

Table III.1. Linear regression analysis – Efficiency of coal and biomass power plants
Root mean square error (RMSE), coefficient of determination (R^2) and p-value (F-statistics) of several models which combine the single independent variable selected previously (Electricity consumption) for the prediction of $\eta_{PP,coal\ and\ biomass}$. The coefficients of each term of the model and its respective p-value (Wald-statistics) are also presented.

Linear regression analysis – efficiency of coal and biomass power plant, $\eta_{PP,coal\ and\ biomass}$							
		RMSE	R^2	p-value (F-stats.)		Estimates	p-value (Wald stats.)
Single independent variable X_1	**Model 1** – Elect. cons.	0.0090	0.6708	0.0899	$\hat{\beta}_0$	0.779	-
					$\hat{\beta}_1$	-0.009	0.0899

Table III.2. Linear regression analysis – Efficiency of natural gas power plants
Root mean square error (RMSE), coefficient of determination (R^2) and p-value (F-statistics) of several models which combine the four independent variables selected previously (precipitation, wind index, Electricity consumption and RES generation) for the prediction of $\eta_{PP,natural\ gas}$. The coefficients of each term of the model and its respective p-value (Wald-statistics) are also presented.

Linear regression analysis – efficiency of natural gas power plant, $\eta_{PP,natural\ gas}$

		RMSE	R^2	p-value (F-stats.)		Estimates	p-value (Wald stats.)
Single independent variable **X_1**	**Model 2** – Precipitation	0.0409	0.7520	0.0569	$\hat{\beta}_0$	0.625	-
					$\hat{\beta}_1$	-1.691×10^{-4}	0.0569
	Model 3 – Wind index	0.0397	0.7671	0.0515	$\hat{\beta}_0$	0.933	-
					$\hat{\beta}_1$	-1.812×10^{-4}	0.0515
	Model 4 – Elect. cons.	0.0669	0.3381	0.3038	$\hat{\beta}_0$	-1.210	-
					$\hat{\beta}_1$	0.034	0.3038
	Model 5 – RES generation	0.0348	0.8207	0.0342	$\hat{\beta}_0$	0.704	-
					$\hat{\beta}_1$	-0.008	0.0342
Two independent variables **$X_1 + X_2$**	**Model 6** – RES generation + Precipitation	0.0332	0.8366	0.1634	$\hat{\beta}_0$	0.688	-
					$\hat{\beta}_1$	-0.006	0.4160
					$\hat{\beta}_2$	-5.518×10^{-5}	0.7021
	Model 7 – RES generation + Wind index	0.0253	0.905	0.095	$\hat{\beta}_0$	0.850	-
					$\hat{\beta}_1$	-0.005	0.2306
					$\hat{\beta}_2$	-9.204×10^{-5}	0.3144
	Model 8 – RES generation + Elect. cons.	0.0143	0.9698	0.0302	$\hat{\beta}_0$	-0.475	-
					$\hat{\beta}_1$	-0.007	0.0231
					$\hat{\beta}_2$	0.023	0.0881

Table III.3. Linear regression analysis – Water supply normalized
Root mean square error (RMSE), coefficient of determination (R^2) and p-value (F-statistics) of several models which combine the five independent variables selected previously (T_{min}, precipitation and wind index) for the parameterization of WS_{norm}. The coefficients of each term of the model and its respective p-value (Wald-statistics) are also presented.

Linear regression analysis – Water supply normalized, WS_{norm}

		RMSE	R^2	p-value (F-stats.)		Estimates	p-value (Wald-stats.)
Single independent variable **X_1**	**Model 9** – T_{min}	1,191.2	0.3563	0.2879	$\hat{\beta}_0$	-7,894.2	-
					$\hat{\beta}_1$	940.3	0.2879
	Model 10 – Precipitation	496.5	0.8882	0.0164	$\hat{\beta}_0$	-1,121.0	-
					$\hat{\beta}_1$	3.319	0.0164
	Model 11 – Wind index	1,156.6	0.3932	0.2576	$\hat{\beta}_0$	-4,195.5	-
					$\hat{\beta}_1$	2.344	0.2576
Two independent variables **$X_1 + X_2$**	**Model 12** – Precipitation + T_{min}	475.4	0.8975	0.1025	$\hat{\beta}_0$	-2,767.2	-
					$\hat{\beta}_1$	3.097	0.0831
					$\hat{\beta}_2$	181.7	0.7113
	Model 13 – Precipitation + Wind index	475.1	0.8976	0.1024	$\hat{\beta}_0$	-107.9	-
					$\hat{\beta}_1$	3.690	0.0883
					$\hat{\beta}_2$	-0.535	0.7099

Table III.4.Linear regression analysis – Run-of-the-river coefficient
Root mean square error (RMSE), coefficient of determination (R^2) and p-value (F-statistics) of several models which combine the five independent variables selected previously (T_{min}, precipitation and wind index) for the parameterization of C_{RoR}. The coefficients of each term of the model and its respective p-value (Wald-statistics) are also presented.

Linear regression analysis – Run-of-the-river coefficient, C_{RoR}

		RMSE	R^2	p-value (F-stats.)		Estimates	p-value (Wald-stats.)
Single independent variable X_1	**Model 14** – T_{min}	0.3941	0.4883	0.1892	$\hat{\beta}_0$	-3.472	-
					$\hat{\beta}_1$	0.408	0.1892
	Model 15 – Precipitation	0.2543	0.7869	0.0448	$\hat{\beta}_0$	-0.303	-
					$\hat{\beta}_1$	0.001	0.0448
	Model 16 – Wind index	0.3875	0.5053	0.1783	$\hat{\beta}_0$	-1.787	-
					$\hat{\beta}_1$	9.859×10^{-4}	0.1783
Two independent variables $X_1 + X_2$	**Model 17** – Precipitation + T_{min}	0.2122	0.8517	0.1483	$\hat{\beta}_0$	-1.913	-
					$\hat{\beta}_1$	9.417×10^{-4}	0.1573
					$\hat{\beta}_2$	0.178	0.4487
	Model 18 – Precipitation + Wind index	0.2498	0.7944	0.2056	$\hat{\beta}_0$	-0.638	-
					$\hat{\beta}_1$	0.001	0.2355
					$\hat{\beta}_2$	1.772×10^{-4}	0.8124

Annex IV. Sensitivity analysis of the residential electricity demand

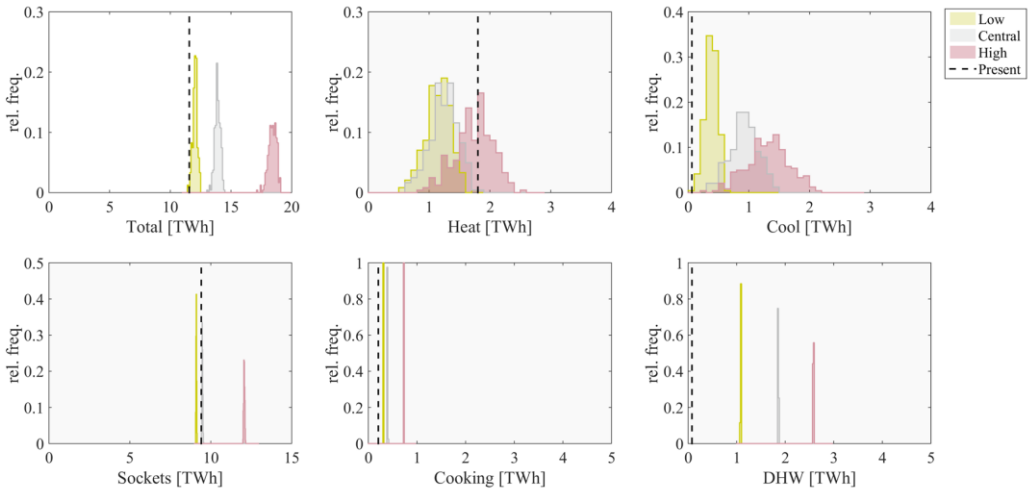

Figure IV.1. Residential electricity consumption per type of demand – RCP8.5
Histograms for the electricity consumption of the different types of demand (total, heat, cool, sockets, cooking and DHW) in the mid-century under RCP8.5 according to the Low, Central and High demand scenarios. The black dashed line shows the present electricity consumption.

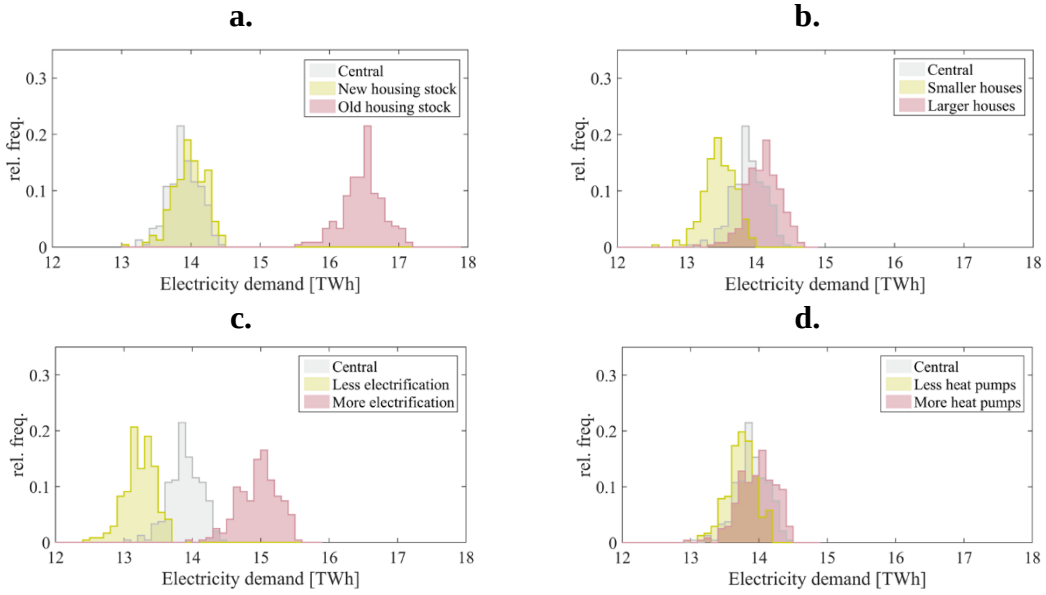

Figure IV.2. Sensitivity analysis on different housing stock development characteristics RCP8.5 – Histograms
Histograms for the sensitivity analysis performed under RCP8.5: a. Household market; b. Floor area of new dwellings; c. Electrification of cooking and DHW; and d. Space heating and cooling.

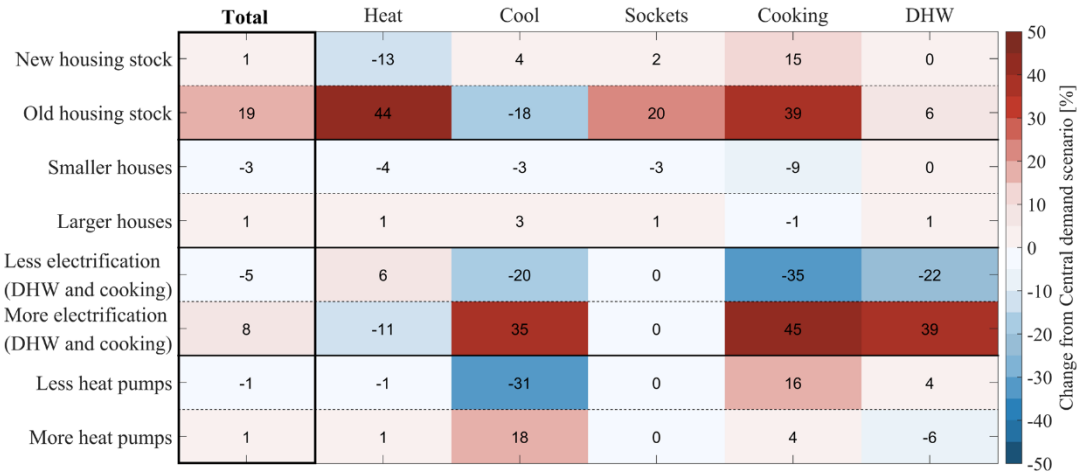

Figure IV.3. Sensitivity analysis on different housing stock development characteristics RCP8.5 – Average
Change in the average electricity consumption relative to the Central scenario for each type of consumption under RCP8.5.

Annex V. Highly renewable power systems (HiRES and HiRES+UB)

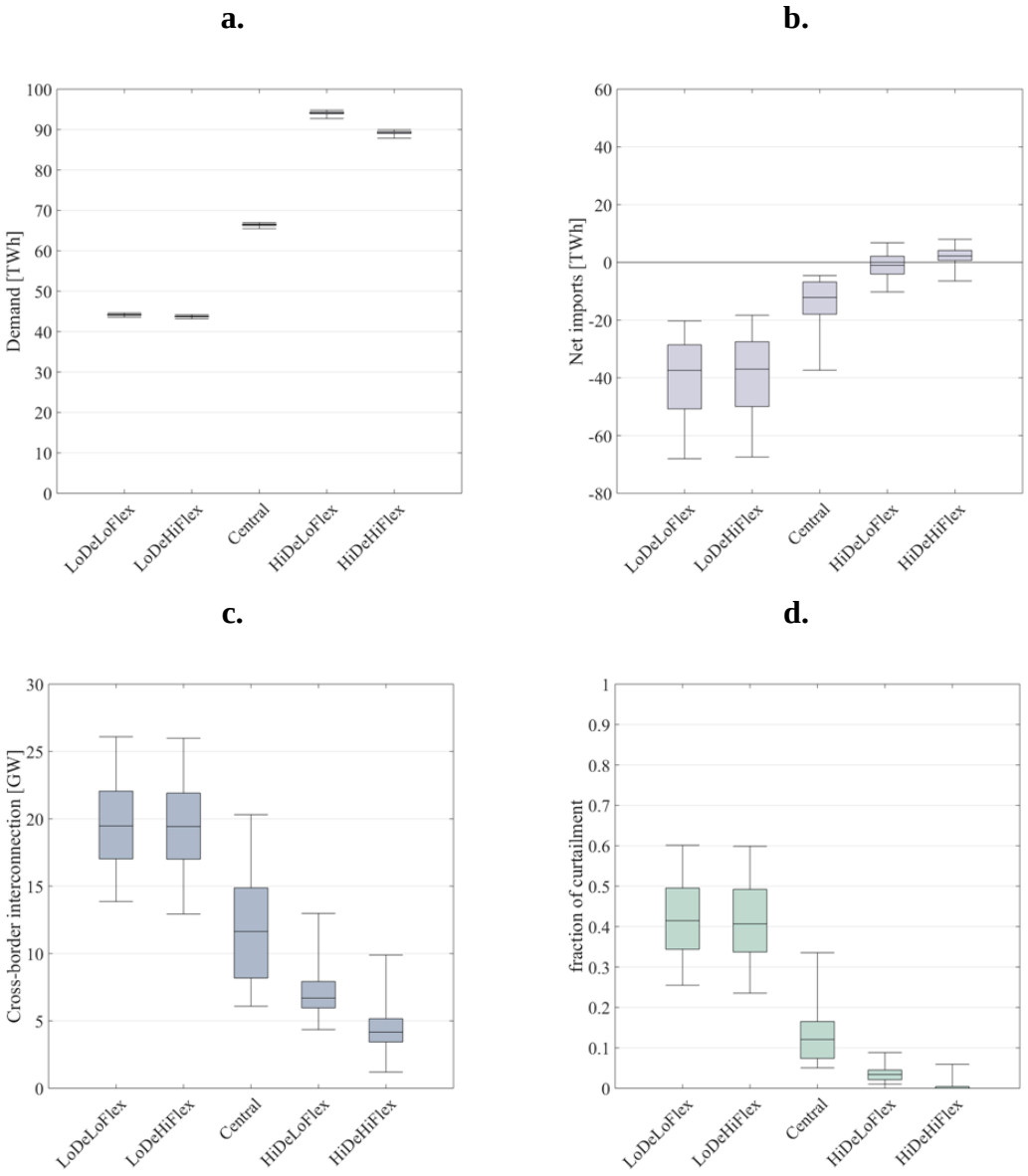

Figure V.1. High renewable penetration power systems – RCP8.5
Performance of the proposed highly-renewable power systems for all ensemble years and each demand-flexibility scenario under RCP8.5 in terms of: a. electricity demand; b. annual net imports (resulting from the difference between annual imports and exports); c. cross-border interconnection requirements; and d. potential energy curtailment (relative to generation). Each boxplot represents the results obtained for all the ensemble years tested.

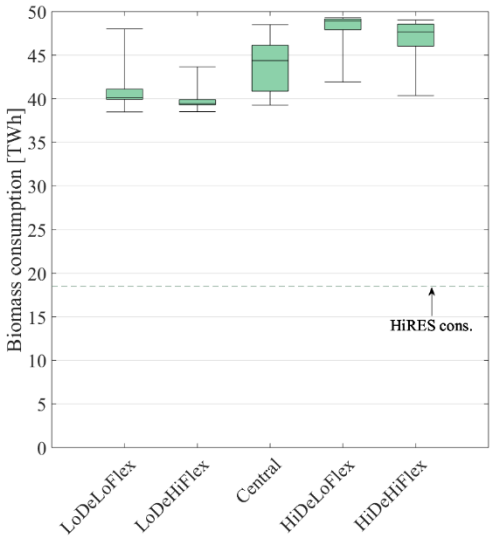

Figure V.2. Biomass consumption in highly renewable power systems – RCP8.5
Comparison between the biomass consumption for all ensemble years and each demand-flexibility scenario under RCP4.5 for HiRES (highly renewable power system) and HiRES+UB (same with unlimited biomass resource) configurations. HiRES is represented in a single dashed line, since its biomass consumption is limited to current values and it is always fully needed. For HiRES+UB, each boxplot represents the results obtained for all the ensemble years tested.

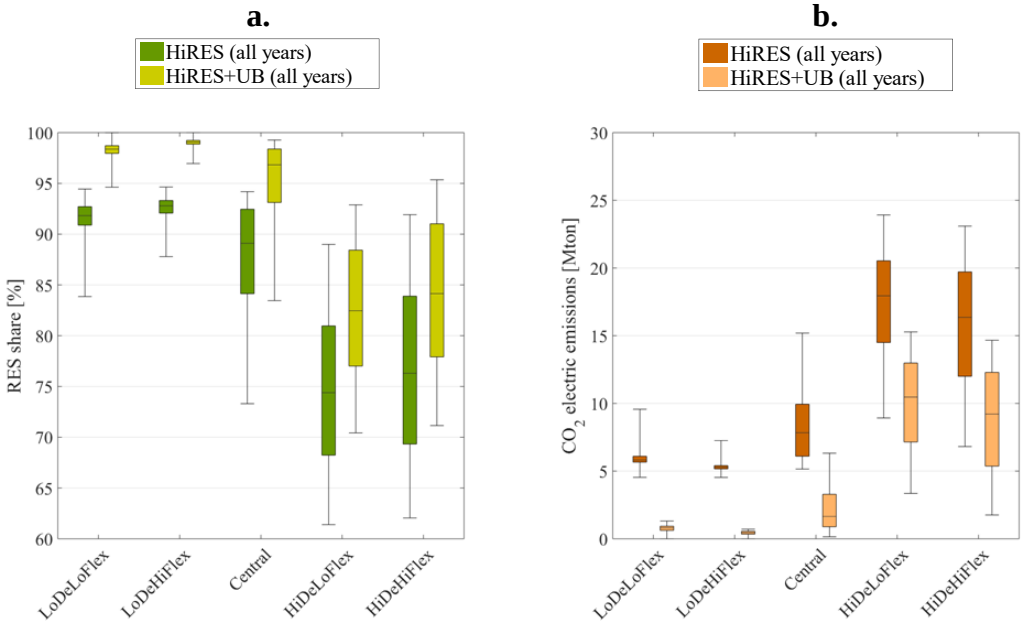

Figure V.3. Renewable share and CO_2 emissions from the power systems HiRES and HiRES+UB – RCP8.5
Comparison between the performance of HiRES (highly renewable power system) and HiRES+UB (same with unlimited biomass resource) configurations for all ensemble years and each demand-flexibility scenario under RCP8.5 in terms of: a. generation share of renewable energy; and b. CO_2 emissions from the power system. Each boxplot represents the results obtained for all the ensemble years tested.

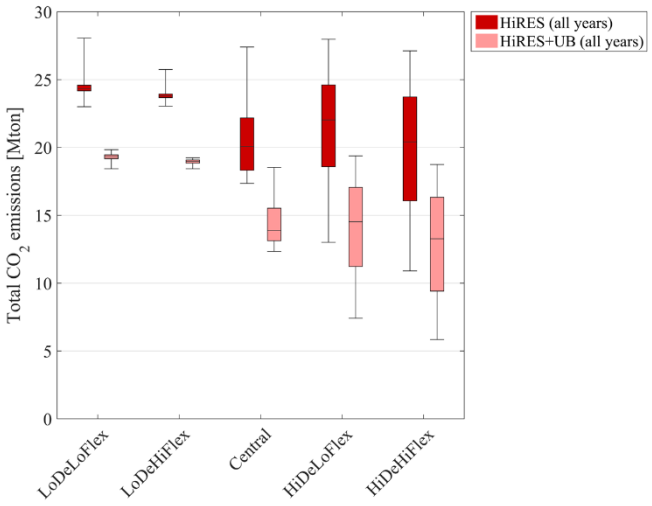

Figure V.4. Total CO_2 emissions – RCP8.5
Comparison between the performance of HiRES (highly renewable power system) and HiRES+UB (same with unlimited biomass resource) configurations for all ensemble years and each demand-flexibility scenario under RCP8.5 in terms of: a. generation share of renewable energy; and b. CO_2 emissions from the power system. Each boxplot represents the results obtained for all the ensemble years tested.

Annex VI. Solar-wind power capacities – HiRES and HiRES+UB

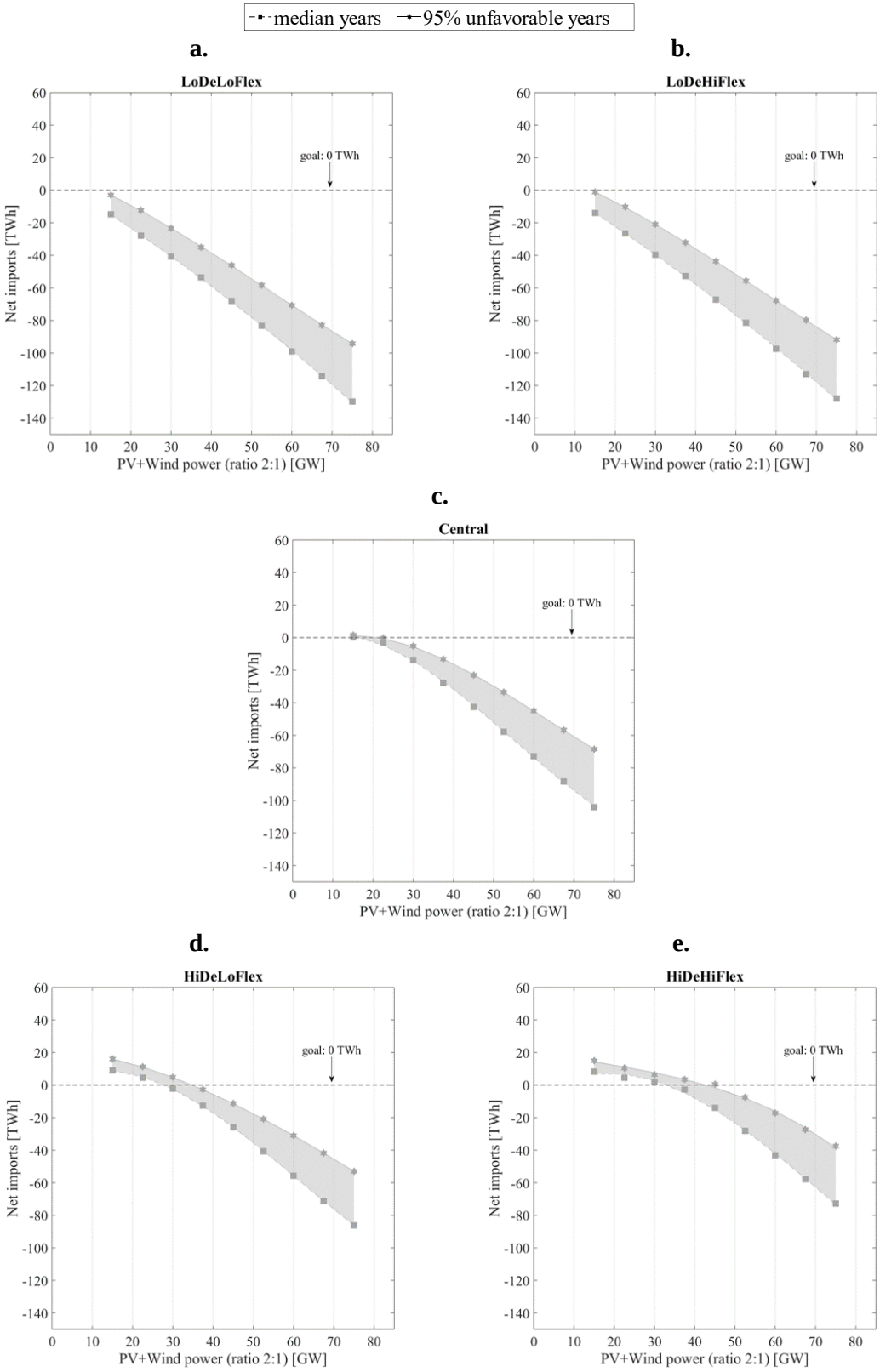

Figure VI.1. Annual net imports variation with PV+Wind installed capacities – RCP4.5
Annual net imports for different PV+Wind installed capacities (ratio 2:1) for different climate conditions and each demand-flexibility scenario under RCP4.5: a. Low demand + Low flexibility (LoDeLoFlex); b. Low demand + High flexibility (LoDeHiFlex); c. Central; d. High demand + Low flexibility (HiDeLoFlex); and e. High demand + High flexibility (HiDeHiFlex). Each marker represents different percentiles of net imports (within all the climate tested): square with dashed line– 50th percentile and hexagram with solid line – 95th percentile.

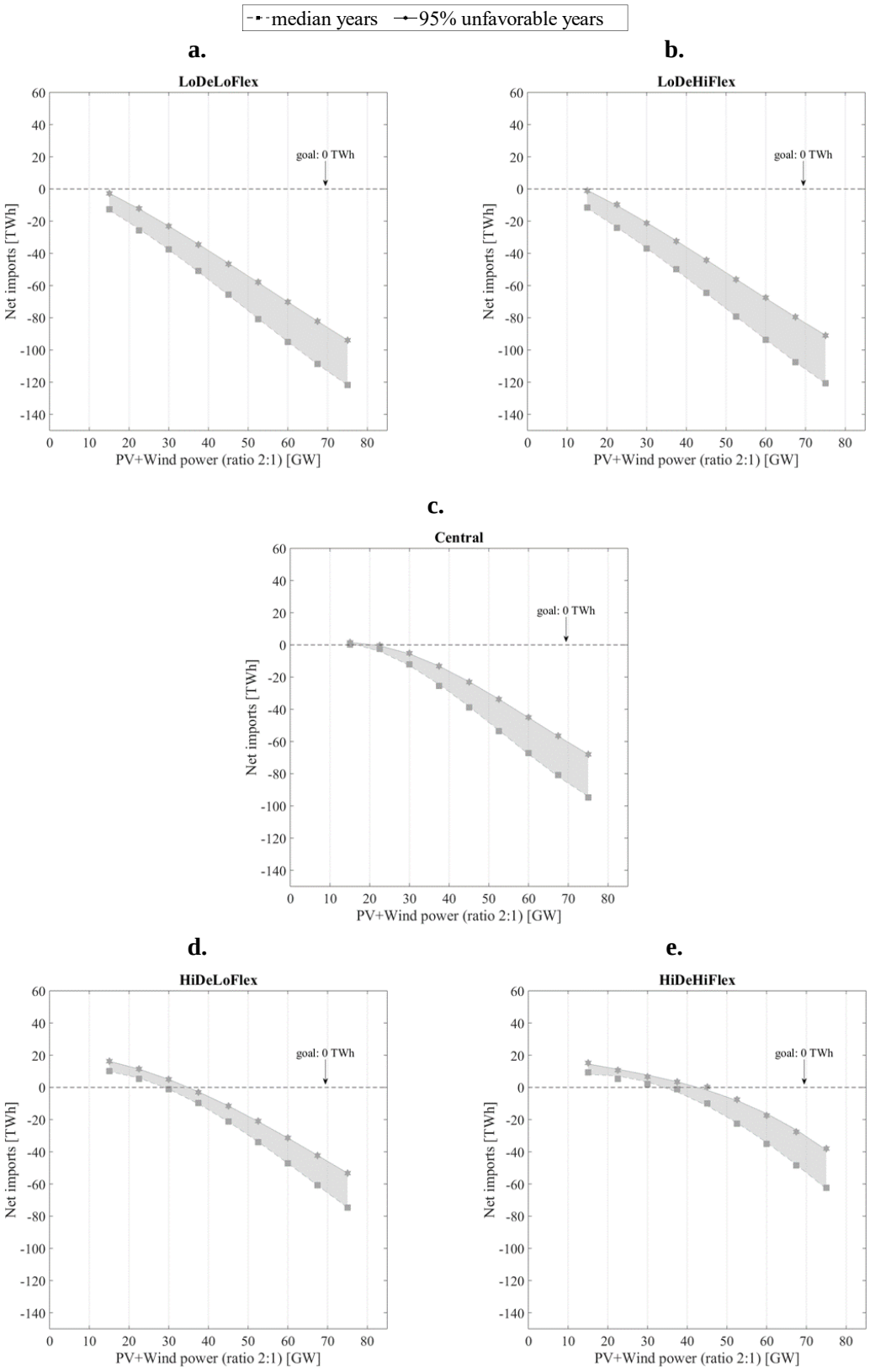

Figure VI.2. Annual net imports variation with PV+Wind installed capacities – RCP8.5
Annual net imports for different PV+Wind installed capacities (ratio 2:1) for different climate conditions and each demand-flexibility scenario under RCP8.5: a. Low demand + Low flexibility (LoDeLoFlex); b. Low demand + High flexibility (LoDeHiFlex); c. Central; d. High demand + Low flexibility (HiDeLoFlex); and e. High demand + High flexibility (HiDeHiFlex). Each marker represents different percentiles of net imports (within all the climate tested): square with dashed line– 50th percentile and hexagram with solid line – 95th percentile.

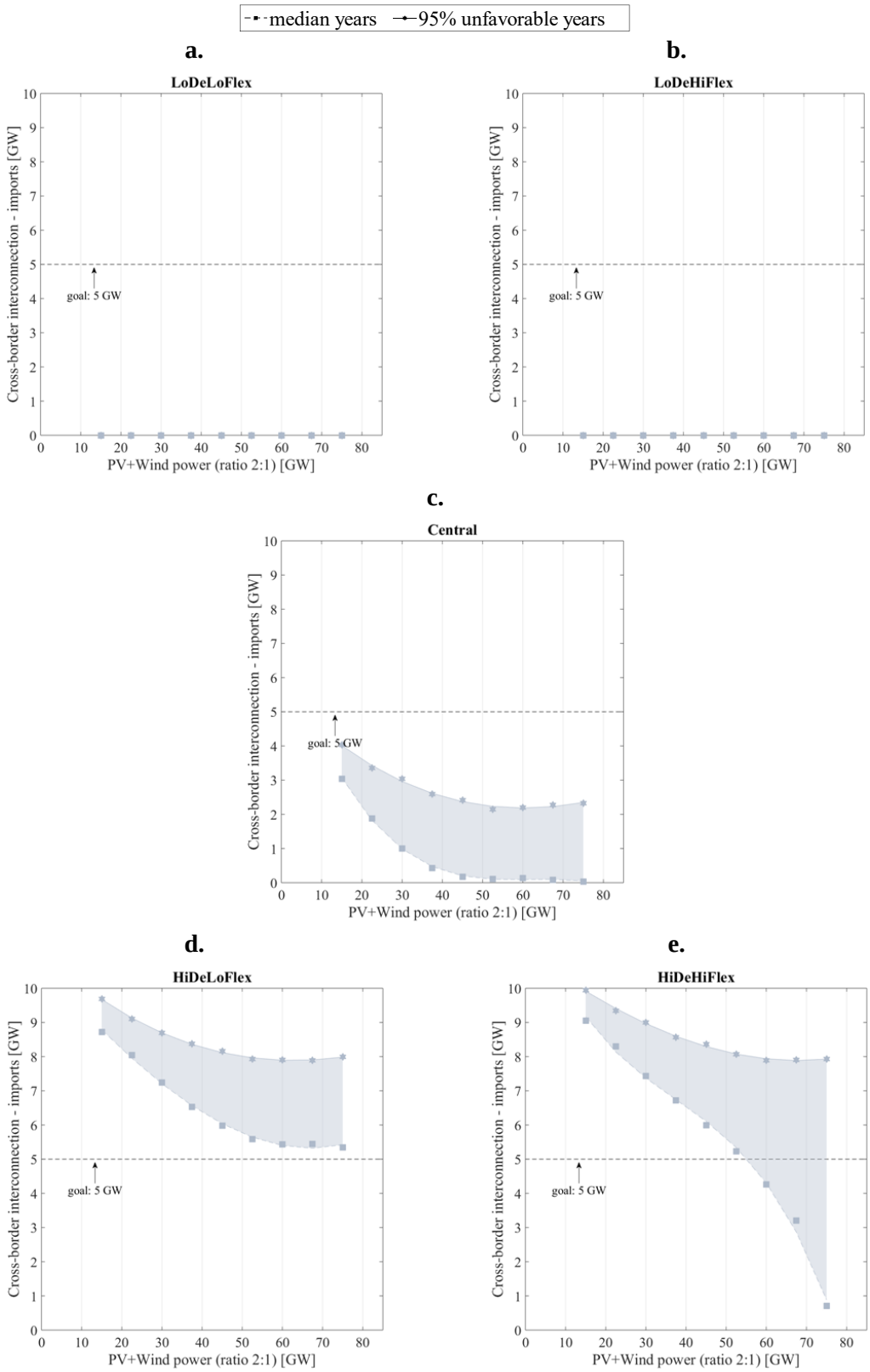

Figure VI.3. Cross-border interconnection for imports and PV+Wind installed capacities – RCP4.5
Cross-border interconnection for imports with different PV+Wind installed capacities (ratio 2:1) for different climate conditions and each demand-flexibility scenario under RCP4.5: a. Low demand + Low flexibility (LoDeLoFlex); b. Low demand + High flexibility (LoDeHiFlex); c. Central; d. High demand + Low flexibility (HiDeLoFlex); and e. High demand + High flexibility (HiDeHiFlex). Each marker represents different percentiles of total CO_2 emissions (within all the climate tested): square with dashed line – 50th percentile and hexagram with solid line – 95th percentile.

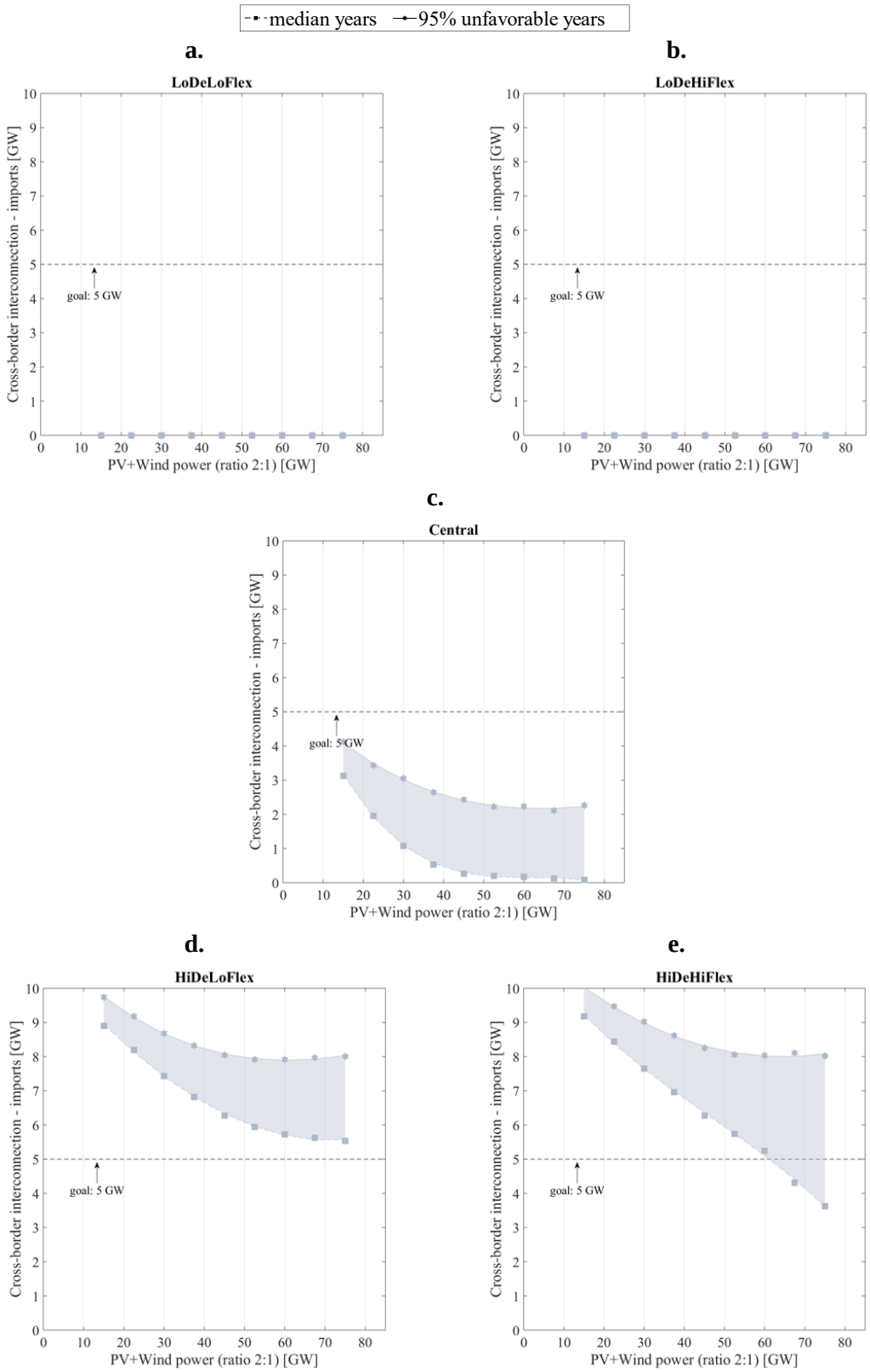

Figure VI.4. Cross-border interconnection for imports and PV+Wind installed capacities – RCP8.5
Cross-border interconnection for imports with different PV+Wind installed capacities (ratio 2:1) for different climate conditions and each demand-flexibility scenario under RCP8.5: a. Low demand + Low flexibility (LoDeLoFlex); b. Low demand + High flexibility (LoDeHiFlex); c. Central; d. High demand + Low flexibility (HiDeLoFlex); and e. High demand + High flexibility (HiDeHiFlex). Each marker represents different percentiles of total CO_2 emissions (within all the climate tested): square with dashed line – 50th percentile and hexagram with solid line – 95th percentile.

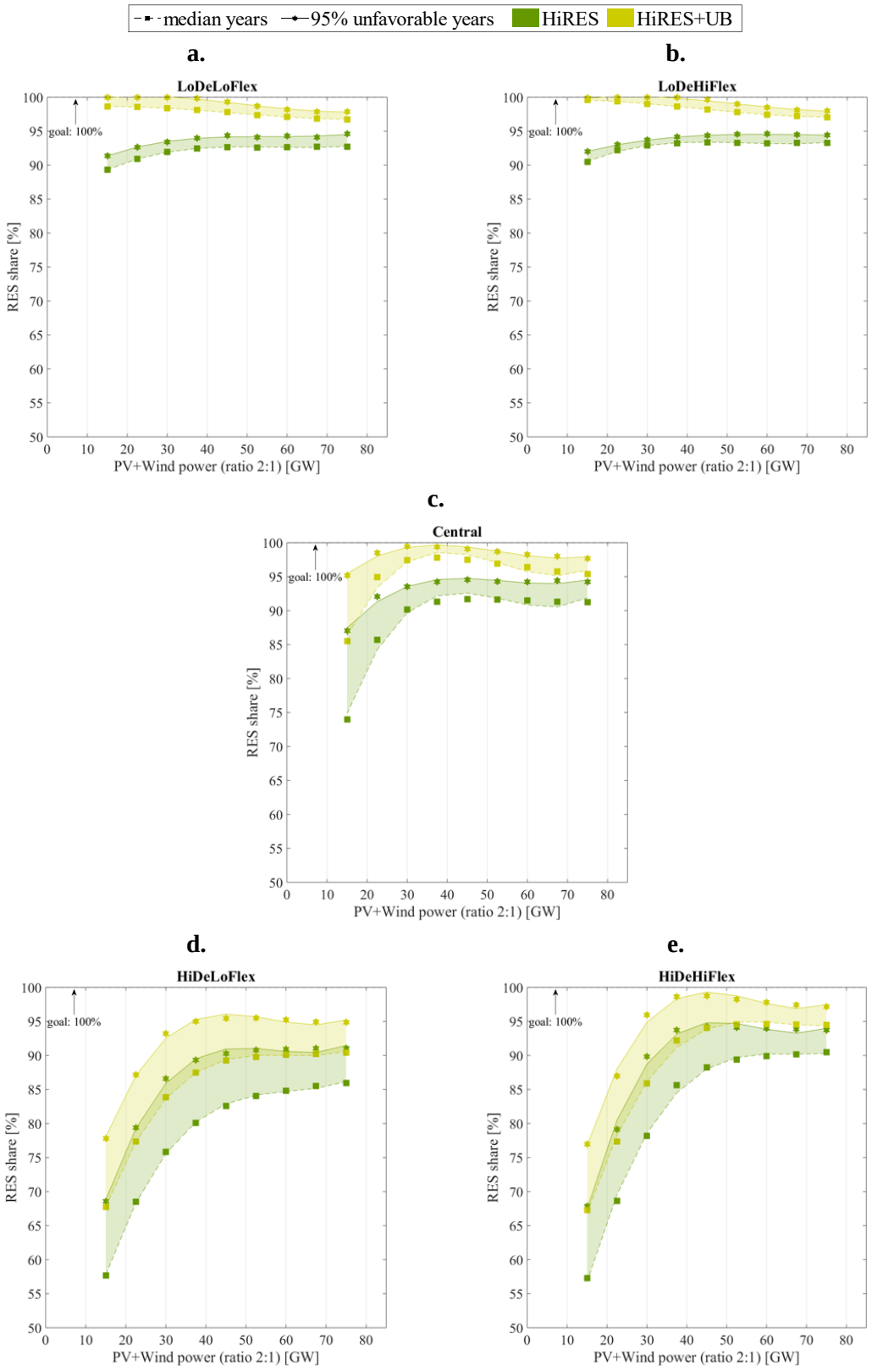

Figure VI.5. Renewable generation share and PV+Wind installed capacities – RCP4.5
Renewable generation share for HiRES and HiRES+UB configurations with different PV+Wind installed capacities (ratio 2:1) for different climate conditions and each demand-flexibility scenario under RCP4.5: a. Low demand + Low flexibility (LoDeLoFlex); b. Low demand + High flexibility (LoDeHiFlex); c. Central; d. High demand + Low flexibility (HiDeLoFlex); and e. High demand + High flexibility (HiDeHiFlex). Each marker represents different percentiles of renewable generation share (within all the ensemble years tested): square with dashed line – 50th percentile and hexagram with solid line – 95th percentile.

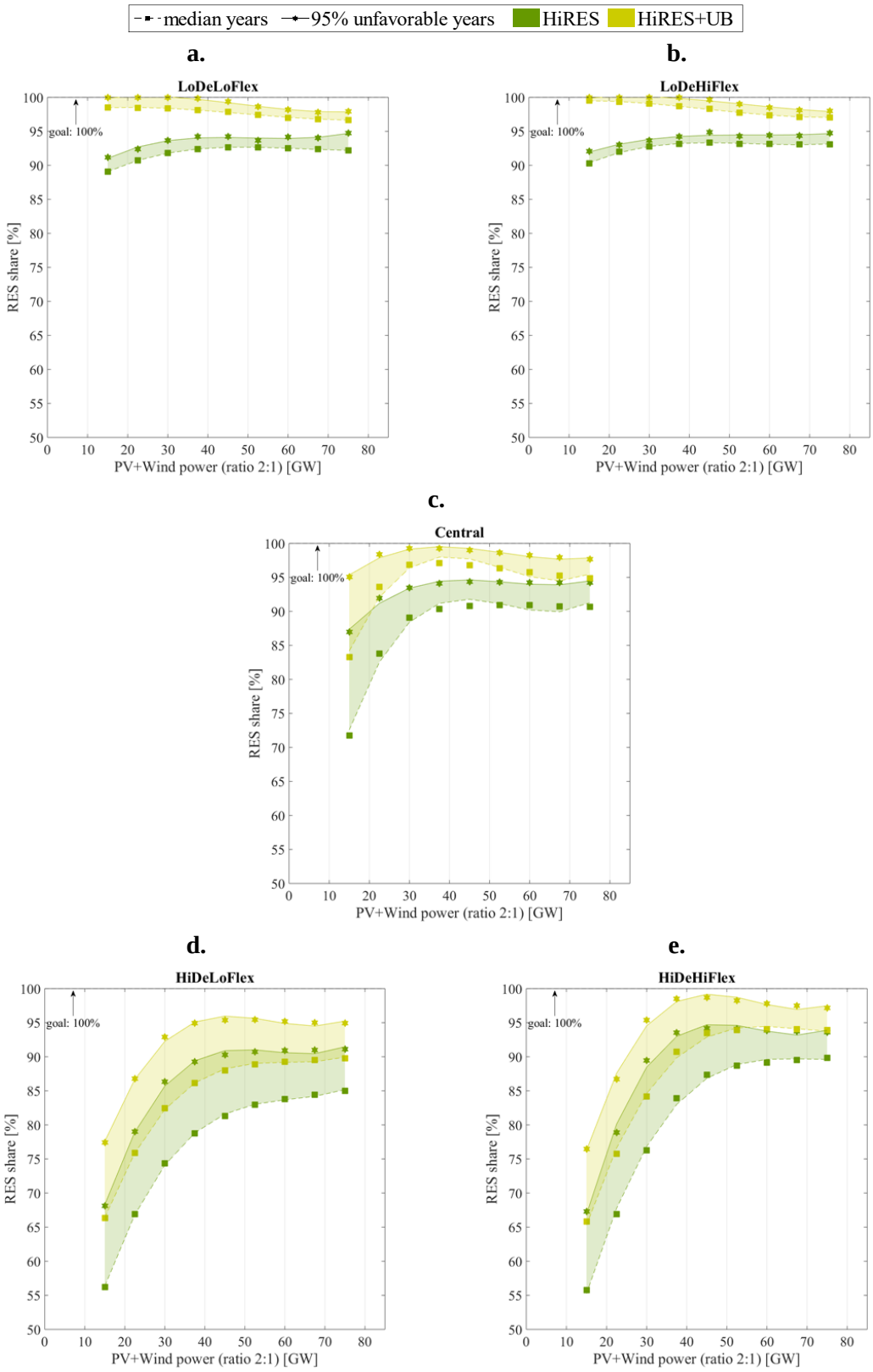

Figure VI.6. Renewable generation share and PV+Wind installed capacities – RCP8.5
Renewable generation share for HiRES and HiRES+UB configurations with different PV+Wind installed capacities (ratio 2:1) for different climate conditions and each demand-flexibility scenario under RCP8.5: a. Low demand + Low flexibility (LoDeLoFlex); b. Low demand + High flexibility (LoDeHiFlex); c. Central; d. High demand + Low flexibility (HiDeLoFlex); and e. High demand + High flexibility (HiDeHiFlex). Each marker represents different percentiles of renewable generation share (within all the ensemble years tested): square with dashed line – 50th percentile and hexagram with solid line – 95th percentile.

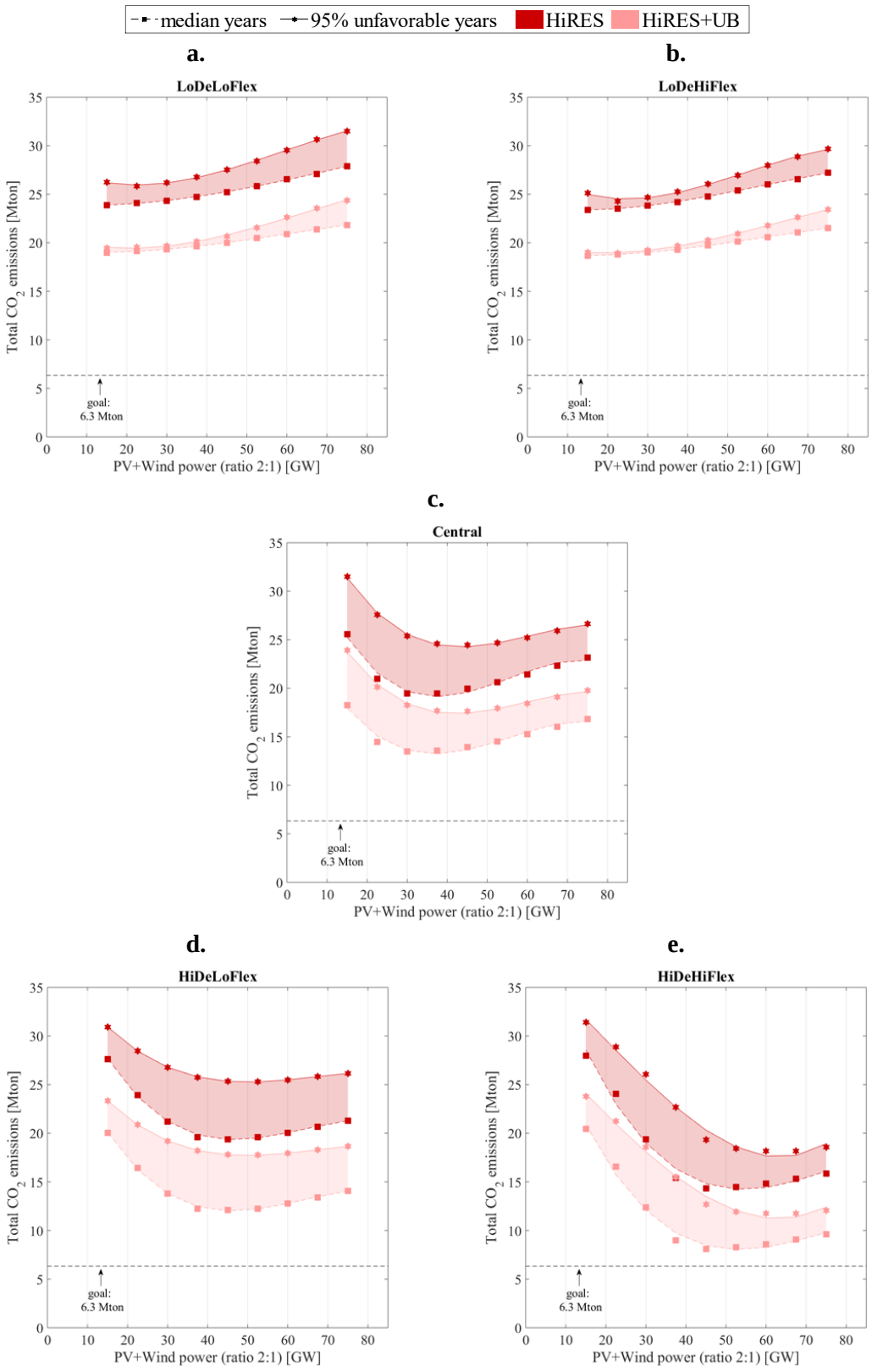

Figure VI.7. Total CO_2 emissions and PV+Wind installed capacities – RCP4.5
Total CO_2 emissions for HiRES and HiRES+UB configurations with different PV+Wind installed capacities (ratio 2:1) for different climate conditions and each demand-flexibility scenario under RCP4.5: a. Low demand + Low flexibility (LoDeLoFlex); b. Low demand + High flexibility (LoDeHiFlex); c. Central; d. High demand + Low flexibility (HiDeLoFlex); and e. High demand + High flexibility (HiDeHiFlex). Each marker represents different percentiles of total CO_2 emissions (within all the ensemble years tested): square with dashed line – 50th percentile and hexagram with solid line – 95th percentile.

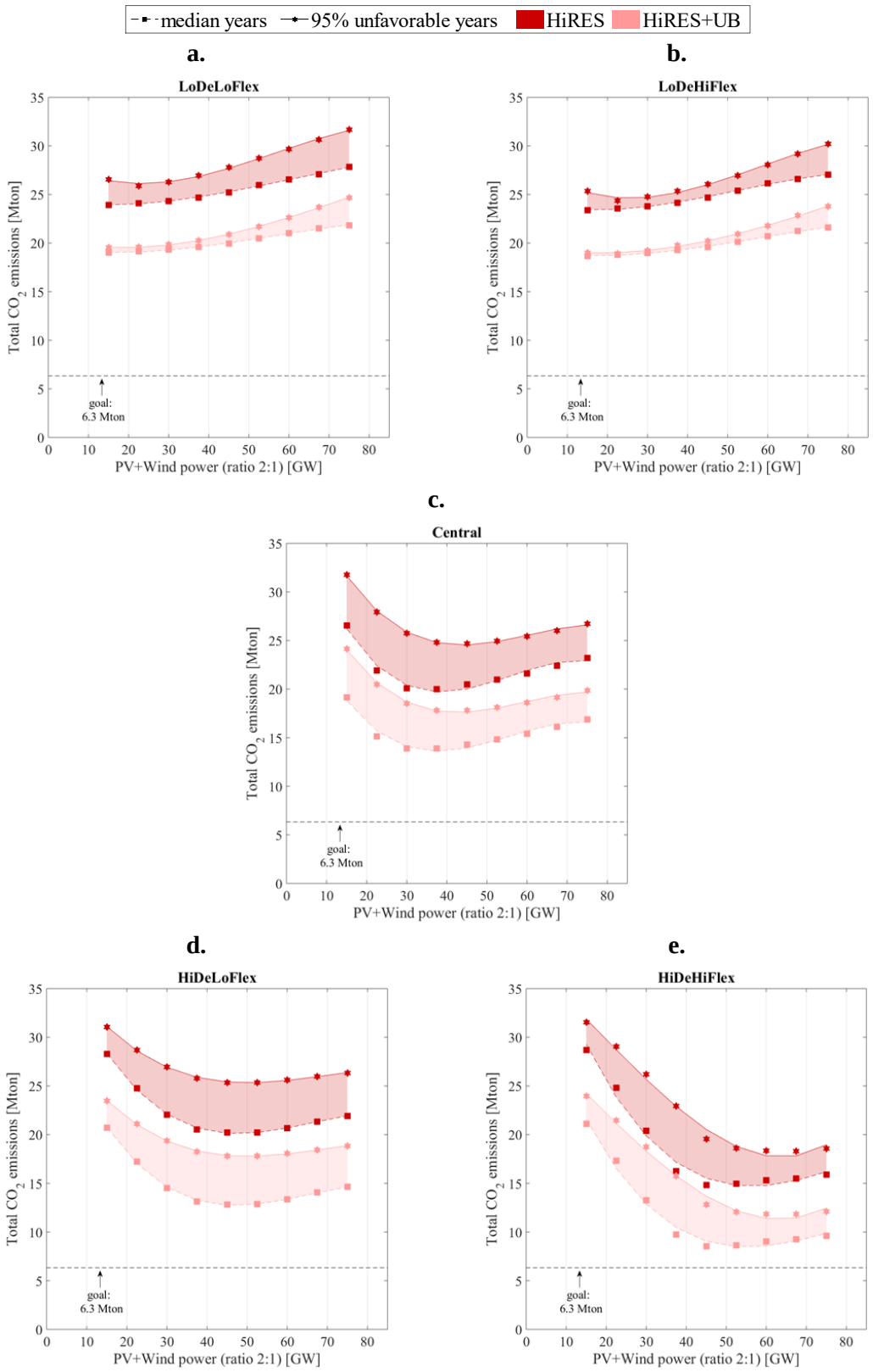

Figure VI.8. Total CO_2 emissions and PV+Wind installed capacities – RCP8.5
Total CO_2 emissions for HiRES and HiRES+UB configurations with different PV+Wind installed capacities (ratio 2:1) for different climate conditions and each demand-flexibility scenario under RCP8.5: a. Low demand + Low flexibility (LoDeLoFlex); b. Low demand + High flexibility (LoDeHiFlex); c. Central; d. High demand + Low flexibility (HiDeLoFlex); and e. High demand + High flexibility (HiDeHiFlex). Each marker represents different percentiles of total CO_2 emissions (within all the ensemble years tested): square with dashed line – 50th percentile and hexagram with solid line – 95th percentile.

Annex VII. Fully renewable power system (100%RES)

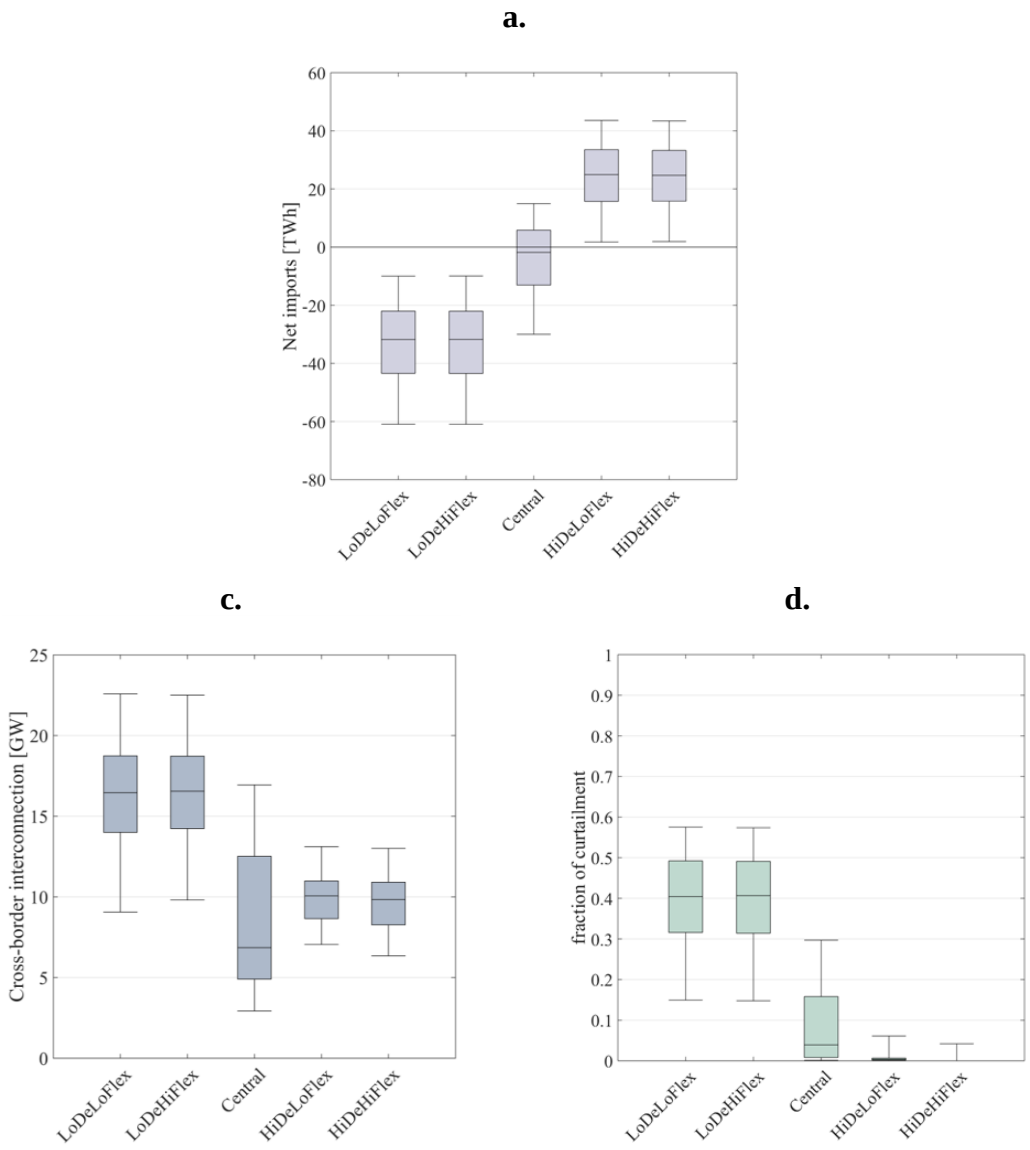

Figure VII.1. Fully renewable power system – RCP8.5
Performance of the proposed 100%RES power system for all ensemble years and each demand-flexibility scenario under RCP8.5 in terms of: a. annual net imports (resulting from the difference between annual imports and exports); c. interconnection requirement; and d. potential energy curtailment (relative to generation). Each boxplot represents the results obtained for all the ensemble years tested.

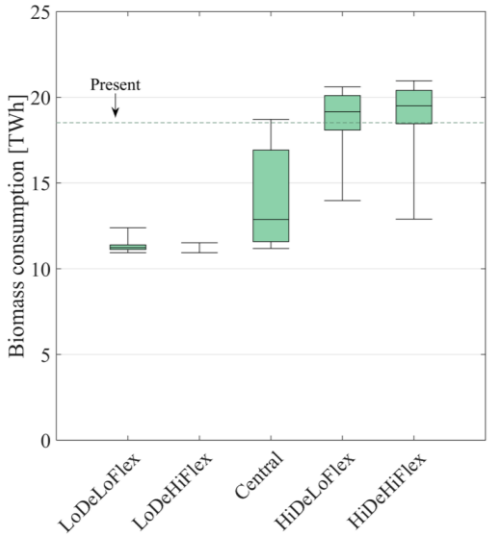

Figure VII.2. Biomass consumption in the fully renewable power system – RCP8.5
Comparison between the biomass consumption for all ensemble years and each demand-flexibility scenario under RCP8.5 for 100%RES (100% renewable power system) and the present consumption. The dashed line represents the present consumption of biomass and each boxplot represents the results obtained for all the ensemble years tested in the 100%RES.

Annex VIII. Required solar-wind capacity – 100%RES

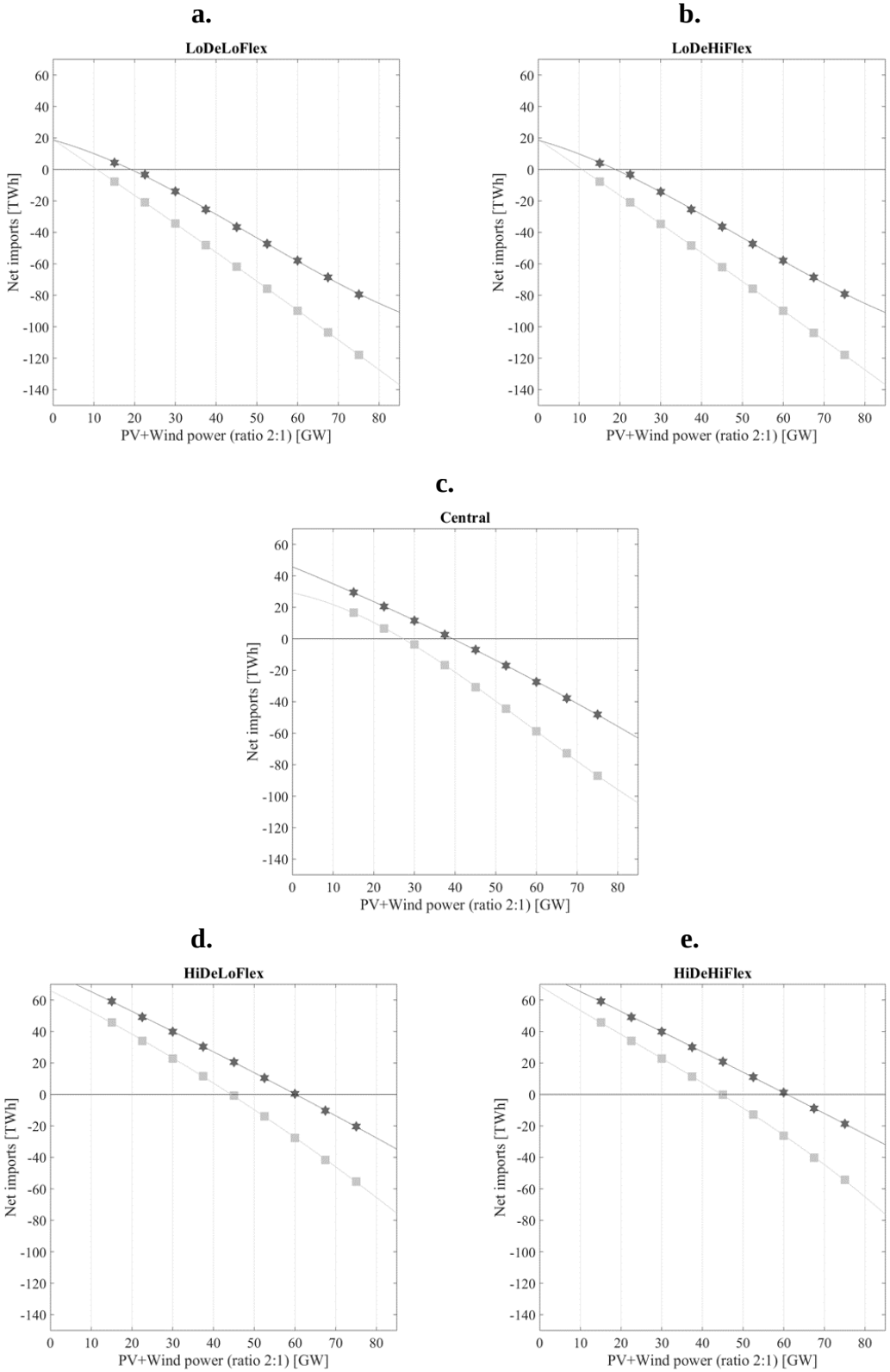

Figure VIII.1. Analysis of the required photovoltaics and onshore wind capacity – RCP4.5
Analysis of the required photovoltaics and onshore wind capacity for different levels of resilience under RCP4.5 for the scenarios: a. Low demand + Low flexibility (LoDeLoFlex); b. Low demand + High flexibility (LoDeHiFlex); c. Central; d. High demand + Low flexibility (HiDeLoFlex); e. High demand + High flexibility (HiDeHiFlex). Each marker represents different percentiles of net imports: square – 50th percentile and hexagram – 95th percentile (95% unfavorable year).

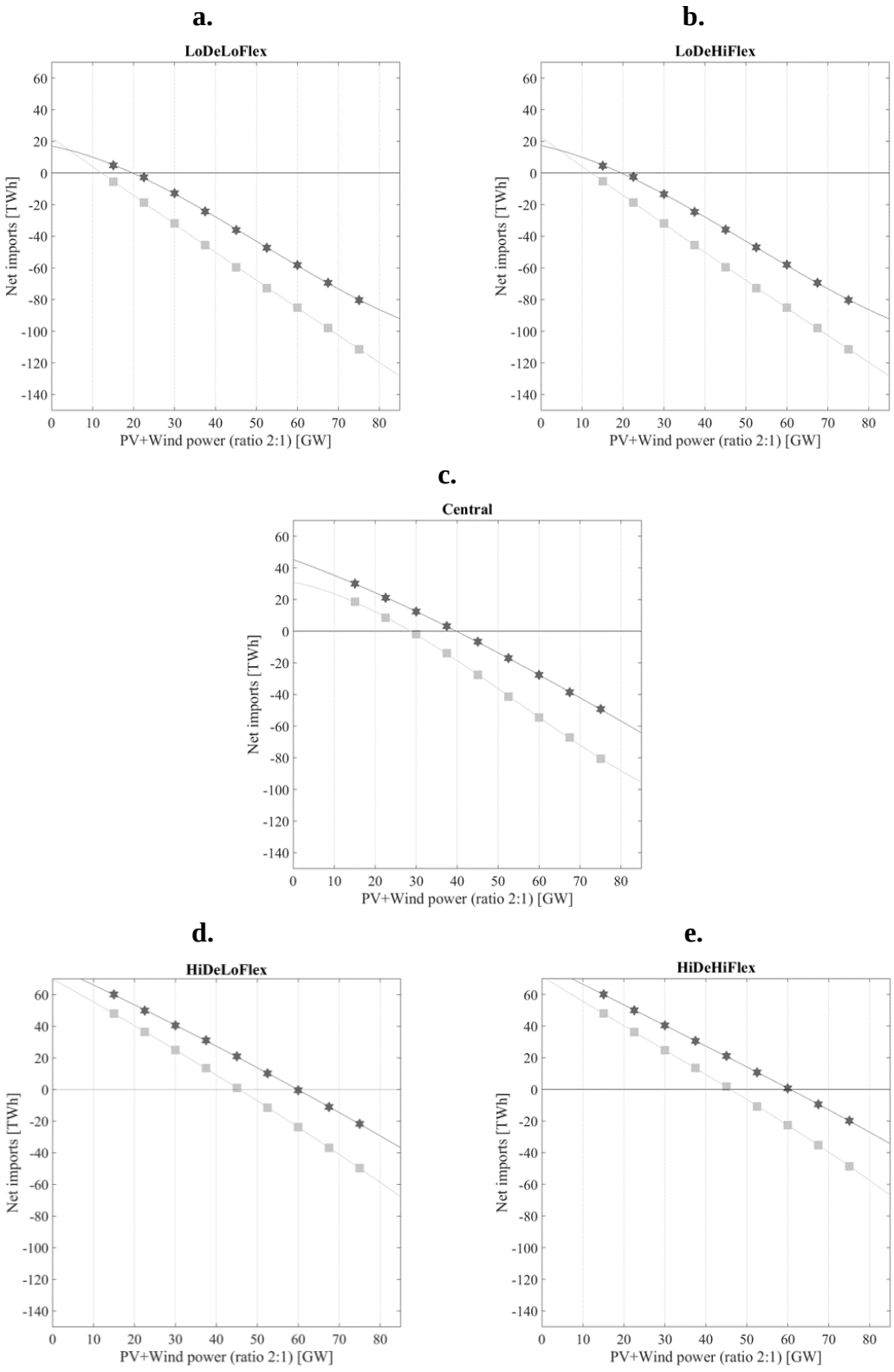

Figure VIII.2. Optimization of the photovoltaics and onshore wind capacity – RCP8.5
Analysis of the required photovoltaics and onshore wind capacity for different levels of resilience under RCP8.5 for the scenarios: a. Low demand + Low flexibility (LoDeLoFlex); b. Low demand + High flexibility (LoDeHiFlex); c. Central; d. High demand + Low flexibility (HiDeLoFlex); e. High demand + High flexibility (HiDeHiFlex). Each marker represents different percentiles of net imports: square – 50th percentile and hexagram – 95th percentile (unfavorable year).

Annex IX. Optimal Power Systems – 100%RES

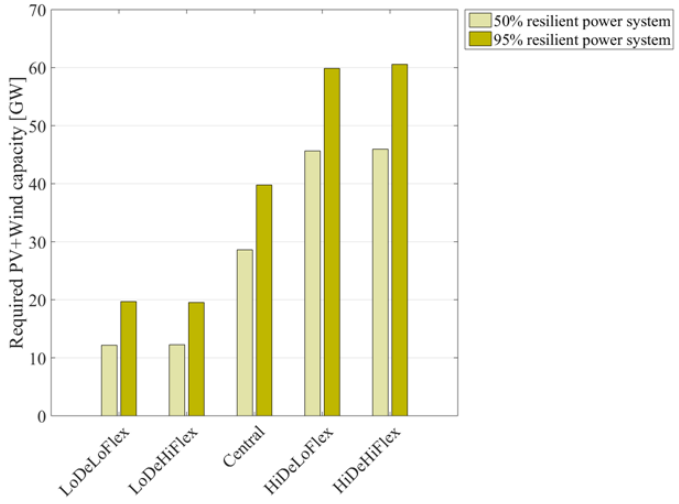

Figure IX.1. Required photovoltaic and wind capacity – RCP8.5
Combined photovoltaics and onshore wind capacities required for having null net imports for the different demand-flexibility scenarios with 50 and 95% resilience under RCP8.5.

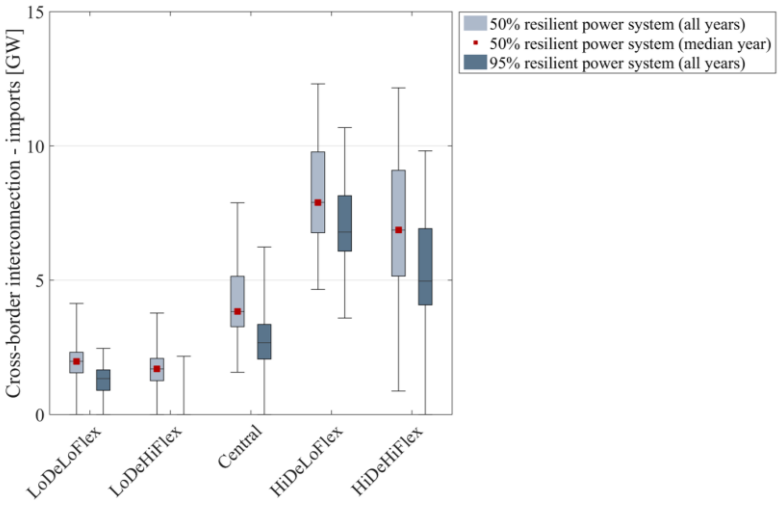

Figure IX.2. Cross-border interconnection requirements – RCP8.5
Cross-border interconnection required for imports for the power systems designed with a level of resilience of 50 and 95% under RCP8.5. Each boxplot represents the results obtained for all the ensemble years tested. The dark red square highlights the median of the 50% resilient power system.

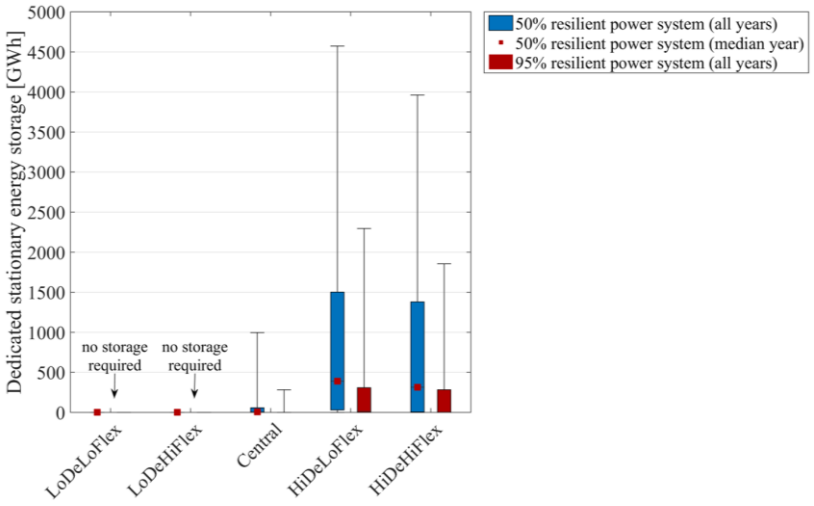

Figure IX.3. Dedicated stationary energy storage – RCP8.5
Dedicated stationary energy storage required for the power system designed with a level of resilience of 50 and 95% under RCP8.5, in order to limit the cross-border interconnection to 5 GW. Each boxplot represents the results obtained for all the ensemble years tested. The dark red square highlights the median of the 50% resilient power system.

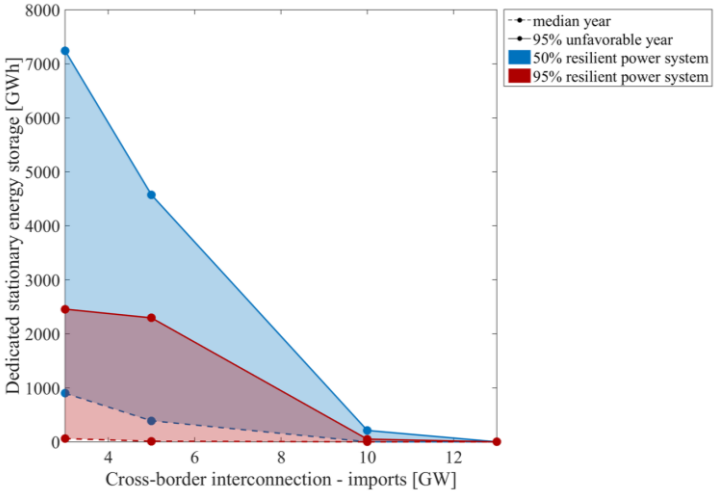

Figure IX.4. Sensitivity analysis on the cross-border interconnection for High demand + Low flexibility – RCP8.5
Dedicated stationary energy storage required according to the cross-border interconnection for the power system designed with a level of resilience of 50 and 95% under RCP8.5. The required dedicated stationary energy storage requirement for different cross-border interconnection capacities is represented in: dashed line– 50th percentile and solid line – 95th percentile.

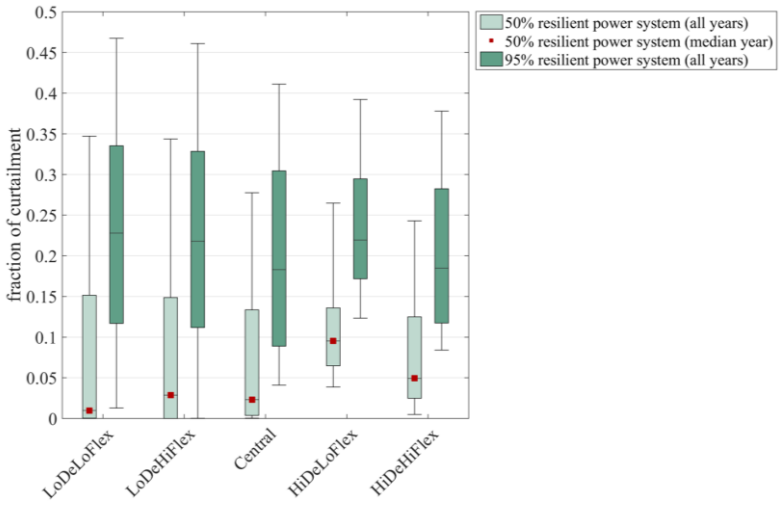

Figure IX.5. Potential energy curtailment – RCP8.5
Generation potentially curtailed for the power systems designed with a level of resilience of 50 and 95% under RCP8.5. Each boxplot represents the results obtained for all the ensemble years tested. The dark red square highlights the median of the 50% resilient power system.